Understanding the fundamentals and application of electrically conductive biofilm in dry digestion

by

Yifei Wang

A thesis

presented to the University of Waterloo

in fulfillment of the

thesis requirement for the degree of

Doctor of Philosophy

in

Civil Engineering - Water

Waterloo, Ontario, Canada, 2023

Examining Committee Membership

The following served on the Examining Committee for this thesis. The decision of the Examining Committee is by majority vote.

External Examiner	George Wells Associate Professor Northwestern University
Supervisor(s)	Tizazu Mekonnen Professor Department of Chemical Engineering
Internal Member	Wayne Parker Professor Department of Civil and Environmental Engineering
Internal-external Member	Trevor Charles Professor Department of Biology
Other Member(s)	Anh Pham Assistant Professor Department of Civil and Environmental Engineering

Author’s Declaration

This thesis consists of material all of which I authored or co-authored: see Statement of Contributions included in the thesis. This is a true copy of the thesis, including any required final revisions, as accepted by my examiners.

I understand that my thesis may be made electronically available to the public.

Statement of Contributions

Yifei Wang was the sole author for Chapters 1, 2, and 7 which were written under the supervision of Dr. Hyung-sool Lee and were not written for publication.

Research in Chapter 3, 4, and 6

This research was conducted at the University of Waterloo by Yifei Wang under the supervision of Prof. Hyung-sool Lee. Yifei Wang carried out all the experimental work and conducted data analysis and interpretation, except for the 16s rRNA sequencing. DNA extraction, 16s rRNA sequencing and raw data from sequencing were carried out and provided in Prof. Keunje Yoo's lab in the Department of Environmental Engineering, Korea Maritime and Ocean University in South Korea.

A version of Chapter 5 was published as the paper: Yifei Wang, Yaohuan Gao, Abid Hussain, and Hyung-sool Lee. "Optimization of biofilm conductance measurement with two-electrode microbial electrochemical cells (MECs)" *Science of the Total Environment*, 858 (2023) 159577

I carried out all the experiments in Chapter 5. Below are my major tasks related to Chapter 5.

- Operation of MECs to develop biofilms on the anodes
- Establishment of analytical instrument and method for *in situ* biofilm conductance measurement
- Data interpretation (biofilm conductance calculation, current density, etc.) under the supervision of Prof. Hyung-sool Lee.

Abstract

The application of microbial electrolysis cell assisted anaerobic digestion (MEC-AD) system for dry digestion to recover methane from food waste (FW) is promising. Understanding the extracellular electron transfer (EET) based syntrophy between ARB and other microorganisms is important to improve the MEC-AD system performance during FW dry digestion. Therefore, the objective of this thesis was (1) to demonstrate an engineered MEC-AD system, bioelectrochemical leach bed reactor (BLBR), for FW dry digestion with enhanced performance, (2) to establish a new standard method for quantification of biofilm conductivity with improved accuracy and reproducibility and to apply the developed method to the anode biofilms in BLBR together with other tools to systematically demonstrate and assess direct interspecies electron transfer (DIET) and conduction-based syntrophy during dry AD process of FW in BLBR.

A traditional leach bed reactor (LBR) was modified for FW dry digestion and methane production. Inoculum should be acclimated with potential inhibitors such as salinity and ammonia which may be encountered with elevated levels in LBR systems before starting the LBR operation, in order to accumulate desired microorganisms adapted to those inhibitors and to achieve the methane production. The cumulative methane yield with the inoculum to substrate ratio (ISR) of 60% was 3.35 times more than that with ISR of 10%, while VS reduction with ISR of 60% decreased by 20% to that with ISR of 10%. Increasing in leachate recirculation also promoted the methane yield. The cumulative methane yield increased by 78% when the recirculation rate increased from 0.3 L/hr to 7.5 L/hr while ISR was kept unchanged. These results displayed the feasibility of LBR application for methane production from FW.

The voltage application in BLBR has proved to improve the acidogenesis and methanogenesis during FW AD process. Optimal applied voltage for methane production was 0.9 V, at which methane yield was 293 mLCH_4/gVS and was 46.7% higher than the control. Further increase the voltage to 1.2 V led to decrease on methane yield. VFA profiles also showed enhanced acidogenesis and acetogenesis with voltage application, with the observed propionate accumulation occurred in the BLBR with 0.3 and 1.2 V but without any significant inhibition on methane yield. The contribution of direct electron transfer through closed circuit on methane yield enhancement was less than 10% and the coulombic efficiency (CE) was less than 6.1%, even with a high conductive anode biofilm in BLBR. The microbial community structure in cathode biofilms indicated the enhanced methane production could be attributed to the enrichment of hydrogenotrophic methanogens through syntrophic methanogenesis because of the enhanced acidogenesis and acetogenesis by applied voltage. Acetoclastic methanogens enriched at the anode may have also improved the methane production via acetate dismutation by directly accepting electrons from ARB in the anode biofilm, although this hypothesis requires future experimental evidence. The results from the present experiments proved the feasibility of BLBR on FW dry digestion and enhanced methane production.

Biofilm conductance is a key parameter to estimate that how feasible the electron could be transferred within it. The biofilm conductance in the MECs showed a sigmoidal profile with anode potential. In comparison, biofilm conductance with a fixed anode potential of -0.4V showed little difference from that without a fixed anode potential, which indicated that anode potential control was not critical for measuring biofilm conductance. The Ohmic-response range was identified at a voltage range between 0 and 100 mV where the current-voltage profile of biofilm followed Ohm's law. Increased monitoring time at each voltage step showed up to 69%

decrease in measured biofilm conductance and further deviation from Ohm's law on the current-voltage profile. The relationship between biofilm conductance and operational parameters also suggested that biofilm conductance should be quantified and displayed with these parameters together for the purpose of comparison. The methods developed in this chapter will be applied to investigate the conductance of biofilms developed in BLBR systems.

Biofilm from LBR and BLBR in previous experiments were developed on the split gold electrodes in the MEC for biofilm conductivity measurement. Although both LBR and BLBR biofilms showed smaller conductivity than *Geobacter*-enriched biofilms, the BLBR biofilm was also reported highly conductive (145.6 ~ 158.9 μS/cm) under the anode potential observed during BLBR operation, indicating that the anode biofilm would be conductive for EET in BLBR. The electron transfer in those methanogenic types of biofilms would be dominated by metallic conduction, because the biofilm conductivity increased against the anode potential. The abundance of *Geobacter* sp. in biofilm community was positively correlated with the biofilm conductivity. Microbial community structure analysis identified similar bacterial and archaea genera in the biofilm communities grown on split gold anodes of MECs and on carbon fiber anodes of BLBR. Therefore, MEC equipped with split gold anodes could be a useful tool for *in situ* study on the bioelectrochemical characteristics including biofilm conductivity of those biofilms grown on electrodes of BLBR and other MEC-AD systems.

Acknowledgements

Without a doubt there are many people to recognize who have helped me along the way, and I greatly appreciate their effort. First and foremost, I would like to express my sincere gratitude to my supervisor, Prof. Hyung-sool Lee, for his expert guidance and continuous support in my research. Meanwhile, I would like to appreciate greatly the support from another supervisor, Prof. Tiz Mekonnen, during the rest of my PhD study after Prof. Lee's leaving. I would also like to thank all other committee members, Prof. Anh Pham, Prof. Wayne Parker, and Prof. Trevor Charles for the assistance they provided during my study. I would like to thank Prof. George Wells from the Department of Civil and Environmental Engineering at Northwestern University for spending his precious time to join the defense as my external examiner.

Special thanks to our technicians, Mark Sobon, Mark Merlau, and Peter Volcic for their assistance in instrument training and troubleshooting and for their commitment to maintain these analytical instruments in good conditions. Without their help, my lab work would be much difficult. Sincere thanks would be given to Prof Keunje Yoo and his colleague from South Korea, for their effort and work spent on DNA extracting and 16s rRNA sequencing of my microbial samples.

In addition, I would like to thank all the members in Department of Civil and Environmental Engineering, for making my experience in Waterloo so exciting. I would like to give my thanks to Dr Abid Hussain and Dr Jangho Lee who taught me with precious experience on the operation of microbial electrolysis cells and meta-omic analysis tools. I should also thank Swakshar Saha and Ziyi Xiong for helping me on leach bed reactor operation for my study.

Last but most importantly, I would like to thank my wife and daughter for their exceptional support they provided to me through my study, even when we were in different countries.

Table of Contents

List of Figures

List of Tables

Nomenclature

AD	Anaerobic Digestion
Ag/AgCl	Silver/Silver Chloride reference electrode
ARB	Anode-Respiring Bacteria
BES	Bioelectrochemical System
BLBR	Bioelectrochemical Leach Bed Reactor
CE	Coulombic Efficiency
CLSM	Confocal Laser Scanning Microscopy
CSTR	Continuous Stirred Tank Reactor
DET	Direct Electron Transfer
DIET	Direct Interspecies Electron Transfer
EET	Extracellular Electron Transfer
EPS	Extracellular Polymeric Substances
FISH	Fluorescence *in situ* Hybridization
FW	Food Waste
GAC	Granular Activated Carbon
GC-FID	Gas Chromatography with a Flame Ionization Detector
GC-TCD	Gas Chromatography with a Thermal Conductivity Detector
HRT	Hydraulic Retention Time
IET	Interspecies Electron Transfer
ISR	Inoculum to Substrate Ratio
LBR	Leach Bed Reactor
LCFAs	Long-Chain Fatty Acids
MECs	Microbial Electrolysis Cells
MEC-AD	Microbial Electrolysis Cell assisted Anaerobic Digestion
MIET	Mediated Interspecies Electron Transfer
OLR	Organic Loading Rate

OUT	Operational Taxonomic Unit
PCR	Polymerase Chain Reaction
SCOD	Soluble Chemical Oxygen Demand
SEM	Scanning Electron Microscopy
SHE	Standard Hydrogen Electrode
SPOB	Syntrophic Propionate-Oxidizing Bacteria
SRT	Solid Retention Time
TAN	Total Ammonia Nitrogen
TCOD	Total Chemical Oxygen Demand
TEM	Transmission Electron Microscopy
TS	Total Solid
VFAs	Volatile Fatty Acids
VS	Volatile Solid
WWTP	Wastewater Treatment Plant

Chapter 1 - Introduction

1.1 Background

As a major organic solid waste from human society, food waste (FW) has become an important economic and environmental issue and gained increasing attention in recent years (Li et al., 2018; Voelklein et al., 2016; Zhang et al., 2022). In North America, United States holds the first place in FW generation per capita in the world (188 kg/capital), followed by Canada in North America (Worldmeters, 2019). In the EU, almost 60 million tons of FW (131 kg/inhabitant) are generated every year with an associated market value estimated at 132 billion euros (Eurostat, 2022). In China, it is estimated that more than 180 million tons of FW will be produced every year by 2026 (Zhang et al., 2022). FW can be originated from harvesting to residential and commercial kitchens which covers almost all steps of the food supply chain (CEC, 2017). Improper disposal of FW would not only lead to generation of leachate and odor which may pollute the environment during collection, transportation, storage, and treatment of FW, but also increase green-house gas emission and affect climate change (Ahmed & Sulaiman, 2001; Han & Shin, 2004; Krcmar et al., 2018; Rocamora et al., 2020).

Enforcement of waste reduction has encouraged a circular economy and enabled waste recycling and resource recovery during waste processing (European Commission, 2020). Anaerobic digestion (AD) is considered a beneficial treatment for FW due to its high treatability and direct conversion to biogas. For example, EU produced about 18.4 billion cubic meters of combined biogas and biomethane (purified biogas) in 2021, with a target of 35 billion cubic meters of biomethane production per year by 2030 (European Biogas Association, Statistical Report 2022).

FW can be a competitive and economic source of biogas production by AD technology, which can achieve the reduction, stabilization, and resourcification for FW with the production of biogas as energy sources and digestate as soil fertilizer (Jang et al., 2019). But AD of FW can accumulate potential inhibitors such as ammonia and medium to long chain fatty acids, thereby affect the AD process (Chen et al., 2008; Shahriari et al., 2012; Xu et al., 2012, 2021).

Single-stage AD is well understood technology for biogas production today. However, the optimum growth conditions for hydrolytic and acidogenic bacteria and methanogens are not the same in the single-stage AD systems, since those systems mostly would prefer methanogens but not for hydrolytic and acidogenic bacteria (Bochmann and Montgomery, 2013; Voelklein et al., 2016). Two-stage AD technologies separate reactors for hydrolytic-acidogenic and methanogenic processes, which allows for individual optimization of hydrolysis and methanogenesis processes and can achieve enhanced process stability and higher rates of organic degradation and biogas yield (Wilson et al., 2016).

Although continuously stirred tank reactors (CSTRs) are commonly used in two-stage AD, they are not ideal for high solid content organic waste (total solid of 20-30%) digestion, such as agricultural waste and FW, because of extremely high operating cost for mixing (Li et al., 2017; Rocamora et a., 2020; Rico et al., 2015; Xiong et al., 2019); hence, dry AD, or high-solids or solid-state digestion, becomes one of the possible FW treatment methods for energy recovery. Dry AD can treat organic materials with solid content as high as 40%. Dry AD also shows a reduced need of water addition, a higher organic loading rate potential, and a reduction on energy cost for mixing in the reactor, making it attractive for organic fraction of municipal solid waste treatment including FW and has shown increase in popularity for organic waste treatment by AD (Guendouz et al., 2010).

Leach bed reactors (LBRs) have gained attention recently due to its capability of treating high-solid content waste, solid-liquid separation, reduced water demand during operation, and low operation and maintenance cost (Swakshar and Lee, 2020; Voelklein et al., 2016; Wilson et al., 2016; Xiong et al., 2019). However, LBRs have mainly employed as hydrolysis reactors of the first stage in the two-stage AD, which means accumulation of VFAs. Integration of hydrolytic-acidogenic and methanogenic processes together in the single LBR for FW treatment is under studying and information on dry AD for FW using single-LBR is limited (Rocamora et al., 2020).

Microbial electrochemical cells (MECs) have gained attention due to resource recovery simultaneously with organic waste and wastewater treatment. MECs combine microbial metabolism of anode-respiring bacteria (ARB) with electrochemistry to capture electrons directly from organic compounds in organic waste and wastewater. Hence, MECs can generate electric power or other high-value products (hydrogen, hydrogen peroxide, ethanol, butanol, etc.), which could contribute to sustainable management of organic waste and wastewater (Lee et al., 2010; Logan and Rabaey, 2012; Logan et al., 2015).

Producing high current density is essential for the success of MEC application, which means that understanding of anode electron transfer kinetics is key for improving current density in MECs (Lee et al., 2016; Torres et al., 2010). Anodic reactions consist of intracellular electron transfer and extracellular electron transfer (EET). Literature has emphasized the significance of electrical conduction of EET for biofilm anodes to generate high current density (Lee, 2018; Lee et al., 2016; Torres et al., 2010). There are two conduction mechanisms of EET. The first is redox conduction in which electrons transport via electron hopping in multiple extracellular cofactors to the anode extracellularly (Li et al., 2016a; Strycharz-Glaven et al., 2011; Yates et al., 2016a & b). The second is metallic-like conduction via electrical pili (e-pili) or other electrically conductive

proteins, and this EET follows Ohm's law in biofilm anodes (Malvankar et al., 2011, 2012a & b, 2015; Tan et al., 2016). Literature has shown that ARB can perform both redox and metallic-like conductive EET, which increases the complexity of conductive EET mechanisms in biofilm anodes (Lee et al., 2016; Lovley, 2017). Lee (2018) has recently reported that Ohm's law can well describes electrical conduction of EET in biofilm anodes where anode potential gradient is less than 200-300 mV, regardless of conduction mechanism.

Biofilm conductivity (or conductance) is the single quantitative parameter to evaluate "electrically conductive biofilms". By measuring current-voltage response through a given biofilm grown on two anodes separated by a non-conductive gap, literature has quantified *in situ* biofilm conductivity of pure *Geobacter sulfurreducens* biofilms and mixed-species biofilms (Li et al., 2016a; Malvankar et al., 2011; Yates et al., 2016a). Although the measurement of biofilm conductivity is the sole method of assessing electrical conduction of EET in biofilm anodes, there is limited information on accuracy and reproducibility of biofilm conductivity measurement. For instance, small current change during measurement can significantly affect conductance value of biofilm anodes. Stable current is critically important for determination of biofilm conductivity, but steady-state current is not defined well for biofilm conductivity measurement in literature. Operational and environmental parameters are not optimized for biofilm conductivity, which means that reported biofilm conductivity might be deviated from true conductivity value. Therefore, existing methods are shallow to ensure the accuracy and reproducibility of biofilm conductivity measurement. An improved and precise method of measuring biofilm conductivity is required to confirm that biofilms are electrically conductive.

Biofilm conductivity has gained more attention as microbial syntrophy based on electrical conduction is proposed for natural and engineered systems such as AD process (Yu et

al., 2018; Lee et al., 2019). Literature has reported that direct interspecies electron transfer (DIET) could occurred between *Geobacter* sp. and some methanogens potentially via electrical conduction in defined co-cultures (Morita et al., 2011; Rotaru et al., 2014 a & b; Shrestha et al., 2014). Combining MECs with AD (called MEC-AD) may improve AD performance by stimulating conduction-based syntrophy between ARB and methanogens (Bo et al., 2014; Lu and Ren, 2014; Wang et al., 2020; Yu et al., 2018; Zhao et al., 2021). This approach is founded on the hypothesis that electrons can be shared between methanogens and ARB through interspecies electron transfer (IET) via conductive EET. Interestingly, few studies have experimentally proved that conduction-based syntrophy truly occurs in MEC-AD systems. Literature has claimed that IET via conductive EET might occur based on improved methane yield or reduction of volatile solid (VS) (Baek et al., 2018; Martins et al., 2018; Wang et al., 2018a, 2021; Zhao et al., 2021). Improvement of AD performance simply by combining MECs with existing AD facilities would be an interesting approach, and the success of the proposed system can contribute to AD and organic waste treatment markets. However, more scientific research is required to prove conduction-based syntrophy in MEC-AD processes. IET via conductive EET and conduction-based syntrophy in the AD processes cannot be accepted without evidences.

1.2 Research Objectives

The primary goal of this study is two-fold. The first is to demonstrate an engineered MEC-AD system, bioelectrochemical leach bed reactor (BLBR), for FW dry digestion with enhanced performance. The second is to establish a new standard method for quantification of biofilm conductivity improving accuracy and reproducibility, including optimization of operating and environmental parameters. Such a method will be applied to the BLBR together with other

tools to systematically demonstrate and assess IET via EET and conduction-based syntrophy during dry AD process of FW in BLBR.

Most of the research was carried out at Waterloo Environmental Biotechnology Laboratory at the University of Waterloo. Several laboratory scale LBRs and BLBRs have been designed, fabricated, and operated for FW dry digestion. MECs equipped with special gold electrodes for *in situ* biofilm conductivity measurement method developing have also been fabricated and operated for this research.

1.3 Thesis outline

This thesis is divided into seven chapters and reference. Chapter 1 provides background information of the research topic under investigation and summarizes the specific goals of the proposed research. Chapter 2 presents a literature review related to the proposed research, focusing on the MEC-AD process for organic waste treatment, syntrophic relationships within specific microorganisms, and biofilm conductance measurement. Chapter 3, 4, 5, and 6 are the main research chapters organized in article format with syntrophic relationship in each chapter. Chapter 7 summarizes the scientific and engineering findings and implications of these results and provides recommendations for future research.

Chapter 2 – Literature Review

2.1 Fundamentals of anaerobic digestion (AD)

The AD process can be divided into four successive steps of substrate degradation: hydrolysis, acidification, acetogenesis, and methanogenesis (Figure 2-1) (Zhou et al., 2018; Lee et al., 2020; Lu et al., 2021). In the first step, the soluble polysaccharides, proteins and lipids produced by FW solubilization are broken down into monosaccharides, amino acids, glycerol and long-chain fatty acids (LCFAs) by the action of different extracellular enzymes secreted by the hydrolytic bacteria. Usually, the hydrolysis of complex organic matters is the rate-limiting step for substrate conversion at this time (Cao et al., 2019). The second step is the acidogenesis, during which the hydrolyzed monomers are fermented to short-chain fatty acids (e.g., acetic acid, propionic acid, butyric acid, etc.) and alcohols, as well as biogas (CO_2 and H_2). Acidogenesis is the fastest step of the AD process, therefore it is likely to lead to the accumulation of volatile fatty acids (VFAs) and a decrease in pH. If the buffering capacity of the digestion system is insufficient and the organic loading rate is high, it will directly lead to the acidification of the AD system and inhibit the metabolism of methanogens (Jang et al., 2014 & 2015).

The third step is called acetogenesis, in which simple organics like ethanol and VFAs will be converted to acetic acid, H_2, and CO_2, while the hydrogen-consuming homo-acetic acid-producing bacteria reduce H_2 and CO_2 to acetic acid. This step is thermodynamically unfavorable under standard conditions at pH 7 and high partial pressure of H_2 (see Eq. 2-1 to 2-3). But consumption of H_2 by homoacetogens and hydrogenotrophic methanogens will the partial pressure of H_2 extremely low, making the entire syntrophic metabolism efficient and

thermodynamically favorable, which provides a good example of syntrophy between acetogenic bacteria and methanogens (Liu et al., 1999; de Bok et al., 2001; Stams & Plugge, 2009; Sieber et al., 2012).

Propionate:

$$CH_3CH_2COO^- + 2H_2O \rightarrow CH_3COO^- + CO_2 + 3H_2 \qquad \Delta G^{0'} = +73.7\ kJ/mol \qquad \text{Eq. 2-1}$$

Butyrate:

$$CH_3CH_2CH_2COO^- + 2H_2O \rightarrow 2CH_3COO^- + H^+ + 2H_2 \qquad \Delta G^{0'} = +49.8\ kJ/mol \qquad \text{Eq. 2-2}$$

Ethanol:

$$CH_3CH_2OH + H_2O \rightarrow CH_3COO^- + H^+ + 2H_2 \qquad \Delta G^{0'} = +9.65\ kJ/mol \qquad \text{Eq. 2-3}$$

VFAs are important intermediate products in the acidogenesis and acetogenesis steps of AD and are produced via different pathways (Zhou et al., 2018; Kamagata et al., 2015; Karki et al., 2021). In general, acetic, propionic, and butyric acid are the main products of acid-producing fermentation (Khatami et al., 2021). Since the hydrolysis of complex compounds greatly limits the efficiency of acidogenesis during AD process, hydrolysis can be accelerated by optimizing operating parameters and pretreating the substrate. Accelerating the rate of hydrolysis, enhancing acidogenesis and mitigating the effects of inhibitory factors are effective strategies to increase the total yield of VFAs (Chen et al., 2013a & b; Jiang et al., 2013; Khatami et al., 2021).

The fourth step is the methane production step, during which methane is mainly produced by two pathways: acetoclastic methanogenesis and hydrogenotrophic methanogenesis (Meena et al., 2020). In the acetate pathway, acetoclastic methanogens split acetic acid to CH_4 and CO_2,

while in the hydrogen-nourishing pathway, hydrogenotrophic methanogens reduce CO_2 to CH_4 by H_2 (or formate). A third pathway, methylotrophic methanogenesis, utilizes methylated compounds including methanol, methylated amines to produce methane (Thauer, 1998). This catabolic pathway is currently exclusively conducted by the species of the family Methanosarcinaceae, among which the genus *Methanosarcina* is the only known genus which can perform all the three pathways for methane production. The genus *Methanosaeta* is strictly acetoclastic, while all other known methanogens produce methane by the reduction of CO_2 (Kendall & Boone, 2006; Hedderich & Whitman, 2006; Sakai et al., 2011; Borrel et al., 2013 & 2014).

Differences in the composition of FW will result in differences in composition of soluble organics (monomers, VFAs, and alcohols) after hydrolysis and acidogenesis steps, and also affect the methanogenesis pathways. In anaerobic digestion of carbohydrate- and fat-rich substrates, the acetoclastic pathway is the predominant methane production pathway, whereas in anaerobic digestion of protein-rich substrates, hydrogenotrophic methanogenesis will predominate (Kurade et al., 2019).

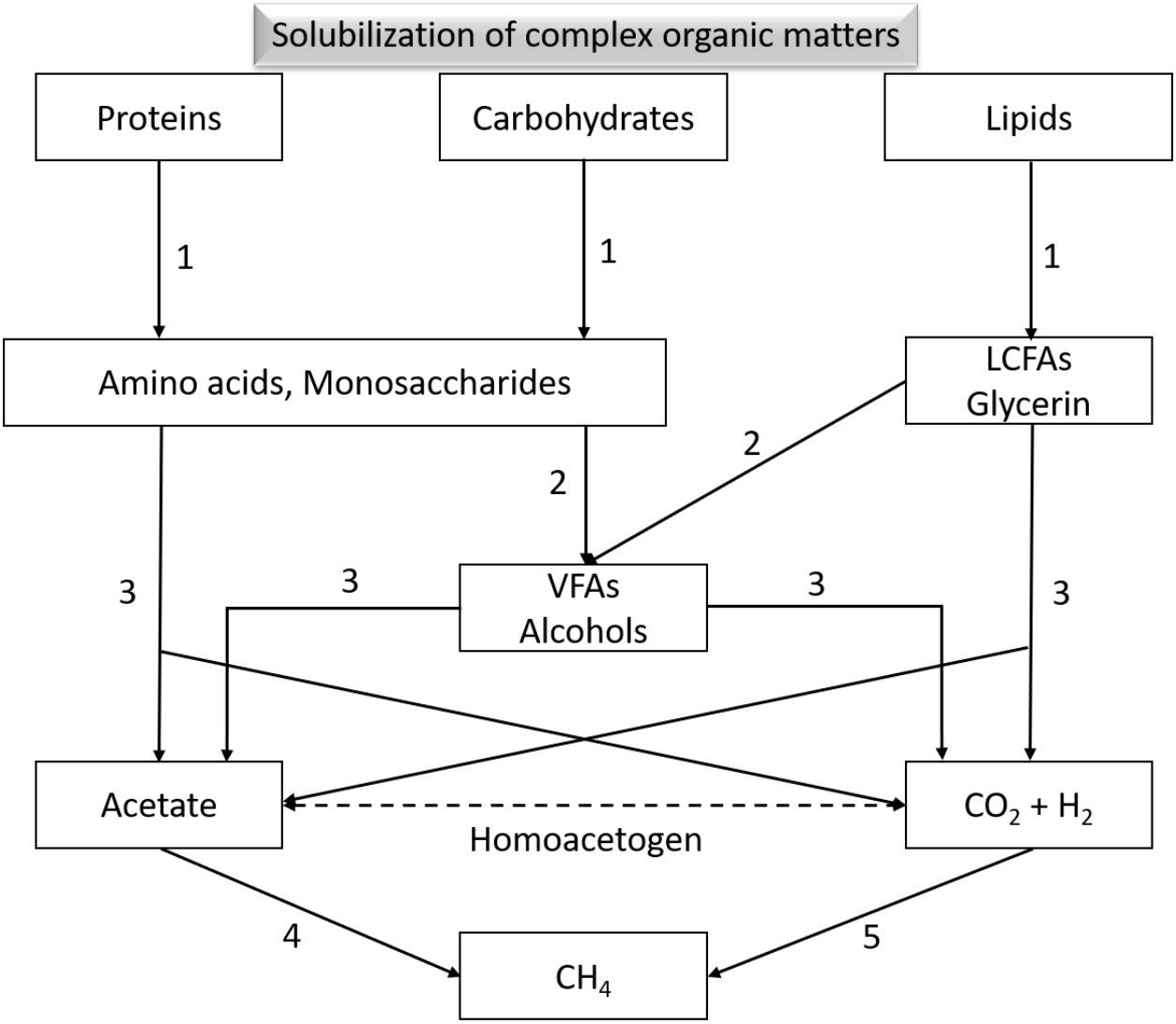

Figure 2-1. Schematic diagram of mechanisms in AD process. 1: Hydrolysis. 2: Acidogenesis. 3: Acetogenesis. 4: Acetoclastic methanogenesis. 5: Hydrogenotrophic methanogenesis.

2.2 Factors affecting dry AD process performance

Different process parameters are critical for batch dry AD operation and need to be analyzed separately. For this reason, inoculum to substrate ratio (ISR), leachate recirculation, hydraulic retention time (HRT) are covered for batch processes, as ISR is a key parameter for

batch process start-up, while leachate recirculation is critical to improve FW substrate homogeneity. Environmental parameters including salinity and pH and inhibitors like fatty acids will also be discussed briefly.

2.2.1 Inoculum to substrate ratio (ISR)

The ISR is a key factor affecting the stability of the AD system and methane production. Different ISR will lead to differences in nutrient content, carbon to nitrogen ratio, and composition of organic matters in the digestion system. FW is rich in biodegradable organic matter such as carbohydrates and can be easily converted to methane through anaerobic digestion. Therefore, increasing the proportion of FW in the feedstock could be an effective way to enhance the methane production of AD system. Inoculum loading at the beginning of the batch digestion process is a way of accelerating the start-up period (or reduce the lag phase of the AD process), and an efficient method to provide the necessary microbial population to the new FW substrate (Chen et al., 2008; Chugh et al., 1999). The common procedures to inoculate the fresh material include the use of digestate from a previous batch, digested manure, or digested sludge from wastewater treatment AD reactors (Karthikeyan and Visvanathan, 2013; Rocamora et al., 2020). For dry AD system like LBR, increasing inoculum addition (hence increasing ISR) would reduce the available volume in the reactor to treat more substrate but can improve biogas yield and maintain system performance by providing more microorganisms responsible for AD process. Reducing ISR would increase substrate treatment capacity of the reactor but may lead to longer retention time and lower methane yields due to inhibitory problems. In addition, the ISR together with the chemical composition of FW would also affect the carbon to nitrogen ratio (C:N) of the FW feedstock. A suitable C:N ratio for AD system is important to maintain the metabolic

activity of microorganisms and C:N values below or above the optimal range may lead to unstable operation of the AD system and reduced biogas production (Hagos et al., 2017).

Although ISR is a key parameter for batch dry AD like LBR systems, different studies have reported different optimum ratio with the variation of system structures, operating conditions, and FW characteristics. For example, Jang et al (2016) showed that the methane yield and methane content increased significantly with increasing the mixing proportion of FW in the feedstock, and the optimal methane production performance of the AD system was achieved at a ISR of 25%. Cheng et al (2020) investigated the effect of different ISR on the AD system and found that the methane production peaked when ISR was 25%. However, Prabhu & Mutruni (2016) found that the highest biogas yield (823 mL/gVS) was achieved at ISR of 66.7%, as compared to other ISR from 33% to 60%. Pan et al (2019) compared the effects of seven ISR on AD performance and found that the highest methane yield was achieved at a ISR of 50%. It also reported shorter lag phase and higher hydrolysis rate as well as 4.5-time increase in the methane yield. Liu et al., (2009) reported almost similar methane yield when the ISR increased from 20% to 40%, which indicated that increasing the inoculum ratio would increase methane yield until a maximum where methane production became independent of FW or inoculum loads. Those differences in optimum ISR may be related to operation modes and types of digestors, composition of FW, and inoculated microorganism. Therefore, for different AD systems, the optimal ISR should be determined carefully according to the type of systems, operation conditions, and FW characteristics.

2.2.2 Leachate recirculation

Although inoculation to start the dry AD process could speed up the AD process and avoid potential inhibitions, it would reduce the reactor volume available for FW treatment. Therefore, leachate recirculation becomes a common solution to reduce the use of inoculum. In addition to a volume increase for FW treatment, it has been reported that leachate recirculation could increase the moisture of the new FW feedstock, increase the contact between hydrolytic bacteria and solid FW substrate, and improve the reactor homogeneity, which in all would promote the reactor performance by achieving the maximum methane yield faster and further increasing the methane production. It has been reported that methane production increased by 4 times and the time to achieve the maximum methane production rate was shorten for 2 days when recirculation was applied (Chan et al. 2002). It has also been reported that solid inoculum could be replaced by using enough leachate from previous batch as initial inoculum and recirculating in the reactor (Kusch et al., 2008).

In addition, leachate recirculation in dry AD systems would help to "wash out" the inhibitors such as ammonia and VFAs present and accumulate in the solid FW substrate. It has been reported that the VFA levels reached their maximum at the beginning of the digestion without any recirculation application, therefore increased the risk of acidification and instability of the dry AD systems (Pezzolla et al., 2017). When recirculation was applied, the VFA concentrations decreased by more than 90% as the recirculation rate increased. The total ammonia nitrogen (TAN) level in the final digestate also followed the similar trend as VFA levels did, which showed a 92% decline in the TAN level with a 2.5-time increase in the methane yield at the highest recirculation rate (Pezzolla et al., 2017).

Studies have reported that both continuous or intermittent recirculation of leachate could increase methane production as compared to those without recirculation (Dearman & Bentham, 2007; Degueurce et al., 2016; Pezzolla et al., 2017; Rico et al., 2015; Wilson et al., 2016). Wilson et al. (2016) achieved similar methane yield with continuous leachate recirculation during operation when the ISR decreased fron 40% to 10%. Rico et al. (2015) applied intermittent recirculation for manure dry AD and found that it would improve the system stability and speed up the AD process. However, recirculation also requires additional energy input for the dry AD system. Recirculation of excessive leachate during dry AD process may also show negative effects on system performance, partially attributed to the fast accumulation of inhibitors like ammonia in the leachate (Chen et al., 2008). Therefore, optimizing recirculation strategies of leachate (continuous or intermittent, rate of recirculation, etc.) is necessary to improve methane production for FW dry AD.

2.2.3 Hydraulic retention time (HRT)

HRT is another key parameter of the AD process, which refers to the contact time between the substrate and anaerobic microorganisms during digestion. HRT equals to solid retention time (SRT) in batch operation mode. HRT can directly affect the efficiency of substrate hydrolysis, as well as the community structure of anaerobic microorganisms, metabolic pathways, and the type and yield of digestate (De Groof et al., 2021; Fernando-Foncillas & Varrone, 2021; Li et al., 2015a & b; Wang et al., 2017). The hydrolysis efficiency and VFAs production increased with longer HRT, and longer HRT was more favorable for the growth of methanogens. HRT is also related to organic loading rate (OLR) of digestion process for batch process, the lower the HRT, the higher the OLR. It was found that the anaerobic digestion system could

operate stably with HRT of 16-40 d, and shorter HRT usually eliminates methanogens and promotes hydrogen production from digestion (Dinesh et al., 2018).

Wang et al. (2020) investigated the effects of HRT on the performance of AD systems and revealed the differences in microbial community structure and the main CH4 metabolic pathways. AD systems with longer HRT (25 d) were enriched with syntrophic *Syntrophomonas* and hydrogenotrophic methanogens, while acid-tolerant bacteria *Lactobacillus* was selectively enriched at HRT 5-d in the system and syntrophic acetate oxidation and hydrotropic methanogenesis became the main methanogenesis pathways. Differentiation of ecological niches within the microbial communities reduced the interspecies competition in the AD system.

However, it was found that the methane yield (314 mL/gVS) of the single-stage AD system at a longer HRT of 25 d was close to that (325 mL/gVS) of the two-phase AD system at a shorter HRT (15 d), suggesting that the effect of HRT on the AD system was also related to the operation modes (Wang et al., 2017). Li et al. (2015a) compared the impacts of different HRT on FW digestion in a continuous AD system and achieved stable performance (334 mL/gVS) with HRT of 7.5-d when the feeding shock was eased, as compared to that (345 mL/gVS) with HRT of 20-d. The high concentration of VFAs produced under high OLR conditions can be converted to methane efficiently without accumulation. The rapid conversion of proteins to ammonium, which provided alkalinity and buffer capacity, was considered as an important factor which affected the stable AD performance under such short HRT. Therefore, careful optimization of HRT (and OLR) is needed to better meet the treatment requirement for different feedstock including FW and to maintain stable system performance for dry AD.

2.2.4 Salinity

Salinity (e.g., Na, K, Ca, Mg, and Cl ions) can be found in FW. NaCl content in FW is generally between 2-5% with value varied significantly depending on the regions and locations (Dai et al., 2013; Zhao et al., 2017). Higher concentrations of salinity in FW would increase the extracellular fluid osmolarity, which would cause cell dehydration and thereby inhibit microorganism growth and reduce methane production in AD system (Chen et al., 2008; Dai et al., 2013). Salinity in the appropriate range can enhance the activity of enzymatic reactions related to anaerobic digestion and maintain and regulate the osmotic pressure balance required for microbial growth. Salinities ranging from 0.1 to 0.23 gNaCl/L would favor the microbial growth in mesophilic AD system including acetoclastic methanogens (Ye et al., 2008). However, higher salinity can lead to a decrease in methane production and even collapse of the anaerobic digestion system. For example, salinities within the range of 2-5 gNaCl/L could improve the hydrolysis and acidification of FW during AD process, but would inhibit methane production (Zhao et al., 2017). It was also reported that methanogens were severely inhibited at salinities >10 g NaCl/L and acidogens were inhibited with salinities up to 50 g NaCl/L (Sakar et al., 2020). Meanwhile, high salinity would affect the conversion of lactic acid to VFAs, resulting in the accumulation of lactic acid and hence the major metabolic pathways alteration in the AD system (Li et al., 2021).

2.2.5 pH

The pH value is an important parameter to maintain the stability of the AD system. Fermentative bacteria in AD systems show different sensitivities to pH, with most of them able

to survive at pH 4.0 to 8.5. Acidogens are believed to be less sensitive and can perform metabolic functions at pH 3.0-11.0, while neutral pH (6.5-7.2) is favorable for the metabolism and growth of methanogenic bacteria (Ward et al., 2008). The rapid hydrolysis of highly biodegradable substrates in the AD system causes a decrease in pH, while maintaining a stable pH reflects the strong buffering capacity of the digestion process. Also, different pH environments would affect the quality of soluble substrates in the digestate that can be utilized by the fermenting flora, which in turn affects the type and concentration of organic matter digested VFAs. Khatami et al (2021) investigated the effects of pH on VFA production during FW digestion and found that acetic acid production was mainly occurred at pH=10, while the main metabolites were propionic and acetic acid at pH=5. Jiang et al (2013) concluded that the concentration and yield of VFAs were highest at pH 6.0, among which acetic and butyric acid were the main organic acid components.

pH less than 5.5 would significantly inhibit methanogenic activity (Braguglia et al., 2018; Ge et al., 2011; Mehariya et al., 2018). Lindner et al (2015) showed that methane production at pH 5.5 was only 40% of the theoretical value. Latif et al. (2017) also observed an 88% reduction in methane production when pH decreased from 7 to 5.5. One study on dry AD of municipal waste showed that the pH dropped to 6.5 when hydrolysis and acidogenesis dominated at the beginning with VFA level up to 12 g/L. pH was then increased to 8 when methanogenesis consumed VFA and decreased its level to 1 g/L (Di Maria et al., 2017). It is reported that maintaining pH between 7.2 and 8.2 was required for stabilization of methane production, as VFAs would become toxic at low pH and at higher pH the ammonium equilibrium in solution would move towards the formation of more toxic free ammonia species. (Chen et al., 2008; Hansen et al., 1998; Karthikeyan and Visvanathan, 2013; Ward et al., 2008). Alkalinity provides

system resistance to sudden changes in pH and is measured for buffer capacity of AD system as an index of process performance (Ward et al., 2008). The buffer capacity is proportional to the concentration of bicarbonate species. Usually, a drop in alkalinity could reflect accumulation of VFAs before the pH variation is observed (Veluchamy et al., 2019). Addition of base or bicarbonate, increasing HRT and reducing OLR, and variation of ISR could affect the buffer capacity of the AD system and maintaining alkalinity of the system would benefit AD process (Ağdağ and Sponza, 2005; Kim & Oh, 2011; Ward et al., 2008; Wu et al., 2016).

In general, considering that the optimum pH of methanogen, maintaining the AD system at neutral or weakly alkaline pH 6.5~7.5 can keep an optimal environment for acidogen and methanogen growth and achieve efficient methane production. Considering its specific characteristics such as the lack of mixing and high solid content in the dry AD system, which would lead to heterogeneity in the system, research may be required prior to the operation of dry AD in order to determine optimum pH range for both fermentative and methanogenic microorganisms.

2.2.6 VFAs

VFAs are important intermediates produced in the acidogenesis and acetogenesis steps of AD. The main VFAs present in the system typically include acetic, propionic, and butyric acids. Accumulation of these VFAs could be observed at the early period during AD process (Massaccesi et al., 2013). It is believed that when the production of VFA was faster than their consumption by acetogen or methanogens, inhibition would occur with the drop in pH and decline of methane yield (Guendouz et al., 2010). Inhibition effect of acetic acid higher than 2

g/L was detected (Karthikeyan & Visvanathan, 2013). And it was reported that approximately 50% and 100% inhibition of methane production occurred at propionate level of 3.5 g/L and 5.0 g/L, and butyrate levels of 15.0 and 25.0 g/L, respectively (Dogan et al., 2005).

The lack of sufficient mixing and the high solid content during dry AD operation can often lead to poor solid liquid mass transfer and accumulation of VFA in some localized areas, producing localized inhibition without affecting the total methanogen in the AD system (Dong et al., 2010). On one hand, the lack of diffusion would contribute to the instability of the process and lead to longer reaction time for dry AD. On the other hand, poor diffusion may indicate that dry AD could be operated at higher VFA levels because methanogens would not get in contact with high VFA directly but in a slow flux leached from solid substrate, therefore avoided the inhibition (Fagbohungbe et al., 2015). In addition, increasing the ISR and introducing leachate recirculation to the dry AD batch system could relief the VFA accumulation (Fernández-Rodríguez et al.,2014; Hashimoto, 1989).

2.3 Direct interspecies electron transfer (DIET) during bioelectrochemical methane production in microbial electrolysis cells assisted anaerobic digestion (MEC-AD) system

The methanogenesis is the last step of AD process, which is highly dependent on interspecies H_2/formate transfer between syntrophic bacteria and methanogens. It faces several limitations: VFA degradation thermodynamically favorable only at very low hydrogen partial pressure, low metabolic rate, accumulation of VFAs under high OLR, pH instability caused loss of methanogens, long operation periods, shift in microbial community towards acidogen-dominant cultures, etc. (Abbas et al., 2021; Beegle et al., 2017; Cheng & Kaksonen., 2017;

Nagendranatha Reddy et al., 2015; Zhao et al., 2014). Therefore, different technologies including pre-treatment, two-stage AD, integration with other technique are developed in practice to accelerate the hydrolysis rate of complex organic matters and break the thermodynamic barrier for acidogenesis in order to improve the efficiency and stability of AD process (Kumar et al., 2021).

MECs combines microbial metabolism of anode-respiring bacteria (ARB) with electrochemistry to capture electrons directly from organic compounds in organic waste and wastewater for electric power and other chemical production. Microbial electrolysis cells (MECs) become a promising alternative technology to enhance the AD process, named MEC-AD. MEC-AD could improve the methane yield by selectively adjusting microbial community structure and promoting interspecies electron transfer (Morita et al, 2011; Yu et al., 2021; Zhao et al., 2020). In addition, recent studies have also shown that the direct interspecies electron transfer (DIET) would be a more effective way for electron transfer than H2/formate mediated interspecies electron transfer, which can enhance the syntrophy between microorganisms in AD system and promote reaction thermodynamically unfavorable, hence improve the AD process (Liu et al., 2016; Xu et al., 2019; Wang et al., 2020b & c; Zhang et al., 2020). Therefore, a comprehensive summary of current understanding on methanogenesis enhancement in MEC-AD will be provided.

2.3.1 DIET in syntrophic methanogenesis

In bioelectrochemical methane production, methane can be produced by CO_2 reduction and the electroactive microbes on the cathode of an engineered system with electric power

supply. The electroactive microbes, like anode-respiring bacteria, can utilize electrons directly from cathode (called biocathode) (direct electron transfer) or they can accept electrons from other sources produced on the electrodes (mediated electron transfer) (Blasco-Gomez et al., 2017; Zhu et al., 2018). Further, direct electron transfer between different microorganisms is also known as direct interspecies electron transfer (DIET) (Lovley, 2011).

Direct microbial electron transfer has been applied to bioelectrochemical synthesis in MECs. On the anode, current is produced by electron transfer from a special group of microorganisms (anode-respiring bacteria, ARB) to the anode. And on the cathode, electron is captured by microbes to produce valuable biochemical product (Choi & Sang, 2016). The electrodes can act as either electron donor or acceptor in the microbial energy metabolisms. The unique cytochromes, e-pili and other appendages of microorganisms allow them to connect and associate with the electrode surface (Pirbadian et al., 2014; Reguera et al., 2005; Summers et al., 2010; Tremblay et al., 2011; Vargas et al., 2013). DIET can take place between mutualistic microorganisms via electrically conductive pili (e-pili) and cytochromes (c-type Cytochromes) (Lovley, 2011) (Figure 2-2a and b). Through e-pili and c-type cytochromes, bacteria can directly transfer electrons generated by intermediates to methanogenic archaea to reduce CO_2 to produce methane. DIET cannot be established between microorganisms lacking e-pili or c-type cytochromes, but the addition of conductive materials can act as electron channels and facilitate the establishment of DIET between microorganisms (Figure 2-2c). Compared with mediated interspecies electron transfer (MIET) (Figure 2-2d), DIET has higher electron transfer rate based on reaction-diffusion-electrochemical model, which could speed up the syntrophy between microorganisms and increase the methane production efficiency (Storck et al., 2015). DIET does not rely on the mediators to transfer electrons or require enzymatic catalysis, which could avoid

the unnecessary energy loss during electron transfer. Besides, electron transfer via DIET is directly to methanogens, avoiding the loss by diffusion.

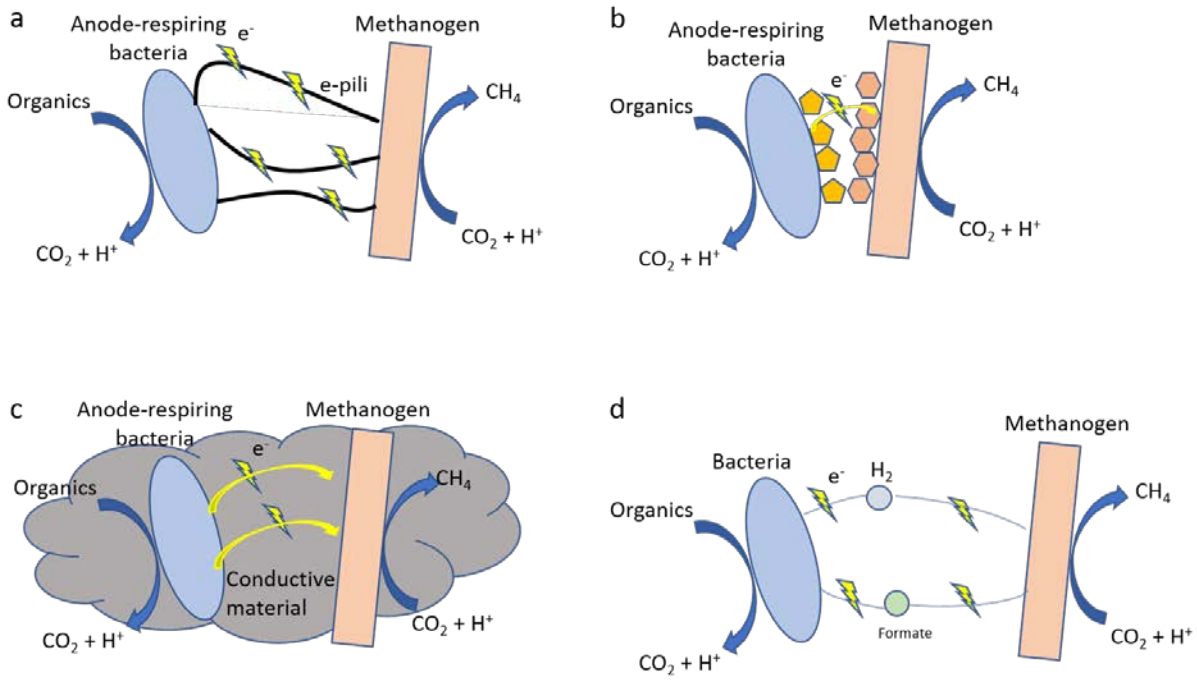

Figure 2-2. Pathways of IET. 2a, electrons transferred via e-pili. 2b, electrons transferred via c-type cytochromes. 2c, electrons transferred via conductive materials. 2d, electrons transferred via mediator like hydrogen molecular.

Rotaru et al. (2014a) studied the metabolism of the aggregates in a defined *Geobacter metallireducens* and *Methanosaeta harundinacea* co-culture by transcriptomics, radiotracer, and genetic analysis. Their results showed that each 1 mol of ethanol produced 1.5 mol of methane, while *G. metallireducens* only converted 1 mol of ethanol into 1 mol of acetate and *M. harundinacea* only converted 1 mol of acetate into 1 mol of methane. This indicated that *M.*

harundinacea not only converted acetate produced from ethanol by *G. metallireducens* into methane, but also utilized the electrons directly transferred from *G. metallireducens* via conductive pili (Reguera et al., 2005; Summers et al., 2010; Malvankar et al., 2011; Rotaru et al., 2014a). This was the first direct proof that methanogenic archaea could participate DIET.

G. metallireducens and *Methanosarcina barkeri* was also proved to produce methane through DIET in a pure co-culture system (Rotaru et al., 2014b). In addition to conductive pili (e-pili), direct electron transfer between syntrophic microorganisms is also possible via cytochrome c. For example, *Geobacter sulfurreducens* can transfer electrons from ethanol oxidation to *G. metallireducens* via cytochrome c during the mutualistic oxidation of ethanol (Rotaru et al., 2014b). This DIET pathway is also present in syntrophic methanogenesis, where methanogens can produce methane using electrons transferred via cytochrome c located in the outer membrane of syntrophic bacteria (Lovley, 2017) (Figure 2-2).

The methane production via DIET is an electronic syntrophy via current, and conductive minerals can act as electrical conductors during the electron transfer process, which would contribute to enhancement of DIET (Figure 2-2). Studies have shown that the addition of conductive minerals stimulated the growth of *Geobacter* in the syntrophic methanogenic system and promoted methane production (Kato et al., 2010, 2012; Nakamura et al., 2009). Rotaru et a., (2014b) studied the role of granular activated carbon (GAC) in the co-culture system of *G. metallireducens* and *M. barkeri*. When the conductive pili (e-pili) of *G. metallireducens* were knocked out, no methane was produced. The addition of GAC resulted in syntrophic methanogenesis, indicating that GAC played a role similar to e-pili in DIET. Li et al. (2015c) found that the addition of nano-Fe_3O_4 into paddy soil would significantly promote the syntrophic butyrate-oxidizing methanogenesis. The improvement then disappeared when nano-Fe_3O_4 was

insulated by SiO_2 wrapping, which also showed for the first time that DIET may exist within syntrophic methanogenesis in natural systems. Ye et al. (2017) found that red mud (mainly hematite) could promote methanogenesis from anaerobic digestion of waste activated sludge. This may be due to the fact that the addition of red mud would facilitate the hydrolysis and acidification of organic matter, increase the activity of key enzymes, enhance the electrical conductivity of the whole reaction system, and promote the DIET between syntrophic bacteria (*Geobacteraceae*) and methanogens (genera *Methanosaeta* and *Methanosarcina*).

Studies have shown that high conductive materials, including carbon-based materials (GAC, biochar, carbon cloth, etc.) and iron-based materials (conductive iron oxides, zero-valent iron, etc.), were able to promote DIET in the engineered AD systems. The addition of different types of conductive materials will affect the enhancement of methane production of AD systems. Kaur et al (2020) found that the addition of biochar to wheat straw would increase the methane yield by 24% (compared to no biochar addition). The addition of biochar promoted the degradation of propionic acid and LCFAs and increased the yield of acetic acid and butyric acid. Chowdhury et al. (2019) compared the effects of adding GAC and magnetite in AD for FW and confirmed that the addition of GAC could significantly shorten the lab phase of AD process, relieve the accumulation of VFAs and increase the methane yield by 50%-80%, as compared to the control and magnetite added systems. The GAC added AD system also showed the highest degradation rate for complex compounds and was selectively enriched with a large number of syntrophic β-oxidizing bacteria (*Syntrophomona*s) for LCFAs and methanogens. Liang et al (2021) concluded that the AD system with the addition of zero-valent iron had the highest amount of cumulative methane yield (394 mL/gVS) compared to those with magnetite and biochar addition, which suggested that zero-valent iron would be the preferred conductive

material candidate to improve the performance and stability of the AD system. Zero-valent iron would significantly enhance the release of soluble organics from substrate, of which proteins and humic acids contain amide groups and cytochromes (electron shuttles) that would contribute to the enhanced DIET between syntrophic microorganisms. Other studies reported that graphite could be used as a conductive material for enrichment of DIET bacteria in AD system, but showed less effective in enhancing the methane yield of the AD system (7.5%-20%) (Muratçobanoğlu et al., 2020; Zhao et al., 2016). Addition of graphite can effectively enrich the DIET participant Methanosaeta and improved interspecies H_2 transfer. It also found that DIET between *Geobacter* sp. and *Methanosaeta/Methanosarcina* would improve the syntrophic degradation of propionic and butyric acid. Therefore, GAC and zero-valent iron may be the better conductive materials to improve the methane production of AD system.

A lot of studies have been done since the discovery of DIET. Besides acetate, other organics such as propionic, butyric, and benzoic acid have also been investigated for their syntrophic DIET mechanisms (Cruz et al., 2014; Li et al., 2015; Zhao et al., 2016b; Zhuang et al., 2015). However, most of the reports focused on syntrophy in lab-scale, engineered systems and only a few studies have been conducted on natural systems. Considering the widespread of conductive materials like iron or iron oxides in ecosystems, potential DIET may occur on a large scale and have important implications for the development of efficient bioenergy sources.

The methanogens that have been confirmed to be able to produce methane via DIET are mainly *Methanosarcina* and *Methanosaeta*, while other species need to be further isolated and identified. The major bacteria that have been found to be capable of syntrophic cooperation with methanogen via DIET include genera *Geobacter*, *Pseudomonas*, *Syntrophomonadaceae*, *Syntrophomonas*, *Sulfurospirillum*, *Tepidoanaerobacter*, *Coprothermobacter*, *Thauera*,

Clostridium, *Bacteroides*, *Streptococcus*, *Sporanaerobacter*, and species in the family Peptococcaceae and Bacillaceae, and more species are still required to be discovered and identified (Dang et al., 2016; Hu et al., 2017; Jing et al., 2016; Lei et al., 2016; Li et al., 2015c; Lin et al., 2017; Yamada et al., 2014; Zhang & Lu, 2016). In addition, the mechanism by which methanogens accept extracellular biotic and abiotic-supplied electrons lacks understanding in detail. Lack of engineering practice of DIET on AD also limits the application of DIET. Current understanding and experience of DIET based on addition of conductive materials needs to be extended to other complex substrates. An efficient anaerobic reactor suitable for long-term operation without interaction with conductive materials has not yet been developed, and the reactor should meet the requirements of retention of enough conductive materials and adequate contact with microorganisms capable of DIET. Long-term operation and observation on the impacts of DIET on the stability and efficiency of AD system are also needed in order to improve the recovery and economic efficiency of the addition of conductive materials for engineering in practice.

2.3.2 DIET during bioelectrochemical methane production

DIET has been applied to bioelectrochemical synthesis in MECs. On the anode, current is produced by electron transfer from a special group of microorganisms (ARB) to the anode. And on the cathode, electron is captured by microbes to produce valuable biochemical product (Choi et al., 2016). The electrodes can act as either electron donor or acceptor in the microbial energy metabolisms. The unique cytochromes, e-pili and other appendages of microorganisms allow them to connect and associate with the electrode surface (Pirbadian et al., 2014; Reguera et al., 2005; Summers et al., 2010; Tremblay et al., 2011; Vargas et al., 2013).

Cheng et al. (2009) first discovered that microorganisms in a bioelectrochemical system (BES) could directly absorb electrons from the cathode surface to reduce CO_2 for methane production, which later was described as "electromethanogenesis" or bioelectrochemical methane production. Methanogenic biofilm (methanogenic biocathodes) was formed on the cathode of the BES after inoculation. The biocathode in the BES system could produce H_2 under certain conditions (Cheng et al., 2007). Hara et al. (2013) found that methanogens can use the H_2 produced by the cathode to reduce CO_2 for methane production. Villano et al. (2010) proved that when the cathode potential in the BES was below -650 mV, methane would be produced through a combination of H_2 reduction of CO_2 and direct absorption of cathode electrons; when the potential was above -650 mV, the yield of H_2 was too low and methane could only be produced through direct absorption of cathode electrons. It is worth noting that many microorganisms containing hydrogenases are also able to produce hydrogen by direct acceptance of electrons from the electrode (Aulenta et al., 2008; Rozendal et al., 2008). Therefore, methane may also be produced by electroactive hydrogen-producing bacteria and hydrogenotrophic methanogens through interspecies hydrogen transfer. Costa et al. (2013) knocked out genes encoding hydrogenase in hydrogenotrophic methanogen and found that this type of methanogen could still grow under conditions where H_2 was not provided. Deutzmann et al. (2015) found that the extracellular enzymes secreted by the cells could mimic the DET mechanism of *M. maripaludis* and directly accept electrons from the cathode for bioelectrochemical methane production, whereas this result did not exclude the possibility of which methanogen could directly accept electrons from the cathode. Lohner et al. (2014) found evidence which excluded the possibility of methanogen using H_2 directly by knocking out genes encoding dehydrogenases in *Methanococcus maripaludis*. Removing the suspended cells in the cathodic chamber also did not

change the methane production rate, suggesting that most of the methanogenesis would be linked to the electrodes, which further confirmed the direct acceptance of cathodic electrons by methanogen for methane production.

At present, studies on the mechanism of electron transfer in bioelectrochemical methane production have focused on hydrogenotrophic methanogen. The mechanisms of electron transfer with the biocathode can be seen in Figure 2-3. First, the bioelectrochemical methane production can be based on the direct electron acceptance from cathode and methanogens would accept cathodic electrons for CO_2 reduction through cytochrome c and other redox factors located on the outer cellular membrane to (Haloua et al., 2015; Reda et al., 2008; Reguera et al., 2005). Bioelectrochemical methane production could also take place by using mediators like hydrogen produced either through electrolysis or by hydrogen-producing bacteria (Garcia et al., 2000; Haloua et al., 2015; Lojou et al., 2002; Tatsumi et al., 1999), or by acetate produced by acetate-producing bacteria (homoacetogens) (Kato et al., 2015; LaBelle et al., 2014; Marshall et al., 2012, 2013; Nevin et al., 2010, 2011; Patil et al., 2015; Rago et al., 2015; Spirito et al., 2014), or by soluble electron carriers including flavins and quinones secreted by microbes or already existed in the system (Angenent et al., 2004; Coursolle et al., 2010; Freguia et al., 2009; Pham et al., 2008; Reguera et al., 2006; Stams et al., 2006). In addition, IET through e-pili, electron carries, or cytochromes can be another route for electron exchange or electric syntrophy (Bond & Lovley, 2003; Bretschger et al., 2007; Cheng & Call, 2016; Gorby et al., 2006; Kato, 2015; Kouzuma et al., 2015; Meitl et al., 2009).

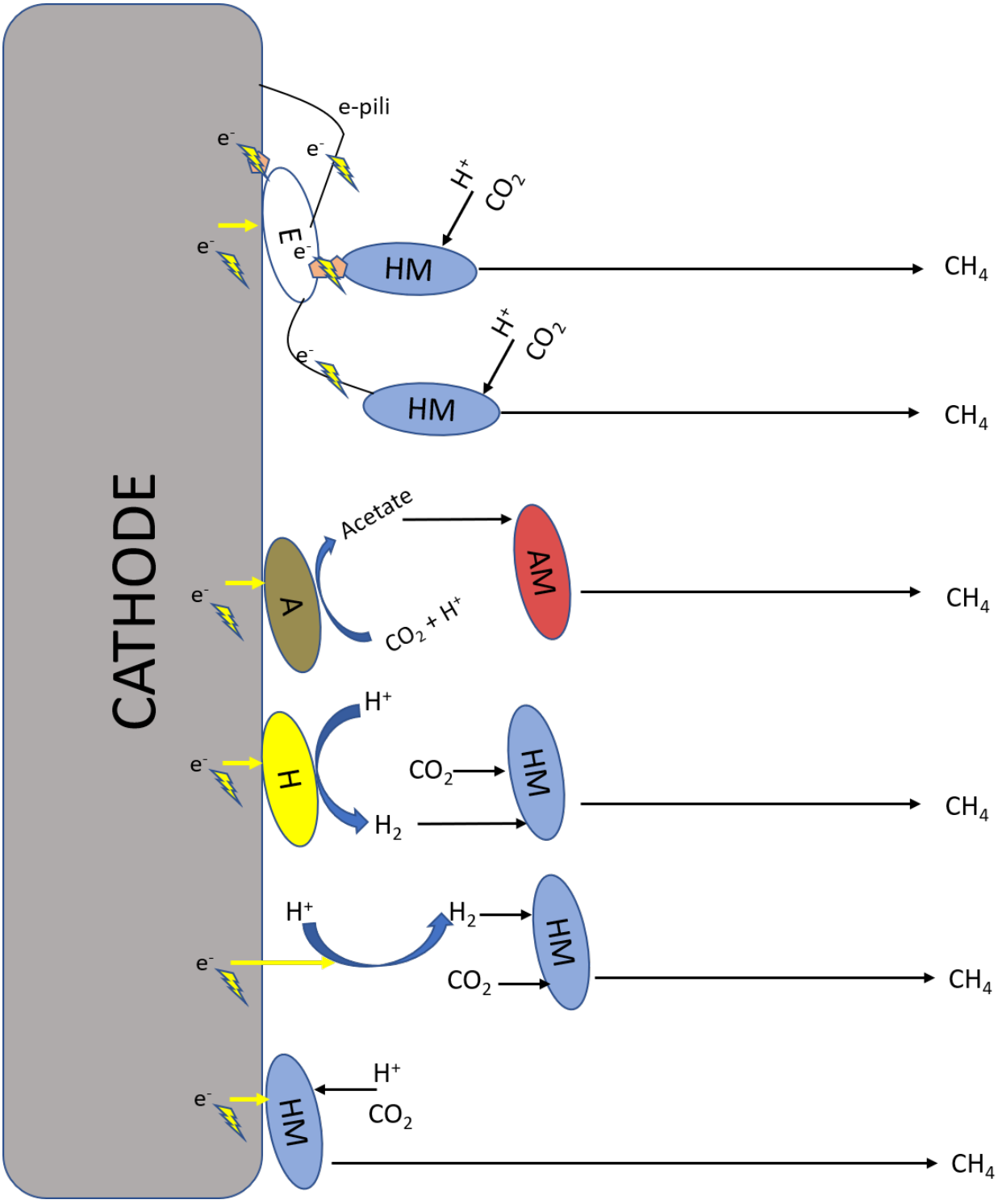

Figure 2-3. Possible mechanisms of electron transfer on biocathode. HM: hydrogenotrophic methanogen. H: hydrogen-producing bacteria. A: acetogen. AM: acetoclastic methanogen. E: electron delivering bacteria.

2.4 Microbial community in the MEC-AD systems

The microbial community on the electrode surface, in suspended liquid or in sludge would determine the EET and DIET pathways and performance of methane production in MEC-AD systems. The structure of the microbial community can be regulated and altered by different factors such as selecting different inoculum sources, pretreatment methods, sources of substrates, and applied voltage.

2.4.1 Bacteria in the MEC-AD systems

A variety of bacteria involved in hydrolysis, acidogenesis, and acetogenesis were found to be significantly increased in the anode biofilm and suspended liquid in the MEC-AD system. The enrichment of hydrolytic bacteria including Acetivibrio, Bacteroides, Cellulomonas, Firmicutes, and Olsenella under applied voltage would accelerate the hydrolysis rate of complex organics and facilitate the following steps of AD (Chen et al., 2016; Feng et al., 2016; Guo et al., 2015; Jain et al., 2015; Wang et al., 2021; Zakaria and Dhar, 2019; Zhao et al., 2016c; Zhen et al., 2017).

Studies also found syntrophic acetogens which could degrade propionate and butyrate into acetate were enriched in the anode biofilms of MEC-AD systems, including *Syntrophobacter*, *Smithella*, *Syntrophomonas*, and *Syntrophothermus*. Therefore, the acetogenesis of VFAs like propionate and butyrate would be accelerated without the risk of VFA accumulation (Gao et al., 2014; Hari et al., 2016; Leng et al., 2018; Wang et al., 2021; Westerholm et al., 2022; Xu et al., 2020; Zhao et al., 2016c).

In addition, anode-respiring bacteria or exoelectrogens, which can perform EET via e-pili and c-type cytochromes, were also found to be selectively enriched in anode biofilm (Hari et a., 2017). Some studies suggested that anode bacteria were dominated by *Geobacter* sp., indicating that *Geobacter* sp. is essential for maintaining the function of anode biofilm. Other researches have detected more than 90 different exoelectrogens, including common ARB of *Geobacter* and *Shewanella*, and bacteria of *Clostridium*, *Bacillus*, *Trichococcus*, and more (Pentassuglia et al., 2018).

Therefore, the enriched hydrolytic bacteria, acetogens, and ARB in the anode biofilm would form a network in which soluble organics including VFAs would be degraded and electrons would be transferred to the anode (Chen et al., 2016; Kato et al., 2015; Kouzuma et al., 2015). As a result, the hydrolysis and acetogenesis would be accelerated and methanogenesis would further be improved.

2.4.2 Archaea in the MEC-AD systems

The bioelectrochemical methane production in MEC-AD mainly occurred on biocathode. (Blasco-G´omez et al., 2017). The structure of the cathode microbial community would directly affect the DIET pathway and methanogenic rate on the biocathodes (Cheng et al., 2009). Studies found that the bioelectrochemical methane production can either through DIET with hydrogenotrophic methanogen by reduction of CO_2 with the electrons accepted from cathode, or by using the hydrogen molecules produced on the cathode for CO_2 reduction (Blasco-G´omez et al., 2017; Wang et al., 2021; Zhao et al., 2021).

It has been found that hydrogenotrophic methanogens, including *Methanobacterium*, *Methanocorpusculum*, and *Methanospirillum*, were dominated in the biocathode community in MEC-AD systems (Cheng et al., 2009; Lin et al., 2019; Liu et al., 2016; Park et al., 2018; Tian et al., 2018; Wang et al., 2021a, b). *Methanosarcina* capable of utilizing both acetate dismutation and CO_2 reduction pathways was also detected in the cathode biofilm (Lee et al., 2017; Park et al., 2018). In addition, the accumulation of VFAs as important intermediates of acidogenesis during AD process would enrich acid-producing bacteria such as *Clostridium* dominated in the cathode biofilm of the MEC-AD system and further promote the enrichment of hydrogenotrophic methanogens (Liu et al., 2016b). The enrichment of hydrogenotrophic methanogens on biocathode would further decrease the hydrogen partial pressure in the system and hence improve the acetogenesis of AD process.

In addition, the major genera of Archaea in the anode biofilm of MEC-AD system were generally dominated by *Methanobacterium* and *Methanocorpusculum* (Cheng et al., 2009; Hari et al., 2017; Liu et al., 2016b). Liu et al. (2016b) also found that *Methanosaeta* would be enriched in anodic biofilm when acidogenesis was improved in the MEC-AD system, which would provide more acetate as substrate for the selective enrichment of *Methanosaeta* in anode biofilm. *Methanosaeta* was also found to accept electrons directly from ARB (*Geobacter*) through e-pili for methanogenesis (Holmes et al., 2017; Zhao et al., 2016c).

2.5 Tools for detection of DIET

Many studies have claimed to discover DIET in the microbial consortium so far, which was highlighted as a main reason to improve methane production in the anaerobic digestor.

Theoretical calculation indicated that DIET would make electron-donating half reactions thermodynamically favorable. But the real energy gain between microbes which participate DIET may still be hard to determine directly, because the interspecies redox potential during electron transfer was unclear (Cheng & Call, 2016). Further, direct proof of DIET should also come from direct detection or observation of electron flow (current) between syntrophic microorganisms (i.e., between ARB and methanogens), together with the enhanced methane production detected in the system, but this type of evidence remains scarce (Wang & Lee, 2021). Only indirect evidence to confirm the occurrence of DIET was provided for most of the situations, or mechanisms other than DIET can explain the performance in some cases (Steendam et al., 2019; Wang et al., 2018a, b). Therefore, to expand our knowledge of DIET and to evaluate the potential application of DIET in natural and engineered systems, current methods of detection and characterization of DIET are summarized and discussed below.

Recent methods used for detecting and characterizing DIET in defined cultures and natural or engineered systems can be classified into these groups. The first group of methods focuses on the detection of specific DIET related species, genes, transcripts, or proteins. The development and application of genetic and meta-omic technology provides the opportunity to identify whether DIET takes place in the objective systems or not. However, the detection of those specific species or genes may not exclude the possibility other than DIET in the system. The absence of some specific species or DIET linked genes may not completely imply the absence of DIET itself. Complementary tests are required to better support the detection of DIET by using this group of methods.

Methods from bioinformatics such as network analysis may provide more information on the interaction between nucleic acids, proteins, and other biomolecules of different cells and

microorganisms (Eisenberg et al., 2000). Graph theory from mathematics together with computer tools has been applied to describe and predict different systems such as protein interaction maps, functional association networks, and signal transduction pathways (Balazasi et al., 2005; Sharan et al., 2007; Huang et al., 2008). Studies based on network analysis have been applied in finding those kinless hubs which have shown highly connected within and between different clusters (i.e., the microorganisms or genes participated in AD), therefore from the theoretical point of view reveal the potential genes or proteins which participate in DIET (Shi et al., 2020; Feng et al., 2017).

The second group of method focused on visualization of cellular components associated with DIET, including pili, cytochromes, redox mediators, and spatial distributions of cells participated in DIET. Visualization of conductive pili and cytochromes may provide valuable evidence to confirm the existence of DIET as they can establish electrical connection with neighboring cells. However, most of these methods can only provide qualitative results (Ha et al., 2017; McGlynn et al., 2015). Cellular spatial distributions via SEM, TEM, and FISH could identify DIET syntrophic partners in the samples and discover how closely cells are positioned to each other and how they are attached together, which may provide correlation between DIET and interspecies cellular distance (Cruz et al., 2014; Liu et al., 2012a; McGlynn et al., 2015; Xu et al., 2016;).

Studies have also found that extracellular polymeric substances (EPS) could be engaged in interspecies electron transfer, with some of the humic- or protein-like substances acting as electron carriers (Ding et al., 2015; Mostafa et al., 2020; Yang et al., 2020; Zhuang et al., 2020). Studies also found the addition of carbon-based conductive materials would increase the EPS amounts as well as the c-type cytochromes components, heme c (Wang et al., 2019, 2020d). The

increase in heme c indicated the enrichment of active microbes which could participate DIET. Therefore, detecting and quantification of those substances in the system may become an index for the indirect evidence of DIET.

DIET via c-type cytochromes requires direct contact of microbial cells. Therefore, formation of microbial aggregates would increase the possibility of cell contact and may further enhance the DIET. Addition of carbon-based conductive materials would enhance the formation of microbial aggregates, sometimes also with the increase in EPS correlated with the enhanced aggregation, which suggested that the microbial aggregates could also be used to qualitatively evaluate the DIET (Wang et al., 2020d; Zhu et al., 2018; Zhuang et al., 2020a, b). Combined with imaging technologies like confocal laser scanning microscopy (CLSM), FISH, and SEM, close association of DIET related microorganisms could be identified in those microbial aggregates (Viggi et al., 2017; Xia et al., 2019).

The third group assesses the methanogenic metabolisms by substrate assays, carbon isotope labeling, and inhibition tests (Wang et al., 2018; Rotaru et al., 2014a, b). These methods are usually performed in batch experiments to evaluate specific metabolic activities related to methanogenesis pathways and are combined with other groups of methods to support the occurrence of DIET in the systems (Seib et al., 2016; Wang et al., 2018). The DIET effect on AD reactions was believed to be mainly associated with the hydrogenotrophic methanogenesis (Baek et al., 2018). Therefore, DIET establishment may be reflected by the enrichment of hydrogenotrophic methanogen and methanogenesis pathways could also be affected by the enhanced DIET.

Some studies have shown that addition of conductive materials would promote hydrogenotrophic methanogenesis, enrich hydrogenotrophic methanogen, and hence enhance AD

performance (Park et al., 2018; Ren et al., 2020; Xie et al., 2020). The shift of methanogenesis pathway may be a useful index for DIET existence. Some studies have also revealed that acetoclastic methanogenesis could be promoted via DIET, with or without the enhancement of hydrogenotrophic methanogenesis. Isotope labeling and inhibitor tests together proved that he addition of carbon-based conductive material could enhance the acetoclastic methanogenesis more than hydrogenotrophic methanogenesis, which suggested possible indirect interspecies electron transfer pathways in the AD system (Lim et al., 2020; Lu et al., 2020; Xiao et al., 2019, 2020). Therefore, the metabolic experiments may provide another way for detecting and discovering possible interspecies electron transfer mechanisms in AD system.

The fourth group of methods focuses on electrochemical characterization, including cyclic voltammetry and conductivity measurement. Those technologies often require to transfer biomass from systems to a bioelectrochemical cell to form biofilms on the electrode and such growth may result in a shift in microbial community structure and may not be similar to the biomass in the system observed. Recent works have reported electrically conductive properties of methanogenic aggregates which may support the existence of direct interspecies electron transfer by electrical conduction. The measurement of the electrical conductivity of the methanogenic aggregates or biofilms ranged from 0.8 ~ 36.7 μS/cm (Barua et al., 2018; Lei et al., 2016; Li et al., 2018; Morita et al., 2011; Shrestha et al., 2014; Wang et al., 2018a & b; Yin et al., 2018; Zhao et al., 2016a, 2018; Zhao & Zhang, 2019). However, these electrical conductivities are several orders of magnitude lower than those found for *Geobacter*-enriched biofilms (Dhar et al., 2016, 2017; Malvankar et al., 2011). In fact, these small values are within error bars of biofilm conductivity for *Geobacter*-enriched biofilms. Such small electrical conductivities of the aggregates/biofilms itself was a question, if they were truly electrically conductive to promote

DET. Moreover, such small biofilm conductivity was measured with nonstandard methods that lower down their reliability. However, it does mean that the increase in conductivity of biofilm may be admitted as hard evidence for DIET, though more concrete evidence from other methods to support the occurrence of DIET will be required (Barua et al., 2018; Li et al., 2017a, 2018a). Therefore, to improve the reliability and accuracy of biofilm conductivity measurement would be a key aspect in the thesis.

Chapter 3 - Enhanced dry digestion of food waste in an anaerobic leachate bed reactor (LBR)

3.1 Introduction

Food waste (FW) represents a large proportion of organic solid waste which has become an important economic and environmental issue and gained more and more attention in recent years. The need for clean, renewable energy generation technologies for zero waste management around the world has led to increased interest in development of waste-to-energy technologies (Li et al., 2018b; Voelklein et al., 2016; Zhang et al., 2022). Anaerobic digestion (AD) can reduce, stabilize and recovery resources from organic solid waste like agricultural and food waste and convert it into energy materials such as methane and hydrogen, and the digestate can be used as fertilizer or soil conditioner (Jang et al., 2016; Rico et al., 2015). Although the high biodegradable content in FW made rapid hydrolysis feasible for AD process, the large accumulation of short-chain fatty acids or volatile fatty acids (VFAs) would cause acidification in the AD system and result in instability or even system collapse. Further, conventional wet AD requires large volumes of water when treating high solid feed stocks like FW and the energy input for mixing is also large, which would technically and economically affect the application of AD (Fierro et al., 2014).

Dry AD like leach bed reactor (LBR) technology is a promising alternative AD process for the treatment of organic wastes with high solid content (total solid > 20%) like FW and municipal solid waste (Guendouz et al., 2010). The lack of internal mixing for dry AD would therefore reduce the energy input compared to conventional wet AD. The reduced water demand

and higher organic loading rate potential for dry AD would make this technology feasible for high solid content treatment (Shahriari et al., 2012). Multi-stage AD system can separate the process of hydrolysis and methanogenesis spatially, which would provide optimal parameters for different microorganisms (Bochmann and Montgomery, 2013). For example, bacteria for hydrolysis and acidogenesis would prefer pH around between 4 and 6.5 and a shorter retention time, at which the two steps would be optimized (Kim et al., 2003; Yu and Fang, 2002). For methanogens, a neutral pH with longer hydraulic retention time (HRT) is required, compared to the hydrolysis stage. Therefore, to apply one single LBR system to complete dry AD for FW must consider those different optimal parameter ranges for different functional microorganisms.

Leachate recirculation is a common operation in dry AD in order to compensate the reduced water content and lack of mixing in the system and increase the contact between microorganisms and solid feedstocks (Wilson et al., 2016). Leachate recirculation could also maintain the functional anaerobic microbial communities in the system (Dearman and Bentham, 2007; Xu et al., 2014). However, leachate recirculation may also accumulate potential inhibitors such as salinity and ammonia in the system, which would affect the methane production in dry AD systems (Chen et al., 2008; Rocamora et al., 2020; Wilson et al., 2016). Therefore, optimal operational practice, including acclimation of inoculum and recirculation strategies, needs to be developed in order to maintain desirable microbial communities in the reactor with the existence potential inhibitors (Rico et al., 2015; Wilson et al., 2016). Table 3-1 summaries the parameters and performance of the FW and other organic waste dry AD from literature.

Table 3-1. Summary of the parameter and performance of FW AD experiments from literature.

Substrate	Reactor type	ISR (%)	HRT (d)	OLR (gVS/L·d)	Recirculation strategy	VS removal (%)	Specific methane yield ($mLCH_4/gVS$)	Reference
Food waste (FW)	Two-stage CSTR	NA	4d (hydrolysis CSTR) 12d (methanogenic CSTR)	6-15 (hydrolysis CSTR); 2-5 (methanogenic CSTR)	NA	NA	371-419	Voelklein et al., 2016
FW	Two-stage; LBR+UASB	NA	18-30d (UASB)	7.1-11.8 (COD based)	0.708 - 4.25 L/hr	51.5-87.5	209-384	Browne & Murphy, 2014
FW	Two-stage; LBR+fixed film reactor	0-60%	16d (LBR)	~1 (COD based)	1.2 L/hr	69.5-73.0	195-260	Wilson et al., 2016
FW	Two-stage; LBR+UASB	~10%	17d (LBR)	4.28 (COD based)	0.016 L/hr	49.7-71.7	180-250	Xu et al., 2011
FW + digested biosolids	LBR	NA	73d	1.3	NA	NA	214-229	Dearman & Bentham, 2007
FW	Single stage; Batch reactor	20-62.5%	25d	0.26-0.8	NA	48.7-93.6	245-518	Liu et al., 2009
FW + Landfill leachate	Single stage; Batch reactor	NA	35d	1.19	NA	NA	369-466	Liao et al., 2014
FW + WAS	Single stage; CSTR	20%	5-30d	2.76-16.2	NA	NA	234-350	Li et al., 2017d

Manure	Solid phase batch AD reactor	60-150%	60d	0.53	0.42-1.25 L/hr	NA	214-227	Rico et al., 2015
Manure	Solid-state AD reactor	50%	50d	NA	0, 1, 2, 4 times per day	NA	120-241	Pezzolla et al., 2017
FW	Single Stage CSTR	47%	8d	4-12	NA	NA	423-535	Chen et al., 2015
FW	Single stage; LBR	10-60%	10d	2.5~2.88	0.3-7.5 L/hr	60.9-76.8%	104-350	This study

The aims of this study were: 1) to investigate the optimal operation conditions of the dry digestion for FW in a leach bed reactor (LBR) system, which would further help understand and improve the operation of bioelectrochemical leach bed reactor (BLBR) system for food waste (FW) dry digestion, and 2) to improve the understanding of the microbial communities in the single-stage, LBR system. A laboratory-scale, single-stage LBR system for FW dry digestion was developed and operated. The impact(s) of operational conditions, including acclimation of inoculum and inoculum to substrate ratio (ISR), were investigated by analyzing and comparing the performance of FW dry digestion in the LBR system. In addition, the effect of different recirculation rates was compared and evaluated in the LBR system for FW dry digestion under the same ISR. Microbial community structures of the leachate and FW was analyzed and compared to track potential community shift after the operation of LBR. Results obtained from these experiments would be the foundation for the operation of BLBR in the next chapters.

3.2 Materials and Methods

3.2.1 Food waste and inoculum collection

FW was collected from a cafeteria at University of Waterloo (Waterloo, Ontario, Canada). After collection, non-biodegradable materials such as bones and egg shells were manually sorted and removed. The sorted FW consisted of vegetables, fruits, and other carbohydrate-rich foods, such as potatoes, bread, etc. Sorted FW were chopped into approximately 1-cm cubes. The chopped FW was then homogenized and stored immediately at -20°C in airtight bags to avoid any deterioration. The FW was thawed at 4°C for 24 hours prior to the experiments. (Swakshar & Lee, 2020; Xiong et al., 2019).

Original AD sludge was collected from the anaerobic digestor of Galt Wastewater Treatment Plant (Cambridge, Ontario, Canada). The sludge was then filtered by mesh to remove large particles prior to experiments.

3.2.2 Reactor configuration

Cylindrical LBRs were made of acrylic glass with an inner diameter of 14 cm and a height of 70 cm and the total volume was 10 L. The reactor body had a removable top cover with a gas outlet and a sprinkling system to spray leachate on FW, a basket sitting in the upper half of the reactor to hold FW, and the lower half as the leachate holding bed (Figure 3-1). The acrylic glass FW basket had an inner diameter of 10 cm and a height of 25 cm, with holes of 5 mm size on its bottom which allowed leachate to percolate through and prevent FW chops from falling into the leachate holding bed. The leachate in the holding bed was recirculated by a digital peristaltic pump (Masterflex L/S Digital Drive, Model no. 07523-80, USA). The leachate in the holding bed was also mixed internally at 60 L/hr using a peristaltic pump (Masterflex L/S Economy Drive, Model no. 07554-90, USA).

The LBR was operated at 35°C, which was kept for mesophilic condition by recirculating heated water from a water heater controller (PolyScience 9702A11C 13-liter Advanced Digital Controller, PolyScience, United States) via PVC tubing tied around the reactor body. A pH controller (Milwaukee, MC-122 pH meter) was coupled to an in-situ pH probe and a pump injecting potassium bicarbonate solution to keep neutral pH and provide alkalinity in the leachate. A gas counter (MilliGas counter, Ritter Apparatus, Bochum, Germany) was connected to the gas outlet line from the top cover of the LBR to record biogas production. Leachate

samples were taken from the mixing line, while biogas samples were taken from the gas outlet line for routine analysis.

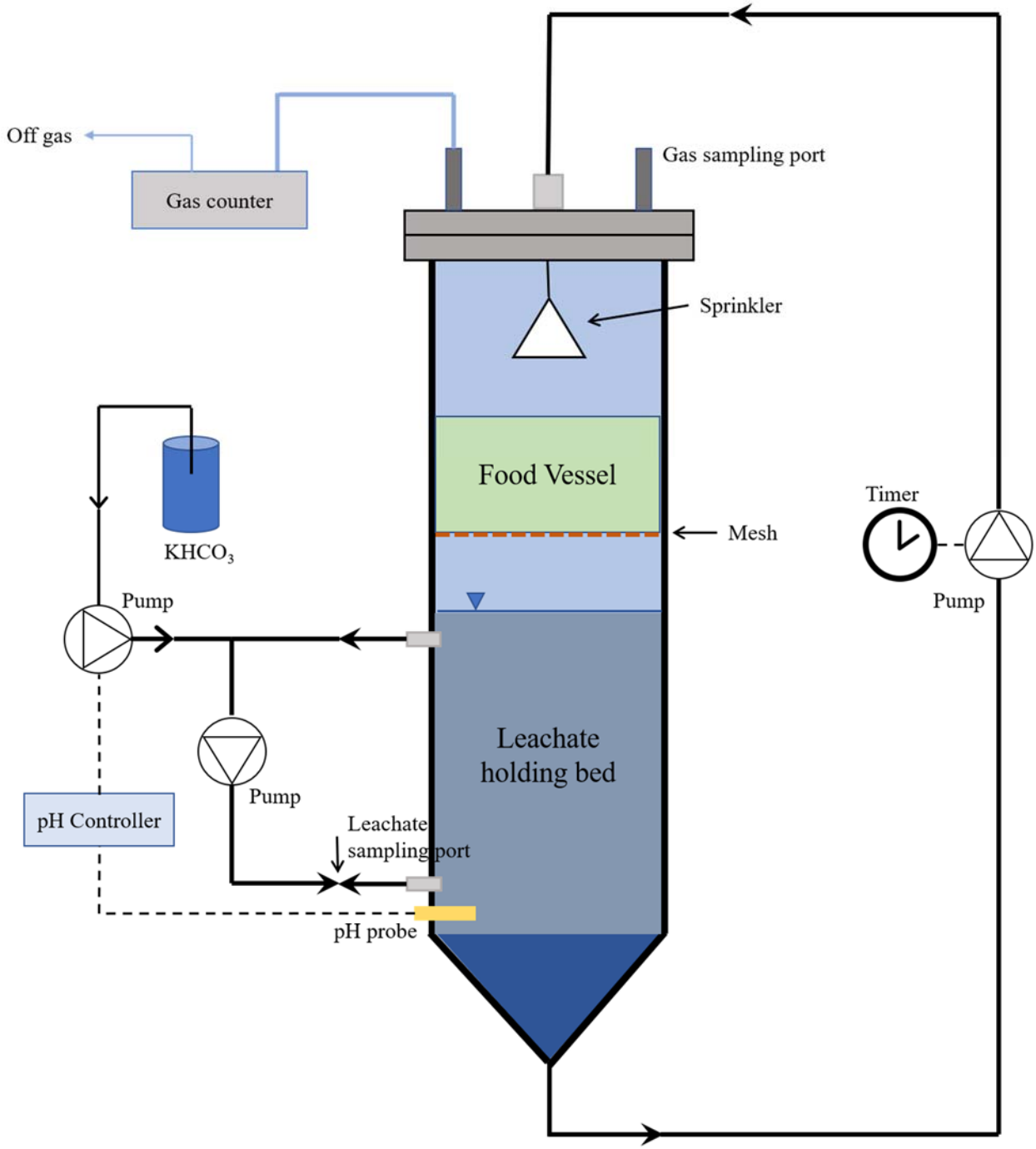

Figure 3-1. Schematic of LBR.

3.2.3 Acclimation of inoculum for LBR

To acclimate a microbial inoculum for the LBR, AD sludge from WWTP was incubated at 35 ℃ in a 4-liter CSTR and fed with FW slurry which was made by a food processor for 3 weeks. The reactor was fed with FW slurry at an organic loading rate (OLR) of 2 g-COD/L·day and a SRT of 30 days. After 3 weeks, the sludge was added to the LBR as inoculum for subsequent experiments. AD sludge without acclimation was also added to a parallel LBR as comparison to evaluate the impact of acclimation on LBR performance.

3.2.4 Reactor operation

(1) Effects of ISR on LBR performance

To evaluate the impacts of inoculum to substrate ratio (ISR) on LBR performance and FW dry digestion, LBRs were fed with acclimated inoculum starting from 10% by VS (10%, 25%, 40%, and 60%) (Table 3-1). To meet a desired ISR value, a certain amount of acclimated AD sludge was added to the LBR diluted with deionized water, and the initial sludge volume was fixed at 2.5 L. A leachate recirculation pump was programmed to be turned on for 15 seconds at every 75 min to sprinkle the leachate on the top of the FW at a rate of 90 L/hr, which corresponded to a leachate recirculation rate of 0.3 L/hr or 7.2 L/day. The initial VS of FW was fixed at about 72 g for all experiments. Before the start of each batch of experiments, the LBR was sparged with N_2 to create anaerobic condition at a flow rate of 0.5 L/min for 30 min. After each batch, the leachate was centrifuged at 9,500 rpm for 20 min and the centrifuged solids were collected as inoculum in the next batch, which would allow enrichment of acclimated microorganisms in the reactor. LBRs were operated for three consecutive batches for each ISR.

Each batch of LBR dry digestion lasted for 10 days. First, the short batch operation period in the LBR was chosen to evaluate the distinctive effects of EET and DIET on FW dry digestion in a bioelectrochemical LBR against the LBR in next chapters. Second, under such short reaction time, the influence of operational changes (i.e., ISR and recirculation rate) on solid reduction and methane production can be assessed well in the LBR. Finally, the feasibility of compact FW dry digestion can be tested by optimizing operating parameters.

Table 3-2. Details of the experiments.

Group	ISR (VS based)	VS of FW (g)	Recirculation Strategy	Recirculation rate (L/hr)
10%	10%	72	Pump at 90 L/hr for 15 seconds every 75 minutes	0.3
25%	25%	72	Pump at 90 L/hr for 15 seconds every 75 minutes	0.3
40%	40%	72	Pump at 90 L/hr for 15 seconds every 75 minutes	0.3
60%	60%	72	Pump at 90 L/hr for 15 seconds every 75 minutes	0.3
R1	25%	72	Pump at 90 L/hr for 15 seconds every 15 minutes	1.5
R2	25%	72	Pump at 90 L/hr for 15 seconds every 3 minutes	7.5

(2) Effects of recirculation strength

To evaluate the impacts of recirculation strength on LBR performance of FW dry digestion, the leachate recirculation pump was programmed to be turned on for 15 seconds at every 3, 15, and 75 minutes to sprinkle the leachate on the top of the FW at a rate of 90 L/hr, which corresponded to leachate recirculation rates of 7.5, 1.5, and 0.3 L/hr or 180, 36, 7.2 L/day, respectively. The ISR was fixed at 25% with an initial VS of FW of 72 g. For each recirculation strength, LBRs were operated for 3 batches, respectively (Table 3-1).

3.2.5 Chemical analysis

Total solids (TS), volatile solids (VS), total suspended solids (TSS), and total volatile solids (VSS) were quantified according to the Standard methods (APHA, AWWA & WEF, 2005). TS and VS of FW were analyzed at the beginning and end of the experiments to determine solid reduction. TCOD, SCOD, volatile fatty acids (VFAs), ammonia nitrogen, pH and alkalinity of leachate were analyzed at Day 0, 2, 4, 7, and 10 during the experiments. COD were analyzed by Hach COD digestion vials (Cat. No. 2125915-CA). Ammonia nitrogen was determined by Hach test kits (TNT832).

Volatile fatty acids (VFAs) were analyzed by GC-FID according to Swakshar & Lee (2020). In brief, leachate samples were filtered through 0.2 μm membrane filters (Whatman, 6751-2502, USA) and were analyzed using a GC (HP 5890 Series II, Hewlett Packard, USA) equipped with a a capillary column (30 m x 0.53 mm x 0.5μm PAG, Supelco, Bellefonte, PA) and a flame ionization detector (FID). The carrier gas was helium (40 psi) and hydrogen and air were used for ignition. To measure the VFA, the GC-FID was programmed to maintain at the

initial temperature of 150 °C for 2 minutes, then increase to 190 °C at a slope of 4°C/min and maintain at that temperature for 3 minutes. The known VFA standard mixtures (Volatile Free Acid Mix, Certified Reference Material, MilliporeSigma™) were used as calibration standard to calculate concentrations of VFA species. VFA concentrations were reported by normalizing each VFA concentration into equivalent concentration of COD.

Biogas composition were monitored daily using a GC-TCD (model 310, SRI Instrument, 51 USA) according to Hussain et al. (2017). In brief, 0.5 mL of biogas sample was collected using a gastight syringe (model 1005 GASTIGHT syringe, Hamilton, Reno, NV) and injected into the GC-TCD equipped with a Porapak Q 80-100 mesh column (Supelco, Bellefonte, PA). The carried gas was argon for hydrogen analysis and the GC-TCD was programed to maintain an initial temperature of 50°C for 1 minute and then increase to 110 °C in at a rate of 10°C/min and maintain for 1 min. For methane analysis, 1.0 mL of biogas sample was injected to another GC-TCD equipped with a packed column (PorapakQ, 6 ft x 1/8 inches, 80/100 mesh, Agilent Tech., USA) and helium was used as carrier gas. The temperatures of the column oven and detector were 41 °C and 200 °C, respectively.

3.2.6 Sample collection, DNA extraction and sequencing process

Leachate samples at the beginning and end of one batch operation, and FW residue samples after one batch operation were collected and preserved by DNA/RNA Shield™ swab collection tubes (Zymo Research) at -20 ℃ before DNA extraction and sequencing.

DNA was extracted from the solid FW residue samples collected by the cotton swabs or 250 µL of liquid leachate sample preserved in DNA/RNA Shield collection tubes (Zymo

Research, Irvine, CA, USA) by using the DNeasy® PowerSoil® Pro Kit (Qiagen, Valencia, CA, USA) according to the manufacturer's instructions. DNA purity was quantified using Nanodrop (Nano-300, Allsheng, Hangzhou, China), and DNA fragment sizes were checked via 2.0% agarose gel electrophoresis. The extracted DNA samples were stored at -80℃ degrees before sequencing. After DNA extraction, PCR amplification via primers, PCR products purification, libraries construction and sequencing were performed by Macrogen Inc. (Seoul, South Korea). The target V4 hypervariable region of the 16S rRNA genes were amplified using primer sets 515F (5'-GTGYCAGCMGCCGCGGTAA-3') / 806rB (5'-GGACTACNVGGGTWTCTAAT-3') and sequencing were performed using Illumina MiSeq platform. Only one sample of leachate and FW residue at each condition was analyzed due to limited resources.

3.2.7. Bioinformatics and statistical analyses

Bacterial and archaeal taxonomy were confirmed by 16s amplicon sequencing analysis. Based on the Mothur software package v1.45.3 (Schloss et al., 2009), Paired-end reads were merged, contigs were generated and primer and barcode trimming, identification and removal of chimeric sequences and high-quality sequences were clustered into operational taxonomic units at a cutoff of 0.03 after quality filtering (Bae and Yoo, 2022). Reads assigned to non-bacterial and non-archaeal origins, such as chloroplast and mitochondrial genomes, were removed and OTUs were classified using training dataset based on the Silva v132 reference database (Kim et al., 2022). Rarefaction curves and alpha diversities were analyzed using Mothur software (Schloss et al., 2009). The rarefaction curves of the samples were used to confirm the sufficient sequencing depth of the various reactors (Kim et al., 2019). The total read counts per sample

were 37722. Excel was used to determine the overall relative abundance of representative sequences at different taxonomic levels. Bacterial and archaea community structures were analyzed and compared separately. Statistical differences in microbial community structure between reactors were tested using the "vegan" package in the R software v4.2.1 (Oksanen et al., 2019) with analysis of similarities (ANOSIM) with 999 permutations.

3.2.8 Calculation

VS removal efficiencies were calculated according to the following equation Eq. (3-1), according to Xu et al., (2011):

$$VS\ Removal\% = \frac{VS_{initial} - VS_{final}}{VS_{initial}} \times 100\% \qquad \text{Eq. (3-1)}$$

where, $VS_{initial}$ (g) and VS_{final} (g) are the total mass of VS in the LBR system at the beginning and end of operation, which included the VS from FW and leachate.

The conversion efficiency of hydrolysis and acidogenesis of FW dry digestion in LBR were calculated according to Eq. (3-2) and (3-3), respectively.

$$Hydrolysis\ \% = \frac{SCOD_{Final} - SCOD_{Initial} + COD_{CH_4}}{TCOD_{FW-added}} \times 100\% \qquad \text{Eq. (3-2)}$$

$$Acidogenesis\ \% = \frac{COD_{VFA-Final} - COD_{VFA-Initial} + COD_{CH_4}}{TCOD_{FW-added}} \times 100\% \qquad \text{Eq. (3-3)}$$

where, TCOD (gCOD) was the total COD of FW added to the LBR; SCOD (gCOD) were the soluble COD in the leachate; COD_{VFA} (gCOD) was the total VFA in the leachate calculated by the COD; the footnote “Final” and “Initial” indicated the COD value in the leachate at the

beginning and end of the operation, respectively; COD_{CH4} (gCOD) was calculated based on 0.388 LCH_4/gCOD.

3.3 Results and discussion

3.3.1 Impact of acclimated and non-acclimated inocula on LBR performance

To determine whether acclimation affected the performance of LBR dry digestion on FW, both acclimated and non-acclimated inocula were tested in parallel with IRS of 25%. The leachate recirculation rate was set at 0.3 L/hr (as described in section 3.2.4).

LBR operation with acclimated inoculum performed slightly better on VS reduction, compared to non-acclimated inoculum (Table 3-2). However, LBR with acclimated inoculum showed more than 5 times higher specific methane yield than that with non-acclimated inoculum (Table 3-2). Meanwhile, SCOD and VFA concentrations of the final leachate showed that there was high level of SCOD which was not converted to methane during the operation of LBR with non-acclimated inoculum, which indicated a relatively good hydrolysis of FW but poor methanogenesis during operation. Both leachates at the end of operation showed similar pH and sodium ion concentrations, but the leachate from non-acclimated LBR had higher alkalinity, which again suggested that methanogenesis function of the non-acclimated microbial community was inhibited.

It is believed that leachate recirculation would cause accumulation of some inhibitors, including ammonia and salinity which are present in FW (Bai & Chen, 2020; Chen et al., 2008; Shahriari et al., 2012). Inhibition caused by salinity (i.e., > 3000 $mgNa^+/L$) has been demonstrated in different studies (Chen et al., 2008; Wilson et al., 2016). Na^+ level higher than

3000 mg/L was detected in leachate both from LBR with acclimated and non-acclimated inoculum, which may explain the poor performance on methane production during operation. Free ammonia at high concentration is also known to be toxic to microorganisms in the AD systems (Liu and Sung, 2002). The degradation of protein and organic nitrogen compounds would produce ammonium and bicarbonate which contribute to the pH buffer capacity in the leachate (Pereira et al., 2013; Shofie et al., 2015). The elevated ammonia level, VFA accumulation, and pH would have complicated interaction and create a steady, inhibition state during AD process (Angelidaki & Ahring, 1993). Although the ammonia nitrogen level in the leachate from non-acclimated inoculum was 1.06-fold than that from acclimated inoculum, the near-neutral pH determined relatively low free ammonia level in both leachate, which was lower than the reported critical concentration of free ammonia (about 200 mgN/L) and therefore the inhibition caused by free ammonia would be minimal (Liu and Sung, 2002; Bai & Chen, 2020). Other studies also showed that acclimated inoculum had better methane production than non-acclimated inoculum since elevated Na^+ level would inhibit methanogenesis, while hydrolysis and acidogenesis may be improved (Calli et al., 2005; Liu and Sung, 2002; Wilson et al., 2016; Zhao et al., 2017b), especially when inoculum was acclimated to high ammonia and salinity level. The results presented here strongly indicated that acclimation of inoculum could maintain desirable microbial communities which are able to tolerate elevated potential inhibitors in LBRs. Therefore, all LBR experiments presented in the thesis were operated with acclimated inoculum.

Table 3-3. Summary of the LBR with non-acclimated and acclimated inocula for FW dry digestion. (n=3)

Group	Non-acclimated	Acclimated
VS reduction	65.0 ± 4.1%	70.5 ± 3.2%
Specific methane yield (mL-CH_4/gVS-added)	28.9 ± 2.1	146.0 ± 4.7
Ammonia-nitrogen (mgN/L)	903 ± 60.1	850 ± 33.1
pH	7.6 ± 0.1	7.7 ± 0.1
Na^+ (mg/L)	4750 ± 177	3810 ± 120
SCOD (gCOD/L)	25.3 ± 2.4	10.3 ± 1.2
Total VFA (gCOD/L)	20.8 ± 1.5	6.34 ± 0.61

3.3.2 Impact of ISR on LBR performance

To determine how inoculum percentages would affect performance of FW dry digestion in LBR operation, experiments were conducted in LBRs inoculated with acclimated sludge before. Figure 3-2 demonstrated an increasing trend on cumulative methane yield when the ISR increased. When operating under 0.6~1.0 gN/L of TAN and 3~4000 mg/L Na^+ conditions, the highest cumulative methane yield was about 350 mLCH_4/gVS-FW, achieved with ISR of 60%. The cumulative methane yield decreased to 251 and 149 mLCH_4/gVS with decreased ISR at 40% and 20%, respectively. At 10% ISR, the lowest yield observed was about 104 mLCH_4/gVS, which was only 30% of the methane yield with 60% ISR. These results demonstrated comparable methane yield with other studies in literature. Wilson et al. (2016) demonstrated methane production as high as 260 mLCH_4/gVS with 60% ISR in LBRs coupled with a fixed-

film anaerobic bioreactor treated OFMSW. Xu et al. (2011) reported methane production between 180 and 250 mLCH_4/gVS in two-stage, LBR coupled with UASB fed with simulated FW. Dearman & Bentham (2007) reported methane yield as high as 229 mLCH_4/gVS with 10% ISR for FW dry digestion in one-stage bioreactor operated for more than 70 days. In another study with single-stage bioreactor system treated with FW for 25 days, methane yields ranged between 185 and 430 mLCH_4/gVS with ISR ranging from 20% to 65% (Liu et al., 2009).

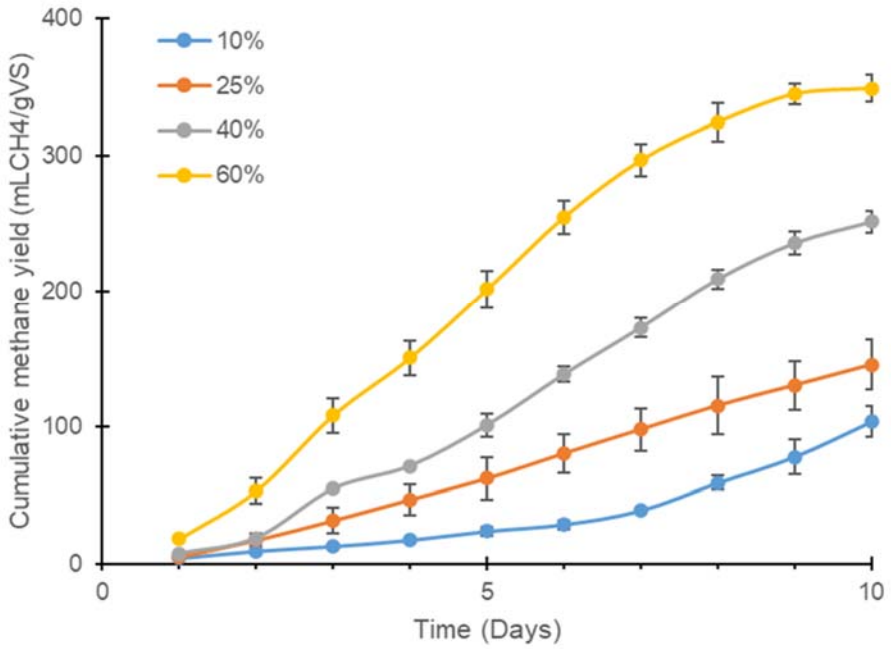

Figure 3-2. Cumulative methane yield during operations in LBRs with different ISR.

Solid removal and hydrolysis and acidogenesis performance were also monitored with different ISR of 10, 25, 40, and 60%, respectively. With 10% ISR, the average VS reduction was 76.8 ± 5.3 %. When ISR to 25% and 40%, VS reduction appeared to decrease to 70.6 ± 3.0% and 70.8 ± 4.5%, which were reduced by less than 10%. respectively. Further, VS reduction

decreased to an average of 60.9±1.9 % when the ISR finally increased to 60%. The VS reduction performance at 25% inoculum is comparable to performance in reactors with 40% ISR. Average VS reduction for LBRs at 10% ISR was a little higher (1.25-fold) than that for LBRs with 60% ISR. In general, the average VS reduction and ISR appeared in a negative correlation (R^2 = -0.840). The slight decrease on VS reduction may be contributed to the increased volatile solid from inoculum and relatively short operation period (10 days of each operation), which would finally increase the volatile solid content in the system. Significant differences were observed by one-way ANOVA in VS reductions among the various ISR (p-value = 0.007), and Tukey's HSD test further identified significant differences only between the mean VS reduction at 60% and all other ISR groups ($p<0.05$). This may indicate that although higher ISR could increase the hydrolytic bacteria in the LBR to improve the solid reduction, the VS removal would still be affected adversely by the increased total amount of volatile solids from the inoculum, considering a relatively short operation time (10 d).

The overall average VS reduction at each ISR were comparable with the observations in other studies (Chen et al., 2008; Lu et al., 2008; Wilson et al., 2016). The average TAN detected in the leachate at the end of every LBR operation ranged from 630 to 1060 mgN/L, while the average Na^+ was between 3790 and 4190 g/L (Table 3-3). One of these studies suggested that high solids AD performed best at TAN concentrations in the range of 600~1000 mg/L (Kayhanian, 2004), while it was also reported 55 ~ 74% of VS reduction obtained when TAN was elevated to 3500 mgN/L in the leachate with inoculum acclimated to such high ammonia before adding to LBRs (Wilson et al., 2016). Other studies have also discovered little inhibition with ammonium level higher than 4000 mg/L and attributed the tolerance to the adaption of microbial communities to elevated ammonia levels (Chen et al., 2008; Dong et al., 2010;

Nakakubo et al., 2008). In contrary, VS reduction inhibition were observed (as low as 40%) in high solid AD reactors for sewage sludge digestion with TAN of 3000~4000 mgN/L (Free ammonia of 300~800 mg/L) (Duan et al., 2012; Song et al., 2004). Therefore, both sides of examples demonstrated the benefit for use of acclimated inoculum under high-level ammonia environment for anaerobic digestion.

Table 3-4. Physical-chemical properties of leachate. (n=3)

Group	**10%**	**25%**	**40%**	**60%**	**R1**	**R2**
pH	7.6 ± 0.2	7.7 ± 0.1	7.8 ± 0.1	7.8 ± 0.1	7.8 ± 0.1	7.7 ± 0.1
TAN (mgN/L)	1062 ± 112	850 ± 33.1	763 ± 45.0	631 ± 42.1	570 ± 41.0	604 ± 58.2
Na^+ (mg/L)	4120 ± 206	3810 ± 120	3790 ± 219	4010 ± 181	4190 ± 496	3630 ± 210
SCOD (gCOD/L)	14.0 ± 0.35	10.3 ± 1.2	9.85 ± 0.66	11.2 ± 0.55	7.15 ± 0.59	5.21 ± 0.91
Total VFA (gCOD/L)	9.37 ± 0.30	6.34 ± 0.61	4.77 ± 0.57	2.83 ± 0.25	4.34 ± 0.34	4.05 ± 0.45

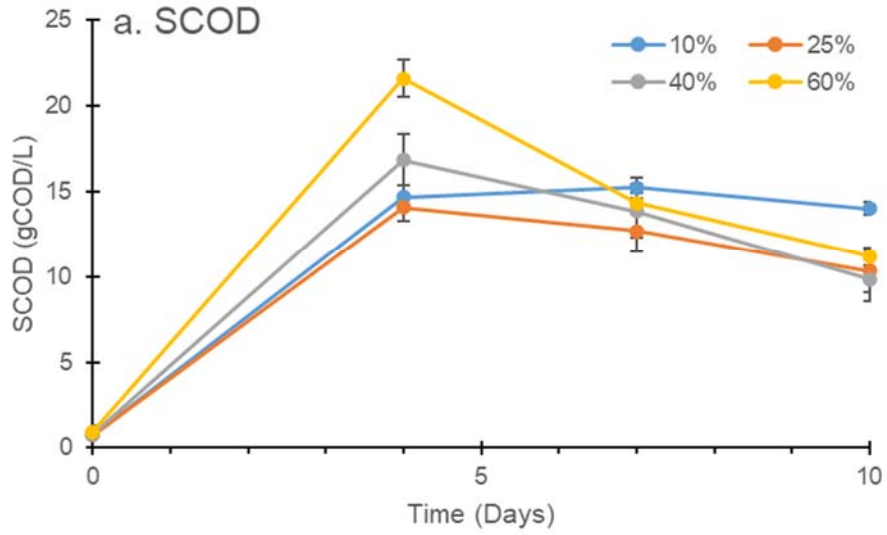
a. SCOD
10%
25%
40%
60%
SCOD (gCOD/L)
25
20
15
10
5
0
0
5
10
Time (Days)

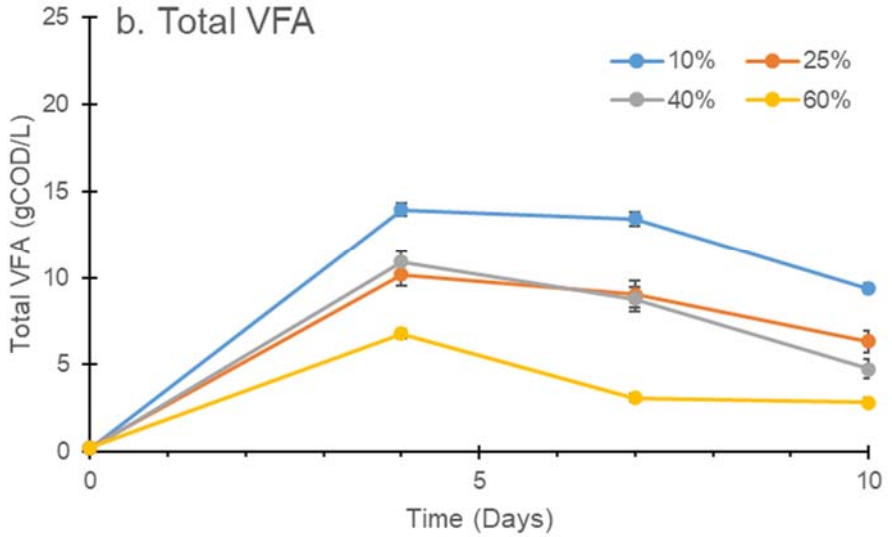
b. Total VFA
10%
25%
40%
60%
Total VFA (gCOD/L)
25
20
15
10
5
0
0
5
10
Time (Days)

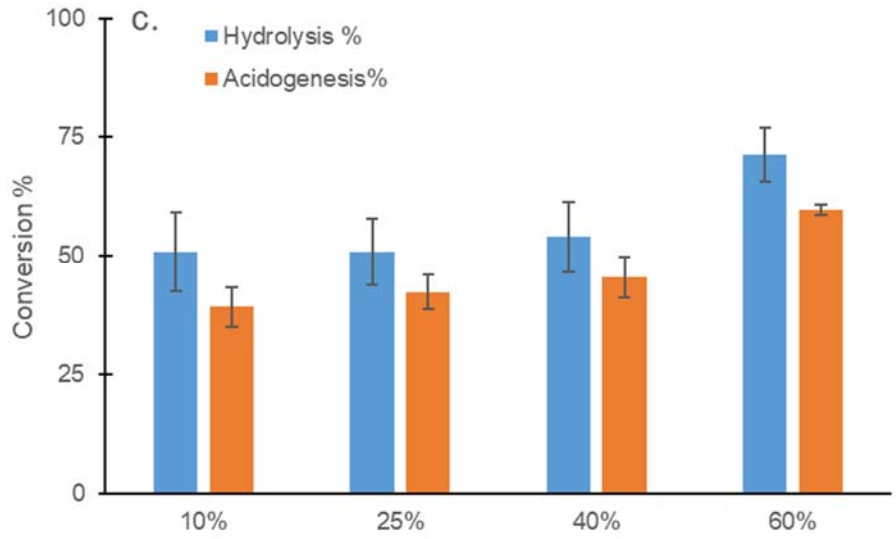

Figure 3-3. SCOD (a), total VFA concentrations (b), and hydrolysis and acidogenesis efficiency (c) during operation of different ISR.

Consistent with VS reduction performance, VFA concentrations in the final leachate demonstrated decreasing trend with increasing inoculum percentages. pH values ranged from 6.6 to 7.8 in the leachate during operations, and the pH of the final leachate of different ISR were comparable (Table 3-3). When starting a new batch, leachate SCOD and VFA levels soon achieved their peaks in the LBR due to the influx of solubilized organics from FW by hydrolysis and acidogenesis, and both gradually reduced as those soluble organics were converted to VFA and methane in the leachate (Figure 3-3). As the ISR increased, more microorganisms were available for hydrolysis and acidogenesis and hence higher SCOD was observed in the leachate (Figure 3-3a). Higher ISR also meant more rapid acetogenesis and methanogenesis in the leachate due to the increase in the acetogens and methanogens and therefore VFA would be converted into methane faster than other lower ISR (Figure 3-3b). In addition, TAN was the

highest in the final leachate with 10% ISR, and decreased gradually when ISR increased. The decrease in TAN could be attributed to the increase in inoculum in LBR, which utilized more nitrogen for cell synthesis and growth. According to the pH and TAN, the free-ammonia (FA) concentrations in each final leachate would be less than 60 mgN/L, which were below the reported critical concentration of 200 mgN/L (Bai & Chen, 2020; Liu & Sung, 2002).

The microbial activities of hydrolysis, acidogenesis, and methanogenesis would determine the efficiency of these important steps of the AD process. It can be seen from Figure 3-3c that both hydrolysis and acidogenesis efficiency increased along with the increase in ISR. Higher ISR would result in higher hydrolysis and acidogenesis efficiency by the increased number of microbes and therefore more VFA would be produced and converted to methane rapidly, which in turn lead to the higher cumulative methane yield and more rapid methane production rate observed in LBR operated with ISR 60%. Therefore, increasing ISR would be effectively improve the methane yield in a short operation time (i.e., 10-day in present experiments).

Thus, the results presented here indicated that an increase in the content of acclimated inoculum can increase methane yield under the existence of ammonia and salinity. Such improvement was mainly due to the increase in the content of microorganisms responsible for the anaerobic digestion process, including hydrolysis, acidogenesis, and methanogenesis. Although solid reduction is believed to be highly affected by original feedstock composition, the addition of more desired microorganisms in the acclimated inoculum would increase the source of hydrolyzing bacteria and thus facilitate the FW hydrolysis (Wang et al., 2010; Zhang et al., 2007). It is also believed that although ISR is important for dry digestion in LBR systems, the

optimum ISR ratio would be affected by many other factors, including system design, operating parameters, and feedstock characteristics (Chen et al., 2008; Di Maria et al., 2013).

3.3.3 Impact(s) of leachate recirculation rates

To study the impact(s) of recirculation rates on methane yield and LBR performance, experiments in LBR with 25% ISR and recirculation rate of 0.3 L/hr was selected as the control. In this study, the VS removal was 66.4 ± 0.04% and 67.7 ± 2.02%, for group R1 and R2, respectively. Compared to the VS removal of the operation with 25% ISR, which was 70.6 ± 3.0%, there was no significant difference among these groups by one-way ANOVA ($p>0.05$). This suggested that the recirculation strategy applied here, which had recirculation rates ranged from 0.3 to 7.5 L/hr, did not strongly affect the solid reduction during the LBR operation. Other studies also reported similar VS removal (69.4~73.0%) when the leachate recirculation rates varied between 0.35 and 1.25 L/hr, respectively (Rico et al., 2015; Wilson et al., 2016; Xu et al., 2014).

In general, all the FW dry digestion experiments were operated for 10 days, while the methane percentage in the biogas increased progressively from the start-up and achieved higher than 50% within 5 days for all the experiments. The methane content from all experiments ended with a range from 62-70%. The control displayed a gradually increased methane yield from the start-up of the operation with a cumulative methane yield of approximate 150 mL CH_4/gVS at the end of operation (Figure 3-4). The daily methane production rate of group 25% was also slow from the beginning, while later became fast and gradually increased, which could be seen from the slope of the methane yield profile (Figure 3-4).

The group R1 displayed a different methane yield profile when the recirculation rate of the LBR increased to 1.5 L/hr and the profile could be divided into two parts (Figure 3-4). After the start-up of the operation, the methane yield increased quite fast, compared to that of control and R2. The methane yield kept growing until Day 5 and the yield reached plateau till the end of the operation, with a cumulative methane yield of about 207 $mLCH_4/gVS$. The daily methane production rate showed rapid methane production rate for the first five days, and then gradually slowed down when the cumulative methane yield reached plateau after Day 6, which indicated a slow but continue methane production if the operation of LBR would extend to longer operation time.

The group R2 displayed another type of methane yield profile when the recirculation rate further increased to 7.5 L/hr (Figure 3-4). At the beginning, the group R2 showed a relatively slow methane yield for the first four days of operation similar to the control, which suggested a low but quite stable daily methane production rate as compared to R1. The methane yield then kept increasing more rapidly from Day 5 and the daily methane production rate also increased rapidly, as compared to the first 4-day operation, and then slowed down again till the end of the operation. The cumulative methane yield of group R2 was about 260 $mLCH_4/gVS$, which was the highest among the control, R1, and R2. Therefore, by increasing the recirculation rate, methane yield in the LBR for FW dry digestion can be improved without increasing ISR.

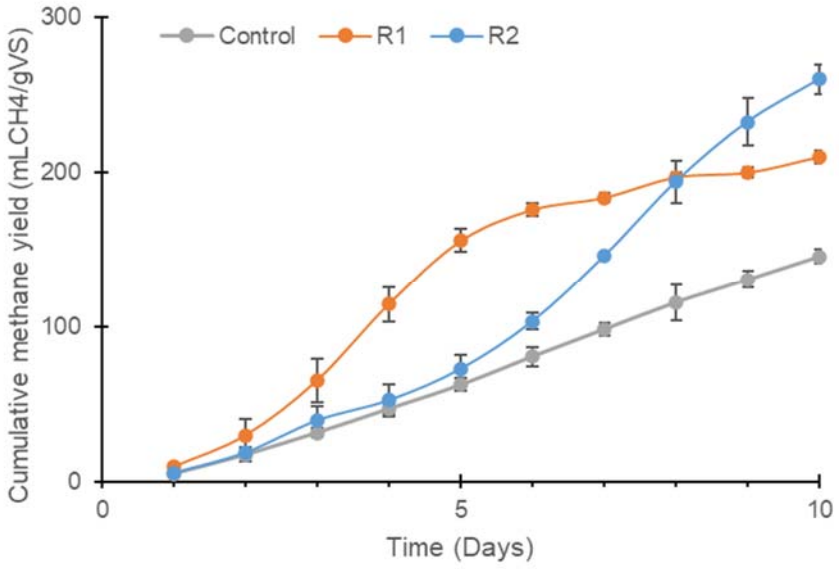

Figure 3-4. Cumulative methane yield for FW dry digestion in LBRs operated with different recirculation rates. (Control: recirculation rate of 0.3 L/hr; R1: recirculation rate of 1.5 L/hr. R2: recirculation rate of 7.5 L/hr)

VFAs and SCOD evolution during the operation of FW dry digestion were shown in Figure 3-5. In general, VFAs and SCOD followed similar trend. At the beginning of the control operation, little VFAs were detected in the leachate because all the inoculum were centrifuged before adding to the LBR. After the operation started, the SCOD and VFA levels in the leachate increased significantly, due to the hydrolysis and acidogenesis of substrate. After reaching a peak at about Day 4, the SCOD and VFA levels were decreased, which indicated more consumption than production in leachate. The SCOD and sum of VFA species concentrations in the leachate of the control were the highest at the end of the operation among the three groups, which was 10.3 and 6.34 gCOD/L, respectively (Figure 3-5a). The highest VFA levels remained in the leachate was correspond with the lowest cumulative methane yield of the control among all three

groups. It also indicated that low ISR (25%) with low recirculation rate could be the reason for the relatively high VFA and SCOD levels remaining in the leachate, which may limit the acetogenesis and methanogenesis.

When the recirculation rate increased to 1.5 L/hr in R1, the VFAs and SCOD levels in the leachate reached peaks at Day 2, which were 7.35 and 9.43 gCOD/L, respectively (Figure 3-5b). The VFAs and SCOD levels then decreased to 4.05 and 5.21 gCOD/L at the end of operation, respectively. This was also in consistence with the methane production in R1. Increasing in the recirculation rate would increase the frequency of contact between microbes and FW, hence may increase the SCOD influx in the leachate. But the faster methane production during the first five-days operation would indicate high SCOD and VFA consumption, which would limit the accumulation of SCOD and VFA in the leachate. While in R2 with recirculation rate of 7.5 L/hr, the maximum VFA and SCOD levels of 19.3 and 20.0 gCOD/L were observed at Day 4 (Figure 3-5c). The VFA and SCOD levels then decreased significantly to 4.34 and 7.15 gCOD/L at the end of operation, respectively, which was the lowest level among the three groups. Higher recirculation rates could provide more contact frequency between microorganisms and substrate even with low ISR, and wash out the VFAs and SCOD into leachate more frequently to avoid VFA and other inhibitor accumulation in LBR. Low ISR would also limit the SCOD and VFA consumption by acetogenesis and methanogenesis at the beginning of operation, which was in consistence with the methane yield in R2.

Figure 3-5 also clearly showed that acetate was the dominant VFA species in the leachate, followed by propionate and butyrate in the control. The remaining volatile fatty acid species were at negligible levels in the leachate. For R1 and R2, acetate also present in higher concentrations than other fatty acid species during dry digestion of FW in LBR, and was

consumed rapidly in the leachate (Figure 3-5b and c). In the scene of control, the maximum level of acetate 6.72 gCOD/L and was consumed about 50% during the dry digestion (Figure 3-5a). The maximum acetate levels in R1 and R2 were 3.50 and 7.70 gCOD/L, respectively. Acetate were both rapidly consumed during the operation of R1 and R2 (Figure 3-5b and c). The maximum propionate and butyrate levels in the control were much lower than that of acetate, and their concentrations remained almost constant or had small decrease during dry digestion operation (Figure 3-5a). While in the leachate of R1, the propionate level was higher (3.77 gCOD/L) than the other two. The propionate concentration remained quite stable and started to decrease at the late period of operation in R1, while butyrate was almost completely degraded at the same time (Figure 3-5b). When the recirculation rate further increased to 7.5 L/hr, the butyrate reached its maximum of (9.87 gCOD/L) after 4-day operation, followed by acetate (7.69 gCOD/L), and was also completely consumed at the end, while propionate level showed slow but steady increase during the operation, which indicated a more active acidogenesis and acetogenesis in the leachate (Figure 3-5c). The rapid decrease in total VFA concentration in R2 in the late operation period was also in consistence with the accelerated methane production rate as shown in Figure 3-4.

The impact of recirculation rates on hydrolysis and acidogenesis efficiency was shown in Figure 3-5d. When the recirculation rate increased from 0.3 L/hr to 7.5 L/hr, the hydrolysis efficiency showed slightly increase from 50.8% of the control to 54.8% in R2, which suggested that increase in recirculation rate may not significantly improve the hydrolysis of complex organics and production of soluble organics. The acidogenesis efficiency increased from 42.3% in the control to 52.7% in R2. The acidogenesis efficiencies in the LBR with higher recirculation rates were significantly different than that in the control ($p < 0.05$), which indicated that

increasing recirculation rate had more impact on VFA production during FW dry digestion. Improved VFA conversion would provide more substrate (acetate, CO_2, and H_2) for methanogenesis, thereby increased the methane yield in the short operation time.

The differences on methane yield and VFA production among different groups have clearly indicated that recirculation strategy could play an important role on the AD process during dry digestion. In the control, low recirculation rate would lead to low moisture content in the FW and low contact frequency between microorganisms and substrate, therefore the hydrolysis process slowed down. Low recirculation rate would also cause VFA accumulation and local pH dropping in the solid substrate of FW, where inhibition of microorganisms including methanogens may occur due to the lack of washout and dilution of VFAs by leachate recirculation. Other studies also observed low methane yield during dry digestion of OFMSW without leachate recirculation (Benbelkacem et al., 2010; Chan et al., 2002; Veeken and Hamelers, 2000).

It was reported that propionate level would show more inhibition on methanogens than other VFA species such as acetate and butyrate (Ahring and Westermann, 1988; Chen et al., 2008; Pullammanappallil et al., 2001; Ward et al., 2008;). However, although the propionate level in R1 and R2 were elevated as compared to the control, methane production was not inhibited in the two group of tests, which may be attributed to the near neutral pH during the operation in R1 and R2. It is reported that microbes utilizing propionate have much lower specific growth rates and larger substrate half-saturation constants than acetate and butyrate. Larger half-saturation constant value of propionate indicates that it would be more difficult for microbes to utilize propionate for growth and proliferation (Li et al., 2020). Therefore, high propionate level may suggest a slow propionate utilization rate in the LBR and hence reflect

different microbial activity levels and VFA degradation and methanogenesis pathways in R1 and R2, which were attributed to the increased leachate rate.

As the recirculation rate increases, it would benefit the internal homogeneity and the washout of potential inhibitors like VFA and ammonia through the solid substrate (Rocamora et al., 2020). Frequent contact between microorganisms in the leachate and solid substrate would improve the hydrolysis and acidogenesis and further increase VFAs available in the leachate for methanogenesis, which would result in higher methane yields and improved process operation performance as shown in the R1 and R2. Although the VFAs remaining in the final leachate of R1 and R2 were still high, considering the relatively short operation time (10-day), it could be expected that the remaining VFAs would be consumed and converted into methane completely when the operation time extends longer, as shown in other studies (Li et al., 2017d; Pezzolla et al., 2017; Rico et al., 2015).

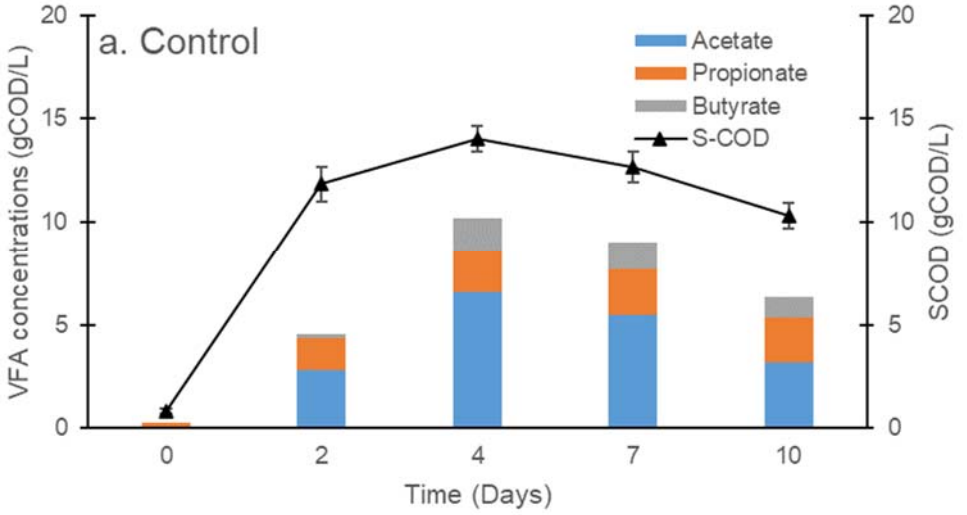
a. Control
Acetate
Propionate
Butyrate
S-COD
VFA concentrations (gCOD/L)
SCOD (gCOD/L)
Time (Days)
0
2
4
7
10
0
5
10
15
20

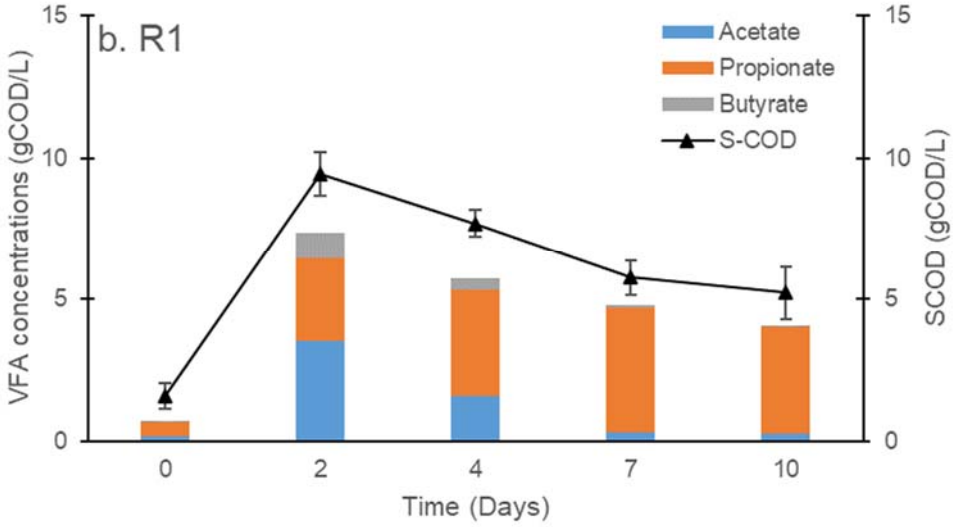
b. R1
Acetate
Propionate
Butyrate
S-COD
VFA concentrations (gCOD/L)
SCOD (gCOD/L)
Time (Days)
0
2
4
7
10
0
5
10
15

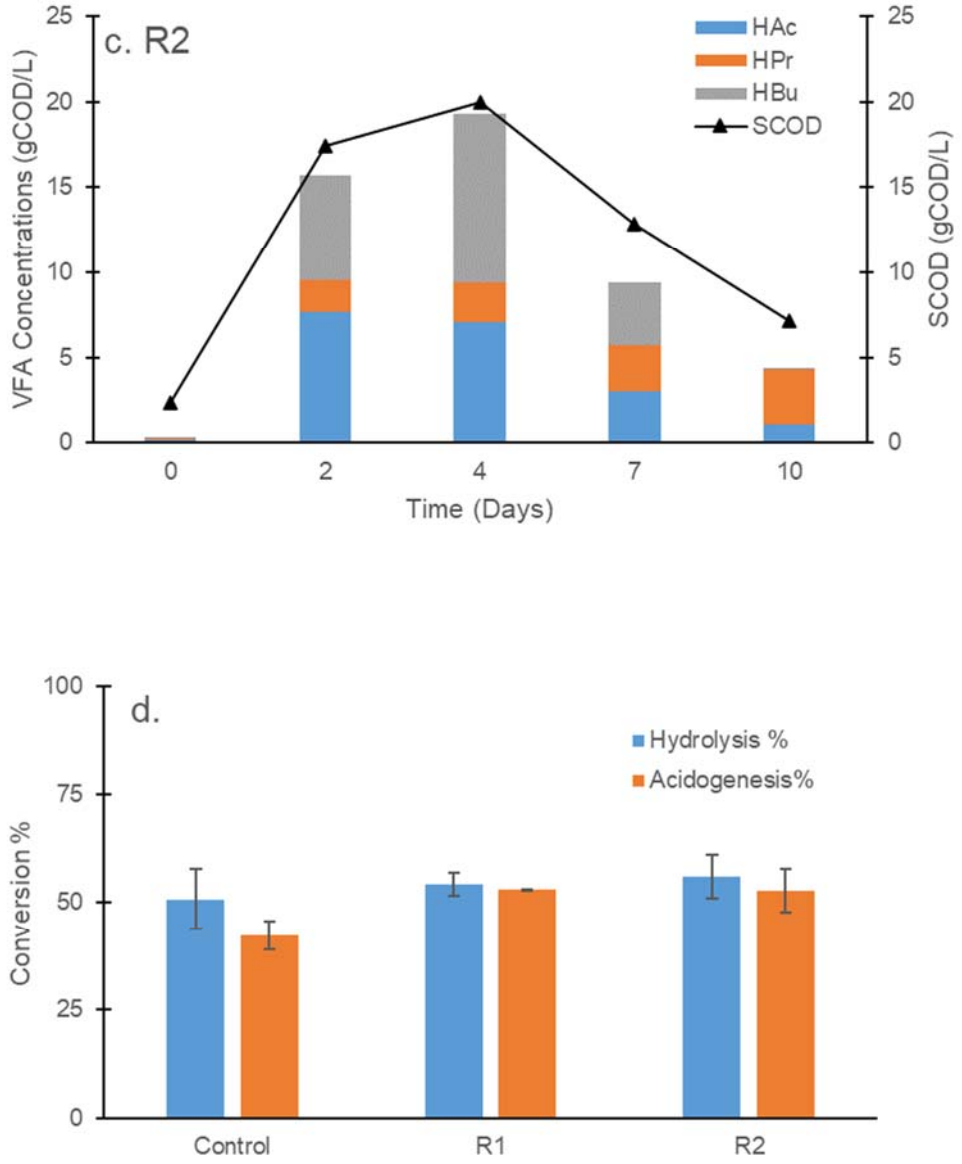

Figure 3-5. VFAs profiles in leachate and hydrolysis and acidogenesis efficiency during FW dry digestion in LBR with different recirculation rates. (a) Control: recirculation rate 0.3 L/hr. (b) R1: recirculation rate of 1.5 L/hr. (c) R2: recirculation rate of 7.5 L/hr. (d) Hydrolysis and acidogenesis efficiency.

3.3.4 Microbial community structure analysis

(1) Enrichment of potential useful microorganisms via acclimation

The microbial community structure in acclimated and non-acclimated leachate samples from the reactors after stable operations were characterized by 16S rRNA sequencing. The highest microbial diversity was obtained in the original WWTP anaerobic digested sludge (Shannon index of 5.59), whereas the Shannon index decreased to 4.67 and 4.26 in the non-acclimated leachate and acclimated leachate, respectively. As an index of biodiversity of community, the decrease in Shannon index indicated that the microbial community of non-acclimated and acclimated were selectively enriched in order to adapt to each specific conditions.

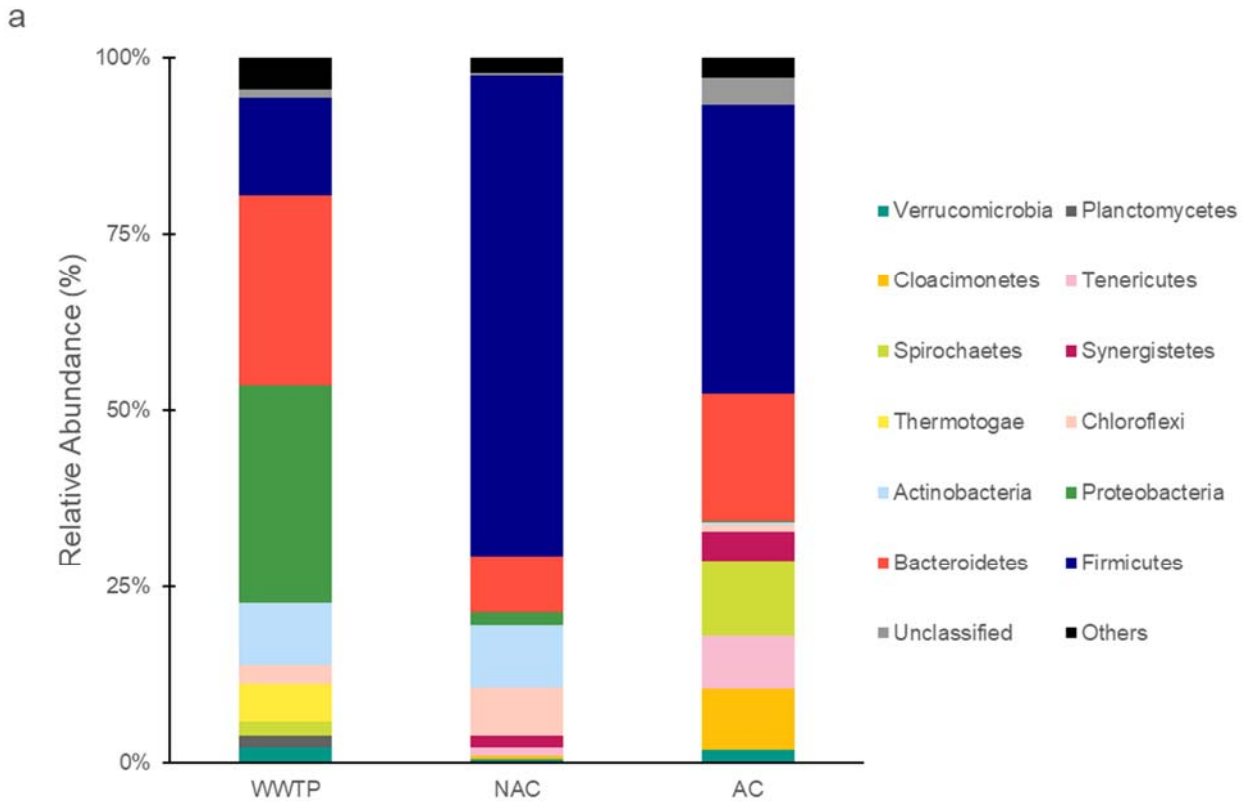

b

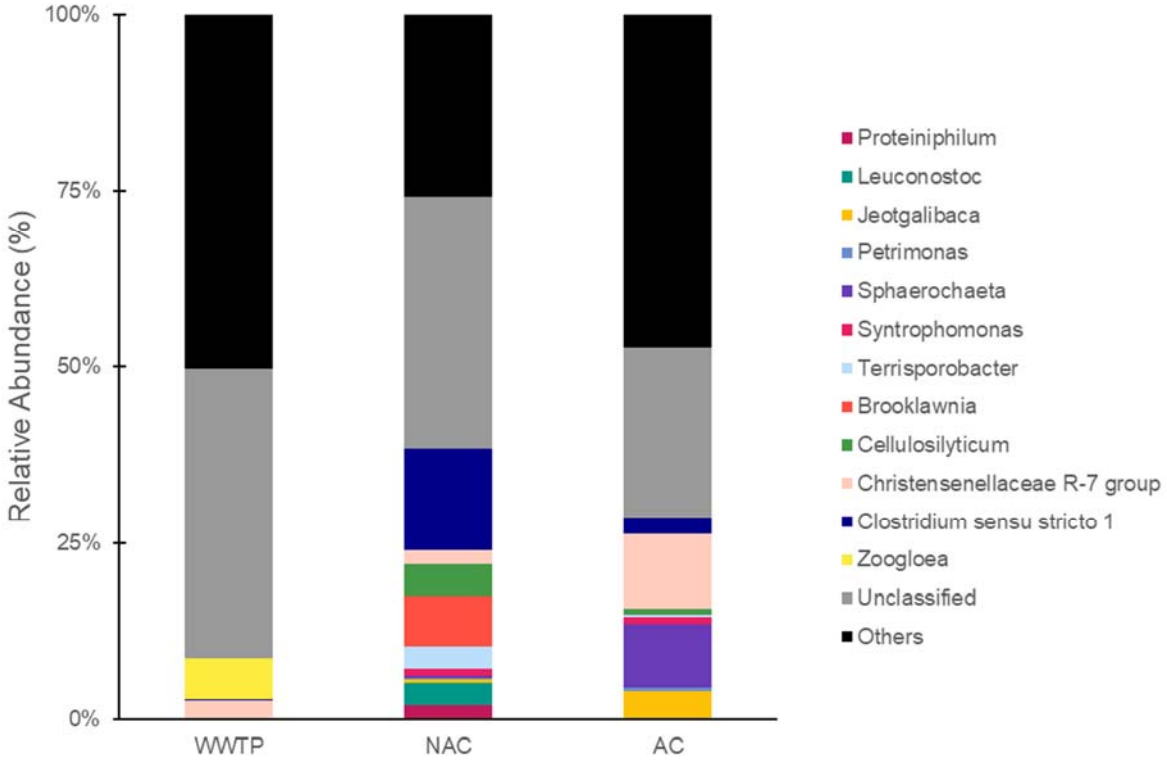
100%
75%
50%
25%
0%
Relative Abundance (%)
WWTP
NAC
AC
Proteiniphilum
Leuconostoc
Jeotgalibaca
Petrimonas
Sphaerochaeta
Syntrophomonas
Terrisporobacter
Brooklawnia
Cellulosilyticum
Christensenellaceae R-7 group
Clostridium sensu stricto 1
Zoogloea
Unclassified
Others

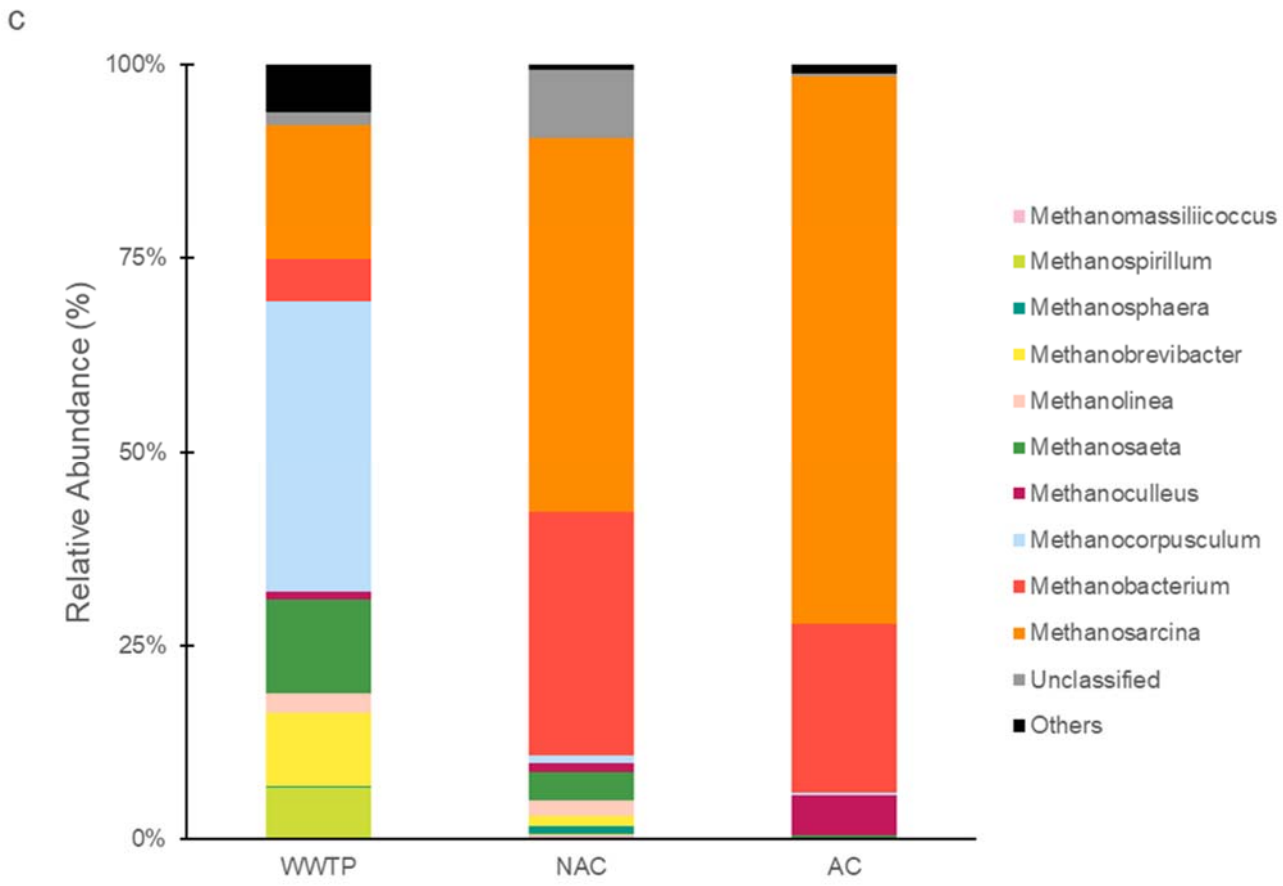

Figure 3-6. Relative abundance of microbial communities in original anaerobic digested sludge (WWTP), leachate from non-acclimated LBR (NAC), and leachate from acclimated LBR (AC) under (a) bacterial phylum level, (b) bacterial genus level, and (c) archaea genus level.

The relative abundance at phylum level in non-acclimated and acclimated leachate samples, as well as the original WWTP digested sludge samples, were shown in Figure 3-6a. Proteobacteria, Bacteroidetes, Firmicutes (Bacillota), and Actinobacteria were dominant in the original WWTP anaerobic digested sludge samples. The phyla Proteobacteria, Bacteroidetes, Firmicutes, and Actinobacteria contain lots of fermentative bacterial species for different

substrates degradation. In the non-acclimated leachate samples, however, the Proteobacteria and Bacteroidetes showed a significant decrease in their relative abundance by 94.1% and 70.2%, respectively, while the phylum Firmicutes abundance was increased by more than 4 times in the original WWTP digested sludge samples. For acclimated leachate samples, similar decrease in the abundance of the phylum Proteobacteria and Bacteroidetes were observed (by 99.4% and 33.2%, respectively), while the phylum of Firmicutes was increased by almost three times than in the original WWTP digested sludge samples.

The relative abundance at genus level in the non-acclimated and acclimated leachate samples were shown in Figure 3-6b. In the non-acclimated leachate sample, the abundance of *Clostridium*, *Brooklawnia*, and *Cellulosilyticum* increased significantly, compared to the original WWTP digested sludge. *Clostridium* contains species for organic compounds fermentation and VFA production, especially butyric acid product (Wiegel et al. 2006). *Brooklawnia* are facultative anaerobic bacteria whose major glucose fermentation products include propionate and acetate (da Costa et al., 2015). *Cellulosilyticum* are obligate anaerobic bacteria which hydrolyze cellulose and xylan and produce acetate as one of the major end products (Cai et al, 2016).

However, in acclimated leachate samples, the relative abundance of *Clostridium*, *Brooklawnia*, and *Cellulosilyticum* were decreased significantly by more than 80%. In contrast, genus *Christensenellaceae* (Christensenellaceae R-7 group), common anaerobic bacteria found in mesophilic digester, dominated in the leachate community with relative abundance of more than 14%. The genus *Sphaerochaeta* and *Jeotgalibaca* also showed significant increase in their relative abundance in the acclimated leachate community. Bacteria from the genus *Christensenellaceae* can utilize various sugars and produce VFAs by fermentation (Morotomi et al, 2012). Furthermore, species in genus *Sphaerochaeta* (8.9%) and *Jeotgalibaca* (3.9%) both

show saline resistance and can grow when salt concentration is as high as 30 gNaCl/L (Miyazaki et al., 2014; Zamora et al., 2017). Therefore, acclimation of the inoculum may help to enrich microbial phylotypes which could tolerate potential inhibitors like saline accumulated in the LBR, hence improve the performance of FW dry digestion.

In addition, the dominant methanogen in the acclimated leachate sample also changed significantly (Figure 3-6c). Compared to the original WWTP anaerobic digester sludge, *Methanocorpusculum* was no longer the dominant methanogen, while *Methanosarcina* showed a 4-time enrichment in abundance (account for 70.6% of archaea) in the leachate community, followed by *Methanobacterium* (21.9%) and *Methanoculleus* (5.2%). Since the genera of *Methanosarcina* and *Methanobacterium* have been proven to have the capability of participating DIET (Cheng et al., 2009; Dinh et al., 2004; Rotaru et al., 2014), the acclimation treatment would benefit the system performance by enhancing the potential DIET when the LBR switches to a bioelectrochemical LBR (BLBR) system.

Although the 16s rRNA data did not indicate the activity of bacteria and archaea in leachate samples, these results could still support that acclimation of inoculum would allow microorganisms which could tolerate potential inhibitors to build up in the leachate. By centrifugation and reusing of the leachate as the inoculum for the next operation, notable improvements in system performance could be expected because such microorganisms can be preserved and concentrated in the inoculum. The increase in ISR would also increase the quantity of inhibitor-tolerant microorganisms in the LBR at the beginning, therefore may benefit the system performance.

(2) Impact of different recirculation rates on microbial community structure.

The improvement on the methane production by increasing the recirculation rates of the LBR raised the question that whether the adjusting of operational parameters would alter the microbial community among them. Therefore, the microbial communities of leachate and food waste residue at the end of operation of LBR with different recirculation rates were examined (Figure 3-7). The highest microbial species diversity was detected in the leachate samples of the control (recirculation rate of 0.3 L/hr) (Shannon index of 4.26), followed by the group with recirculation rate of 1.5 L/hr (Shannon index of 4.10) and 7.5 L/hr (Shannon index of 3.66), respectively, which may indicate that changing recirculation rates would selectively enrich microorganisms and hence decrease the microbial diversity in the community.

When the recirculation rate increased from 0.3 (control) to 1.5 L/hr (R1), the dominant genus *Christensenellaceae*, as well as the genus *Sphaerochaeta*, decreased dramatically in the leachate sample community as compared to those in the control. Bacteria from those two genera could produce acetate as major fermentation product (Morotomi et al., 2012; Ritalahti et l., 2012). In contrast, the genus *Trichococcus* became the dominant genus with a relative abundance of 17.4% in the community, followed by *Jeotgalibaca* (10.4%) and *Brooklawnia* (8.5%), respectively (Figure 3-7a). Bacteria from genus *Jeotgalibaca* showed saline resistance during their growth. The genus *Trichococcus* was reported to be capable of fermentation and could produce acetate and ethanol as fermentation products (Liu et al., 2002), while the genus *Brooklawnia* could produce propionate and acetate from fermentation (da Costa et al., 2015). This may explain the elevated level of propionate during the operation. When the recirculation rate further increased to 7.5 L/hr (R2), the abundance of genus *Jeotgalibaca*, a group of bacteria which have saline-tolerance in their growth condition, further increased to more than 30% in the

leachate community (Miyazaki et al., 2014; Zamora et al., 2017). The genus *Clostridium* also showed a 3.4-time increase as compared to that in the control. In addition, the relative abundance of *Christensenellaceae* in R2 returned to the same level as in the control, whose mainly fermentation products were acetate and a small amount of butyrate (Morotomi et al., 2012). That may explain the elevated butyrate and acetate levels in the leachate of R2. However, the abundance of the genus *Trichococcus* and *Brooklawnia* in the leachate of R2 decreased significantly compared to those in the leachate of R1, while the genus *Sphaerochaeta* remained similar abundance level in R2 as in group R1, which were both much lower than that in the control. Therefore, changing the recirculation rates could effectively enrich specific microorganisms and alter the microbial community structure and hence the metabolism pathways during dry AD process.

In addition, several possible microorganisms isolated or co-cultivated are responsible to degrade propionate between the syntrophic propionate-oxidizing bacteria (SPOB) and methanogens (Stam, 1994; Westerholm et al., 2022), including species belong to the genera *Smithella*, *Syntrophobacter*, *Pelotomaculum*, *Desulfotomaculum* and *Cloacimonetes* (de Bok et al., 2001; Galushko and Kuever, 2019; Imachi et al., 2007; Liu et al., 1999; McInerney et al., 2008; Nilsen et al., 1996; Pelletier et al., 2008). Among them, *Smithella propionica* is the only SPOB known to carry out dismutation of propionate to acetate and butyrate (Liu et al., 1999; de Bok et al., 2001). Butyrate can be further oxidized by *Syntrophomonas* to acetate and hydrogen for methane production with its syntrophic methanogen partner (Liu et al., 1999). Others like *Syntrophobacter* could oxidize propionate to acetate and CO_2/H_2 associated with sulfate reduction (Galushko and Kuever,2019). 16s rRNA analysis indicated that the leachate of the control had the highest abundance of SPOB (9.7% in total), followed by R2 (4.3%) and R1

(2.9%), respectively. The low abundance of SPOB, together with the lower specific growth rates and larger substrate half-saturation constants when using propionate as substrate and short operation periods, may explain the relatively high propionate levels and slow propionate utilization rates observed in R1 and R2 (Ito et al., 2012; Jannat et al., 2021; Li et al., 2020; Liu et al., 2011; Westerholm et al., 2022).

When the recirculation rate was low (control), the genera *Methanosarcina* and *Methanobacterium* dominated (total abundance > 90%) in the archaea community of the leachate samples (Figure 3-7b). *Methanosarcina* is capable of acetate dismutation for methane production, while *Methanobacterium* is sole hydrogenotrophic methanogen (Sowers et al., 1984; Whitman et al., 2014). It is estimated that about two-third of the methane is produced from acetate under mesophilic condition, which may explain the high abundance of *Methanosarcina* in the control and R1 and R2 (Liu & Whitman, 2008). With the increase in the recirculation rate, the archaea community structure changed (Figure 3-7b). In R1, the genus *Methanosarcina* (61.1%) still dominated in the methanogen community, while the genus *Methanocorpusculum*, a hydrogenotrophic methanogen, raised up to 26.1%. The genus *Methanobacterium* decreased to 9.8% in the leachate, which was the smallest among the control, R1, and R2. It has been reported that *Methanobacterium* may not be capable of methanogenesis under high propionate level, therefore the elevated propionate concentration observed in R1 may not be suitable for *Methanobacterium* growth (Zhang et al., 2019b). When the recirculation rate further increased to 7.5 L/hr (R2), the relative abundance of genus *Methanosarcina* decreased to 45.9%, although it was still the dominant methanogen genus. The genus *Methanocorpusculum* further increased to 30.7%, while the genus *Methanobacterium* returned to 21.4%, which was similar to that in the control. The increase in the abundance of SPOB in R2 may help *Methanobacterium* abundance

recover by syntrophic propionate oxidization between SPOB and *Methanobacterium*, by which utilized the propionate in the leachate. The archaea community seemed to switch from acetoclastic-dominated to a community with more hydrogenotrophic methanogens, which indicated that the change of recirculation rate would also affect the archaea community structure and selectively enrich specific methanogens in the system.

In addition, increasing the recirculation rate would relief the differences between microbial community structures in the leachate and from the food waste residue (FWR) (Figure 3-7a). When the recirculation rate was low (0.3 L/hr), the contact between microorganisms in the leachate and solid food waste was less frequent and may selectively prefer those solid-associated, hydrolysis and fermentative bacteria to remaining on the solid food waste (Degueurce et al., 2016; Lu et al., 2008; Wang et al., 2010). However, such differences on bacterial community structure were improved and diminished along with the increasing contact frequency between leachate and solid food waste by increasing the recirculation rate.

Therefore, increasing the recirculation rates during the operation of LBR would significantly change the microbial community structure by selectively enrichment of some specific microorganisms including the genera *Jeotgalibaca*, *Trichococcus*, *Brooklawnia*, and *Clostridium* which are capable of fermenting organic compounds and producing VFAs or have saline-tolerance in the leachate; hence improve the methane production with enhanced acetogenesis and acidogenesis. This result proved that adjusting operation parameters such as recirculation rate was critical for maintaining an ideal microbial community structure which would benefit LBR operation and system performance. However, microbial community structure analysis could not provide the activity or abundance data of those key enzymes (or functional genes) which are critical for hydrolysis, fermentation, and methanogenesis. Future studies are

required to reveal the relationship between the activity of enzymes involved in the anaerobic digestion processes and the control on operational parameters of LBR.

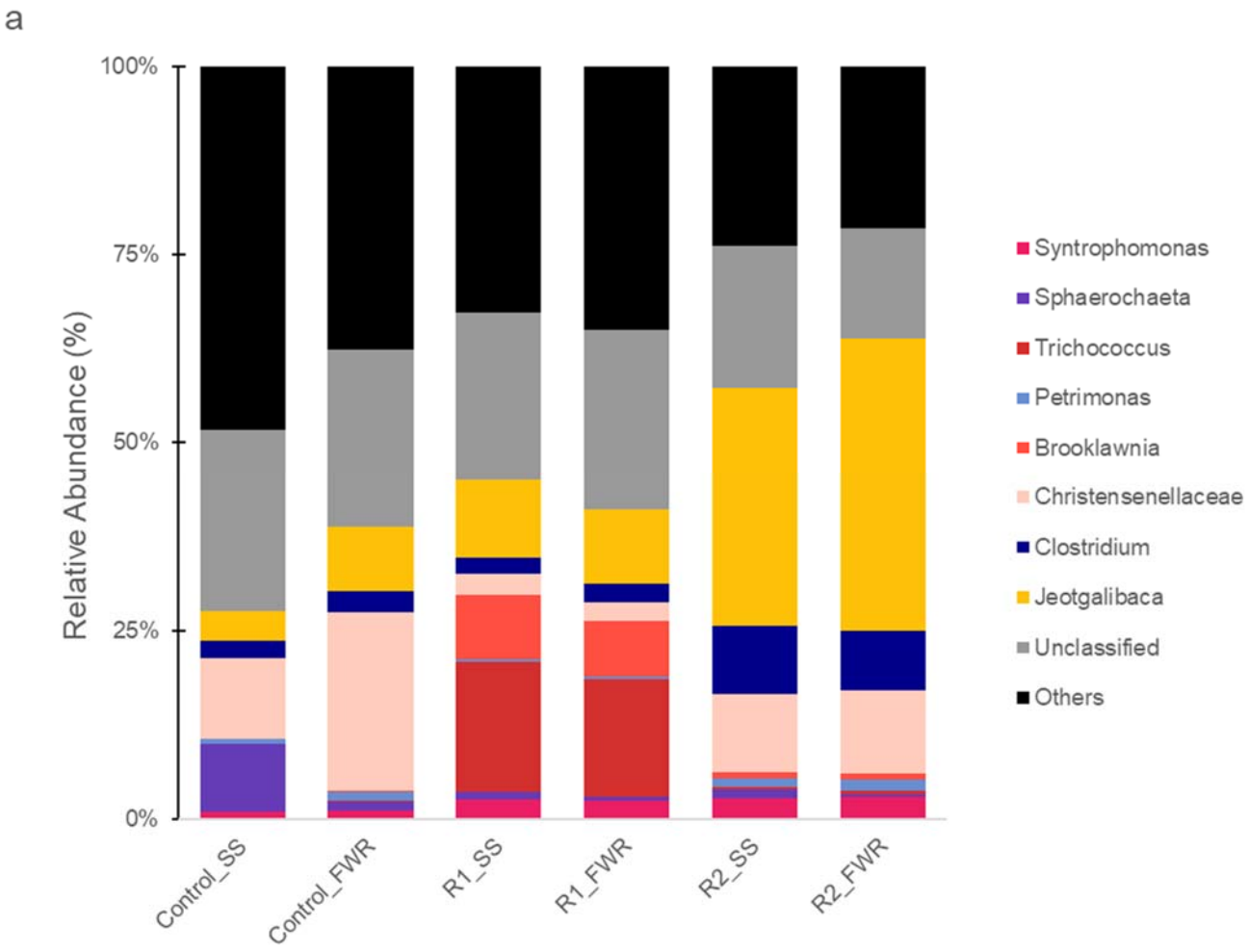

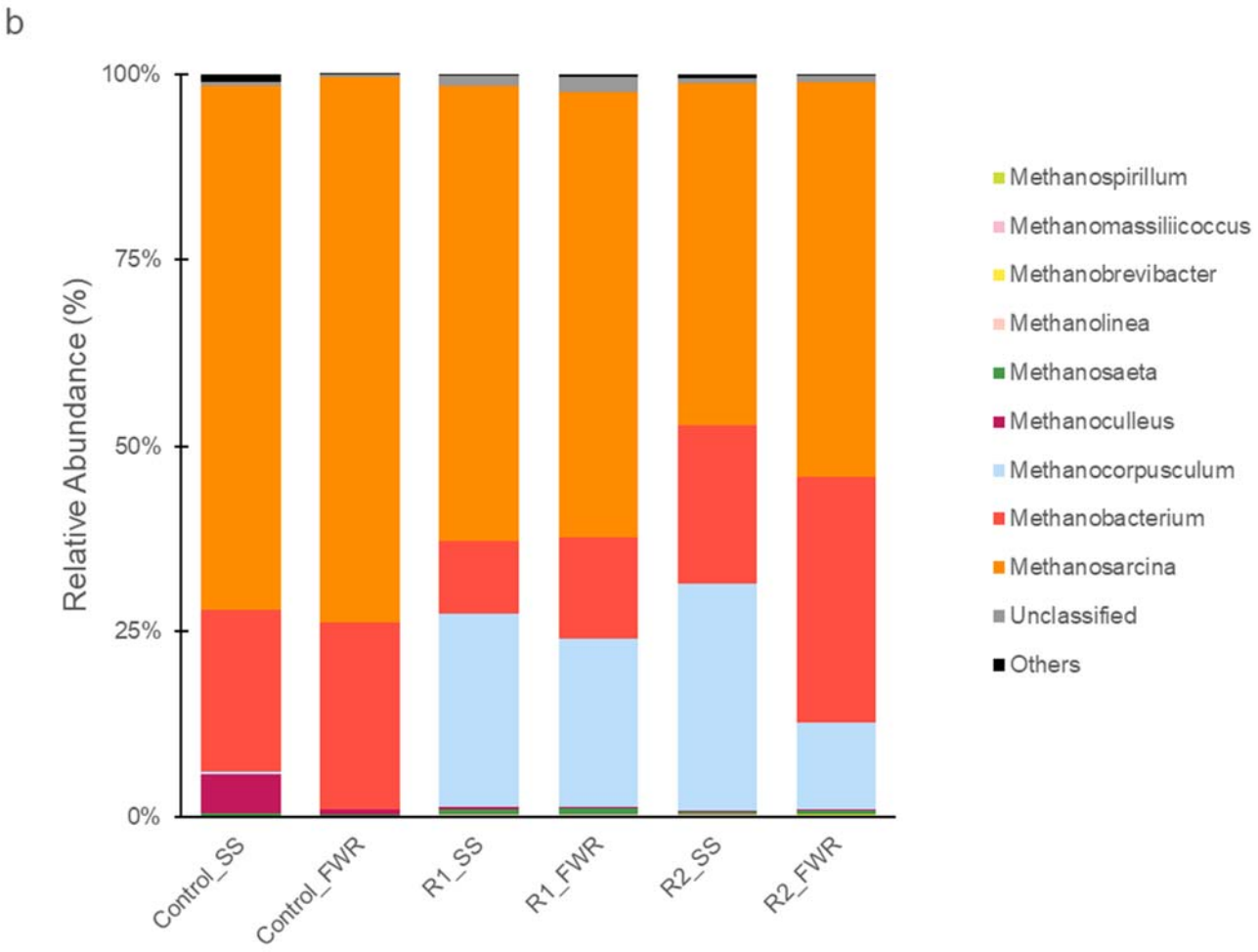

Figure 3-7. Relative abundance of microbial communities in leachate and food waste residue samples of LBR with different recirculation rates under (a) bacterial genus level, and (b) archaea genus level.

Control_SS: leachate in LBR with recirculation rate of 0.3 L/hr.

Control_FWR: food waste residue in LBR with recirculation rate of 0.3 L/hr.

R1: LBR with recirculation rate of 1.5 L/hr.

R2: LBR with recirculation rate of 7.5 L/hr.

3.4. Conclusion

This study has demonstrated that inoculum should be acclimated with inhibitors such as salinity and ammonia which may be encountered with elevated levels in LBR systems in order to accumulate desired microorganisms. The effects of different ISR on methane yield and process performance for FW dry digestion in the LBR systems were studied. Within the ISR range of 10 to 60%, methane yield was positively related to ISR while the VS reduction showed a negative relation to ISR. Higher methane yield was achieved when more inoculum was added to LBR. Increasing in leachate recirculation rate would also promote the methane yield and speed up the dry digestion process, allowing the LBR system operated with an ISR of 25% in a short operation time. The results obtained from this study would be used as a basis for the experiments in next chapters for FW dry digestion with bioelectrochemical leachate bed reactor (BLBR).

Chapter 4 - Enhanced methane production for FW dry digestion using bioelectrochemical leach bed reactor (BLBR)

4.1 Introduction

Dry anaerobic digestion (AD) process refers to the anaerobic digestion technology where the total solids of the feedstock is usually above 20% (Rocamora et al., 2020). Compared with conventional wet anaerobic digestion, the high solids content of food waste (FW) and biodegradable compounds makes dry anaerobic digestion a preferred technology for food waste treatment in engineering because dry AD like leach bed reactor (LBR) can handle higher organic loading rate, decrease the water requirement, and reduce energy input on internal mixing (Kumar & Samadder, 2020; Pera et al., 2021; Rocamora et al., 2020; Westerholm et al., 2020). Operation stability of dry AD depends on a variety of factors, including feedstock characteristic, organic load rate (OLR), hydraulic retention time (HRT), inoculum to substrate ratio (ISR), and recirculation strategy, and different studies have provided different recommend values of those factors for dry AD (See Table 3-1, Chapter 3) (Kothari et al., 2014; Kumar et al., 2021; Rocamora et al., 2020; Zhang et al., 2022).

Complex microbial metabolisms are involved in dry AD system. Solid organic matter of FW is first hydrolyzed and acidified to produce a variety of volatile fatty acids (VFAs) such as acetic acid, propionic acid and butyric acid, among which, except for acetic acid, which can be directly completed to produce methane, the rest must be converted to acetic acid and CO_2 and H_2 before methane can be produced (Tang et al., 2015; Zhang et al., 2022). The Gibbs free energy during the conversion of propionic acid and butyric acid to acetic acid is positive

(thermodynamically unfavorable), which limits the methanogenic rate of the whole system and prolongs the anaerobic digestion time (Wang et al., 2022). The large accumulation of short-chain fatty acids also tends to cause acidification in the AD system, leading to unstable digestion and even the AD system would collapse (Mu et al., 2020; Rocamora et al., 2020).

Microbial electrolysis cells (MECs) can use organic matters to produce hydrogen or methane by converting the organic matter and transferring the donor electrons from anode to cathode through an external circuit by anode-respiring bacteria (ARB) under an applied voltage (Cheng & Logan, 2007; Escapa et al., 2013; Hamelers et al., 2010; Wang et al., 2021a). The addition of electrodes to anaerobic processes including AD with an applied voltage would increase the degradation rate of organic matter, enhance the methane production, and enable some non-spontaneous reactions to occur (Cheng et al., 2009; Hamelers et al., 2010). Studies have shown methane production from synthetic wastewater with MECs and found that hydrogenotrophic methanogens could use the hydrogen molecules produced on cathode to reduce CO_2 for methane production, which indicated the novel interspecies electron transfer pathways, making MEC-AD a promising technology for CO_2 capture and methane production (Cheng et al., 2009; Clauwaert & Verstraete, 2009; Logan & Rabaey, 2012; Zhao et al., 2015).

The operation of MEC assisted AD (MEC-AD) can be efficiently achieved with introducing electrodes within an AD system (Lee et al., 2019). The performance of MEC-AD system depends on several biological and operation factors like microbial community structure, applied voltage, electrode material, temperature, pH, and organic loading rate (Wang et al., 2022). Studies have shown that an optimum applied voltage to the MEC-AD system would play an important role in organic degradation and methane production (Chen et al., 2016; Choi et al., 2017; Lim et al., 2017; Vologni et al., 2013), however, no studies have attempted to improve

methane production in dry AD by integrating MECs with dry anaerobic digesters, although proper engineering can improve energy recovery, as well as operating costs in FW dry anaerobic digesters (Feng et al., 2015; Guo et al., 2013; Lee et al., 2019; Tartakovsky et al., 2009).

Therefore, based on the studies FW dry digestion in LBR in the previous chapter, this study aimed to evaluate the performance of the novel, bioelectrochemical leach bed reactor (BLBR) on FW dry digestion. To establish the contribution of applied voltage on microbial electrolysis assisted anaerobic digestion, food waste was tested for dry digestion in the BLBR system with different applied voltage. An equivalent system to the BLBR was tested without applied voltage as control. The effect(s) of applied voltage was evaluated on different steps of AD processes and microbial community structures. Results from this study would be used to qualitatively discuss the possible mechanisms and explain how microbial electrolysis can enhance methane production in the BLBR.

4.2 Materials and Methods

4.2.1 Food waste and inoculum collection

FW was collected from a cafeteria at University of Waterloo (Waterloo, Ontario, Canada). After collection, FW was sorted, chopped, and frozen at -20°C as described in Chapter 3. The FW was thawed at 4°C for 24 hours prior to the experiments (Swakshar & Lee, 2020; Xiong et al., 2019).

Original AD sludge was collected from the anaerobic digestor of Galt Wastewater Treatment Plant (Cambridge, Ontario, Canada). The sludge was then filtered by mesh to remove

large particles prior to experiments. AD sludge was acclimated before added into the BLBR systems as inoculum. The acclimation process can be seen in Chapter 3.

4.2.2 Reactor configuration

Two cylindrical BLBRs were made of acrylic glass with an inner diameter of 14 cm and a height of 70 cm and the total volume was 10 L (Figure 4-1). The reactor body had a removable top cover with a gas outlet and a sprinkling system to spray leachate on FW, a basket sitting in the upper half of the reactor to hold FW, and the lower half as the leachate holding bed. The acrylic glass FW basket had an inner diameter of 10 cm and a height of 25 cm, with wholes of 5 mm size on its bottom which allowed leachate to percolate through and prevent FW chops from falling into the leachate holding bed. The leachate in the holding bed was recirculated by a digital peristaltic pump (Masterflex L/S Digital Drive, Model no. 07523-80, USA). The leachate in the holding bed was also mixed internally at 60 L/hr using a peristaltic pump (Masterflex L/S Economy Drive, Model no. 07554-90, USA).

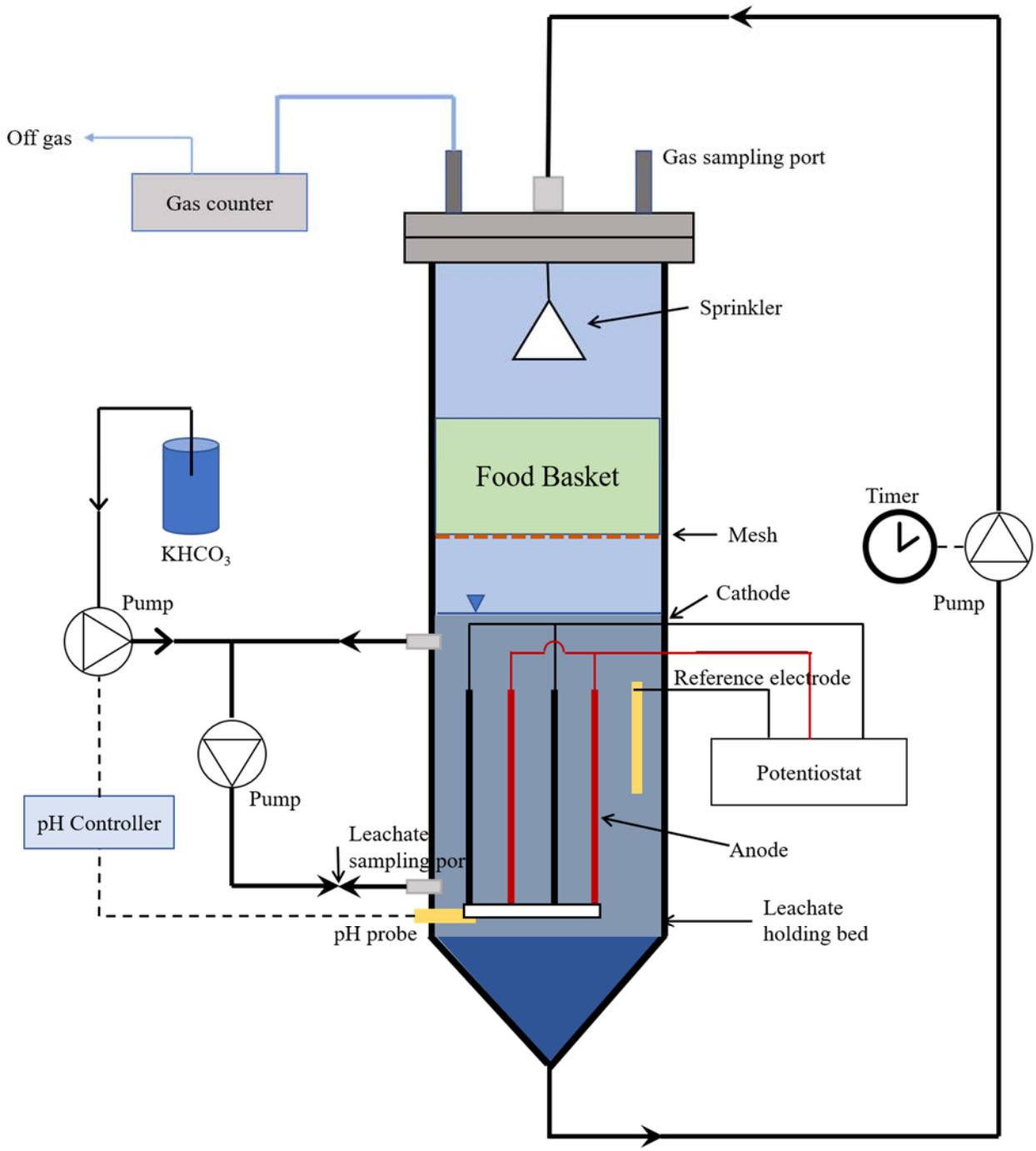

Figure 4-1. Schematic of the BLBR system.

The BLBRs were operated at 35°C, which was kept for mesophilic condition by recirculating heated water from a water heater controller (PolyScience 9702A11C 13-liter Advanced Digital Controller, PolyScience, United States) via PVC tubing tied around the reactor body. A pH controller (Milwaukee, MC-122 pH meter) was coupled to an in-situ pH probe and a pump injecting sodium bicarbonate solution to keep neutral pH and provide alkalinity in the leachate. A gas counter (MilliGas counter, Ritter Apparatus, Bochum, Germany) was connected to a gas line from the top cover of the BLBRs to measure biogas production. Leachate samples were taken from the mixing line, while biogas samples were taken from the gas line for routine analysis.

4.2.3 Reactor operation

BLBRs were fed with acclimated inoculum with ISR 25% and the initial leachate volume was fixed at 2.5 L. The leachate in the holding bed was continuously mixed at a rate of 60 L/hr with a peristaltic pump (Masterflex L/S Digital Drive, 115/230 VAC, Model no. 07523-80, USA). A leachate recirculation pump was programmed to be turned on for 15 seconds at every 75 min to sprinkle the leachate on the top of the FW at a rate of 90 L/hr, which corresponded to a leachate recirculation rate of 0.3 L/hr or 7.2 L/day. The initial VS of FW was fixed at about 72 g for all experiments. Before the start of each batch of experiments, all the BLBRs were sparged with nitrogen gas to create anaerobic conditions at a flow rate of 0.5 L/min for 30 min. After each batch, the leachate was centrifuged at 9,500 rpm for 20 min and the centrifuged solids were collected as inoculum in the next batch, which allowed enrichment of acclimated fermentative and methanogenic microorganisms in the reactors.

Prior to start-up, two pairs of carbon fiber anodes and stainless-steel cathodes, which were used to enrich *Geobacter* sp. in a mother MEC in Chapter 5, were placed in the leachate holding bed in each BLBR (Figure 4-1). The distance between anode and cathode was 1.5 cm. The ends of electrodes were connected to a potentiostat (Bio-logic, VSP, Gamble Technologies, Canada) which would provide the voltage. A reference electrode (Ag/AgCl, MF-2052, Bioanalytical System Inc., USA) was placed at a distance of 5 mm from the anode and also connected to the potentiostat. One BLBR was ran for control without applied voltage (open-circuit mode, OCM) and the other was operated under applied voltage between 0.3 and 1.2 V. The applied voltages were fixed at 0.3 V, 0.6 V, 0.9 V, and 1.2 V with the potentiostat, respectively. Current, electrode potentials and other parameters were monitored and recorded every minute using the potentiostat and EC-Lab v10.23 software installed on a computer. BLBRs were operated for three consecutive batches for each applied voltage to get reproducible results. Each batch of the BLBR run lasted for 10 days. This very short reaction time was chosen to evaluate the effects of applied voltage on anaerobic digestion in a shorter hydraulic retention time (meaning higher organic loading rate) in the BLBR.

4.2.4 Chemical Analysis

Total solids (TS), volatile solids (VS), total suspended solids (TSS), and total volatile solids (VSS) were quantified according to the Standard methods (APHA, AWWA & WEF, 2005). TS and VS of FW were analyzed at the beginning and end of the experiments to determine solid reduction. pH and ORP were measured using a pH meter TCOD, SCOD, volatile fatty acids (VFAs), ammonia nitrogen, pH and alkalinity of leachate were analyzed at Day 0, 2,

4, 7, and 10 during each operation. COD were analyzed by Hach COD digestion vials (Cat. No. 2125915-CA). Ammonia nitrogen was determined by Hach test kits (TNT832).

Volatile fatty acids (VFAs) including acetic acid, propionic acid, and butyric acid were analyzed by GC-FID as described in Chapter 3 (Swakshar & Lee, 2020). VFA concentrations were reported by normalizing each VFA species into equivalent concentration of COD. Biogas composition produced from the BLBR were monitored daily using a GC (model 310, SRI Instrument, 51 USA) equipped with a thermal conductivity detector (TCD) as described in Chapter 3. (Hussain et al., 2020). All measurement were carried out with triplicate.

4.2.5 Calculation

The VS removal, conversion efficiency of hydrolysis and acidogenesis of FW dry digestion in the BLBR were calculated according to Eq. (3-1), (3-2) and (3-3) in Chapter 3, respectively.

The coulombic efficiency (CE) of the BLBR was calculated using Equation (4-1), according to Lee et al., (2009):

$$CE = \frac{e^-_{transferred}}{\Delta e^-_{donor}} \qquad \text{Eq. (4-1)}$$

where $e^-_{transferred}$ is the total electrons transferred from anodes, which could be calculated via the integral of the current recorded and the time the experiment lasted; Δe^-_{donor} is the total electron equivalents converted from the organic electron donor, which could be calculated based on the substrate consumption.

Assuming that all the electrons transferred from the anodes in the BLBR were used for methane production through extracellular electron transfer, the theoretical volume of methane produced from electrons via EET could be calculated using Equation (4-2):

$$V_{EET} = V_m \frac{\int idt}{nF} \qquad \text{Eq. (4-2)}$$

where, V_{EET} is the cumulative methane yield from electrons via EET; V_m is the molar volume of gas; i is the current recorded by the EC-lab software during experiments; n is the number of electrons (equals to 8) to reduce one mole of CO_2 to CH_4; F is the Faraday constant 96,485 C/mol (Liu et al., 2016; Zhao et al., 2021).

Energy balance was calculated for energy consumption and recovery from methane for the BLBR, respectively. Energy consumption for the BLBR was calculated for pump operation and electric energy input, using Eq (4-3) to (4-5) (Li et al., 2016c; Xiong et al., 2019).

For pump operation energy consumption:

$$W_P = \frac{Q\gamma Ht}{1000} \qquad \text{Eq. (4-3)}$$

where, W_P is the energy consumption by the pumps (kWh); Q is the flowrate (m^3/s); γ is the specific weight (9,800 N/m^3); H is the hydraulic pressure head (m). For the BLBR in present experiments, the hydraulic pressure head was 0.25 m for mixing the leachate at a rate of 60 L/hr, and 0.64 m for leachate recirculation at a rate of 0.3L/hr. t is the operation time (240 hr).

For electric energy input:

$$W_E = IEt \qquad \text{Eq. (4-4)}$$

where, W_E is the electric energy input (kWh); I is the average current during the BLBR operation (A); E is the applied voltage for the BLBR (V); t is the operation time (240 hr).

For energy recovery from methane produced in the BLBR:

$$W_{CH_4} = \frac{\Delta H_S V_{CH_4}}{V_m \times 3600} \quad \text{Eq. (4-5)}$$

where, ΔH_S is the gross heating value of methane (890.3 kJ/mol); V_{CH4} is the cumulative methane production in the BLBR (L); V_m is the molar volume of gas under 25 ℃ (24.8 L/mol) (Li et al., 2016c).

4.2.6 Sample collection, DNA extraction and sequencing process

Leachate samples at the beginning and end of one batch operation, and FW residue samples after the same batch operation were collected and preserved by DNA/RNA Shield™ swab collection tubes (Zymo Research) at -20 ℃ before DNA extraction and sequencing.

DNA was extracted from the solid FW residue samples collected by the cotton swabs or 250 μL of liquid leachate sample preserved in DNA/RNA Shield collection tubes (Zymo Research, Irvine, CA, USA) by using the DNeasy® PowerSoil® Pro Kit (Qiagen, Valencia, CA, USA) according to the manufacturer's instructions. DNA purity was quantified using Nanodrop (Nano-300, Allsheng, Hangzhou, China), and DNA fragment sizes were checked via 2.0% agarose gel electrophoresis. The extracted DNA samples were stored at -80℃ degrees before sequencing. After DNA extraction, PCR amplification via primers, PCR products purification, libraries construction and sequencing were performed by Macrogen Inc. (Seoul, South Korea). The target V4 hypervariable region of the 16S rRNA genes were amplified using primer sets

515F (5’-GTGYCAGCMGCCGCGGTAA-3’) / 806rB (5’-GGACTACNVGGGTWTCTAAT-3’) and sequencing were performed using Illumina MiSeq platform. Only one sample of leachate, biofilms, and FW residue at each condition was analyzed due to limited resources.

4.2.7 Bioinformatics and statistical analyses

Bacterial and archaeal taxonomy were confirmed by genomics analysis. Based on the Mothur software package v1.45.3 (Schloss et al., 2009), paired-end reads were merged, contigs were generated and primer and barcode trimming, identification and removal of chimeric sequences and high-quality sequences were clustered into operational taxonomic units at a cutoff of 0.03 after quality filtering (Bae & Yoo, 2022). Reads assigned to non-bacterial and non-archaeal origins, such as chloroplast and mitochondrial genomes, were removed and OTUs were classified using training dataset based on the Silva v132 reference database (Kim et al., 2022). Rarefaction curves and alpha diversities were analyzed using Mothur software (Schloss et al., 2009). The rarefaction curves of the samples were used to confirm the sufficient sequencing depth of the various reactors (Kim et al., 2019). The total read counts per sample were 37722. Excel was used to determine the overall relative abundance of representative sequences at different taxonomic levels. Bacterial and archaea community structures were analyzed and compared separately. Statistical differences in microbial community structure between reactors were tested using the "vegan" package in the R software v4.2.1 (Oksanen et al., 2019) with analysis of similarities (ANOSIM) with 999 permutations.

4.3 Results and Discussion

4.3.1 Effect of different voltages on methane production

The cumulative methane yield with different voltages were displayed in Figure 4-2. In the control (open-circuit mode) which was set as the control, the methane yield was 199 $mLCH_4/gVS$. The methane production increased gradually for the first five days and slowed down to the end of operation. The cumulative methane yield in the BLBR with applied voltage 0.3V was 212 $mLCH_4/gVS$, which was similar to that of the control. For applied voltage 0.6 V, the methane yield increased to 240 $mLCH_4/gVS$, 20.6% higher than the control. When the applied voltage increased to 0.9 V, the cumulative methane yield was the highest at 293 $mLCH_4/gVS$, while it slightly reduced to 236 $mLCH_4/gVS$ at applied voltage 1.2 V. Although operation time was kept as short as 10 days in the BLBR, the methane yield was improved by 47.2 % over the control, indicating that EET on electrodes may contribute to the improvement of methane production in anaerobic digestion of FW. In addition, those BLBR tested with 0.6, 0.9, and 1.2 V showed faster methane production rate than that in the control during the first 5 days of operation. The improvement of methane yield and methane production rate with applied voltage was in consistence with other studies conducted in different MEC-AD systems in literature (Chen et al., 2016; Lee et al., 2019; Wang et al., 2021a; Zhao et al., 2016c). The decline in the methane yield when the applied voltage was further increased to 1.2 V was also consistent with other studies (Chen et al., 2016; Ding et al., 2016; Lee et al., 2019). This may attribute to the low cathode potential at higher applied voltage which would cause alkaline condition and high pH may inhibit some methanogens and therefore decrease methane production (Feng et al., 2015). The final pH in the leachate in the BLBR with 1.2 V was 8.2, which was higher than that in the BLBR with 0.3, 0.6, and 0.9 V (pH 7.8, 7.9, and 8.0,

respectively), and high pH may result in the decreased in methane yield in the BLBR with 1.2 V by inhibiting the activity of methanogens and decreasing methanogenesis (Chen et al., 2016; Feng et al., 2015; Wang et al., 2022).

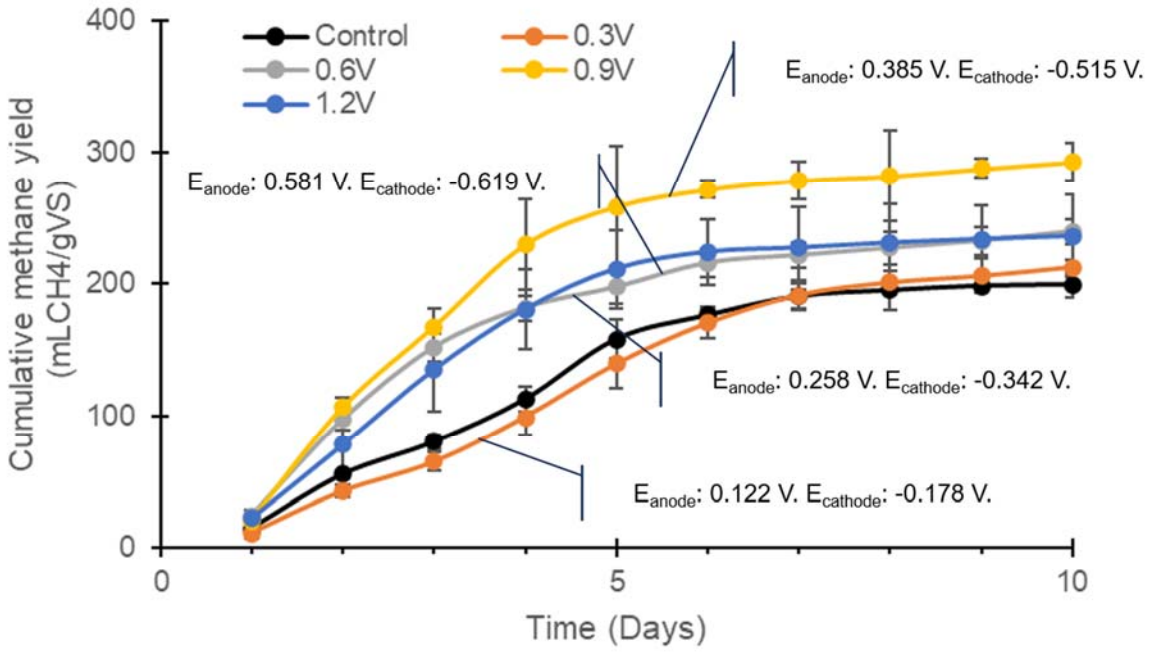

Figure 4-2. Cumulative methane yield in the BLBRs with different applied voltage. Anode and cathode potential under each applied voltage were also displayed.

4.3.2 Organic removal and solubilization

The impacts of applied voltage on solid removal involved in the BLBR against the control were investigated (Figure 4-3). VS removal in the control was 74.3%, which was slightly improved to 75.6%, 77.6%, 74.7%, and 75.2% in the BLBR at applied voltage of 0.3 V, 0.6 V,

0.9 V, and 1.2 V, respectively, but no significant differences were observed between the BLBR with applied voltage and the control ($p>0.05$). Some studies suggested that the hydrolysis of FW and other organic waste could be promoted with applied voltage, while others showed little promotion on the hydrolysis during AD (Chen et al., 2020; Sun et al., 2015; Yu et al., 2018; Zhao et al., 2021). The present study also showed little enhancement on FW hydrolysis in the BLBR with applied voltage, which also indicated that applied voltage did not improve the hydrolysis during AD of FW. In addition, hydrolysis of solid FW relies on the secretion and metabolism of different hydrolases, while the hydrolysis of FW in the BLBR occurred in the FW basket which was not submerged in the leachate with the electrodes (Chen et al., 2020; Duong et al., 2019). Therefore, FW solubilization in the basket may not be affected directly by the applied voltage.

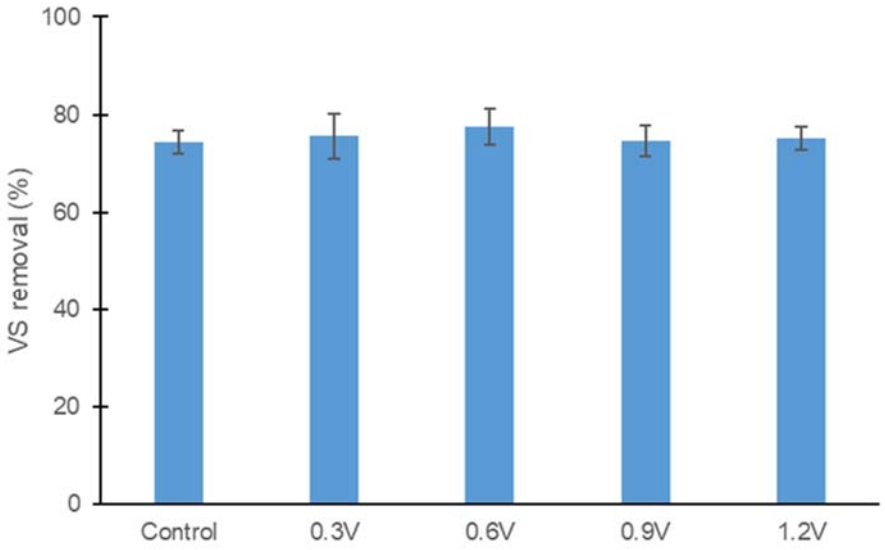

Figure 4-3. VS removal in the BLBR operated with different applied voltage.

As shown in Figure 4-4a, SCOD (containing VFAs and other soluble organic matters) increased in the early time of the operation as result of the hydrolysis of solid organic matters, and decreased due to methane production. The accumulation time of SCOD in the BLBR continued for two days, while the SCOD accumulated during the first four days in the control. For the BLBR at 0.3 V applied voltage, the SCOD concentrations reached a peak value of 16.8 gCOD/L after 2 d, which was almost twice the peak SCOD level in the control. The BLBR at other applied voltages consistently showed steeper increase and decrease of SCOD than the control. This result implies that applied voltage would indirectly stimulate solubilization and accelerate fermentation (e.g., acidogenesis) in BLBR, although VS removal was not affected much. Under applied voltage, enhancement of fermentation and methanogenesis in the BLBR can pull solubilization of organic matters thermodynamically (Wang et al., 2022).

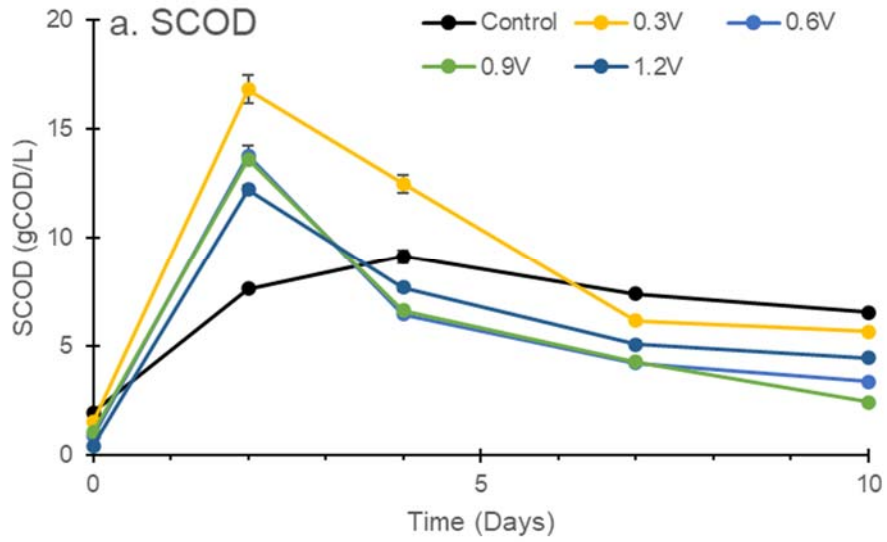
a. SCOD
Control
0.3V
0.6V
0.9V
1.2V
SCOD (gCOD/L)
20
15
10
5
0
0
5
10
Time (Days)

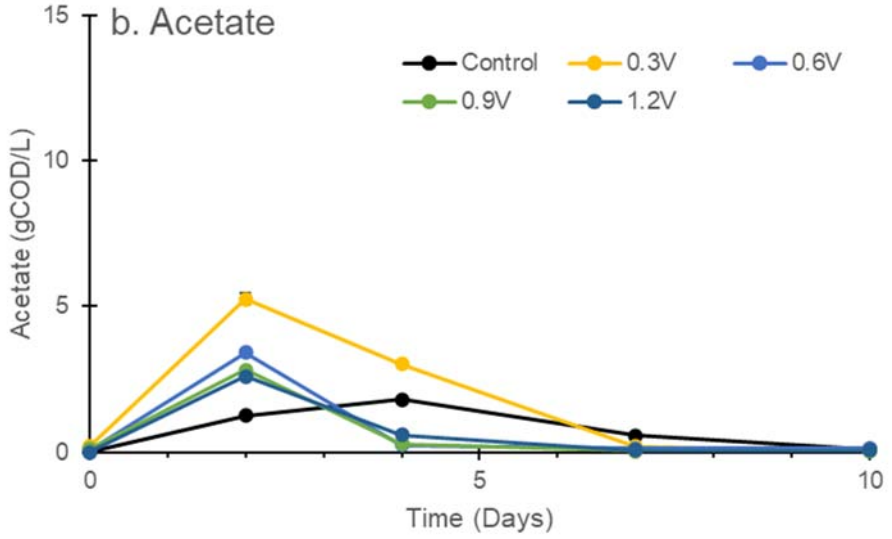
b. Acetate
Control
0.3V
0.6V
0.9V
1.2V
Acetate (gCOD/L)
15
10
5
0
0
5
10
Time (Days)

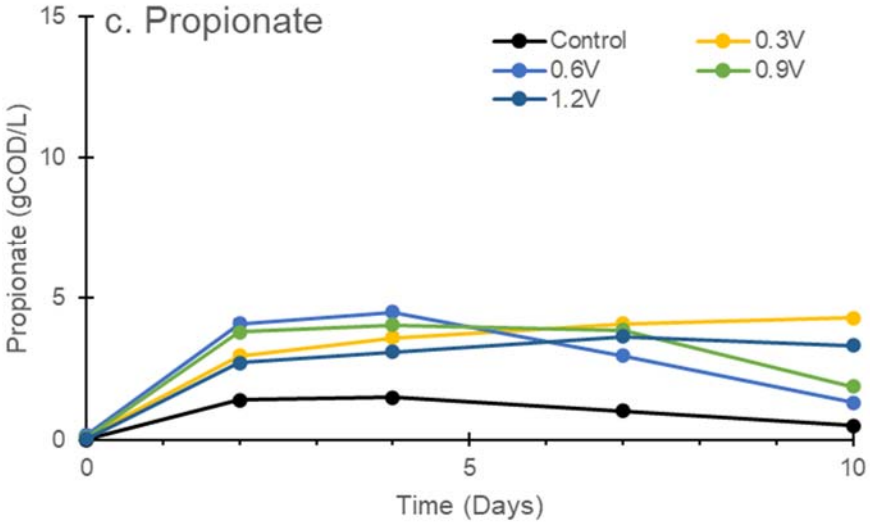
c. Propionate
Control
0.3V
0.6V
0.9V
1.2V
Propionate (gCOD/L)
15
10
5
0
0
5
10
Time (Days)

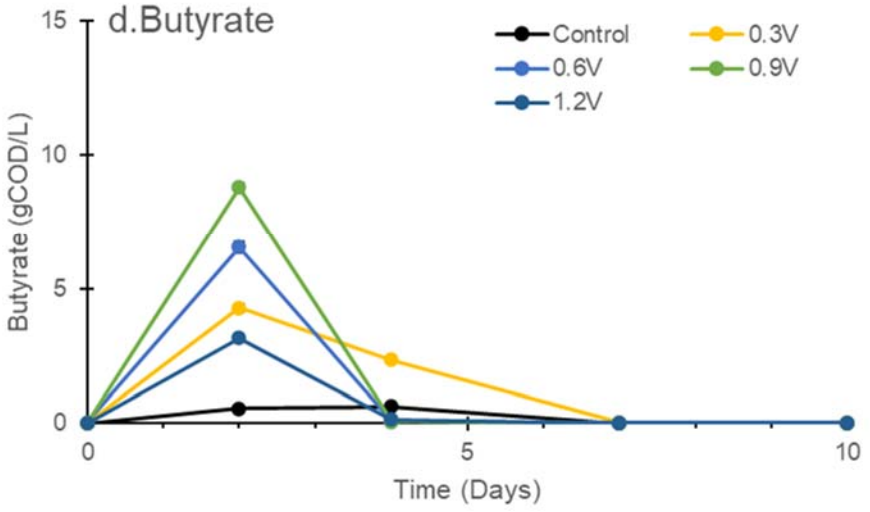
d.Butyrate
Control
0.3V
0.6V
0.9V
1.2V
Butyrate (gCOD/L)
15
10
5
0
0
5
10
Time (Days)

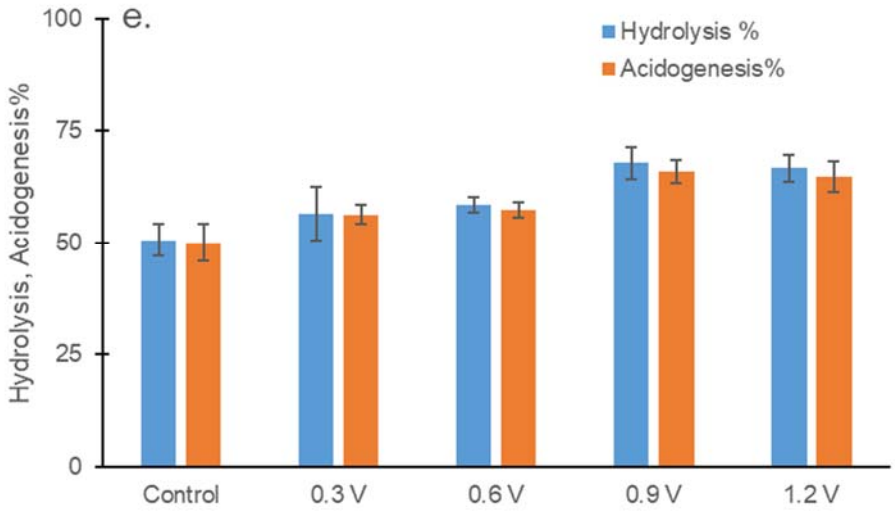

Figure 4-4. SCOD (a), acetate (b), propionate (c), butyrate level (d), and hydrolysis and acidogenesis efficiency (e) during operation.

Figure 4-4b, 4-4c, and 4-4d showed VFA profiles during operation with different applied voltages. Acetate, propionate, and butyrate were the major VFAs in the leachate for all runs in the BLBR and the control, accounting for more than 70% of the SCOD within 2 days of operation. Acetate, which was a favorable substrate for methanogens, showed a rapid increase consistent to SCOD profile (Figure 5-4b). After 2 days of operation, acetate reached its peak values: 5.23 gCOD/L (0.3 V), 3.41 gCOD/L (0.6 V), 2.82 gCOD/L (0.9 V), and 2.60 gCOD/L (1.2 V). After that, acetate was rapidly consumed, and it was below 0.1 gCOD/L (<1.56 mM acetate). In comparison, acetate gradually increased and reached a plateau of 1.50 gCOD/L after 4 days of operation in the control, which was also consistent with the SCOD trend in the control. Acetate is an important intermediate during AD process and can be produced by acidogenesis and acetogenesis. The elevated acetate concentrations during the early period of operation in the

BLBR system indicated that applied voltage would improve production of acetate both from fermentation and acetogenesis under applied voltage. Acetate is the substrate for acetoclastic methanogen, by which methane is produced by acetate dismutation. Elevated acetate levels may also improve the acetoclastic methanogenesis and therefore enhance the methane production. In addition, increased acetate may stimulate ARB like *Geobacter* to use acetate as substrate for EET and DIET, and improve the methane production with the syntrophic interactions between hydrogenotrophic methanogen and ARB (Clauwaert & Verstraete, 2009; Liu et al., 2019; Zakaria & Dhar, 2019; Zhang et al., 2019; Zhao et al., 2021). The competition for substrate between ARB and acetoclastic methanogen may also alter the microbial community structure and further affect the EET and DIET pathways on anode (Xiao et al., 2020).

Propionate profiles did not show any abrupt changes, compared to acetate and butyrate (Figure 4-4c), although propionate concentration in the leachate of the BLBR was higher than that of the control. In the BLBR with 0.3 V applied voltage, the propionate level kept increasing until the end of operation and reached as high as 4.3 gCOD/L (38.5 mM). When the applied voltage increased, the propionate level also increased. The BLBR with 0.6 and 0.9 V showed declines in the propionate concentration after 4 days of operation, while the propionate level in the BLBR with 1.2 V was quite similar to that in the BLBR with 0.3 V. This result indicated that MEC-AD would improve the acidogenesis for propionate production at a certain voltage range.

Propionate is a common intermediate for acidogenesis step, which is normally fermented to acetate and hydrogen via acetogenesis (Wang et al., 2022). However, the acetogenesis of propionate into acetate and hydrogen is thermodynamically unfavorable under standard conditions with a positive Gibbs free energy of +76.1 kJ/L. Syntrophic acetogenesis of propionate relies on the consumption of hydrogen produced from the fermentation of propionate

by the hydrogenotrophic methanogens (Dhar et al., 2013; Feng et al., 2015; Siriwongrungson et al., 2007). Therefore, the balance between the production (acidogenesis) and consumption (acetogenesis) terms partially explained those quite stable propionate concentrations with time in the BLBRs.

Moreover, studies on MEC assisted AD systems have shown little evidence of propionate accumulation at the end of operations. A possible explanation is that the enrichment of hydrogenotrophic methanogen would rapidly utilize hydrogen produced from propionate fermentation and maintain an extremely low hydrogen partial pressure (Cerrillo et al., 2017; Chen et al., 2016; Hari et al., 2017; Liu et al., 2016b; Wang et al., 2021b; Zhao et al., 2016c, 2021). Considering the longer operation time (20-135 days) in those studies and shorter time (10 days) in present study, the almost stable level of propionate in the BLBR may also decrease with extended operation time. Future experiments with longer operation time on the BLBR are needed to further identify the fate and pathway of propionate during AD process in the BLBR.

Butyrate accumulation and degradation also showed similar trend to acetate (Figure 4-4d). In the BLBR, butyrate concentration increased rapidly within 2 days of operation followed by abrupt consumption. The peak value of butyrate increased from 4.2 gCOD/L in the BLBR with 0.3 V, to 8.8 gCOD/L in the BLBR with 0.9V which was the maximum among all the BLBR operations. When the applied voltage further increased to 1.2 V, the butyrate peak level went back to 3.2 gCOD/L. As comparison, butyrate was only reached to 0.6 gCOD/L in the control after 4 days of operation, which was 14.6 times lower than the maximum butyrate concentration in the BLBR with 0.9 V. The maximum butyrate concentration and rapid consumption in the BLBR may indicate that acidogenesis and acetogenesis of butyrate were both improved under applied voltage. Acetogenesis of butyrate for acetate and hydrogen would also

become thermodynamically favorable with extremely low hydrogen partial pressure, which would also be achieved by the enrichment of hydrogenotrophic methanogen in MEC-AD system (Wang et al., 2021a; Zhao et al., 2021).

Under applied voltage, the microbial activities would determine the efficiency of hydrolysis, acidogenesis, and methanogenesis during the AD process (Figure 4-4e). When the applied voltage increased from 0.3 V to 0.9 V, the hydrolysis and acidogenesis efficiencies both increased and these efficiencies achieved the maximum values at 0.9 V. When the applied voltage further increased to 1.2 V, the hydrolysis and acidogenesis efficiencies both slightly decreased, which suggested mild inhibition on hydrolysis and acidogenesis during operation. Significant differences on the hydrolysis and acidogenesis efficiencies were observed by one-way ANOVA ($p < 0.05$) among the BLBR with applied voltages and the control. These results indicated that voltage application could improve the hydrolysis and acidogenesis within a certain voltage and therefore more substrate for methanogenesis would be produced to promote the methane production in the BLBR. Therefore, 0.9 V could be selected as the optimal applied voltage for enhanced methane production when using the BLBR for FW dry digestion.

4.3.3 Microbial community structure under applied voltage

The microbial community structures of electrode biofilm samples under each applied voltage, as well as the leachate and food waste residue, were characterized by 16s rRNA sequencing. The Shannon index in each condition showed a decrease from leachate samples to the electrode (anode and cathode) biofilm and food waste residue (Table 4-1). A greater reduction in the Shannon index was found in the anode and cathode biofilms of all conditions,

compared to the food waste residue samples. It also worth noting that the Shannon index of cathode biofilm at applied voltage 0.9V decreased from 4.38 (leachate samples) to 3.64, and at applied voltage 0.3V the Shannon index of cathode biofilm decreased from 4.42 to 3.56. Shannon Index represents the diversity of species in the microbial communities and a decrease in Shannon Index suggests a decrease in the diversity of microbial species in these samples. This indicated that an applied voltage would selectively enrich those functional microorganisms in electrode biofilms, especially cathode biofilm, which may benefit and improve the BLBR system performance.

Table 4-1. Shannon index of different samples under different conditions.

Condition	Leachate	Anode	Cathode	Food waste residue
OCM	4.42	3.77	3.76	3.92
0.3V	4.42	3.83	3.56	4.05
0.6V	4.47	3.87	3.98	4.07
0.9V	4.38	3.81	3.64	4.13
1.2V	4.57	3.98	4.07	4.28

(1) Bacteria in the BLBR

The relative abundance of different phylotypes in the leachate, electrode biofilms, and food waste residue samples were shown in Figure 4-5a. Firmicutes, Bacteroidetes, and Actinobacteria were dominant in all the samples. Especially, they accounted for more than 80% of the bacterial phylum in those anode and cathode biofilms in the BLBR. Firmicutes, Bacteroidetes, and Actinobacteria contain a large number of fermentative bacterial genera

(*Chlostridium*, *Trichococcus*, *Brooklawnia*, *Corynebacterium*, etc.) which are capable of conducting hydrolysis and acidogenesis. With applied voltage, the abundance of those bacterial phyla showed increase to different extent in those electrode biofilms, as compared to the leachate samples. It is also worth noting that the phylum Proteobacteria, including a variety of bacterial genera capable of electron-producing and EET (i.e., *Geobacter*), was more enriched in the anode biofilm (1.97%) than in the cathode biofilm (0.69%) at applied voltage 0.9V, which may contribute to the enhanced performance of methane production.

Figure 4-5b shows the relative abundance of bacterial genera in the leachate, electrode biofilms, and food waste residue samples under different conditions. The genus *Clostridium*, which is capable of carbohydrates fermentation and VFA production including acetate and butyrate, had high abundance in the BLBR (Wiegel et al., 2006). Specifically, the highest abundance of this genus was observed in the anode biofilms at applied voltage of 0.6V and 0.9V, which were both 5.3 times higher than that in the leachate samples, respectively. The genus *Corynebacterium* is also capable of fermentation and was low in abundance in the control's samples, but it also showed elevated abundance in those electrode biofilms than in the leachate samples in the BLBR (Tauch & Sandbote, 2014). The abundance of other fermentative bacteria, including *Christensenellaceae, Trichococcus*, *Brooklawnia*, and *Syntrophomonas*, remained stable or had small variation between leachate and electrode biofilms. In contrast, the genus *Jeotgalibaca* decreased significantly from all the samples in the BLBR, compared to the control. The genus *Jeotgalibaca* was observed with relative high abundance in those LBR operated without electrodes (Chapter 3, Figure 3-7a). Therefore, such bacterial genus may not be adapted to the environment in a bioelectrochemical system. The bacterial community structures between food waste residue and leachate samples at all conditions were quite similar, suggesting that

metabolic reactions in the FW basket of the BLBR and in suspension would not be changed much between the BLBR and control. In addition, the total abundance of fermentative bacterial genera (mainly *Clostridium*, *Christensenellaceae*, *Trichococcus*, and *Brooklawnia*) decreased in the cathode biofilm than in the anode biofilm in the BLBR. These results indicate that the applied voltage would selectively enrich fermentative bacteria in the anode biofilms for organic fermentation and VFA production.

Several possible microorganisms isolated or co-cultivated are responsible to degrade propionate between the syntrophic propionate-oxidizing bacteria (SPOB) and methanogens (Stam, 1994), including species belong to the genera *Smithella*, *Syntrophobacter*, *Pelotomaculum*, *Desulfotomaculum* and *Cloacimonetes* (de Bok et al., 2001; Galushko and Kuever, 2019; Imachi et al., 2007; Liu et al., 1999; McInerney et al., 2008; Nilsen et al., 1996; Pelletier et al., 2008). Among them, *Smithella propionica* is the only SPOB known to carry out dismutation of propionate to acetate and butyrate (Liu et al., 1999; de Bok et al., 2001). Butyrate can be further oxidized by *Syntrophomonas* to acetate and hydrogen for methane production with its syntrophic methanogen partner (Liu et al., 1999). Others like *Syntrophobacter* could oxidize propionate to acetate and CO_2 associated with sulfate reduction (Galushko and Kuever,2019). Studies about syntrophic propionate oxidization raised a hypothetical syntrophic network for complete propionate oxidation. In the network, SPOB like *Smithella* associated with *Methanobacterium* would play an important role in dismutation of propionate into acetate and butyrate. The butyrate produced would be further degraded by *Syntrophomonas* and its associated methanogen (Jannat et al., 2021; Liu et al., 2011; Westerholm et al., 2022).

On one hand, the abundance of these SPOB were relatively low (<4%) in leachate and electrode biofilm samples of the BLBR and the control, among which the butyrate-oxidizing

bacteria *Syntrophomonas* accounted for the highest abundance (77-92%) (Figure 4-6a). The low abundance of SPOB may indicate the syntrophic propionate oxidizing pathway by SPOB was not active in the BLBR, in which higher propionate concentrations were observed. On the other hand, it is reported that SPOB have much lower specific growth rates and larger substrate half-saturation constants than acetate and butyrate. Larger half-saturation constant value of propionate indicates that it would be more difficult for microbes to utilize propionate for growth and proliferation (Li et al., 2020). Therefore, the elevated propionate levels may suggest a slow propionate utilization rate in the BLBR and hence reflect different microbial activity levels and VFA degradation and methanogenesis pathways under applied voltage. However, this result could not exclude other pathways for propionate degradation in the BLBR. The lack of active SPOB in the leachate and anode biofilms may be attributed to the short operation time (10 days) in present experiments. Considering the very low abundance of SPOB (0.23%) in the original WWTP anaerobic digested sludge, longer operation or acclimation period for enrichment of more active SPOB in the inoculum in order to promote syntrophic propionate degradation could be an effective way to improve the propionate degradation and methane production when built the microbial communities in the BLBR (Wang et al., 2021a; Chen et al., 2016; Jannat et al., 2021; Westerholm et al., 2022).

Potential ARB including *Geobacter*, *Desulfomicrobium*, and *Desulfobulbus,* which could participate EET between microorganisms and electrodes, were also detected in the anode biofilms in the BLBR (Holmes et al., 2004; Müller et al., 2016; Pfeffer et al., 2012; Rabaey et al., 2004; Scholz et al., 2019). With the increase in applied voltage from 0.3 to 1.2V, the relative abundance of *Geobacter* in the anode biofilm increased by 25.0%, 66.7%, 212%, and 514%, respectively. Furthermore, the total abundance of those potential ARB capable of EET also

increased along with the increase in applied voltage, although the highest population was only 1.78% of the anode biofilm community. The low abundance of *Geobacter* detected on anode biofilm may be attributed to the positive anode potential in the BLBR. For example, the anode potential varied between +0.3 and +0.4 V (vs SHE) in the BLBR with 0.9 V applied voltage during operation and *Geobacter* population would not dominate the community under this positive anode potential, which was in consistence with other study (Dhar et al., 2016). In addition, several bacterial genera including *Clostridium*, *Trichococcus*, *Syntrophomonas*, *Corynebacterium*, and *Petrimonas* have been reported with the potential to participate EET or DIET within biofilm community (Baek et al., 2015; Jiang et al., 2022; Li et al., 2016c; Lin et al., 2022; Liu et al., 2010b; Ren et al., 2020; Saheb-alam & Persson, 2019; Zhao et al., 2012). Their total abundance accounted for 35.2-40.0% in the anode biofilm of the BLBR, compared to that of 22.7% in the control. As a result, the anode biofilm in the BLBR may also show high conductivity for electron transfer via EET and DIET, even with low *Geobacter* abundance. A survey has also identified more than 90 microbial species already existed which are electroactive and more potential species capable of EET and DIET exist in natural and artificial engineered systems (Koch & Harnisch et al., 2016). Therefore, the potential EET-based syntropy, or "electric syntrophy", in the anode biofilm may be more widespread than expected to improve the methane production in the BLBR (Kouzuma et al., 2015).

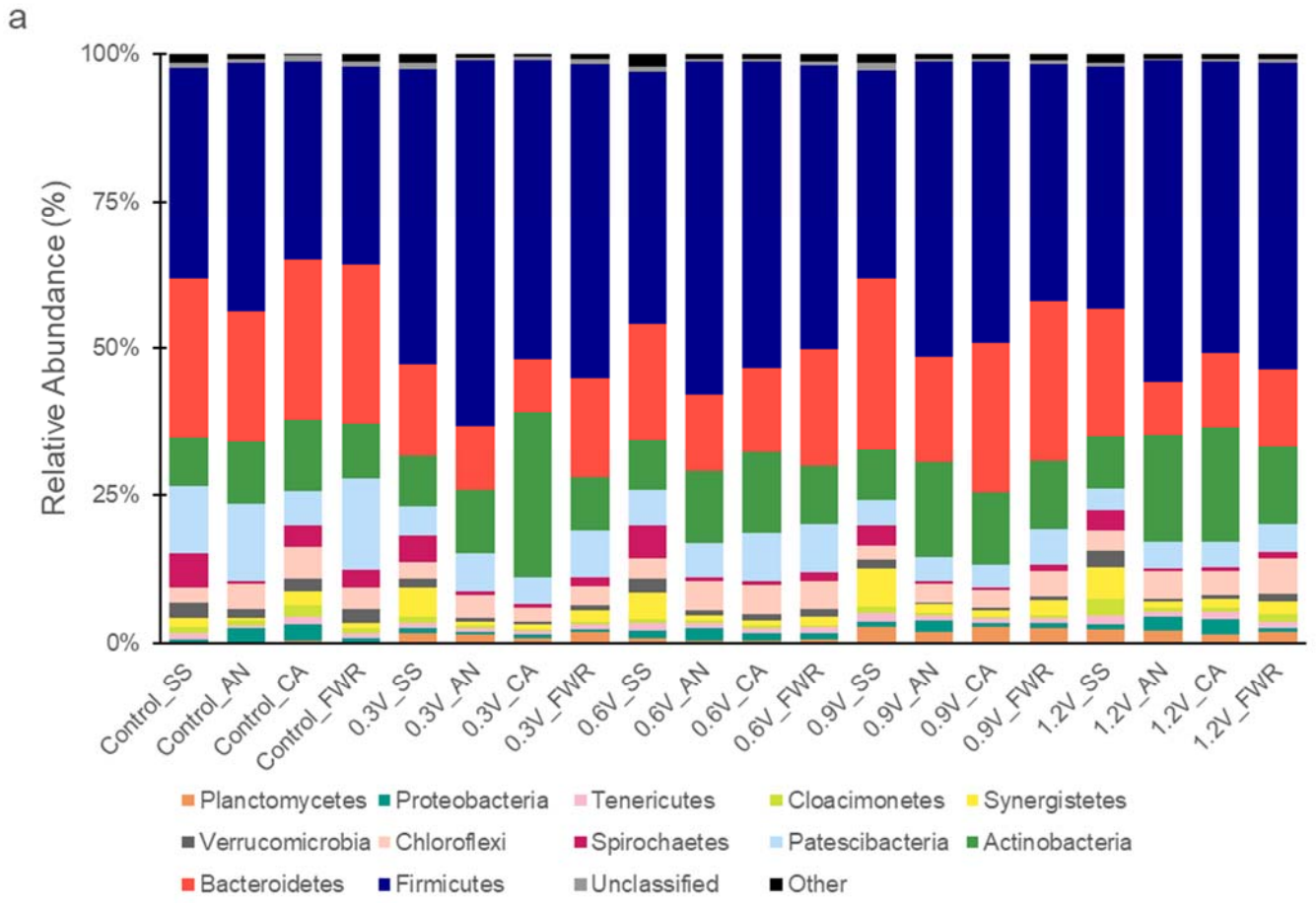
a
100%
75%
50%
25%
0%
Relative Abundance (%)
Control_SS
Control_AN
Control_CA
Control_FWR
0.3V_SS
0.3V_AN
0.3V_CA
0.3V_FWR
0.6V_SS
0.6V_AN
0.6V_CA
0.6V_FWR
0.9V_SS
0.9V_AN
0.9V_CA
0.9V_FWR
1.2V_SS
1.2V_AN
1.2V_CA
1.2V_FWR
Planctomycetes
Proteobacteria
Tenericutes
Cloacimonetes
Synergistetes
Verrucomicrobia
Chloroflexi
Spirochaetes
Patescibacteria
Actinobacteria
Bacteroidetes
Firmicutes
Unclassified
Other

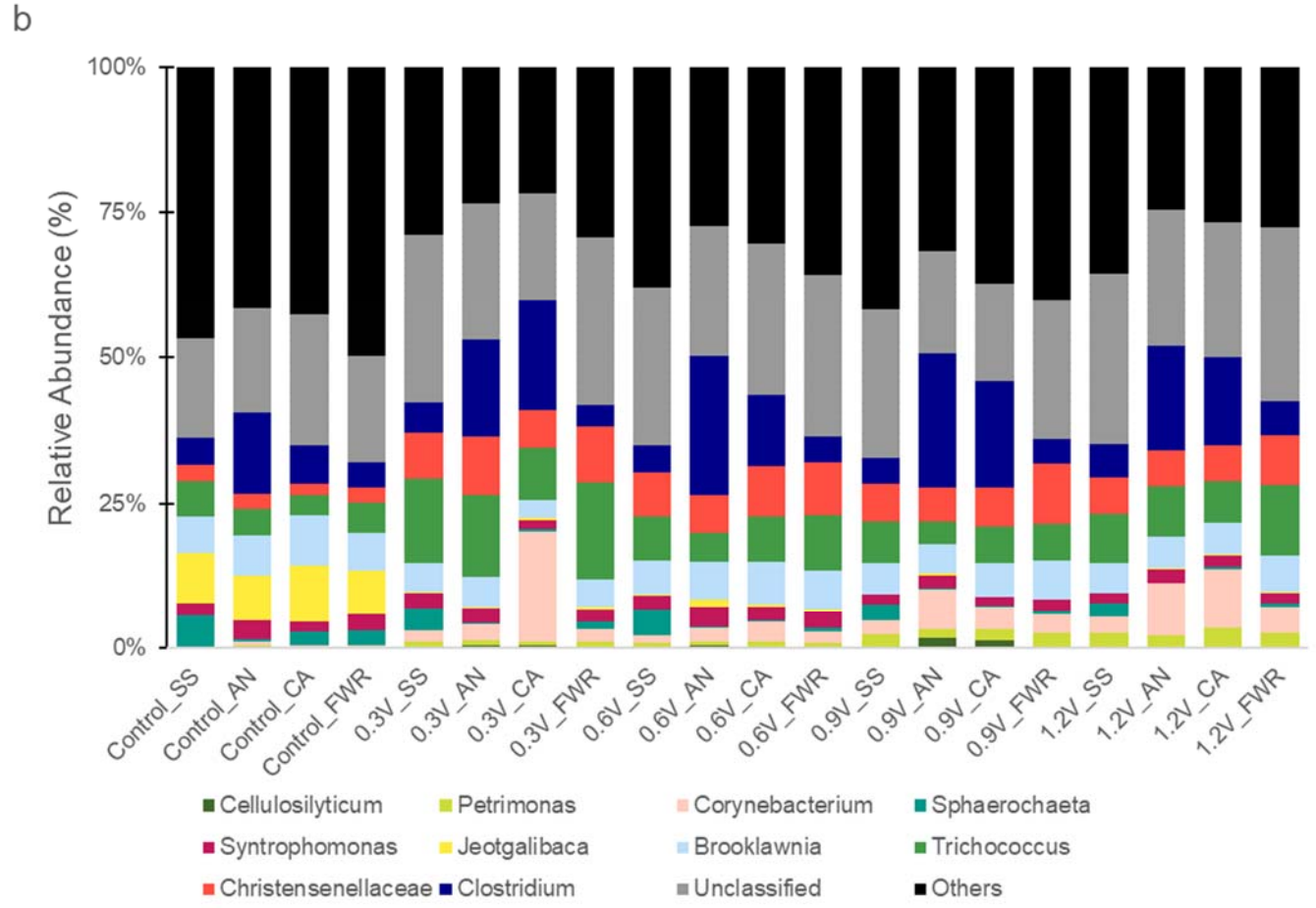
b
100%
75%
50%
25%
0%
Relative Abundance (%)
Control_SS
Control_AN
Control_CA
Control_FWR
0.3V_SS
0.3V_AN
0.3V_CA
0.3V_FWR
0.6V_SS
0.6V_AN
0.6V_CA
0.6V_FWR
0.9V_SS
0.9V_AN
0.9V_CA
0.9V_FWR
1.2V_SS
1.2V_AN
1.2V_CA
1.2V_FWR
Cellulosilyticum
Petrimonas
Corynebacterium
Sphaerochaeta
Syntrophomonas
Jeotgalibaca
Brooklawnia
Trichococcus
Christensenellaceae
Clostridium
Unclassified
Others

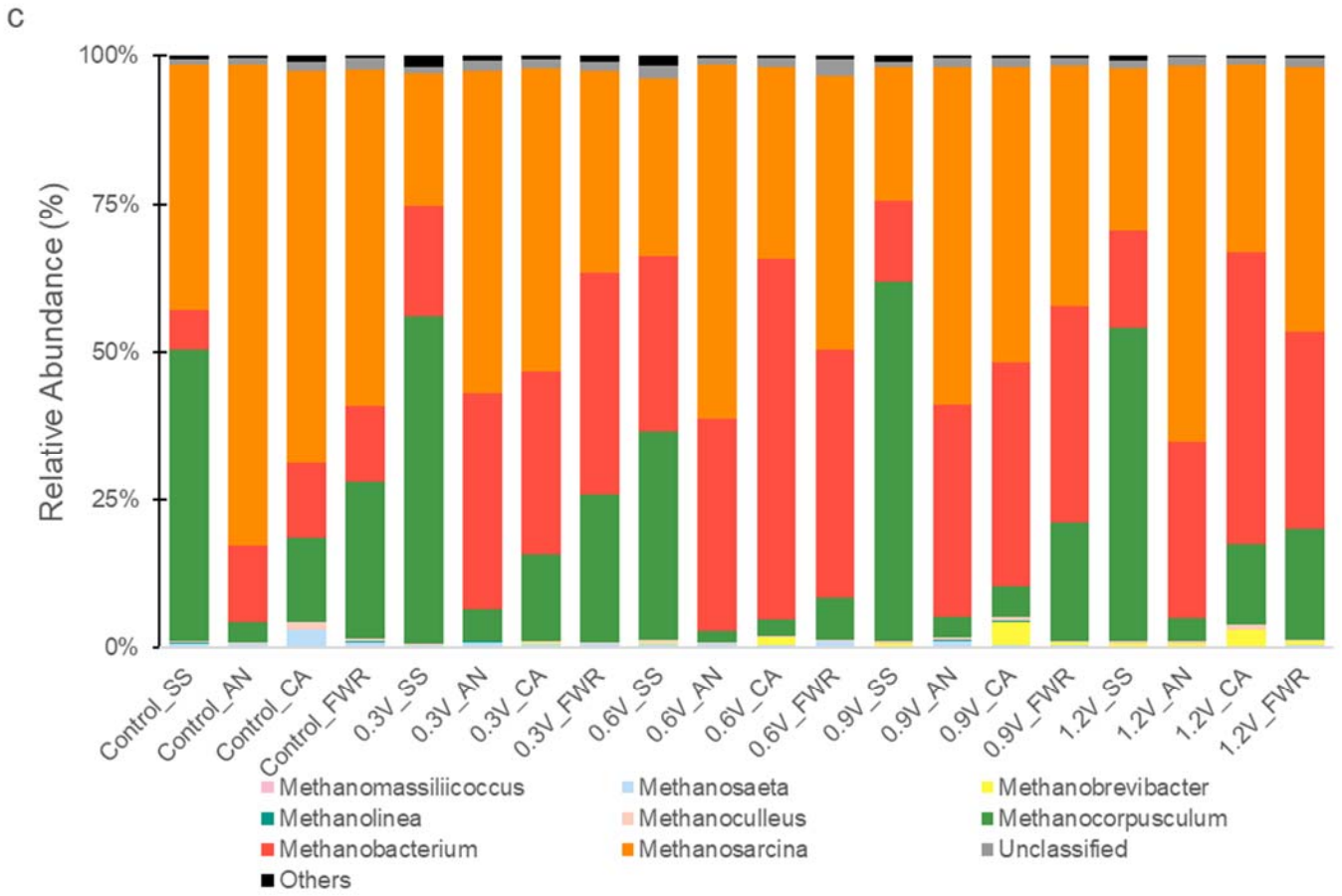

Figure 4-5. Relative abundance of microbial communities in leachate, electrodes, and food waste residue of the BLBR under different conditions at (a) bacterial phylum level, (b) bacterial genus level, and (c) archaea genus level. SS: leachate. AN: anode. CA: cathode. FWR: food waste residue.

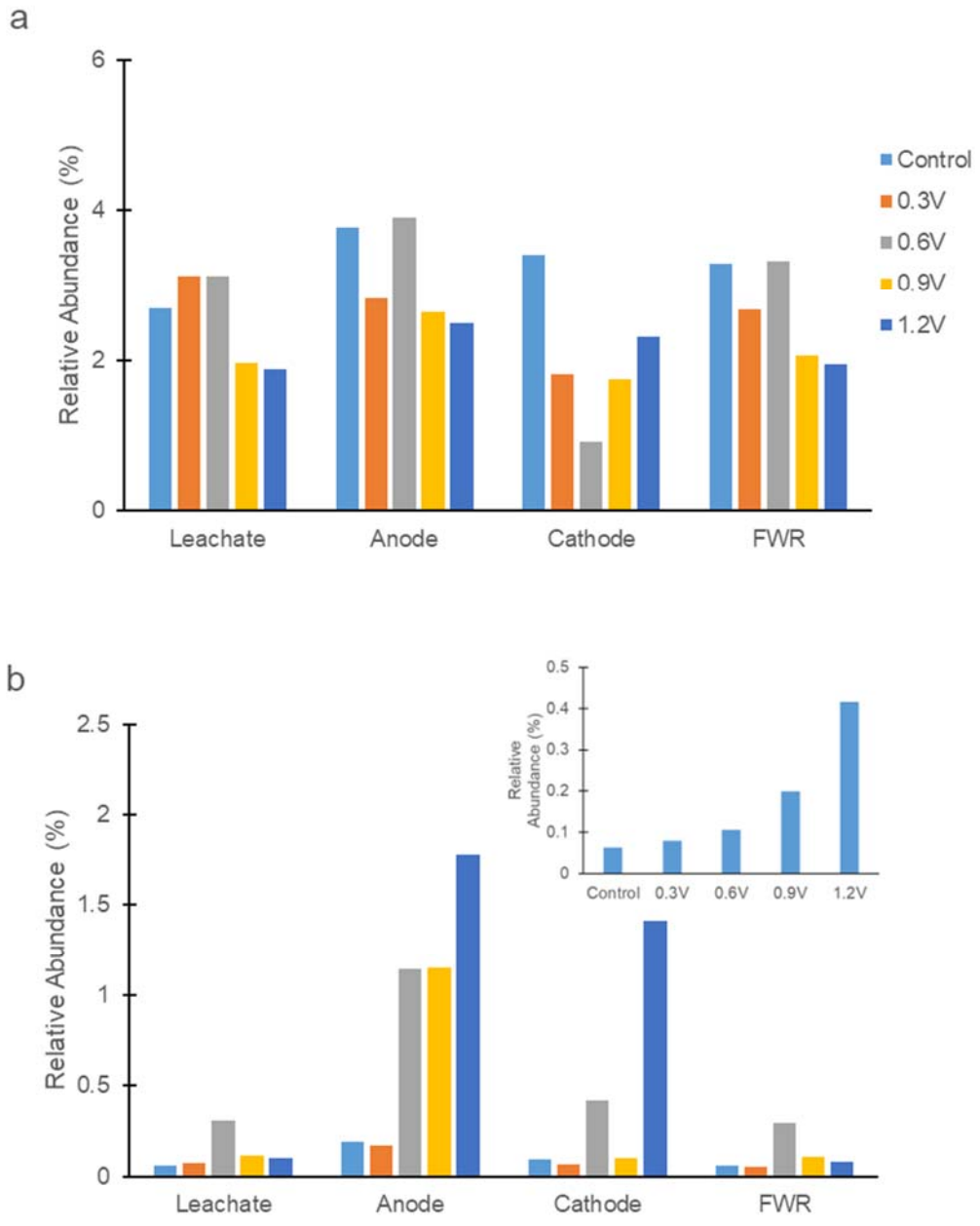

Figure 4-6. Relative abundance of (a) SPOB and (b) total bacteria genera which could participate EET in the leachate, electrode biofilms, and FW residue samples under different conditions. Inset: relative abundance of the genus *Geobacter* in the anode biofilm samples under different conditions.

(2) Archaea in the BLBR

When the BLBR was operated with applied voltages, the dominant methanogens in the cathode biofilm changed distinctively (Figure 4-5c). *Methanobacterium*, a hydrogenotrophic methanogen, was shown significant increase in all the cathode biofilm samples in the BLBR over the control (12.5% of archaea in the biofilm). The highest abundance of *Methanobacterium* was observed with 61.0% in the cathode biofilm at applied voltage 0.6V, while other conditions also had 39.4 to 40.9% abundance in their cathode biofilms, compared to that of 12.5% in the cathode biofilm in the control. This genus has been proven to participate direct or indirect interspecies electron transfer in syntrophic methanogenesis (De Vrieze et al., 2018). Meanwhile, the genus *Methanosarcina*, which can perform both acetate dismutation and CO_2-reduction for methane production and be capable of accepting electrons from nonbiological extracellular surfaces, also accounted for a relatively high abundance (31.8 - 51.2%) of the archaea community in the cathode biofilm in the BLBR (Rotaru et al., 2014a). Therefore, the prevailing abundance of *Methanobacterium* and *Methanosarcina* (accounting for 82.2 - 93.6% in total) in cathode biofilm indicated that the cathode biofilm might accept electrons from the cathode for methane production more effectively and promote the methane production.

In addition, the anode biofilm also showed dominant abundance of *Methanobacterium* and *Methanosarcina*, accounting for totally 91.1 - 95.8% of the archaea in anode biofilm under different applied voltages, which was quite similar to the total abundance of 94.3% in the anode biofilm for the control (Figure 4-5c). The high abundance of *Methanobacterium* and *Methanosarcina*, together with the small but increasing number of bacteria capable of EET, may also suggest that those anode biofilms could become another possible place for syntrophic methanogenesis between ARB and methanogens via DIET.

The present experimental results indicated that the BLBR with applied voltage improved the methane production. Literature have proved that enhanced methanogenesis in those MEC assisted AD systems was related to the enrichment of hydrogenotrophic methanogens with CO_2 reduction by receiving electrons directly from cathode or by using hydrogen produced on the cathode (Wang et al., 2021a; Zhao et al., 2021). As a result, electrons from VFAs were transferred to anode and further to cathode, where electrons were captured by hydrogenotrophic methanogen for carbon dioxide reduction. Therefore, the theoretical methane production from this type of EET in the BLBR could be estimated and further used to identify the contributors to the enhanced methane production (Table 4-2).

The highest theoretical methane yield from EET via closed-circuit at an applied voltage of 1.2 V was 1.69 L, which accounted for only 10.1% of the total methane yield during the operation. Under this situation, the CE of the BLBR was only about 6% with an average current density of 7.4 A/m^2. The theoretical methane yield via EET in the BLBR system was far smaller than the total methane production, which indicated that methane production via EET through closed circuit could not contribute to the improved methane yield. The enhanced methane production may be attributed more to the improved acidogenesis and acetogenesis under applied voltage which increase the substrate (VFAs) for methane production (Wang et al., 2021a).

Table 4-2. Theoretical methane production and Coulombic efficiency (CE) of the BLBR with each applied voltage

Group	0.3 V	0.6 V	0.9 V	1.2 V
V_{EET} (L)	0.026	0.49	1.62	1.69
V_{Total} (L)	15.3	17.3	21.1	17.0
% of V_{EET} in total methane production	0.17	2.88	7.66	10.1
CE (%)	0.10	1.51	4.96	6.08

V_{EET}: theoretical methane production assuming all electrons transferred from anode are used for methane production.

The relatively low theoretical methane production via EET and low CE were attributed to the low electron transferred via closed circuit from the anode to the cathode. This result may indicate either only a small portion of electrons were delivered by ARB to the anode or the anode biofilm was not as conductive as expected. The conductivity of biofilm was often believed to result from the abundance of *Geobacter* (Barua et al., 2018; Dhar et al., 2016; Li et al., 2016a, 2018a). The microbial community structure analysis revealed that the abundance of the genus *Geobacter* in the anode biofilm showed increase with the increasing applied voltage, but the relative abundance of *Geobacter* was still lower than 0.5% (Figure 4-6b inset). Other genera including *Desulfomicrobium* and *Desulfobulbus* also known to participate EET were also found with low abundance in the anode biofilm (Figure 4-6b). However, the measured biofilm conductivity of those BLBR biofilm grown on split gold electrodes showed a biofilm conductivity about 150 μS/cm when the anode potential ranged between +300 and +400 mV,

which was 10% less than that of *Geobacter*-enriched biofilm. Details about the biofilm conductivity will be shown in Chapter 6. Therefore, the anode biofilm could still be recognized as conductive for electron transfer.

In addition, bacteria other than common ARB such as *Geobacter* could also participate in EET and DIET. For example, in one study the anode biofilm of the MEC-AD was detected with low abundance of *Geobacter* but high in *Clostridium* and the MEC-AD still showed improved methane production as compared to the control, with CE of 43% and current density of 51.4 A/m^2 in the system (Li et al., 2016c). This result indicated that anode biofilm with low ARB abundance could still be active in metabolizing the substrate and delivering electrons to anode.

Further, interspecies substrate competition between different microbes in anode biofilm may also increase the current generation and EET (Xiao et al., 2021). Interspecies substrate competition would increase the metabolic activities of ARB and benefit the conductive biofilm formation on the anodes, which would improve EET and current generation by up-regulating proteins expressions related to biofilm formation, c-type cytochromes synthesis, and flavin secretion (Xiao et al., 2021). Those results proved the complexity and diversity of the EET-based syntrophy in anode biofilms and showed the potential of such anode biofilms for high current generation in the BLBR.

On the other hand, the low number of electrons delivered from anode to cathode would limit the electrons that could participate DIET-induced methanogenesis on the cathode, but this would not exclude other types of DIET-induced methanogenesis. As can be seen from Figure 4-5c, the genus *Methanocorpusculum*, which can carry out methane production by CO_2 reduction, was maintained higher abundance in the leachate than in the electrode biofilms in the BLBR. The elevated VFAs in the leachate would promote the syntrophic or DIET-induced methanogenesis

with *Methanocorpusculum* by metabolizing the substrates to acetate, CO_2 and H_2 for ARB and hydrogenotrophic methanogens and hence enhance the methane production (Feng et al., 2018; Li et al., 2016c; Liu et al., 2016b). In addition, the genus *Methanosarcina* was also found with high abundance (54.4~63.5%) in the anode biofilm (Figure 4-5c) and *Methanosarcina* is the genus which can use both acetate and CO_2 for methane production. The elevated level of acetate may promote the acetoclastic methanogenesis by *Methanosarcina* in the BLBR. Further, ARBs in anode biofilm may also improve the methane production by DIET between ARBs and acetoclastic methanogen such as *Methanosarcina*. Studies have shown that the acetoclastic methanogenesis pathway can be improved via increased electron donor and enhanced EET by ARB (Holmes et al.,2017; Inaba et al., 2019; Li et al., 2018c; Xiao et al., 2019, 2020). Therefore, the methane production was still improved in the BLBR, even when the electron transferred from anode to cathode was limited.

4.3.4 Energy balance

The energy consumption and recovery from methane production in FW dry digestion in the BLBR was calculated and summarized in Table 4-3. For the BLBR with applied voltage, the calculated energy consumption ranged from 0.21 to 0.44 kWh/kg-VS, compared to 0.20 kWh/kg-VS of the control. The highest voltage application would increase the energy consumption by 2.10 times. For all the tested conditions, the net energy output was positive (greater than 2.00 kWh/kg-VS). The highest net energy output of 2.90 kWh/kg-VS was obtained when the BLBR was operated with 0.9 V, which was in agreement with the highest cumulative methane production. Under this condition, the net energy output was 45% higher than that of the control. Therefore, 0.9 V could be considered as the optimal operation voltage for FW dry digestion in

the BLBR. The positive net energy output of the BLBR operation and enhanced methane yield could further compensate part of the energy requirement to maintain the BLBR system at mesophilic condition (35 ℃), which was not included in the above energy balance calculation.

Table 4-3. Energy consumption and recovery from FW dry digestion in the BLBR.

	Energy consumption (kWh/kg-VS)	**Energy recovery (kWh/kg-VS)**	**Net energy output (kWh/kg-VS)**
Control	0.20	2.20	2.00
0.3 V	0.21	2.34	2.13
0.6 V	0.24	2.66	2.42
0.9 V	0.35	3.25	2.90
1.2 V	0.44	2.61	2.17

4.4 Conclusions

The application of voltage in the BLBR has proved to improve the acidogenesis and methanogenesis during AD process for FW. Methane yield in the BLBR was successfully enhanced at all applied voltages. The maximum methane yield was 293 mLCH_4/gVS at applied voltage 0.9 V, which was 46% higher than the control. No significant difference was observed in VS removal among these operation with different applied voltage.

The contribution of direct electron transfer on methane yield enhancement was less than 10%. The microbial community structure in cathode biofilms indicated the enhanced methane production could be attributed to the enrichment of hydrogenotrophic methanogens through syntrophic methanogenesis because of the enhanced acidogenesis and acetogenesis by applied voltage. However, acetoclastic methanogen directly accepting electrons from ARB could also occur in the anode biofilm, although this hypothesis requires future experimental evidence.

The findings from these experiments proved the efficiency of the BLBR on FW dry digestion and methane production, which would help to broaden the understanding of applied voltage on FW dry digestion in the MEC assisted AD systems and provide fundamental and practical information for engineering of the BLBR in the future.

Chapter 5 - Optimization of biofilm conductance measurement with split gold electrode in microbial electrolysis cells (MECs)

5.1 Introduction

A microbial electrochemical cell (MEC) is one type of bioelectrochemical systems in which anode-respiring bacteria (ARB) or exoelectrogens carry out metabolism by converting chemical energy to electrical energy or the opposite (Hussain et al., 2021; Lee, 2018; Logan & Rabaey, 2012;). ARB deliver electrons to a solid electrode through extracellular electron transfer (EET), which usually serves as the terminal step in anode-respiration (Dhar et al., 2016; Lee et al., 2016; Malvankar et al., 2012a). EET, thus, affects the current density in MECs, as well as their application. Several EET mechanisms have been reported (Lee, 2018; Malvankar et al., 2011, 2012c; Snider et al., 2012; Strycharz-Glaven et al., 2011; Strycharz-Glaven & Tender, 2012; Yates et al., 2016a & b). Among them, conductive EET receives great attention because it is believed that this type of EET enables explains the high current density in MECs (Dhar et al., 2016; Lee, 2018; Torres et al., 2010).

Metallic conduction (Ohmic conduction) and redox conduction (long-range electron hopping) are the two types of conductive EET mechanisms that have been proposed (Lee, 2018; Malvankar et al., 2011; Yates et al., 2016a & b). In metallic conduction, the biofilm matrix acts as synthetic organic metallic polymers (*i.e*., polyaniline) in which EET generally follows Ohm's law (Dhar et al., 2016 & 2017; Malvankar et al., 2011, 2012a & b, 2015; Tan et al., 2016). *Geobacter spp.* can produce conductive pili (e-pili) with conductivity higher than 250 S/cm to conduct metallic EET and extend to biofilm anodes (Adhikari et al., 2016; Tan et al., 2016 &

2017). In redox conduction, electrons are transported to the solid electrode via electron hopping between adjacent multiple extracellular cofactors referred to redox sites throughout biofilm (Li et al., 2016b; Snider et al., 2012; Strycharz-Glaven et al., 2011; Yates et al., 2016a). Lee et al. (2016) proposed that Ohm's law can well describe conductive EET (metallic and redox conduction) in high current density biofilm anodes where potential gradient is small at 100-200 mV.

Biofilm conductivity or conductance in biofilm anode has received attention more as a means to understand EET mechanisms and facilitate EET engineering for carbon capture and utilization and renewable energy (Dhar et al., 2016, 2017, 2019; Hussain et al., 2021). However, methodology for biofilm conductance measurement with high accuracy, which is important for quantitatively and accurately studying EET kinetic in MECs, is yet to be established. In parallel, the significance of an accurate biofilm conductance has grown as the possibility of conduction-based syntrophy among microorganisms (e.g., direct interspecies electron transfer (DIET)) has been demonstrated (Baek et al., 2018; Barua & Dhar, 2017; Li et al., 2017a; Lu & Ren, 2016). Although advanced microscopic techniques such as conductive atomic force microscopy (AFM) and other electrochemical technique can be applied to examine the conductive property of cell appendages (*e.g.*, e-pili) (Castro et al., 2014; Hubenova et al., 2020; Steidl et al., 2016; Wanger et al., 2013), quantification of biofilm conductivity and conductance is still important for the understanding of conductive EET at biofilms in macro-scale by using split electrodes (Summers et al., 2010; Malvankar et al., 2011, 2012a; Morita et al., 2011; Liu et al., 2012, 2020; Dhar et al., 2016, 2017, 2018; Lee et al., 2016; Li et al., 2016a & b; Yates et al., 2016a & b).

Several environmental factors, including proton concentration within anodic biofilm, anode potential, substrate concentration, and microbial population, have shown impacts on EET

kinetics and biofilm conductance/conductivity (Malvankar et al., 2011, 2012a & b; Matsuda et al., 2011; Dhar et al., 2016, 2017, 2018). Malvankar et al. (2012) compared multiple parameters including biofilm thickness, current density, and biofilm conductivity between different *Geobacter* species and reported that limitations in mass transfer may affect current density and biofilm conductivity (Malvankar et al., 2012b). Dhar et al. (2017) assessed the pH effect on biofilm conductivity and current density by varying phosphate buffer concentration from 2.5 to 100 mM and reported that the lowest buffer concentration (2.5 mM phosphate) caused acidic pH in inner biofilm and the biofilm conductivity showed a 69.0% decrease, along with a decrease of current density, comparing to these values at 100 mM phosphate buffer (Dhar et al., 2017). It was also reported that long-term starvation (~4 days) significantly decreased biofilm conductivity (Dhar et al., 2018).

Impacts of anode potential on EET kinetics have also been studied and discovered (Liu et al., 2010a; Matsuda et al., 2011; Snider et al., 2012; Srikanth et al., 2010; Torres et al., 2009). Dhar et al. (2016) proved that anode potential itself does not directly influence biofilm conductivity within the anode potential ranging from - 0.2 V to + 0.2 V (vs SHE) when a biofilm anode was enriched with *Geobacter sulfurreducens* (Dhar et al., 2016). Instead, anode potential can change the microbial population on biofilm anodes, and as a result, biofilm conductivity could vary (Dhar et al., 2016; Lee, 2018). In addition, I-V curves show non-linear curves during biofilm conductance measurement as anode potential was more polarized (Boyd et al., 2015). It seems that the effects of anode potential on biofilm conductance and EET kinetic need more work for clarification.

Previous works have quantified biofilm conductance under different conditions by adjusting parameters like anode potential, monitoring time, gap size, voltage range, buffer

concentrations, and substrate concentrations (Malvankar et al., 2011, 2012b; Liu et al., 2012, 2020; Dhar et al., 2016, 2017, 2018; Li et al., 2016a & b; Yates et al., 2016a & b). For these reasons, a wide range of biofilm conductance has been reported (Table 5-1). Such different conditions and methods for biofilm conductance measurement cause inconsistency in biofilm conductance. For instance, biofilm conductance fluctuated even for the same bacteria species; biofilm conductance of *G. sulfurreducens* ranged from approximately 3.3 μS to 5.7 mS. Such a large deviation of biofilm conductance casts doubts on the accuracy and reproducibility of existing methods. It is also questionable that the literature has used standardized operating conditions and monitoring parameters since they can readily affect electric current during biofilm conductance measurement. To accurately measure the current passing through the split electrodes, the steady-state current (rather than transient current) should be used to measure and report biofilm conductance or conductivity due to many factors including current variation by charging of pseudo-capacitance and non-Faradaic current induced by counterions transferring (Dalton et al., 1990; Li et al., 2016a & b, 2018a; Malvankar et al., 2011). A clear definition of "steady-state current" for quantification of biofilm conductance is also missing, although the concept of the steady-state current is critical for the determination of biofilm conductance. Despite the significance of the steady-state current, few studies have reported detailed information on the steady-state current and decay of transient current when reporting the measurement of biofilm conductance. Operating conditions can also change biofilm conductance, such as recording time or frequency of tests under the same conditions. Small interference or change of current caused by different operating conditions may deviate electric current, consequently changing the value of biofilm conductance and conductivity (Malvankar et al., 2011, 2012b; Dhar et al., 2016, 2017, 2018; Li et al., 2016a & b).

Table 5-1. Measurement of biofilm/aggregate conductance by two split gold electrodes method.

Material	Voltage selection	Selection of waiting time and Current recording	Electrode characterization	Conductance (mS)*	Reference
Biofilm	0~50 mV; 25 mV step	Unknown waiting time; average the steady-state current within 100 seconds	A 2-Au electrode with a 50-μm gap	0.13~5.68	(Malvankar et al., 2011, 2012a & b)
Biofilm	0~50 mV; 25 mV step	Unknown waiting time, average the current within 100 seconds	A 2-Au electrode with a 50-μm gap	0.034	(Vargas et al., 2013)
Biofilm	0~50 mV; 25 mV step	Not available	A 2-Au electrode with a 50-μm gap; different substrate concentrations	0.34~1.04	(Dhar et al., 2016, 2017, 2018, 2019)
Biofilm	0~75 mV; 25 mV step	Wait for 20 min, then record current data every 30 seconds for 3 min	2-Au electrodes with the gap width from 50~1000 μm	2.12×10^{-3} ~ 8.79×10^{-1}	(Li et al., 2016a & b, 2018a & b)
Biofilm	0~50 mV; 25 mV step	Not available	A 2-Au electrode with a 100-μm gap	0.63	(Lee et al., 2016)

Biofilm	0~50 mV; 25 mV step	Unknow waiting time; record the current every second for 5 minutes	A 2-Au electrode with a 20-μm gap	3.3×10^{-3} ~ 3.28×10^{-2}	(Liu et al., 2020)
Biofilm	0~50 mV; 25 mV step	Not available	A 2-Au electrode with a 20-μm gap	0.27~1.24	(Hussain et al., 2021)
Wastewater Aggregates	-0.3 to +0.3 V; 25mV step	Record the current 10 seconds after setting the voltage	A 2-Au electrode with a 50-μm gap	6.1~7.2 (μS/cm)	(Morita et al., 2011)
UASB granules	-0.3 to +0.3 V; 25mV step	Record the current 10 seconds after setting the voltage	A 2-Au electrode with a 50 μm gap	0.8~36.7 (μS/cm)	(Shrestha et al., 2014)
Activated sludge	-0.3 to +0.3 V; 25 mV step	Record current data for 120 seconds after steady-state	A 2-Au electrode with a 0.5 mm gap	1.02×10^{-4} ~8.38×10^{-3}	(Zhao et al., 2016a)
Activated sludge	-0.3 to +0.3 V; 25 mV step	Not available	2 probes with a 1-cm gap	1.0×10^{-2} ~2.4×10^{-2}	(Zeng et al., 2019)

* Unless specified by the unit, the data listed in this column were the conductance

In this study, to improve the reliability and accuracy of biofilm conductance measurement, the effects of operational parameters on biofilm conductance were evaluated by using MECs equipped with split gold electrodes, including anode potential, substrate concentration, voltage range, and measurement time at each voltage step and optimal conditions for quantification of biofilm conductance were proposed. Further, the methods developed from the above experiments will be used for biofilm development and in situ conductance measurement for those biofilms grown on the anodes of BLBR in Chapter 4.

5.2. Materials and methods

5.2.1 MEC configuration

Two dual-chamber MECs equipped with two split gold electrodes (2-Au electrode) as the anode and a graphite plate as the cathode was used (Figure 5-1a). MECs were designed and manufactured using plexiglass material with an anode chamber of 20 mL. The 2-Au anode (40 mm × 36 mm × 10 μm, L × W × H) was manufactured by nanoFAB Center (University of Alberta, Edmonton, Canada). It has a glass base and a non-conductive gap of 10 μm in the middle of the Au coating. The total geometric surface area of the 2-Au anode was 14.4 cm^2. ARB biofilm was developed on top of the Au anode. A graphite plate (Isomolded Graphite Plate 203101, Fuel Cell Earth, USA) was employed as the cathode. The working volumes of the anodic and cathodic chambers were 15 mL for each, and they were separated by an anion exchange membrane (AMI-7001, Membranes International Inc., USA). A reference electrode (Ag/AgCl, MF-2052, Bioanalytical System Inc., USA) was placed at a distance of 5 mm from the anode surface during the acclimation of ARB biofilms and tests later.

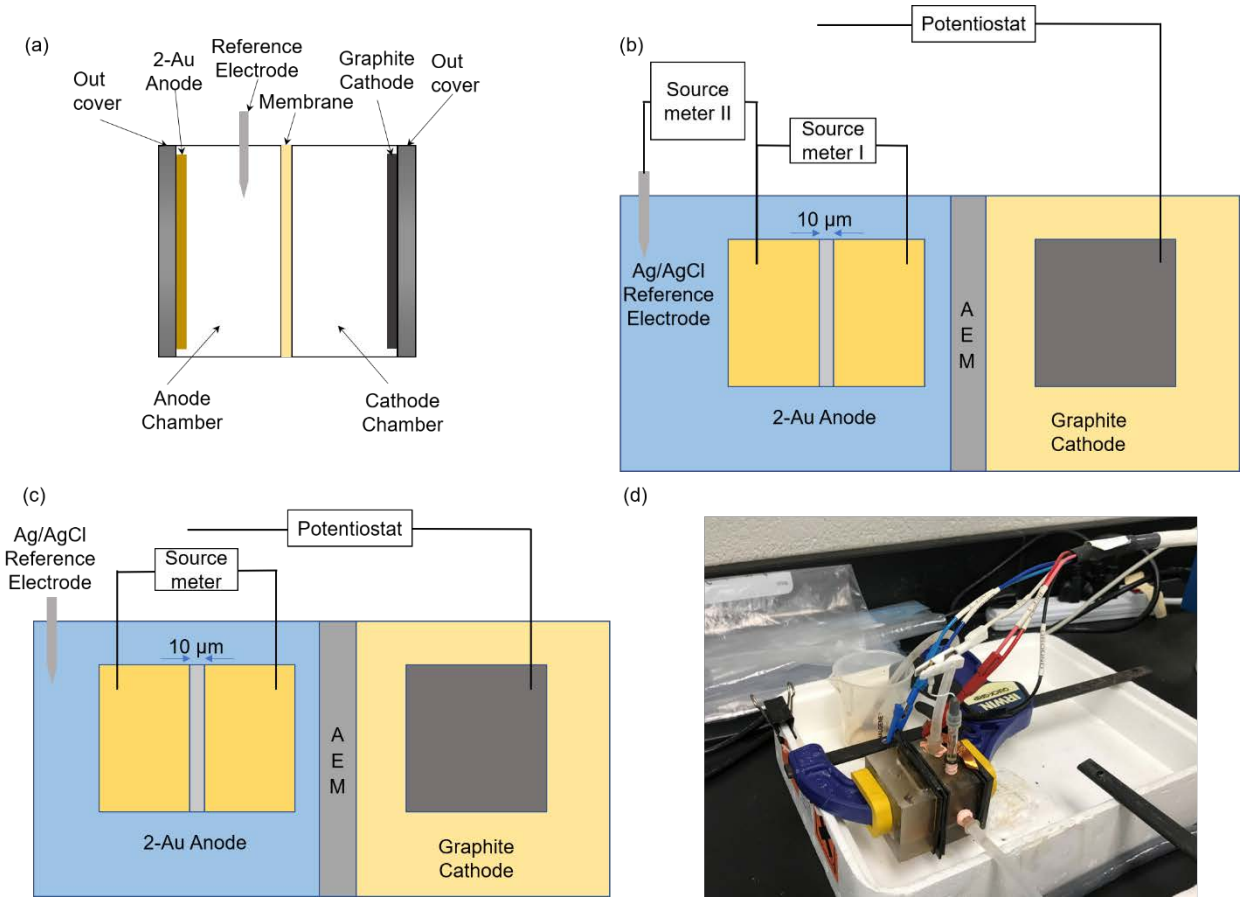

Figure 5-1. (a) Schematic diagram of MECs; (b) biofilm conductance measurement in open circuit mode; (c) anode potential control experiments; and (d) photo of a 2-Au MEC.

5.2.2 Inoculation and operation

Acetate medium (25 mM acetate) was used as the primary source of electron donor and carbon source for ARB proliferation during the experiments, except the experiments for the effects of substrate concentration. The medium (per L of 18.2 MΩ.cm MilliQ water) included 2,050 mg CH_3COONa, 37mg NH_4Cl, 25 mg $MgCl_2 \cdot 6H_2O$, 6 mg $MnCl_2 \cdot 4H_2O$, 5 mg EDTA,

1 mg $CO(NO_3)_2 \cdot 6H_2O$, 0.5 mg $ZnCl_2$, 0.2 mg $NiCl_2 \cdot 6H_2O$, 0.2 mg $NiCl_2$, 0.1 mg $AlK(SO_4)_2$, 0.1 mg $NaHSeO_3$, 0.1 mg H_3BO_3, 0.1 mg $Na_2WO_4 \cdot 2H_2O$, 0.1 mg $Na_2MoO_4 \cdot 2H_2O$, 0.1 mg $CuSO_4 \cdot 5H_2O$, and 0.01 mg $CaCl_2 \cdot 2H_2O$. Supplemented with 100 mM phosphate buffer, the medium was autoclaved and later purged with ultra-pure N_2 gas (99.999%) for 30 min. During purging, the N_2 gas was filtered through a 0.45 µm membrane filter (RK-02915-14, Cole-Parmer, USA) to avoid any contamination. Then, $Na_2S \cdot 9H_2O$ (77 mM) and $FeCl_2 \cdot 2H_2O$ (20 mM) were added to the medium (1 mL of each per L medium), respectively. The pH of the medium was maintained at 7.5 ± 0.1. The anodic chambers of the MECs were inoculated with the effluent and biofilms collected from a mother MEC from a mother MEC with almost pure *G. sulfurreducens* in biofilms (Dhar et al., 2018). The anodic chamber filling with fresh acetate medium after inoculation was then deoxygenated with ultra-pure N_2 gas for approximately 20 min. The cathodic chamber was fed with distilled water. The working potential was fixed at -0.4 V (vs Ag/AgCl) with a potentiostat (Bio-logic, VSP, Gamble Technologies, Canada) during the experiments including the acclimation of ARB biofilms. Such inoculation procedures could produce a *Geobacter*-dominant anodic biofilm in the MECs (Dhar et al., 2016). Current, electrode potentials and other parameters were monitored and recorded every minute using the potentiostat and EC-Lab v10.23 software installed on a computer. The MECs were operated in batch mode, according to the literature (Dhar et al., 2018) and after confirming repetitive current-time profiles we started to measure the biofilm conductance. The MECs were operated at a controlled temperature of 25 ± 1 °C during the experiments. To assess the reproducibility of the biofilm conductance data, two identical MECs were operated in parallel. All potentials in this study were reported against Ag/AgCl unless otherwise specified.

5.2.3 Biofilm conductance measurement

To measure the biofilm conductance of the anode biofilm, MECs were temporarily disconnected and kept in open circuit mode during the measurement (Figure 5-1b). If not specified, the MECs were fed with 25mM acetate medium. One source meter (Keithley 2400, Keithley Instruments Inc., USA) would apply a linear voltage ramp, for example, from 0 to100 mV with a step of 25 mV, between the two separate gold electrodes of the anode. At each voltage step, the current was recorded continuously at a frequency of 1 Hz over a minimum period of 100 seconds by using a LabVIEW data acquisition system (National Instruments, Texas, USA). The observed biofilm conductance (G_{obs}, S) could be obtained directly from the slope of current-voltage curve (I-V profile). Each biofilm conductance measurement was run in triplicate and the average was reported. An abiotic 2-Au MEC was used to measure the ionic conductance in the acetate medium, and we followed the same procedure for biofilm conductance measurements.

5.2.4 Assessment parameters for quantification of biofilm conductance

To characterize biofilm conductance with and without anode potential (E_{anode}) control, one source meter (Keithley 2400, Keithley Instruments Inc., USA) was used to apply a gate voltage (V_{gate}) between the gate (*i.e.*, the Ag/AgCl reference electrode) and the source-drain electrodes (*i.e.*, 2-Au anode) to create the electrolyte gate field effect (Figure 5-1c) (Malvankar et al., 2011). The value of V_{gate} was the same as the E_{anode} during MECs operation (Malvankar et al., 2011). Another source meter of the same model was used to apply a voltage between the two separate electrodes of the anode (source-drain) to perform biofilm conductance measurement as

described above. Biofilm conductance was measured while E_{anode} was controlled at -0.4 V (vs Ag/AgCl). To further evaluate E_{anode} effect on biofilm conductance, we measured biofilm conductance as E_{anode} was varied from -0.6 V to +0.6 V (vs Ag/AgCl). A voltage ramp from 0 to 100 mV was applied between the two separate Au electrodes with a step of 25 mV and a monitoring time of 100 seconds at each voltage condition.

To examine the effect of substrate concentration on biofilm conductance measurement, three acetate concentrations were studied: 1) 25 mM acetate, 2) 1.8 mM acetate close to the apparent half-maximum-rate concentration (K_s) of *Geobacter sp.* (Lee et al., 2009), and 3) acetate-free growth medium. For each substrate concentration, the MECs were operated until they reached steady-state current density. A voltage ramp from 0 to 100 mV with a step of 25 mV was applied between the two separate Au electrodes. Each voltage step was kept for 100 seconds and the current data was monitored during that time. The voltage ramp which was applied between the separate two Au electrodes was also varied from 0 to 500 mV with an increasing step of 25 mV while keeping the monitoring time of 100 seconds at each voltage step unchanged. E_{anode} was fixed at -0.4 V for these experiments.

The steady-state current and decay of transient current during biofilm conductance measurement was also assessed by monitoring the current for a relatively long period of over 20 min and determined the time required to reach steady-state current at each voltage step during biofilm conductance measurement. We changed monitoring time from 100 to 500 and 1,500 seconds, respectively, while voltage was applied across the two separate Au electrodes from 0 to100 mV with an increasing step of 25 mV with E_{anode} control.

5.2.5 Calculation and analysis

The intrinsic biofilm conductance, G_{bio}, can be calculated using Eq. 5-1.

$$G_{bio} = G_{obs} - G_{control} \quad (5\text{-}1)$$

Where G_{obs} is the observed biofilm conductance (S) measured with the biotic MEC, and $G_{control}$ is the ionic conductance (S) measured with the abiotic MEC (Malvankar et al., 2011; Dhar et al., 2016, 2017, 2018). The pH values were measured with a pH benchtop meter (PHB-600R, OMEGA, Canada) connected with a pH probe (RK55500-40, Accumet MicroProbe combination electrode, Cole-Parmer, Canada). Acetate was quantified with a gas chromatography (GC) (Model: Hewlett Packard HP 5890 Series II) equipped with a flame ionization detector (FID) (Hussain et al., 2021). Before GC-FID analyses, the samples were filtered by 0.2 µm membrane filters (DISMIC-25 HP, Toyo Roshi Kaisha Ltd., Japan) and then acidified using 1 N phosphoric acid. All samples were analyzed in triplicate.

5.3 Results and discussion

5.3.1 Effects of anode potential on the biofilm conductance

The measured biofilm conductance was $2.37 \pm 0.14 \times 10^{-4}$ S in the MECs fed with 25 mM acetate medium when E_{anode} was not controlled. During the measurement, E_{anode} was stable at -0.072 ± 0.011 V (vs Ag/AgCl) without E_{anode} control. When E_{anode} was fixed at -0.1 V, the biofilm conductance was $2.42 \pm 0.06 \times 10^{-4}$ S, which was only 2.1% greater than the biofilm conductance without E_{anode} control. When E_{anode} was fixed at -0.4 V, the measured biofilm conductance was $2.12 \pm 0.10 \times 10^{-4}$ S, about 10% smaller than that without E_{anode} control.

Figure 5-2 showed the profile of biofilm conductance against E_{anode}. The biofilm conductance increased steadily as E_{anode} was gradually increased from -0.6 V to +0.6 V. The highest biofilm conductance of $3.56 \pm 0.058 \times 10^{-4}$ S was found at E_{anode} +0.6 V (vs Ag/AgCl). Literature reported a wide range of biofilm conductance from 2.12×10^{-6} to 5.68×10^{-3} S (Table 5-1), while E_{anode} was neither controlled nor monitored in literature (Li et al., 2016a & b, 2018a & b; Liu et al., 2020; Malvankar et al., 2012a & b; Vargas et al., 2013; Shrestha et al., 2014; Zhao et al., 2016a; Zeng et al., 2019). Due to the ambiguous relationship between E_{anode} and biofilm conductance, such a wide range of reported biofilm conductance would cast doubt on the measured biofilm conductance because potential bias may exist between "true biofilm conductance" in a given condition and the measured value. Our experimental results indicated that although Eanode control may not be critical for measuring biofilm conductance regardless the slightly change on biofilm conductance, but the biofilm conductance should be reported together with the anode potential during measurement (i.e., either measured or controlled anode potential) for the purpose of comparison. This is consistent with the literature reporting that a highly conductive biofilm anode was kept despite E_{anode} change (Dhar et al., 2016; Lee et al., 2016, 2019; Li et al., 2016a & b, 2018a & b; Lee, 2018). This result also implied that parameters other than E_{anode} would mainly result in the large deviation of biofilm conductance in literature.

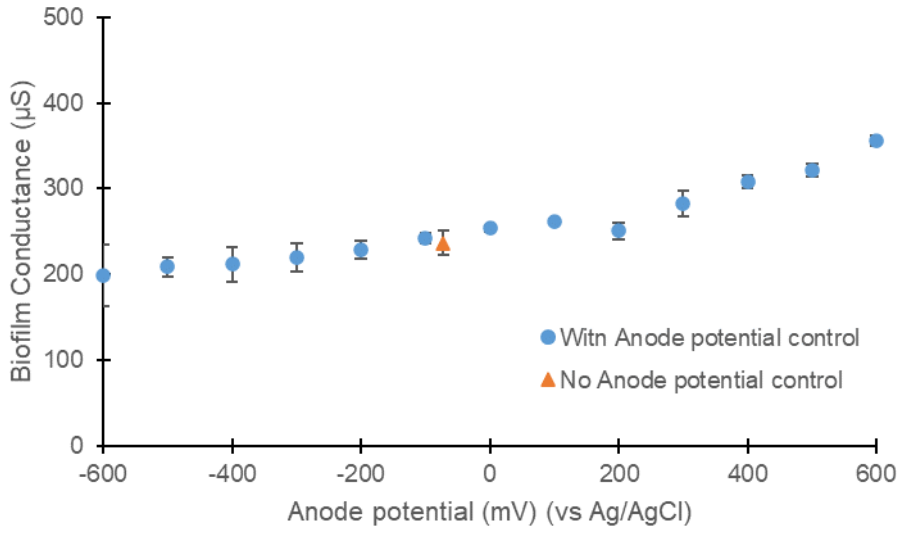

Figure 5-2. Measured biofilm conductance at different anode potentials. The orange triangle data represents the biofilm conductance measured without anode potential control, and the blue circles indicate the biofilm conductance with anode potential control. Error bar represents standard deviation (n = 5).

5.3.2 Effects of substrate concentration on the biofilm conductance

Figure 5-3 showed the change of biofilm conductance when the acetate concentration in anodic chamber decreased from 25 mM to 1.8 mM and then to 0 mM. The biofilm conductance with 25 mM acetate was $2.12 \pm 0.25 \times 10^{-4}$ S, which was measured under anode potential control (E_{anode} = - 0.4 V). When the substrate concentration decreased to 1.8 mM acetate, which was the half-saturation concentration of acetate (Lee et al., 2016), the intrinsic biofilm conductance decreased to $1.95 \pm 0.20 \times 10^{-4}$ S. The MECs were further operated in an acetate-free condition (0 mM acetate) and the measured biofilm conductance decreased to $1.78 \pm 0.06 \times 10^{-4}$ S. This

pattern well agrees to literature reporting that metabolic conditions in an anode biofilm influenced biofilm conductance (Dhar et al., 2017, 2018; Hussain et al., 2021). For instance, biofilm conductivity decreased from 0.87 to 0.27 mS/cm (69.0% decline) when inner biofilms were partially acidified with current density reduction from 2.38 to 0.64 A/m^2 (Dhar et al., 2017). The biofilm conductivity was conserved when fed with no substrate medium temporarily, but its reduction was as large as 69% in a 4-d, "long-term" starvation (Dhar et al., 2018). Our study shows the same declining trend of biofilm conductance after 2 weeks of starvation, but its reduction was relatively small at 16%, as compared to the biofilm conductance at 25 mM acetate concentration. Biofilm characteristics, anode material, or combined effect could cause such different levels of biofilm conductance reduction. The literature and this study commonly used *Geobacter spp.* enrichment as inoculum and gold electrodes as the anodes, and hence the two parameters would not cause such a difference in biofilm conductance reduction (Dhar et al., 2016, 2017, 2018). The reduction difference might be related to measurement methods of biofilm conductance. For instance, this study measured biofilm conductance with a voltage ramp from 0 to 100 mV (five-point calibration) with a step of 25 mV for a constant waiting period of 100 seconds at each voltage step to ensure "pseudo-steady-state current". In comparison, the voltage ramp was as small as 50 mV (three-point calibration) without a defined waiting period for steady-state current at individual voltage conditions in the literature. The previous method used in the literature could bias pseudo-steady-state current at each voltage, leading to deviation of measured biofilm conductance. This analysis explains why the measurement protocol of biofilm conductance and the definition of the pseudo-steady-state current can be important for biofilm conductance measurements, and data reliability and accuracy.

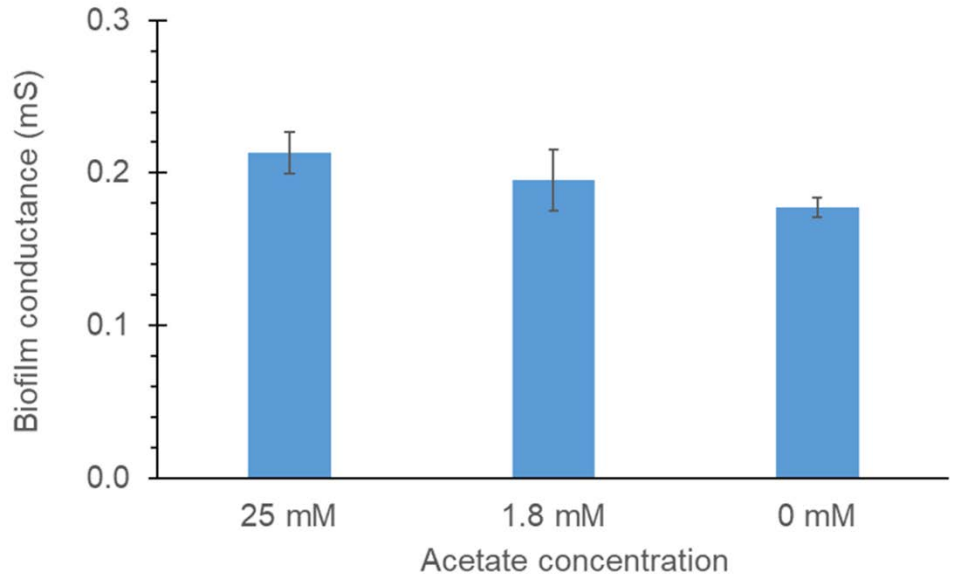

Figure 5-3. Biofilm conductance measured at different acetate concentrations. (The r^2 of the linear regression of I-V profile with 25 mM, 1.8 mM and 0 mM acetate was 0.99, 0.96, and 0.95, respectively.) Error bar represents standard deviation (n = 5).

5.3.3 Effects of the voltage range on the biofilm conductance

As illustrated in Figure 5-4, the I-V profile with E_{anode} control during biofilm conductance measurement displayed a visual deviation from Ohm's Law when the applied voltage gradually increased to 500 mV. The I-V profile stayed within Ohm's Law when the applied voltage was less than 100 mV and the biofilm conductance was 1.81×10^{-4} S (with E_{anode} controlled at – 0.4 V vs Ag/AgCl). The slope of the I-V profile (*i.e.*, the conductance) then decreased when the applied voltage was greater than 100 mV. The calculated biofilm conductance decreased by 88% within the range of 100 to 400 mV, and by 71% within the range of 400 and 500 mV, respectively. On one hand, this result indicated the resistance of electrons passing through the anodic biofilm first increased significantly at an applied potential gradient over 100 mV, then

decreased partly at a higher potential gradient over 400 mV. On the other hand, Ohm's law could solely account for the decrease of biofilm conductance with the increasing potential gradient, which would support the complexity of the extracellular electron transport in the biofilm anode: metallic conduction (Ohmic conduction), redox conduction (non-Ohmic conduction), and combined one (Malvankar et al., 2011; Lee et al., 2016; Li et al., 2016a & b; Lee, 2018).

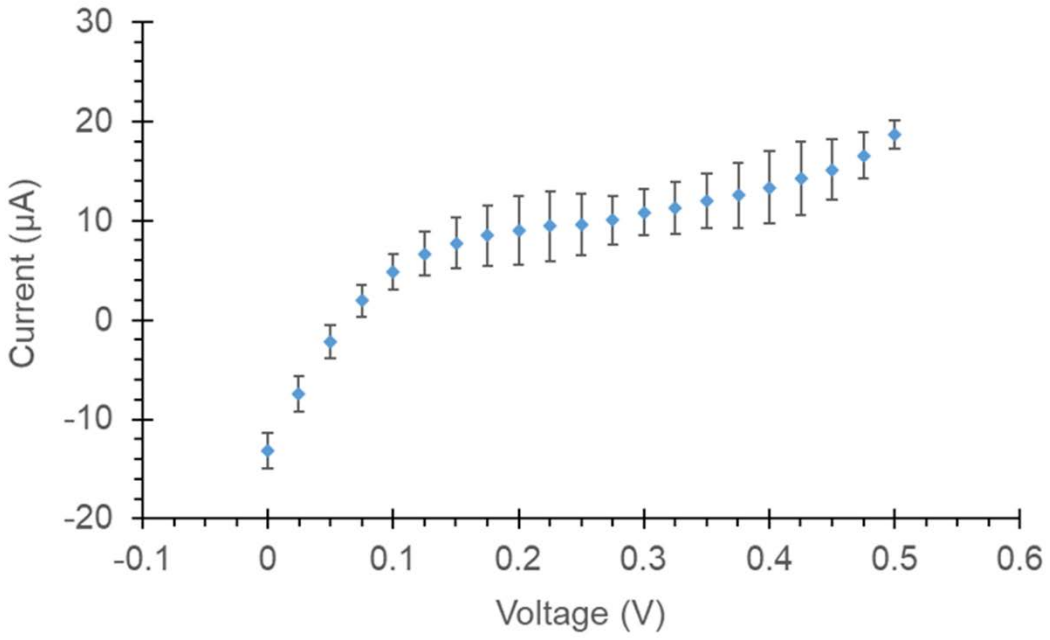

Figure 5-4. I-V profile during the biofilm conductance measurement with the voltage range from 0 mV to 500 mV, with Eanode = -0.4 V (vs Ag/AgCl). Error bar represents standard deviation (n=5).

Under redox conduction, microorganisms can produce several types of extracellular redox cofactors acting as redox mediators in the electroactive biofilm (Holmes et al., 2006; Nevin et al., 2009; Snider et al., 2012; Shu et al., 2016; Yates et al., 2016a & b). These

extracellular redox cofactors, such as cytochromes, have different redox potentials (Magnuson et al., 2001; Qian et al., 2011; Santos et al., 2015; Dantas et al., 2017). In electroactive biofilms, electrons were conducted between adjacent redox sites via an electron self-exchange reaction, which involves both reduced and oxidized redox sites. Electron hopping was limited when those redox sites were oxidized or reduced completely within the redox sites network in the biofilm (Strycharz-Glaven et al., 2011). A majority of extracellular redox cofactors in the biofilm would be oxidized forms at higher applied voltage bias (*i.e.*, > 100 mV) while reduced forms of the cofactors would be limited, which may alter the distribution of redox sites within the biofilm. The counterion mobility in the conductive biofilm under larger voltage bias may be also limited and therefore, the electron transport may suffer higher resistance within the biofilm. The measured biofilm conductance was therefore smaller than that at lower applied voltage.

Nevertheless, it is still possible that EET follows Ohm's Law in the biofilm anode when the applied voltage is small (*i.e.*, less than 100 mV), regardless of the conduction mechanism; for those small applied voltages in biofilm anodes, even redox conduction would stay with Ohm's Law (Yates et al., 2016b). The results here indicated that the I-V profile would follow Ohm's Law within the Ohmic-response range (from 0 to 100 mV), and the voltage range greater than 100 mV would bring deviation on the biofilm conductance measurement due to increased resistance to electron transfer.

5.3.4 Biofilm conductance measurement at a longer monitoring period

Three different monitoring periods (100, 500, and 1500 seconds) were selected as the defined monitoring time at each voltage step from 0 to 100mV (the Ohmic-response region) with

an increasing step of 25 mV. The current data collected at each voltage step clearly showed the decay of transient current, followed by the steady-state current, which indicated the importance of the time allowing those current to dissipate during monitoring (Figure 5-5) (Dalton et al., 1990; Li et al., 2016a). Further comparison of the coefficient of variation of the time-averaging value of current suggested that the whole 100 seconds of data had larger dispersion than the last 20 seconds of data in the monitoring period of each voltage step (Table 5-2). Both 500-second and 1500-second also showed the same trends that the last 20% (time-sequencing) of the data had much smaller dispersion than that of the whole period. Therefore, we selected the current in the last 20 seconds as the steady-state current value for 100-second tests to calculate the observed biofilm conductance. For 500-second and 1500-second periods, the current data in the last 100 seconds and 300 seconds were selected as the steady-state current to compute the biofilm conductance, respectively (Figure 5-6a).

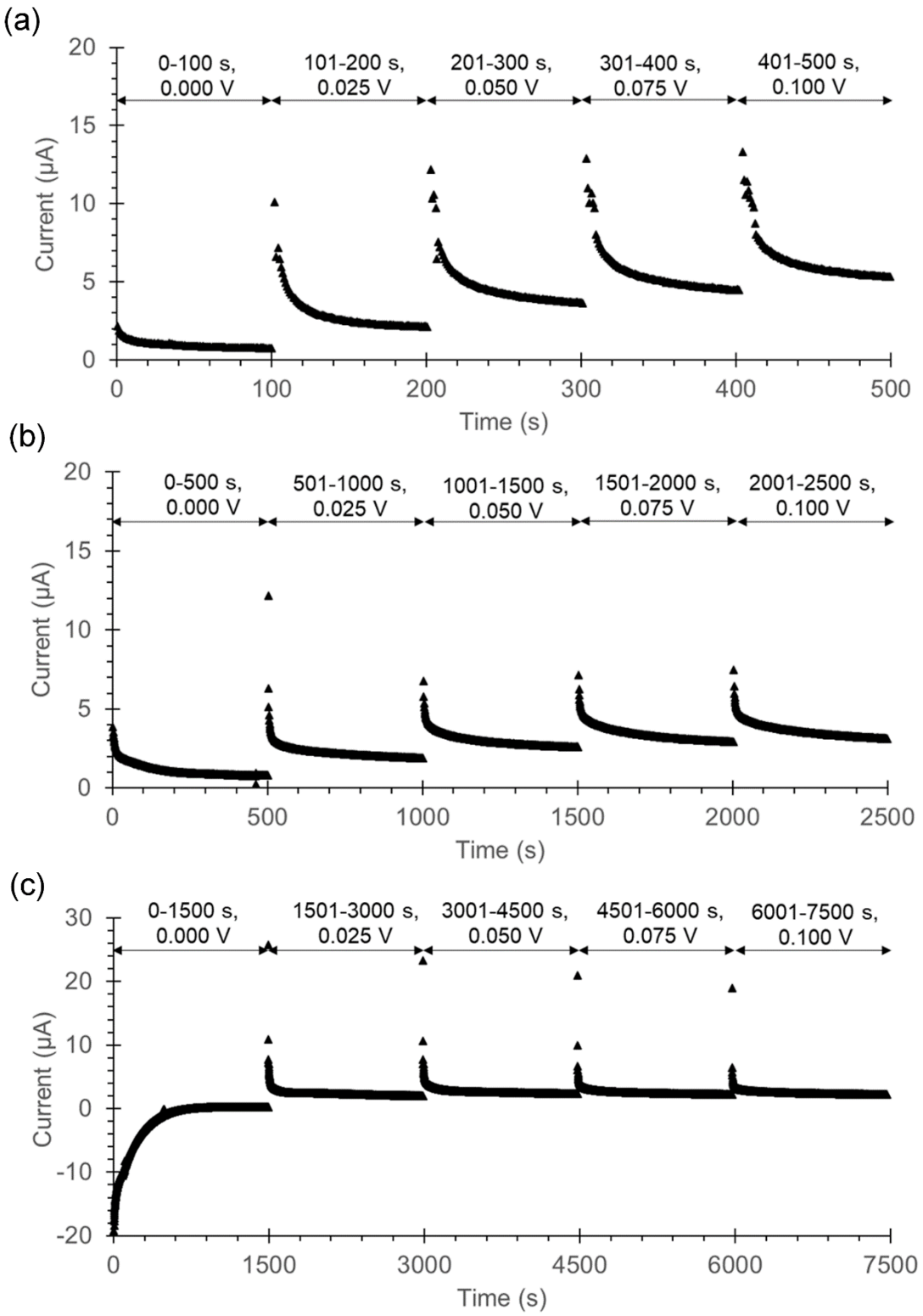
(a)
0-100 s, 0.000 V
101-200 s, 0.025 V
201-300 s, 0.050 V
301-400 s, 0.075 V
401-500 s, 0.100 V
Current (μA)
Time (s)
(b)
0-500 s, 0.000 V
501-1000 s, 0.025 V
1001-1500 s, 0.050 V
1501-2000 s, 0.075 V
2001-2500 s, 0.100 V
Current (μA)
Time (s)
(c)
0-1500 s, 0.000 V
1501-3000 s, 0.025 V
3001-4500 s, 0.050 V
4501-6000 s, 0.075 V
6001-7500 s, 0.100 V
Current (μA)
Time (s)

Figure 5-5. The current data recorded during the biofilm conductance measurement with 100-second (a), 500-second (b), and 1500-second (c) at each voltage step.

Table 5-2. Comparison of CV* of the average value of all and the last 20% of the data in each period.

100-second		**500-second**		**1500-second**	
All	20%	All	20%	All	20%
22.18	3.64	21.89	2.15	26.91	1.45

*: Coefficient of Variance (CV) was the ratio of the standard deviation to the mean value (%).

Figure 5-6a compared the intrinsic biofilm conductance calculated using all (the blue column) and the last 20% of the current data (the orange column) collected at each monitoring period. In general, the biofilm conductance using the last 20% (time-sequence) of the data collected during the monitoring time of each voltage step was slightly smaller than the corresponding value using all the data collected. The two biofilm conductance values were significantly different ($p<0.05$) for all the three different monitoring periods. Those results indicated that the final reported conductance depends on the selection of monitoring period for the pseudo-steady-state current. During the pseudo-steady-state, the transient non-Faradaic current due to counter-ion diffusion and capacitive effect of the electroactive biofilm would decline and become negligible (Adhikari et al., 2016; Li et al., 2016b). Since the non-Faradaic current upon potential shift is influenced by factors other than the electroactive biofilm, such as electrodes (*i.e.*, material and configuration) and electrolytes, it is essential that current data in the

pseudo-steady state is used for biofilm conductance quantification (Holtan et al., 2019; Jacobs et al., 1994; Li et al., 2017c; McGrath et al., 1995; Ren et al., 2014b; Soleymani et al., 2009).

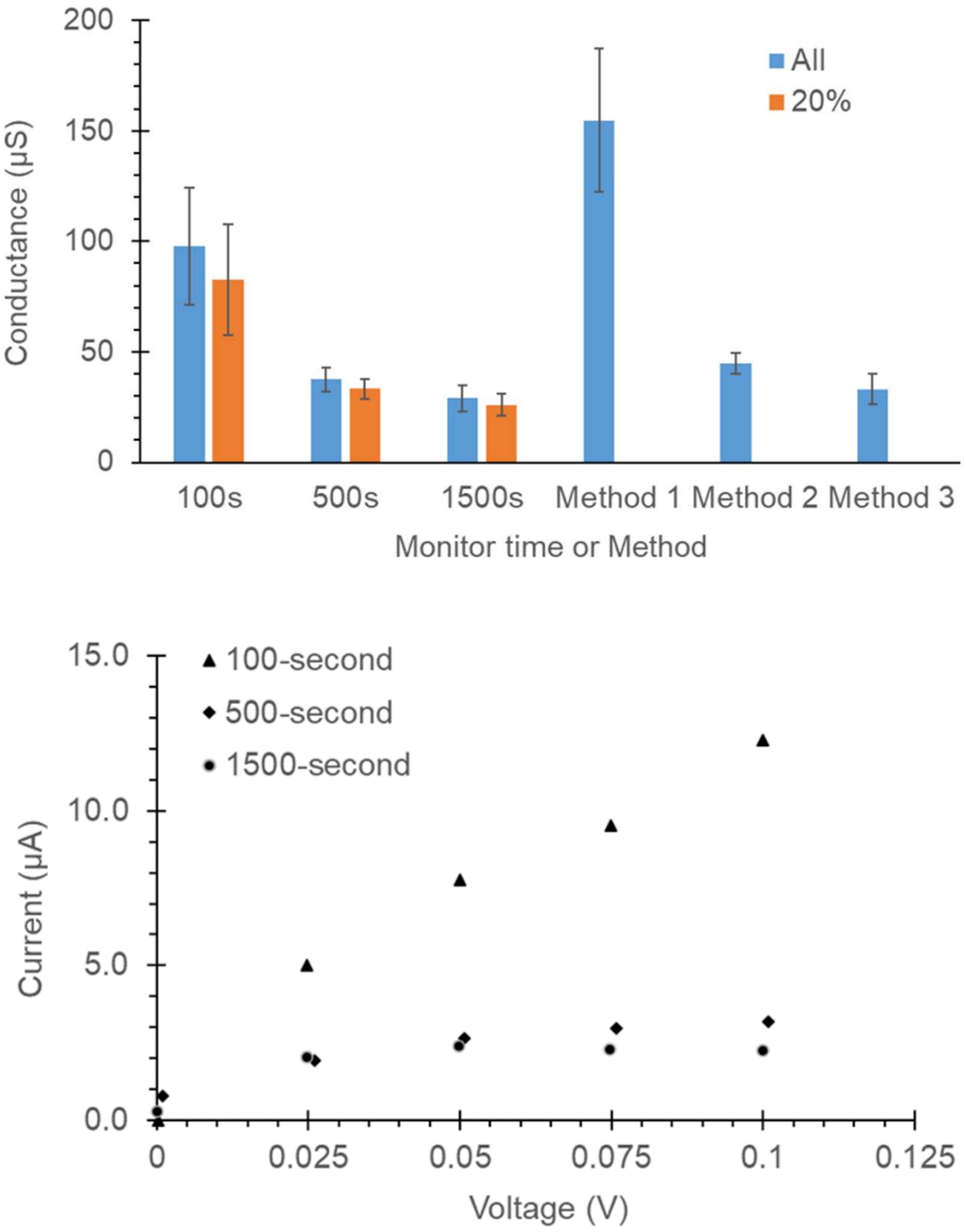

Figure 5-6. Biofilm conductance and its response to voltage. (a) Intrinsic biofilm conductance from different measurement times. Error bar represents standard deviation (n = 5). "All" means all the data collected is averaged for calculation, while "20%" means only the last 20% of the

data recorded in each period is averaged. Method 1: voltage range 0~50 mV with an increasing step of 25 mV and an average steady-state current of 100 seconds (Malvankar et al., 2011). Method 2: voltage range 0~50 mV with an increasing step of 25 mV and an average of the current of 5 min (Liu et al., 2020). Method 3: voltage range 0~75 mV with a step of 25 mV and wait for 20 min and then record current data every 30 seconds for 3 min (Li et al., 2016a; Li et al., 2016b). (b) time-averaged current and voltage profile of 100-second, 500-second, and 1500-second monitoring time. Error bar represents standard deviation (n = 5).

Figure 5-6a showed the gradual decrease in the biofilm conductance as the increase in the measurement time period from 100 to 1500 seconds at each voltage step. In general, a biofilm conductance varied from 26 to 155 μS was obtained using different monitoring period during measurements. The biofilm conductance of 100-second test was almost 2.5 times larger than that of 500-second test, while the value of 1500-second test was only 31% of that of 100-second test. When the monitoring time for each voltage step was 100 seconds, the time-averaged current and voltage followed Ohm's Law, which showed a high linear correlation ($r^2 = 0.99$) (Figure 5-6b). However, the time-averaged current and voltage gradually derived from Ohm's Law when the monitoring time increased to 500 seconds and 1500 seconds. The derivation from Ohm's Law was more serious when the monitoring time was 1500 seconds ($r^2 = 0.70$). Keeping the anode biofilm in open circuit mode for longer period may also alter the metabolic state of the biofilm or affect the structures of microbial assemblages like e-pili and should be avoided during the measurement (Li et al., 2016a). Therefore, these results indicated that whether the electric response of a biofilm follows Ohm's Law may depend on the monitoring time and the

monitoring time at each voltage step should be carefully selected to avoid long-term open-circuit of anode biofilms.

Two types of electrical conduction, metallic (ohmic conduction) and redox conduction are widely applied to explain the conductive EET between the electrode surface and attached microorganisms (Lee, 2018; Li et al., 2017a; Zacharoff & El-Naggar, 2017). Some researchers have attributed the biofilm conductance to metallic conduction, which is featured by the conductive pili (e-pili) of *G. sulfurreducens* (Malvankar et al., 2011, 2012d, 2015). Others have suggested that non-ohmic, redox conduction by multistep electron hopping within the network of cytochromes, would dominate the conduction in biofilms (Snider et al., 2012; Steidl et al., 2016; Zacharoff & El-Naggar, 2017). Although the dominance of the two mechanisms on biofilm conductance and EET requires further evidence and study, these two conduction mechanisms may occur simultaneously in a live anodic biofilm (Steidl et al., 2016). Even if redox conduction does not follow a linear I-V pattern, at a small potential gradient (*i.e.*, the potential gradient when measuring the biofilm conductance), redox conduction can still follow Ohm's law (Yates et al., 2016b). However, our results from the 500- and 1500-second monitoring time tests suggested that keeping the MECs at open-circuit status at a long time may alter the characteristics of the live electroactive biofilm in terms of its charge-holding capability and potentially the morphology of the biofilm. Hence, the electrochemical properties of the biofilm may be altered in a longer monitoring time, which would finally affect the accurate measurement of biofilm conductance and introduce more errors and deviations to the measured biofilm conductance (Heijne et al., 2018). Because the duration of the open-circuit period affected biofilm conductance, the 100-second condition was selected as the optimum monitoring time in this study and was applied for all biofilm conductance measurements.

5.4 Conclusions

In this study, the biofilm conductance in the MECs increased along with the increase in anode potential from -0.6 V to +0.6 V (vs Ag/AgCl), with the highest conductance value occurred at E_{anode} of +0.6 V. However, biofilm conductance with a fixed anode potential of -0.1V showed a small difference from that without a fixed anode potential, which indicated that Eanode control was not critical for measuring biofilm conductance, while it could still slightly change biofilm conductance. The Ohmic-response range was identified at a voltage range between 0 and 100 mV where the current-voltage profile of biofilm stayed within Ohm's law. Increased monitoring time at each voltage step showed up to 69% decrease in biofilm conductance and further deviation from Ohm's law on the current-voltage profile. The relationship between biofilm conductance and operational parameters suggested that biofilm conductance should be displayed with these parameters together for the purpose of comparison. The methods developed in this chapter will be applied to investigate the conductance of biofilms developed in BLBR systems.

Chapter 6 - Conductivity of different types of anodic biofilms from LBR and BLBR enriched on split gold electrodes in microbial electrolysis cells (MECs)

6.1 Introduction

Methanogenesis is an important process for biofuel production and energy recovery from organic waste. It is believed that interspecies electron transfer (IET) plays an important role on the methanogenic processes and affect the metabolism in the microbial communities of anaerobic digestion process (Thauer et al., 2008). Usually, IET are achieved by mediators such as hydrogen or formate (mediated interspecies electron transfer, MIET) (Baek et al., 2018; Lovley, 2017; Mostafa et al., 2020). Recently, direct interspecies electron transfer (DIET) via conductive pili (e-pili) or c-type cytochromes has been recognized as an alternative, effective pathway for syntrophic methanogenesis and may contribute to the enhanced system performance in those microbial electrolysis cells assisted AD (MEC-AD) systems, as compared to MIET (Malvankar & Lovley, 2014; Rotaru et al., 2014a, b; Wang & Lee, 2021).

The achievement of DIET requires microorganisms to establish electrical connection via e-pili, c-type cytochromes, or conductive materials (electric syntropy) in order to transfer electrons directly between microorganisms (Kouzuma et al., 2015). Studies have been conducted on the conductive mechanisms of electron in pure culture biofilms like *Geobacter sulfurreducens* and mixed species, current-generating biofilms and two mechanisms were proposed. Some studies believed that the biofilm would act as synthetic organic metallic polymers such as polyaniline and extracellular electron transfer (EET) would generally follow Ohm's law (metallic conduction) (Dhar et al., 2016; Malvankar et al., 2011, 2012a, b; Tan et al., 2016). Other studies

suggested that electrons would be transported via electron hopping between adjacent redox cofactors in the biofilm (Li et al., 2016a; Snider et al., 2012; Yates et al., 2016a).

Electrical conductivity is a recognized property of for high-current producing biofilms. Further, the EET-based syntropy like DIET among microorganisms in the microbial electrolysis cells assisted AD (MEC-AD) systems relies on the high conductivity of biofilms grown on the electrodes in order to make electron transfer feasible within the system. Besides, to better understanding the mechanisms of MEC-AD enhancement on methane production also requires to accurately quantify the biofilm conductance, as the conductance (conductivity) would significantly affect the electron conduction pathway (Baek et al., 2018; Barua & Dhar, 2017; Li et al., 2017a; Lu & Ren, 2016; Wang et al., 2021a, 2022). Therefore, reliable methods for biofilm conductance measurement to quantitatively and accurately study DIET kinetic in biofilms of AD and MEC-AD systems need to be established. Recent studies also suggested that those methanogenic biofilm and aggregates also showed electrical conductance (Morita et al., 2011; Shrestha et al., 2014; Li et al., 2018a), and those value were varied greatly from less than 1 to 40 μS/cm, while biofilm conductance of *G. sulfurreducens* ranged from approximately 5 μS to 5 mS (Table 5-1). Such a large deviation of biofilm conductance casts not only doubts on the accuracy and reproducibility of existing methods but also raise the demand for reliable biofilm conductance measurement methods.

In addition, ARB like *Geobacter* sp. within the methanogenic and current-generating biofilm are often believed to be electroactive and their abundance are often associated with the biofilm conductance (conductivity) (Dhar et al., 2016; Malvankar et al., 2011, 2012a; Morita et al., 2011; Summers et al., 2010) , but the characterization of microbial community in the MEC-AD systems found more IET-related microorganisms, including genera *Geobacter*,

Desulfobacula, *Desulfomicrobium, Deferribacter*, *Syntrophus*, and *Pseudomonas*, while more bacteria species were found to have the potential or be able to participate DIET in the methanogenic mixed species biofilms (Holmes et al., 2004; Koch & Harnisch, 2016; Müller et al., 2016; Pfeffer et al., 2012; Rabaey et al., 2004; Scholz et al., 2012; Steendam et al., 2019). Therefore, the relationship between biofilm conductance (conductivity) and microbial community structure in those methanogenic biofilms from MEC-AD systems should be investigated.

This study aimed to quantify the conductivity of methanogenic types of biofilms grown on split gold electrodes using methods developed in Chapter 5. Methanogenic biofilms enriched from inoculum in LBR and BLBR were developed on the split gold electrodes of MECs for analysis. Fermentative biofilms enriched from the same inoculum were used for comparison. Biofilm community structures were sequenced and analyzed in order to discover possible relationship between conductivity and major community components.

6.2 Materials and methods

6.2.1 Biofilm growth in MECs

Anaerobic sludge collected from the centrifuged LBR and BLBR leachate were used as inoculum for growing anode biofilms, respectively. As comparison, fermentative inoculum was prepared by heating the anaerobic sludge at 75 C for 15 minutes to inhibit all the methanogens in it before use. All the biofilms were developed on the same 2-Au electrodes in the MECs as described in Chapter 5. In brief, the anodic chambers of the MECs were inoculated with LBR and BLBR leachate, and fermentative inoculum, respectively. The MECs inoculated with LBR leachate were fed with a growth medium amended with 50 mM phosphate buffer containing 100

mM sodium acetate, 20 mM sodium propionate, and 10 mM sodium butyrate with pH adjusted around 7.0. In particular, the BLBR MECs were fed with the filtrate of the BLBR leachate to simulate the syntrophic interactions between ARB and methanogens in biofilm anodes. The MECs inoculated with fermentation sludge were fed with the growth medium containing 3.75 g/L of glucose to simulate the proliferation of fermenting bacteria. pH was adjusted to 5.5 to inhibit methanogenesis. The anodic chambers after inoculation were then deoxygenated with ultra-pure N_2 gas for approximately 20 min. The cathodic chambers were fed with distilled water. The working potential was fixed at +0.3 V (vs Ag/AgCl) with a potentiostat (Bio-logic, VSP, Gamble Technologies, Canada) for BLBR biofilm inoculated MECs during the experiments. All MECs were tested in duplicate and run at 35 ℃.

6.2.2 Conductance measurement

To measure the biofilm conductance of the anode biofilm, the method developed in Chapter 5 was used here. In brief, MECs were temporarily disconnected from potentiostat and one source meter (Keithley 2400, Keithley Instruments Inc., USA) would apply a linear voltage ramp from 0 to100 mV with a step of 25 mV between the two separate gold electrodes of the anode. The current was recorded continuously at a frequency of 1 Hz over a period of 100 seconds by using a LabVIEW data acquisition system (National Instruments, Texas, USA) at each voltage step. The observed biofilm conductance (G_{obs}) could be obtained from the slope of current-voltage curve (I-V profile). Each biofilm conductance measurement was run in triplicate and the average was reported.

To further characterize biofilm conductance at variable anode potential (E_{anode}), one source meter (Keithley 2400, Keithley Instruments Inc., USA) was used to set the anode

potential between the Ag/AgCl reference electrode and one of the source-drain electrodes (2-Au anode). Another source meter of the same model was used to apply a voltage between the two separate electrodes of the anode (source-drain) to perform biofilm conductance measurement as described above. Biofilm conductance was measured while E_{anode} was varied from -0.6 V to +0.6 V (vs Ag/AgCl). A voltage ramp from 0 to 100 mV was applied between the two separate Au electrodes with a step of 25 mV and a monitoring time of 100 seconds at each voltage condition. The biofilm conductance was calculated as described above.

6.2.3 Biofilm thickness measurement

The biofilm thickness (L_f) was measured using the method described in literature (Bonanni et al., 2013; Dhar et al., 2017). In general, the change of resistance between a working electrode (the gold anode disconnected from the potentiostat) and a microelectrode in a microsensor were monitored for biofilm thickness quantification. As illustrated in Figure 6-1, a stainless-steel needle used as the microelectrode was connected with a multimeter (Fluke 179/TPAK, Fluke Electronics Canada LP, Canada) and moved toward the gold anode by a micromanipulator (MM33, Unisense A/S, Denmark). Before measurement, the anode chamber will be evacuated with nitrogen gas to remove all the liquid. At the beginning of the measurement, the microelectrode was positioned in the headspace of the anode chamber in the vicinity of the biofilm without touching the biofilm, giving an extremely high or infinite resistance read from the multimeter. The microelectrode was then moved through the biofilm at a 5-µm step. When the microelectrode touched the outmost layer of the biofilm, the resistance decreased to the range of million Ohm due to moisture of the biofilm. When the microelectrode finally touched the gold anode surface, resistance was substantially decreased to almost zero.

The biofilm thickness was then calculated from the number of steps between the first sudden change in resistance when touching biofilm outmost surface and last sudden change when touching the anode surface. Each measurement was completed in 20 min to mitigate adverse effects of oxygen on those anaerobic microorganisms (Dhar et al., 2016, 2017 & 2018). The biofilm thickness (L_f) was measured at three different points on the anodic biofilm and the average was used to calculate the biofilm conductivity.

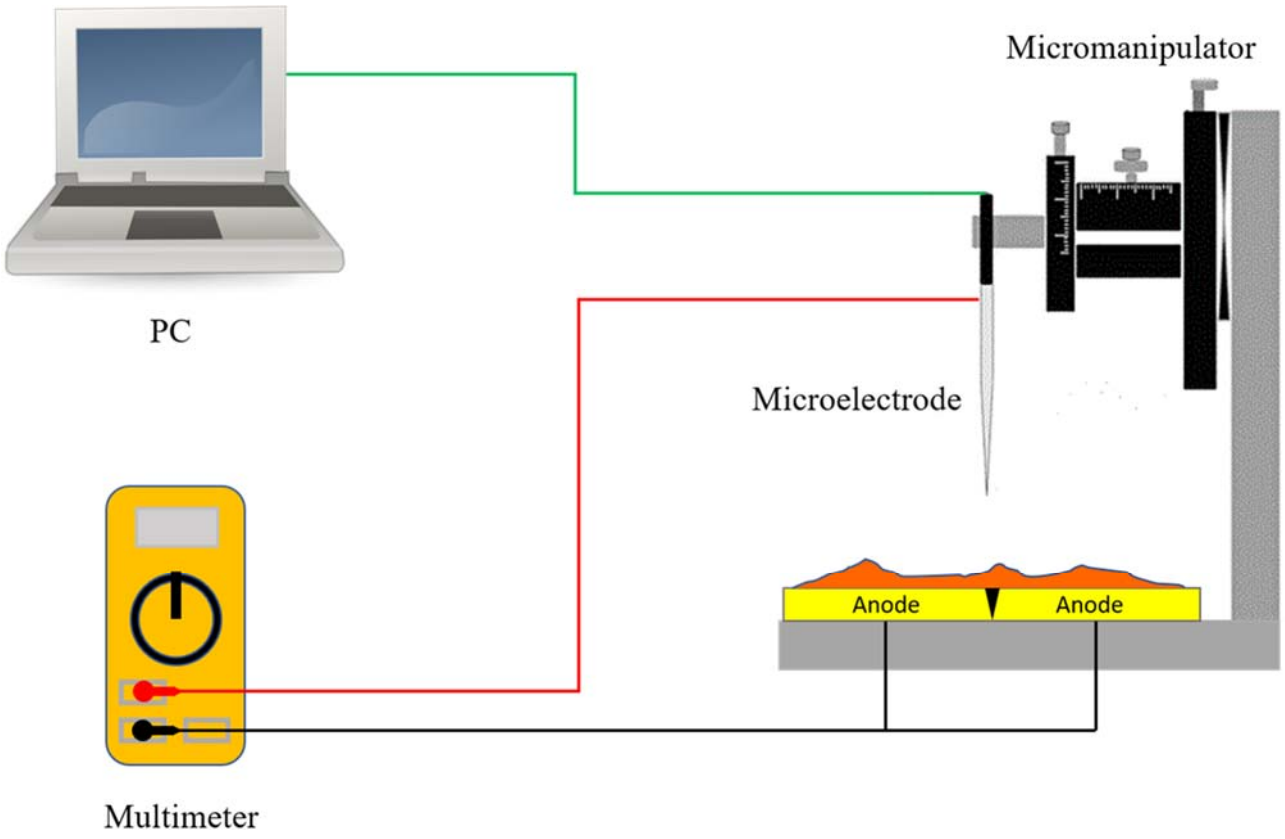

Figure 6-1. Schematic set-up for biofilm thickness (L_f) measurement.

6.2.4 Quantification of Biofilm conductivity

The intrinsic biofilm conductance, G_{bio}, was calculated using Eq. 5-1 in Chapter 5.

$$G_{bio} = G_{obs} - G_{control} \qquad (5\text{-}1)$$

Where G_{obs} is the observed biofilm conductance (S) measured with the biotic MEC, and $G_{control}$ is the ionic conductance (S) measured with the abiotic MEC.

The intrinsic biofilm conductance was then used to quantify the biofilm conductivity across the 10-μm non-conductive gaps with Eq. (6-1) (Kankare & Kupila, 1992; Dhar et al., 2016; Hussain et al., 2021):

$$K_{bio} = \frac{\frac{G_{bio}\pi}{L}}{\ln\left(\frac{8L_f}{\pi a}\right)} \qquad (6\text{-}1)$$

Where, K_{bio} (μS/cm) is the biofilm conductivity; G_{bio} (μS) is the intrinsic biofilm conductance; L is the length of the gold electrodes (3.6 cm); L_f (μm) is the biofilm thickness; a is the half of the non-conductive gap between the two split gold electrodes (25 μm).

6.2.5 Sample collection, DNA extraction and sequencing process

Anodic biofilm samples at the end of experiments from each type of MECs were collected and preserved by DNA/RNA Shield™ swab collection tubes (Zymo Research) at -20 ℃ before DNA extraction and sequencing. DNA was extracted from the biofilm samples collected by the cotton swabs preserved in DNA/RNA Shield collection tubes (Zymo Research, Irvine, CA, USA) by using the DNeasy® PowerSoil® Pro Kit (Qiagen, Valencia, CA, USA) according to the manufacturer's instructions. DNA purity was quantified using Nanodrop (Nano-300, Allsheng, Hangzhou, China), and DNA fragment sizes were checked via 2.0% agarose gel

electrophoresis. The extracted DNA samples were stored at -80℃ degrees before sequencing. After DNA extraction, PCR amplification via primers, PCR products purification, libraries construction and sequencing were performed by Macrogen Inc. (Seoul, South Korea). The target V4 hypervariable region of the 16S rRNA genes were amplified using primer sets 515F (5'-GTGYCAGCMGCCGCGGTAA-3') / 806rB (5'-GGACTACNVGGGTWTCTAAT-3') and sequencing were performed using Illumina MiSeq platform. Only one sample of each biofilm was analyzed due to limited resources.

6.2.6 Bioinformatics and statistical analyses

Bacterial and archaeal taxonomy were confirmed by 16s amplicon sequencing analysis. Based on the Mothur software package v1.45.3 (Schloss et al., 2009), Paired-end reads were merged, contigs were generated and primer and barcode trimming, identification and removal of chimeric sequences and high-quality sequences were clustered into operational taxonomic units at a cutoff of 0.03 after quality filtering (Bae and Yoo, 2022). Reads assigned to non-bacterial and non-archaeal origins, such as chloroplast and mitochondrial genomes, were removed and OTUs were classified using training dataset based on the Silva v132 reference database (Kim et al., 2022). Rarefaction curves and alpha diversities were analyzed using Mothur software (Schloss et al., 2009). The rarefaction curves of the samples were used to confirm the sufficient sequencing depth of the various biofilm samples (Kim et al., 2019). The total read counts per sample were 37722. Excel was used to determine the overall relative abundance of representative sequences at different taxonomic levels. Bacterial and archaea community structures were analyzed and compared separately. Statistical differences in microbial community structure

between samples were tested using the "vegan" package in the R software v4.2.1 (Oksanen et al., 2019) with analysis of similarities (ANOSIM) with 999 permutations.

6.3 Results and discussion

6.3.1 Conductivity of different biofilms grown on anodes of MECs

In the 120-day inoculation, biofilms began to form and cover the non-conductive gaps of the split gold electrodes in all MECs. The conductance of biofilms grown on the anodes of LBR and BLBR MECs gradually increased over the inoculation and the biofilm conductance and reached the plateau after about 100 days (for LBR biofilm) and 70 days (for BLBR biofilm) (Figure 6-2). The LBR biofilm conductance increased to 76.6 µS, while the conductance of BLBR biofilm increased to 93.3 µS. In comparison, the conductance of fermentative biofilm reached a plateau of 3.7 µS after 40 days of inoculation and was maintained at this level for 120 days of MEC operation (Figure 6-2A). Methane production was detected 5 days after the inoculation of the sludge in both LBR and BLBR MECs, but not detected in the fermentative MECs. The methane production, as long with the consumption of acetate in the effluent of LBR and BLBR MECs, indicated that active anodic biofilms was formed in those MECs. The LBR and BLBR biofilms thickness were measured after 120 days of operation and the average biofilm thickness was 37.3 ± 2.8 and 52.5 ± 2.4 µm, respectively, for the LBR and BLBR which were both much lower than that of fermentative biofilm over 700 µm (747 ± 26.5 µm) (Table 6-1). Fermentative biofilm grown on the carrier in different bioreactor for wastewater treatment and other purposes typically has thickness of several hundred micrometers, while glucose in the medium can also stimulate biofilm thickness (Li et al., 2018a; Nguyen et al., 2020; Tam et al.,

2008). Factors including substrate, reactor hydraulic conditions, and carriers would affect the biofilm thickness (Arabgol et al., 2020; Fowler et al., 2023; Li et al., 2016a & 2018a; Nguyen et al., 2020; Suarez et al., 2019; Teodósio et al., 2011; Wagner et al., 2010). Biofilm conductivity was then calculated at the end of inoculation, according to the conductance and biofilm thickness data (Table 6-1). The average conductivity of LBR biofilm was 48.8 ± 2.8 μS/cm, which was comparable to conductivity of methanogenic biofilm developed from anaerobic sludge (16.8 ~ 50.6 μS/cm) (Li et al., 2017). The conductivity of LBR biofilm was about 20% smaller than the BLBR biofilm (61.6 ± 2.4 μS/cm), but was 65 times higher than the fermentative biofilm (0.75 ± 0.01 μS/cm) (Table 6-1). As comparison, the conductivity of LBR and BLBR biofilms were 33.2% and 41.8% of the conductivity of the *Geobacter*-enriched biofilm studied in Chapter 5 (147.2 ± 10.6 μS/cm).

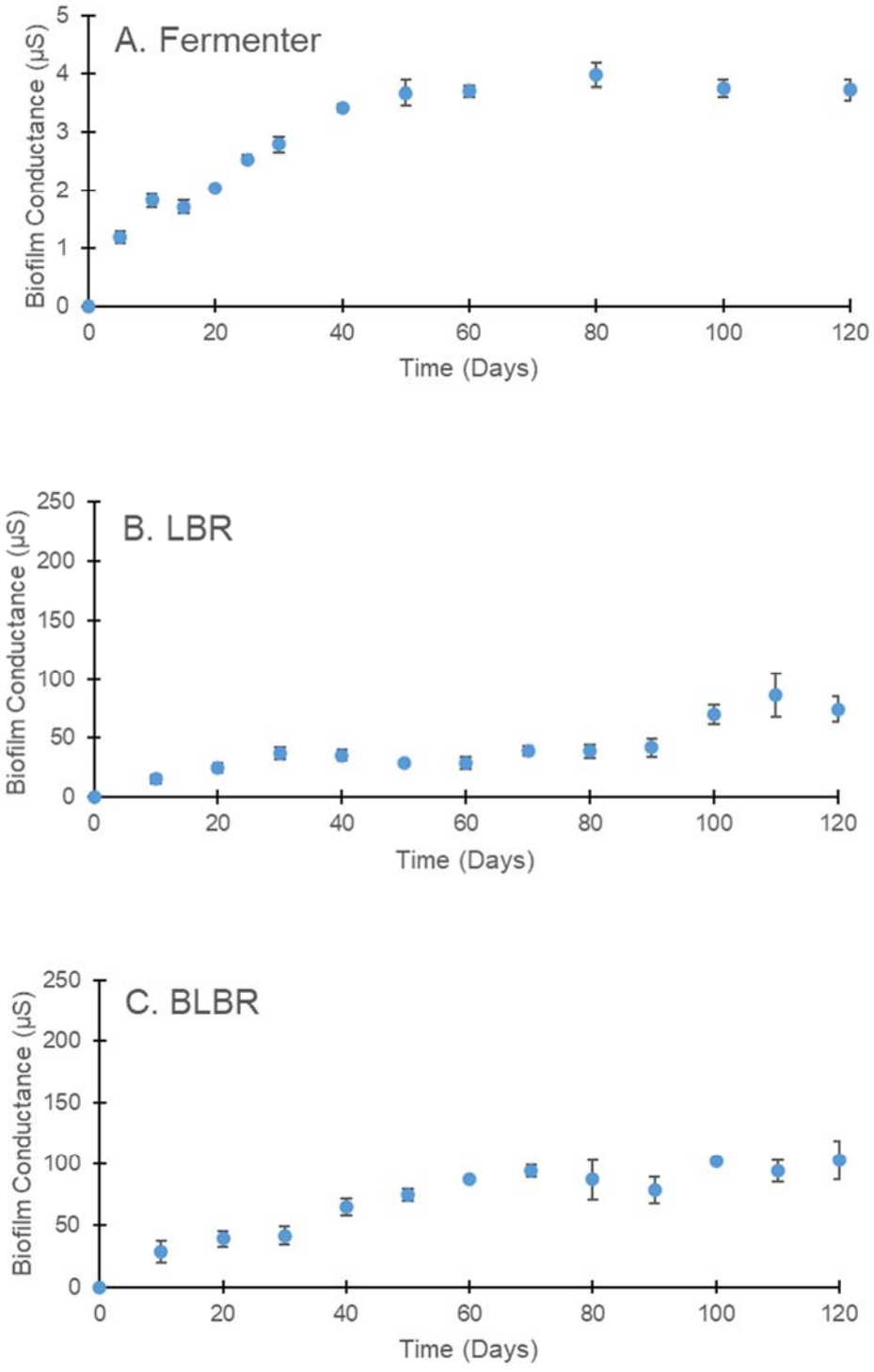

Figure 6-2. Biofilm Conductance measured over inoculation. A. Fermentative biofilm. B. LBR biofilm. C. BLBR biofilm. Error bars represent standard error with 3 replicates (n=3).

Table 6-1. Average biofilm thickness and conductivity of different types of biofilms.

Biofilm types	**Fermentative**	**LBR**	**BLBR**
Biofilm thickness (μm)	747 ± 26.5	37.3 ± 2.8	52.5 ± 2.4
Conductivity (μS/cm)	0.75 ± 0.01	48.8 ± 2.8	61.6 ± 2.4

Biofilm conductivity was the value with anode potential of -0.4 V (vs Ag/AgCl). Error bars represent standard error with 3 replicates (n=3).

6.3.2 Biofilm conductivity against variation of anode potentials

Conductivity of LBR and BLBR biofilms against anode potential were measured in order to explore possible mechanisms (Figure 6-3). From -600 mV to -200 mV (vs Ag/AgCl, the same as below), the biofilm conductivity in the LBR MECs showed a gentle increase and had a small peak with a conductivity of 52.8 μS/cm at -300 mV. Starting from -200 mV, the biofilm conductivity kept increasing till +600 mV and the conductivity at +600 mV was 2.45 times more than that at -600 mV (Figure 6-3). BLBR biofilm showed a conductivity profile against anode potential similar to that of LBR biofilm, but had higher conductivity (Figure 6-3). However, fermentative biofilm conductivity did not increase with the increase of anode potential until it increased to more positive than 200 mV. Overall, the biofilm conductivity of LBR and BLBR increased with increasing anode potential from -600 mV to +600 mV (vs Ag/AgCl); the conductivity of BLBR biofilm at +600 mV was 4.77 times higher that at -600 mV. It was also worth noting that the conductivity of BLBR biofilm at anode potential of +300 to +400 mV (145.6 ~ 158.9 μS/cm) were about 10% less than those of *Geobacter*-enriched biofilm (Figure 6-3 inset), while this anode potential range just covered the normal anode potential in the BLBR with the applied voltage of 0.6 and 0.9 V. Therefore, the anode biofilms in the BLBR at applied

voltage 0.6 and 0.9 V may also have comparable conductivity as those in the MECs, which would be favorable for conductive EET in anode biofilm of BLBR. Abiotic MEC experiments using the same split electrode but had no biofilm growth did not exhibit any conductance response, which indicated that the both biofilms were electronically conductive.

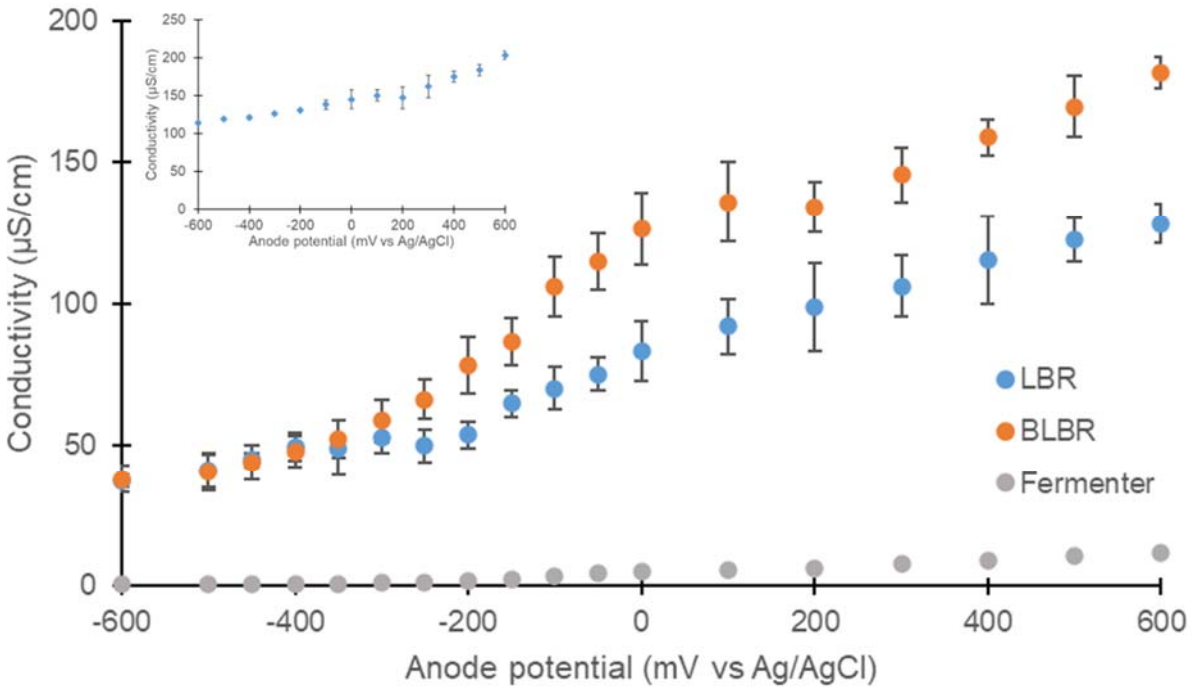

Figure 6-3. Conductivity of LBR, BLBR, and fermentative biofilms against anode potential variation. Inset: Conductivity of *Geobacter*-enriched biofilm against anode potential.

The profiles of the conductivity against anode potential of the LBR and BLBR biofilms were quite different from previous studies on methanogenic biofilm or granules (Li et al., 2016a, 2018a). In those studies, a peak-manner response against anode potential was observed in both methanogenic and mixed culture ARB biofilms, with the peak conductivity of about 75 μS /cm at

anode potential of -175mV (vs Ag/AgCl) observed in the methanogenic biofilm (Li et al., 2018a). Conductivity of the same biofilm decreased dramatically to as low as 5.0 μS/cm when anode potential varied more negative than -450 mV or more positive than 200 mV (Li et al., 2018a). However, the profiles of the conductivity against anode potential for BLBR biofilm was quite similar to that discovered in the *Geobacter*-enriched anodic biofilms (Figure 6-3 inset) (Malvankar et al., 2011 & 2012a). This response was also consistent with the conductance profile observed in organic metals (Lindsay, 2006; Zotti et al., 1995).

Redox conduction mechanism believed that *in situ* application of a small voltage between the split electrodes covered by conductive biofilms would result in electrolysis of redox species near electrode surface till steady state of the concentration gradients of these reduced and oxidized redox species was achieved (Dalton et al., 1990; Strycharz-Glaven et al., 2011). The gradient may also provide the driving force for electron transport in those redox polymers where electrons would diffuse from high to low concentrations. Therefore, redox polymers (i.e., conductive anodic biofilms) would show a characteristic maximum conductance when its redox potential creates equal ratio of reduced and oxidized species and conductance becomes poor as the polymer is poised at a potential far positive or negative of its redox potential due to overwhelming majority of reduced and oxidized redox species (Heller, 2006; Lindsay, 2006; Tran et al., 2004; Zotti et al., 1995).

The increase of biofilm conductivity with increasing anode potential indicates the characteristic of conductance similar to that in synthetic organic metal (Lindsay, 2006; Zotti et al., 1995), which could not be attributed to redox conduction associated with extracellular redox cofactors such as cytochromes. When anode potential became more positive (more highly oxidizing potential), the redox conduction relied on cytochrome-like cofactors would predict a

suppression in conductivity, which was not observed in the LBR and BLBR biofilm (Figure 6-3). In organic metals, charges (electrons) are delocalized and spread throughout the polymers (biofilms in our case). Literature suggested that this type of conductivity pattern could be related to electronically conductive pili (e-pili) or appendages of *G. sulfurreducens*. The electrical connections conferred by e-pili of *Geobacter* sp. resembled those of synthetic organic metals like polyaniline, in which charges are delocalized and spread throughout the polymer (Chen et al., 2014a & b; Liu et al., 2014; Malvankar et al., 2011, 2012a & b; Rotaru et al., 2014a & b). It is suggested that aromatic amino acids could play an important role on ohmic conduction of e-pili because overlapping π-orbitals of aromatic moieties can confer the delocalized charge distribution for metallic conductivity, and mutant of *G. sulfurreducens* which lacks key aromatic amino acids in their pilin monomers would only produce non-conductive pili (Lee et al., 2006; Liu et al., 2014; Malvankar et al., 2011; Vargas et al., 2013). Direct visualization of charge propagation along the e-pili and computational homology modelling further proved the delocalization of charges along e-pili similar to organic metals (Lovley and Malvankar, 2014; Malvankar et al., 2014, 2015;). Therefore, conductivity in BLBR biofilms would be closely related to ohmic conduction from e-pili of *Geobacter* sp. in the biofilms, and the increased conductivity with positive anode potential can favor the conductive EET in anode biofilm of BLBR systems.

6.3.3 Biofilm conductivity and biofilm community structures

The conductivity and microbial community structures of the LBR and BLBR biofilms were compared with those of fermentative biofilms to seek potential correlation in conductivity and community structures. Conductivity of both LBR and BLBR biofilms were higher than

fermentative biofilm (Table 6-1), but much less than that of a *Geobacter*-enriched biofilm. Further analysis also found positive correlation (r = 0.90) between the *Geobacter*'s population in biofilm microbial community and the biofilm conductivity (Figure 6-4). Similar correlation between the conductivity and *Geobacter* sp. abundance in methanogenic and mixed-species biofilms was also observed (Li et al., 2016a & 2018a). In the present biofilm community, *Geobacter* sp. accounted for 0.10% in the LBR biofilm, 0.21% in BLBR biofilms, and only 0.01% in fermentative communities. In comparison, *Geobacter* sp. commonly comprised more than 85% of the electronically conductive anodic biofilms, while it only comprised of 0.12% and 0.20% in the bacterial community in the anode biofilms from the control and the BLBR run at applied voltage 0.9 V, respectively (Figure 6-4 and Figure 6-5 inset) (Dhar et al., 2016; Hussain et al., 2021). Therefore, the BLBR biofilms inoculated from the leachate of BLBR enriched exoelectrogens like *Geobacter* sp. during the inoculation of MECs and the biofilms grown on the anodes of MECs under similar anode potential as in the BLBR 0.9V condition would show similar ARB abundance to those in BLBR systems.

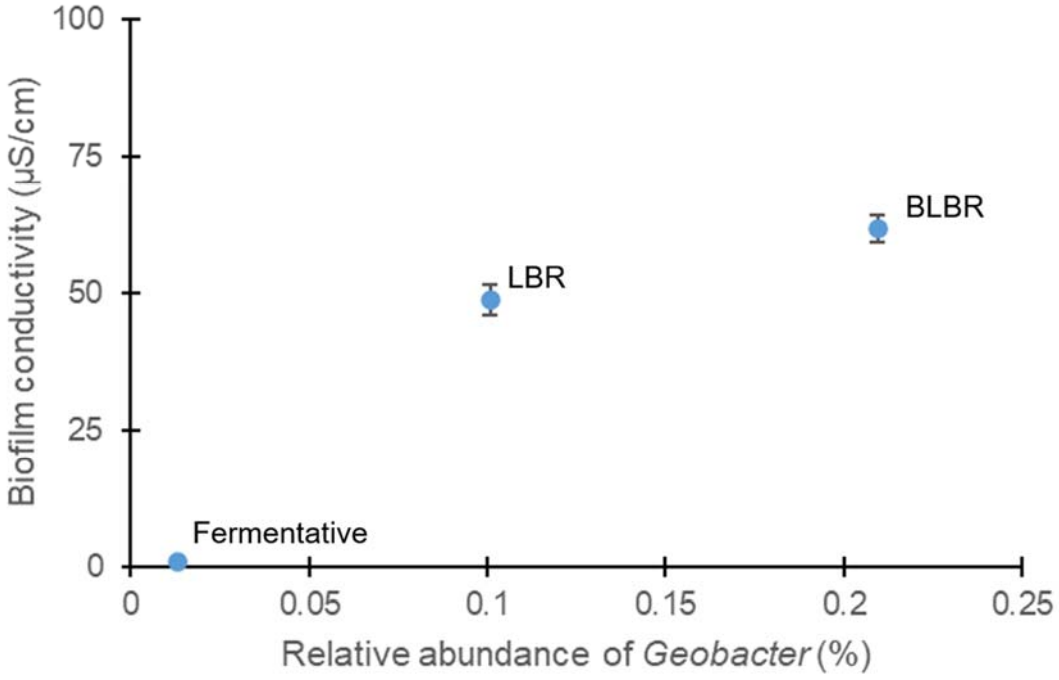

Figure 6-4. Biofilm conductivity and relative abundance of genus *Geobacter* in different biofilms. Error bars represent standard error (n=3).

Community structure analysis has shown the most abundant bacterial genera in those different biofilms (Figure 6-5a). *Clostridium*, *Trichococcus*, *Brooklawnia*, *Jeotgalibaca*, *Christensenellaceae*, and *Syntrophomonas* are all detected with high abundance in both LBR and BLBR biofilms. Bacteria from these genera can carry out organic fermentation and VFA production for AD process. Both LBR and BLBR biofilms had similar structure of major bacterial genera in the biofilm communities. Further comparison also proved that BLBR biofilm owns similar or comparable relative abundance of dominant bacterial genera as the anodic biofilm from BLBR at applied voltage 0.9V. This may be attributed to the similar anode

potential maintained in the MECs for BLBR biofilm growth and in the BLBR with 0.9V voltage application (Figure 6-5a). Especially, it was noted that the BLBR biofilms in MECs showed similar *Geobacter* abundance as the anodic biofilms of BLBR 0.9V group (0.21% vs 0.20%). In addition, the LBR biofilm also displayed similar biofilm community structure to the anodic biofilm in the control reactor (BLBR under open circuit mode) (Figure 6-5a). The bacterial community structures of these anode biofilm from MECs anodes and BLBR anodes were deviated from the leachate samples of BLBR 0.9 V conditions, which indicated that applied voltage would selectively enrich and modify the bacterial communities in the anode biofilms in both MECs and BLBRs, leading to similar bacterial community structure in the two systems.

The relative abundance of archaea genera was also compared for LBR and BLBR biofilms and leachate and anode biofilms from control BLBR and the one at applied voltage 0.9 V (Figure 6-5b). In BLBR biofilm, the genera *Methanosarcina* and *Methanobacterium* together dominated the archaea community, similar to that in the anode biofilm from BLBR 0.9 V condition. It was also observed that the genus *Methanocorpusculum* decreased significantly in the anode biofilm samples, as compared to the leachate sample from BLBR 0.9 V condition. Therefore, the applied voltage would selectively enrich the genera *Methanosarcina* and *Methanobacterium* in the anode biofilm of MEC, as well as in the anode biofilm of BLBR systems.

Therefore, it can be estimated that the anodic biofilm in BLBR systems with 0.9 V voltage applied would show similar biofilm conductivity to the biofilms grown on the 2-Au anodes in MECs because of the similar microbial community structures, and higher conductivity (~180 μS/cm at anode potential of +400 mV) could also be expected for those anode biofilms in BLBR systems, where the anode potential would range from +300 to +400 mV during operation.

These results proved that the biofilm grown on the anode of MECs could represent the anodic biofilms in the BLBR systems, which would provide a convenient way for future study on electrochemical characteristics of those conductive biofilms and EET procedures within the biofilms.

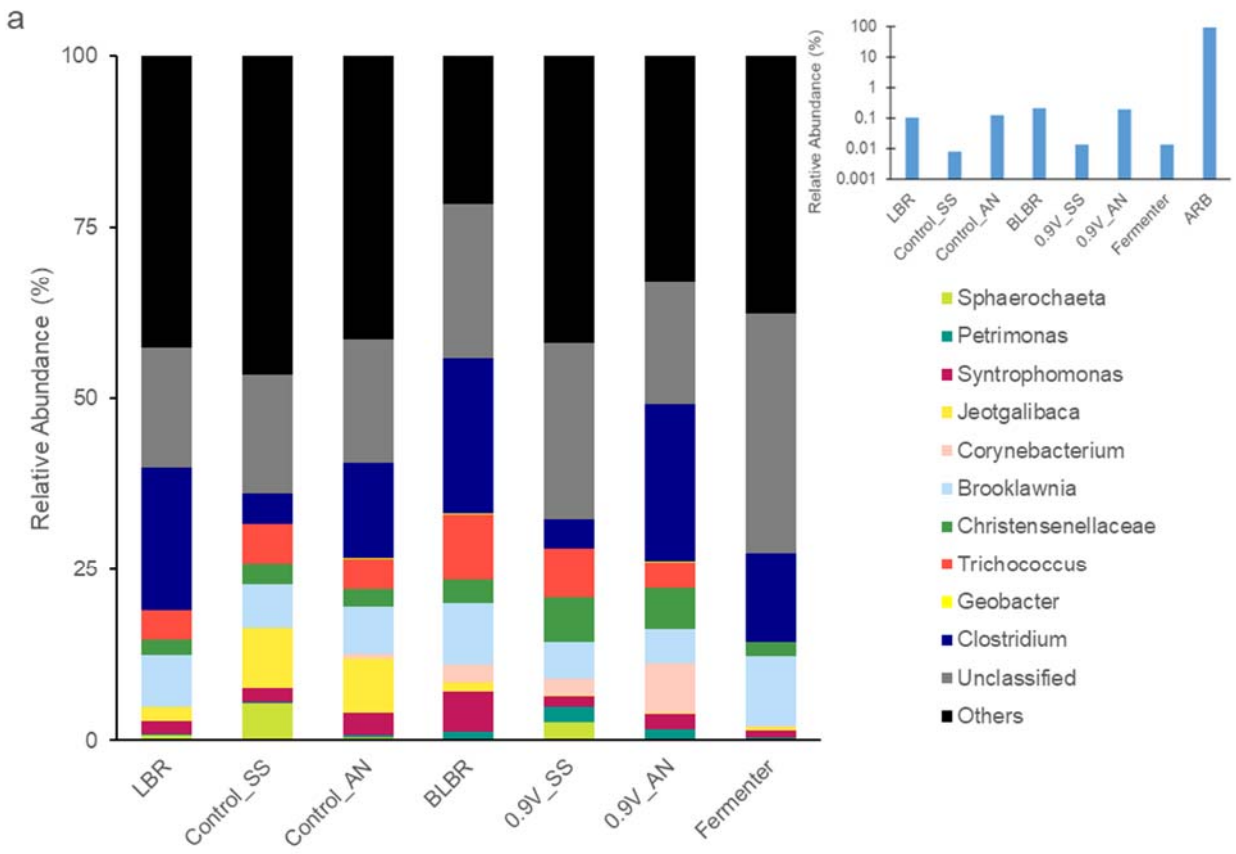
a
Relative Abundance (%)
100
75
50
25
0
LBR
Control_SS
Control_AN
BLBR
0.9V_SS
0.9V_AN
Fermenter
Relative Abundance (%)
100
10
1
0.1
0.01
0.001
LBR
Control_SS
Control_AN
BLBR
0.9V_SS
0.9V_AN
Fermenter
ARB
Sphaerochaeta
Petrimonas
Syntrophomonas
Jeotgalibaca
Corynebacterium
Brooklawnia
Christensenellaceae
Trichococcus
Geobacter
Clostridium
Unclassified
Others

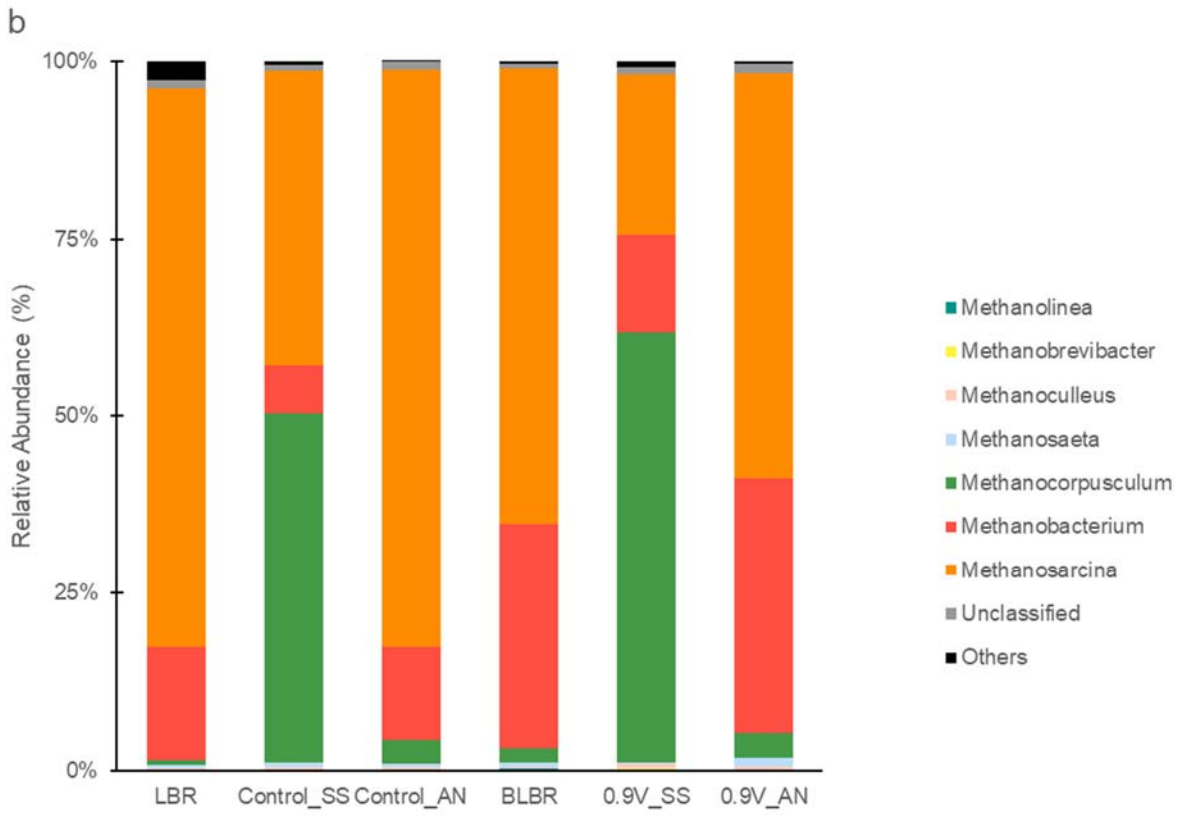

Figure 6-5. Relative abundance of (a) bacterial genera and (b) archaea genera in LBR and BLBR biofilm communities. Samples of leachate and anode biofilms from BLBR under control and 0.9V were also listed for comparison. SS: leachate samples. AN: anode biofilm samples. Inset: Relative abundance of genus *Geobacter* in these samples.

The correlation between *Geobacter* sp. and conductivity indicated that *Geobacter* sp. may be the major component of conductive biofilms which enables EET and DIET in anode biofilms and an active participant of syntrophic methanogenesis and DIET, although the low relative abundance of *Geobacter* sp. was observed in the anode biofilms. In addition, multiple genera including *Desulfomicrobium*, *Desulfobulbus*, and *Pseudomonas* which could also participate DIET between microorganisms and electrodes were also detected in the BLBR

biofilms (Holmes et al., 2004; Müller et al., 2016; Pfeffer et al., 2012; Rabaey et al., 2004; Scholz et al., 2012). Those potential ARB capable of EET were also selectively enriched in the BLBR biofilm of MECs under applied voltage, which accounted for about 1.07% of the anode biofilm community.

Although *Geobacter* sp. is often recognized as the major participant of EET and DIET with hydrogenotrophic methanogen, some studies discovered the relative abundance of *Geobacter* less than 5% in those MEC-AD system (Wang et a., 2021a; Zhao et al., 2021), compared to the abundance of *Geobacter* higher than 85% in those current-generating biofilm (Dhar et al., 2016; Hussain et al., 2021). And it still requires solid evidence that a threshold abundance of major EET participants like *Geobacter* may exit in mixed-species biofilm in order to maintain high biofilm conductivity, even the present study and other researches proved that there was correlation between biofilm conductivity and the abundance of *Geobacter* in biofilm community (Dhar et al., 2016; Li et al., 2016a & 2018a).

The low Coulombic efficiency (CE) (<7%) and low *Geobacter* abundance obtained during BLBR operation indicated that only a small portion of electrons were delivered by ARBs to the anode through the anode biofilm. The relatively low abundance of ARBs like *Geobacter* may limit the number of electrons which could be transferred from substrate to anode, thereby limiting the electrons delivered to cathode and accepted by those hydrogenotrophic methanogens for CO_2-reduction methane production. *Geobacter* abundance above 25% and CE as high as 43% were reported in those MEC-AD system (Li et al., 2016c; Wang et al., 2021a; Zhao et al., 2016c). Therefore, pre-enrichment of *Geobacter* and other ARBs in the anode and leachate before starting the BLBR operation may increase the electron transferred via EET to the anode and hence improve the methane production on cathode.

Studies have also indicated the complexity of EET-based syntrophy, or "electric syntrophy", in anode biofilm. On one hand, the BLBR biofilm community showed higher abundance of several bacterial genera including *Clostridium* (22.6% in BLBR biofilm vs 20.8% in LBR biofilm), *Trichococcus* (9.53% in BLBR biofilm vs 4.30% in LBR biofilm), *Syntrophomonas* (5.88% vs 1.88%), *Corynebacterium* (2.59% vs 0.08%), and *Petrimonas* (1.06% vs 0.28%). Studies have indicated that above bacteria can, or have the potential to carry out EET or DIET within the biofilm community (Baek et al., 2015; Doloman et al., 2022; Engel et al., 2020; Izadi et al., 2021; Jiang et al., 2022; Lin et al., 2022; Liu et al., 2010b; Ren et al., 2020; Saheb-alam et al., 2019; Zhao et al., 2012). Besides, *Geobacter* abundance of almost zero and CE as high as 43% were reported in a MEC-assisted AD system with improved methane production, which further indicated that bacteria other than ARB could participate in EET and high current generation (Li et al., 2016c). Further, a survey has also identified more than 90 microbial species already existed which are electroactive and there are more potential microbial species capable of EET and DIET existing in natural and artificial engineered systems (Koch & Harnisch, 2016).

On the other hand, interspecies substrate competition between different microbes in anode biofilm may also increase the current generation and EET (Xiao et al., 2021). Interspecies substrate competition would increase the metabolic activities of ARB and benefit the conductive biofilm formation on the anodes, which would improve EET and current generation by up-regulating proteins expressions related to biofilm formation, c-type cytochromes synthesis, and flavin secretion (Xiao et al., 2021). Those results proved the complexity and diversity of the EET-based syntrophy in anode biofilms and showed the potential of such anode biofilms for high current generation and active EET in BLBR.

In addition, it can be seen from Figure 6-5b that the relative abundance of *Methanosarcina* was more than 60% in BLBR biofilm from MECs, which indicated that this methanogen may also participate in syntrophic methanogenesis or DIET-induced methanogenesis with ARB involved in the anodic biofilm (Guo et al., 2019; Logan et al., 2019; Ringeisen et al., 2006; Tang et al., 2007). Further, some studies also proved that acetoclastic methanogenesis was also stimulated by the syntrophy between ARB and acetoclastic methanogen, which would become an important and beneficial complement for enhanced methane production in those engineered MEC-AD systems like BLBR (Xiao et al., 2019 & 2020). Considering the abundance of *Methanosarcina* which is capable of both hydrogenotrophic and acetoclastic methanogenesis in the anode biofilm, electrons delivered by ARB would be accepted by *Methanosarcina* for methane production via acetate dismutation and DIET-induced CO_2 reduction and such electron transfer pathways could not be excluded in the MEC-AD systems. More work is needed to find the proportion of electrons transferred to anode and participating DIET for acetoclastic methanogenesis in anode biofilm during BLBR operation and to identify the factors which would affect the efficiency of the two electron transfer pathways in the BLBR system.

6.4 Conclusion

In the present study, biofilm conductivity results displayed that the methanogenic types of biofilms showed smaller conductivity than *Geobacter* enriched biofilms. The BLBR biofilm also reported highly conductive under the anode potential of which was observed in the BLBR systems, which proved that the anode biofilm would be conductive for EET during BLBR

operation. The electron transfer in those methanogenic types of biofilms would be dominated by metallic conduction, because the biofilm conductivity increased against the anode potential.

The abundance of *Geobacter* sp. in biofilm community was positively correlated with the biofilm conductivity. Several bacterial and archaea genera with the potential of EET and DIET were also found with elevated abundance in BLBR biofilm community, which also suggested a possible way of optimizing EET and DIET in those biofilms by alternating microbial community structure. Microbial community structure analysis also identified similar bacterial and archaea genera components in the biofilm communities grown on anodes of MECs and BLBRs. Therefore, MECs could provide a useful and convenient tool for future *in situ* study on the bioelectrochemical characteristics of those biofilms grown in electrodes of BLBR and other MEC-AD systems.

These findings would expand and deepen our understanding of extracellular electron transfer within fermentative and methanogenic microbial communities in the engineering systems. Further investigation and studies on this topic are important for improvement in bioenergy recovery in MEC assisted AD systems and would also provide innovative understanding of other biogeochemical or bioelectrochemical processes in anaerobic environments.

Chapter 7 – Conclusions and recommendations

7.1 Conclusions

The application of microbial electrolysis cell assisted anaerobic digestion (MEC-AD) system for food waste (FW) dry digestion to recovery methane from organic waste is promising. And understanding the extracellular electron transfer (EET) based syntrophy between ARB and other microorganisms is important to improve the MEC-AD system performance for dry digestion and to further expand the application of the innovative bioelectrochemical leach bed reactor (BLBR) for sustainable energy recovery technology. The present study in the thesis first to develop an engineered MEC-AD system, the BLBR, for FW dry digestion with applied voltage. The second is to establish a new standard method for quantification of biofilm conductivity with improving accuracy and reproducibility, including optimization of operating and environmental parameters. Such a method will be applied to the anode biofilm in the BLBR together with other tools to systematically demonstrate and assess interspecies electron transfer via EET and conduction-based syntrophy during dry AD process of FW in BLBR. The key conclusions from the present study are summarized below.

A traditional leach bed reactor (LBR) was modified for FW dry digestion and methane production. Inoculum should be acclimated with potential inhibitors such as salinity and ammonia which may be encountered with elevated levels in LBR systems before starting the LBR operation, which in order to accumulate desired microorganisms adapt to those inhibitors and to achieve the methane production. The cumulative methane yield with inoculum to substrate ratio (ISR) 60% was 3.35 times more than that with ISR 10%, while VS reduction with 60%

decreased by 20% to that with ISR 10%. Increasing in leachate recirculation also promoted the methane yield. The cumulative methane yield increased by 78% when the recirculation rate increased from 0.3 L/hr to 7.5 L/hr while ISR was kept unchanged. These results displayed the feasibility of LBR application for methane production from FW.

The voltage application in BLBR has proved to improve the acidogenesis and methanogenesis during AD process for FW. Methane yield in the BLBR was enhanced at all applied voltages compared to the control. Optimal applied voltage for methane production was 0.9 V, at which methane yield was 46.7% higher than the control. Further increase the voltage to 1.2 V led to decrease on methane yield. No significant difference was observed in VS removal among these operation with different applied voltage. VFA profiles also showed enhanced acidogenesis and acetogenesis during AD with voltage application, and the observed propionate accumulation occurred in the BLBR with 0.3 and 1.2 V, but did not display any significant inhibition on methane yield. The contribution of direct electron transfer through closed circuit on methane yield enhancement was less than 10% and the coulombic efficiency (CE) was less than 6.1%, even with a high conductive anode biofilm in BLBR. The microbial community structure in cathode biofilms indicated the enhanced methane production could be attributed to the enrichment of hydrogenotrophic methanogens through syntrophic methanogenesis because of the enhanced acidogenesis and acetogenesis by applied voltage. Acetoclastic methanogen enriched at anode may also improve the methane production via acetate dismutation by directly accepting electrons from ARB in the anode biofilm, although this hypothesis requires future experimental evidence. The results from the present experiments proved the feasibility of BLBR on FW dry digestion and enhanced methane production.

Biofilm conductance is a key parameter to estimate that how feasible the electron could be transferred within it. The biofilm conductance in the MECs showed a sigmoidal profile corresponding to an increase in anode potential from -0.5 V to +0.2 V (vs Ag/AgCl). In comparison, biofilm conductance with a fixed anode potential of -0.4V showed a small difference from that without a fixed anode potential, which indicated that anode potential control was not critical for measuring biofilm conductance, while it could still slightly change biofilm conductance. The Ohmic-response range was identified at a voltage range between 0 and 100 mV where the current-voltage profile of biofilm stayed within Ohm's law. Increased monitoring time at each voltage step showed up to 69% decrease in measured biofilm conductance and further deviation from Ohm's law on the current-voltage profile. The relationship between biofilm conductance and operational parameters also suggested that biofilm conductance should be quantified and displayed with these parameters together for the purpose of comparison. The methods developed in this chapter will be applied to investigate the conductance of biofilms developed in BLBR systems.

Finally, biofilm from LBR and BLBR in previous experiments were developed on the split gold electrodes in the MEC for biofilm conductivity measurement. Biofilm conductivity results displayed that both LBR and BLBR biofilms showed smaller conductivity than Geobacter-enriched biofilms. The BLBR biofilm also reported highly conductive (145.6 ~ 158.9 μS/cm) under the anode potential of which was observed in the BLBR systems, indicating that the anode biofilm would be conductive for EET during BLBR operation. The electron transfer in those methanogenic types of biofilms would be dominated by metallic conduction, because the biofilm conductivity increased against the anode potential. The abundance of *Geobacter* sp. in biofilm community was positively correlated with the biofilm conductivity. Several bacterial and

archaea genera with the potential of EET and DIET were also found with elevated abundance in BLBR biofilm community, indicating that high biofilm conductivity may also be related to those potential electroactive bacteria in the anode biofilm. Microbial community structure analysis identified similar bacterial and archaea genera components in the biofilm communities grown on split gold anodes of MECs and on carbon fiber anodes of BLBR. Therefore, MEC equipped with split gold anodes could be a useful tool for *in situ* study on the bioelectrochemical characteristics including biofilm conductivity of those biofilms grown on electrodes of BLBR and other MEC-AD systems.

7.2 Suggestion

The findings in the present study have proved the possibility of integration of MEC and LBR into one MEC-AD system and the feasibility of BLBR for enhanced methane production on FW dry digestion. MEC equipped with split gold electrodes has also displayed its advantage for study bioelectrochemical characteristics of those conductive biofilm from MEC-AD systems. However, more studies are required to deeper understanding the electric syntrophy among the anode and cathode biofilm in the BLBR and improve the performance of BLBR for solid waste dry digestion and energy recovery. For these purposes, some future research topics are summarized here.

In terms of MEC-AD system operations, future studies are needed to expand the types of wastes which can be treated in BLBR, including solid waste like FW, agricultural waste, and municipal solid waste, and wastewater like brewing wastewater, pig manure, and industrial wastewater.

Second, more work is required to optimize the operation parameters including organic loading rate, hydraulic retention time, applied potential, and internal fluid kinetics for BLBR dry digestion on FW and other organic waste in order to improve the solid removal, methane production rate and methane yield, and decrease the energy consumption during treatment. Studies should focus on the materials and structures of electrodes in order to facilitate the selection and enrichment of electroactive and DIET related microorganisms in the BLBR in order to improve the methane production. Third, long-term operation on the BLBR for FW and other organic waste dry digestion should be carried out, when the above two points are satisfied. The present studies of 10-day operation are not able to evaluate the system performance stability and economic feasibility of BLBR for scale-up and long-term operation.

In terms of microbial mechanisms in MEC-AD systems, although many studies have been conducted to demonstrate effect of DIET on the enhanced performance in MEC-AD system, many challenges still remain. For example, unlike pure culture systems, most of the studies have been conducted to speculate whether microorganisms in the complex microbial community capable of extracellular electron transfer are involved in DIET during anaerobic digestion, based on the specific enrichment of microorganisms by conductive materials, and the results need to be further validated. The database of functional DIET microorganisms will be expanded through long-term sequencing validation based on 16S rRNA analysis combined with metagenomic, metatranscriptomic, and proteomic techniques to identify microorganisms involved in inhibitor degradation as well as capable of DIET in anaerobic systems. While investigating the promotion on anaerobic digestion by DIET, a comprehensively consideration is needed to establish the correspondence between the physical-chemical characteristics of electrodes and DIET mechanisms on AD performance enhancement.

In addition, hydrogenotrophic methanogenic bacteria have been recognized as the major participant involved in DIET, however, in a reaction system dominated by hydrogenotrophic methanogenic bacteria, mediated interspecies electron transfer via hydrogen may also be promoted. It requires detail studies to verify the dominance of DIET in AD process. The hypothetical DIET-induced acetoclastic methanogenesis between ARB and acetoclastic methanogens on anode biofilm also requires more work. Future studies should find out the efficiency between the two possible pathways, acetoclastic methanogenesis induced by DIET in anode biofilm and hydrogenotrophic methanogenesis accepting electrons from cathode, and identify the factors that would affect the efficiency of the two pathways during BLBR operation.

Finally, design and application of synthetic electroactive microbial community for MEC-AD system would be a good alternative for natural electroactive microbial community. Compared with natural community, synthetic electroactive microbial community will have a clear structure, fewer metabolic pathways, and high specificity on substance metabolisms, and thus may have higher efficiency in mediating energy conversion and electron transfer. A strategy combining adaptive co-evolution and modification should be developed to engineer synthetic electroactive microbial community to improve their EET and other catalytical functions. The adaptive strategy here can enable the co-evolution of each strain within a colony under the induction of specific environmental stress, thus enabling the colony to acquire superior traits. Many unknown targets can be obtained through co-evolving which can provide an important reference for establishing the theoretical basis of design and engineering synthetic electroactive microbial community. A mathematical model of the design and construction on synthetic electroactive microbial flora can be developed and combined with computational technique, which will provide the optimal solution for precise regulation of synthetic electroactive microbial

community. On this basis, a modular platform for synthetic electroactive microbial community could be developed and improve the efficiency of synthetic electroactive microbial community construction, which will benefit its wide industrial application.

Bibliography

Abbas, Y., Yun, S., Wang, Z., Zhang, Y., Zhang, X., Wang, K., 2021. Recent advances in bio-based carbon materials for anaerobic digestion: A review. Renewable and Sustainable Energy Reviews, 135:110378.

Adhikari, R.Y., Malvankar, N.S., Tuominen, M.T., and Lovley, D.R., 2016. Conductivity of individual Geobacter pili. RSC Adv. 6 (10), 8354–8357.

Ağdağ, O.N., Sponza, D.T., 2005. Effect of alkalinity on the performance of a simulated landfill bioreactor digesting organic solid wastes. Chemosphere 59, 871–879.

Ahmed, A.M., and Sulaiman, W.N., 2001. Evaluation of groundwater and soil pollution in a landfill area using electrical resistivity imaging survey. Environmental Management, 28(5), 655-663.

Ahring, B.K., Westermann, P., 1988. Product inhibition of butyrate metabolism by acetate and hydrogen in a thermophilic coculture. Appl. Environ. Microbiol. 54, 2393e2397.

Angenent, L.T., Karim, K., Al-Dahhan, M.H., Wrenn, B.A., Domíguez-Espinosa, R., 2004. Production of bioenergy and biochemicals from industrial and agricultural wastewater. Trends Biotechnol. 22, 477–485.

Anderson, L.B., Reilley, C.N., 1965. Thin-layer electrochemistry: steady-state methods of studying rate processes. J. Electroanal. Chem. 10 (4), 295–305.

Angelidaki, I., Ahring, B.K., 1993. Thermophilic anaerobic-digestion of livestock waste–the effect of ammonia. Applied Microbiology and Biotechnology, 38(4): 560-564.

Angelidaki, I., Ellegaard, L., Ahring, B.K., 1993. A mathematical model for dynamic simulation of anaerobic digestion of complex substrates: focusing on ammonia inhibition. Biotechnol. Bioeng. 42, 159e166.

Appels, L., Lauwers, J., Degrève, J., Helsen, L., Lievens, B., Willems, K., Van Impe, J., and Dewil, R., 2011. Anaerobic digestion in global bio-energy production: Potential and research challenges. Renew. Sustain. Energy Rev. 15, 4295–4301.

Arabgol, R., Vanrolleghem, P.A., Picullell, M., Delatolla, R., 2020. The impact of biofilm thickness-restraint and carrier type on attached growth system performance, solids characteristics and settleability. Environ. Sci.: Water Res. Technol., 2020,6, 2843-2855.

Arbeli, Z.; Brenner, A.; and Abeliovich, A., 2006. Treatment of high-strength dairy wastewater in an anaerobic deep reservoir: Analysis of the methanogenic fermentation pathway and the rate-limiting step. Water Res. 40, 3653–3659.

Association, A.P.H., Association, A.W.W., Federation, W.E., 2005. Standard Methods for the Examination of Water and Wastewater. American Public Health Association (APHA), Washington DC, USA.

Aulenta, F., Canosa, A., Majone, M., Panero, S., Reale, P., Rossetti, S., 2008. Trichloroethene dechlorination and H2 evolution are alternative biological pathways of electric charge utilization by a dechlorinating culture in a bioelectrochemical system. Environ Sci Technol, 42: 6185–6190.

Bae, S., Yoo, K., 2022. Microplastic contamination and microbial colonization in coastal area of Busan City, Korea. Front. Mar. Sci., Front. Mar. Sci. 9:1030476.

Baek, G., Kim, J., Cho, K., Bae, H., Lee, C., 2015. The biostimulation of anaerobic digestion with (semi)conductive ferric oxides: their potential for enhanced biomethanation, Appl. Microbiol. Biotechnol. 99, 10355–10366.

Baek, G., Kim, J., Kim, J., and Lee, C., 2018. Role and Potential of Direct Interspecies Electron Transfer in Anaerobic Digestion. Energies, 11(1), 107.

Bai, X., Chen, Y., 2020. Synergistic effect and supernatant nitrogen reduction from anaerobic co-digestion of sewage sludge and pig manure. Bioresource Technology Reports, 10 100424.

Balazsi, G., Barabasi, A.L., Oltvai, Z.N., 2005. Topological units of environmental signal processing in the transcriptional regulatory network of *Escherichia coli*. Proc. Natl. Acad. Sci. U.S.A., 102, 7841-6.

Bao, H., Yang, H., Zhang, H., Liu, Y., Su, H., Shen, M., 2020. Improving methane productivity of waste activated sludge by ultrasound and alkali pretreatment in microbial electrolysis cell and anaerobic digestion coupled system. Environmental Research, 180, 108863.

Barua, S., Zakaria, B.S., and Dhar, B.R., 2018. Enhanced methanogenic co-degradation of propionate and butyrate by anaerobic microbiome enriched on conductive carbon fibers. Bioresource Technology, 266, 259-266.

Batstone, D.J., and Virdis, B., 2014. The role of anaerobic digestion in the emerging energy economy. Curr Opin Biotechnol, 27, 142-149.

Beegle, J.R., Borole, A.P., 2017. An integrated microbial electrolysisanaerobic digestion process combined with pretreatment of wastewater solids to improve hydrogen production. Environ Sci Water Res Technol, 3:1073e85.

Benbelkacem, H., Bayard, R., Abdelhay, A., Zhang, Y., Gourdon, R., 2010. Effect of leachate injection modes on municipal solid waste degradation in anaerobic bioreactor. Bioresour. Technol. 101, 5206–5212.

Blasco-G´omez, R., Batlle-Vilanova, P., Villano, M., Balaguer, M., Colprim, J., Puig, S., 2017. On the edge of research and technological application: a critical review of electromethanogenesis. Int. J. Mol. Sci. 18 (4), 874.

Bo, T., Zhu, X., Zhang, L., Tao, Y., He, X., Li, D., and Yan, Z., 2014. A new upgraded biogas production process: Coupling microbial electrolysis cell and anaerobic digestion in single-chamber, barrel-shape stainless steel reactor. Electrochemistry Communications, 45, 67-70.

Bochmann, G., Montgomery, L., 2013. Storage and pre-treatment of substrates for biogas production. In: Wellinger, A., Murphy, J.D., Baxter, D. (Eds.), The Biogas Handbook. Woodhead Publishing, Oxford, Cambridge, Philadelphia, New Delhi, pp. 95–96.

Bonanni, P.S., Bradley, D.F., Schrott, G.D., and Busalmen, J.P., 2012. Limitations for current production in *Geobacter sulfurreducens* biofilms. ChemSusChem, 6, 711-720.

Bond, D.R. and Lovley, D.R., 2003. Electricity production by *Geobacter sulfurreducens* attached to electrodes. Applied and environmental microbiology, 69(3), 1548-1555.

Boone, D.R., Johnson, R.L., and Liu, Y., 1989. Diffusion of the interspecies electron carriers H2 and formate in methanogenic ecosystems and its implications in the measurement of Km for H2 or formate uptake. Appl. Environ. Microbiol., 55, 1735–1741.

Borole, A.P., Reguera, G., Ringeisen, B., Wang, Z.W., Feng, Y., and Kim, B.H., 2011. Electroactive biofilms: current status and future research needs. Energy & Environmental Science, 4(12), 4813-4834.

Borrel, G., Toole, P.W., Harris, H., Peyeret, P., Brugere, J.F., Gribaldo, S., 2013. Phylogenomic data support a seventh order of methylotrophic methanogens and provide insights into the evolution of methanogenesis. Genome Biol Evol, 5:1769–1780.

Borrel, G., Parisot, N., Harris, H.M.B., Peyretaillade, E., Gaci, N., 2014. Comparative genomics highlights the unique biology of Methanomassiliicoccales, a Thermoplasmatalesrelated seventh order of methanogenic Archaea that encodes pyrrolysine. BMC Genomics, 15:679.

Boyd, D., Snider, R.M., Erikson, J.S., Roy, J.N., Strycharz-Glaven, S.M., and Tender, L.M., 2015. Theory of Redox Conduction and the Measurement of Electron Transport Rates Through Electrochemically Active Biofilms. Chapter 6, Biofilms in Bioelectrochemical Systems: From Laboratory Practice to Data Interpretation, edited by Haluk Beyenal, Jerome T. Babauta.

Braguglia, C.M., Gallipoli, A., Gianico, A., 2018. Anaerobic bioconversion of food waste into energy: A critical review. Bioresource Technology, 248:37-56.

Bretschger, O.; Obraztsova, A.; Sturm, C.A.; In, S.C.; Gorby, Y.A.; Reed, S.B.; Culley, D.E.; Reardon, C.L.; Barua, S.; Romine, M.F., 2007. Current production and metal oxide reduction by Shewanella oneidensis MR-1 wild type and mutants. Appl. Environ. Microbiol. 73, 7003–7012.

Browne, J.D., Allen, E., and Murphy, J.D., 2013. Improving hydrolysis of food waste in a leach bed reactor. Waste Management, 33(11), 2470-2477.

Browne, J.D., Murphy, J.D., 2014. The impact of increasing organic loading in two phase digestion of food waste. Renew. Energy 71, 69-76.

Cadavid-Rodríguez, L.S., and Horan, N.J., 2014. Production of volatile fatty acids from wastewater screenings using a leach-bed reactor. Water Research, 60, 242-249.

Cai, S., Shao, N., Dong, X., 2016. Cellulosilyticum. In Bergey's Manual of Systematics of Archaea and Bacteria (eds W. B. Whitman, F. Rainey, P. Kämpfer, M. Trujillo, J. Chun, P. DeVos, B. Hedlund and S. Dedysh).

Calli, B., Mertoglu, B., Inanc, B., Yenigun, O., 2005. Effects of high free ammonia concentrations on the performances of anaerobic bioreactors. Process Biochem. 40(3–4), 1285–1292.

Cao, S., Sun, F., Lu, D., 2019. Characterization of the refractory dissolved organic matters (rDOM) in sludge alkaline fermentation liquid driven denitrification: Effect of HRT on their fate and transformation. Water Research, 159: 135-144.

Castro, L., Vera, M., Munoz, J.A., Blazquez, M.L., Gonzalez, F., Sand, W., and Ballester, A., 2014. *Aeromonas hydrophila* produces conductive nanowires. Research in Microbiology, 165, 794-802.

CBC. (2019, Sept. 25). How bad is Canada's food waste problem? among the world's worst, report finds; Retrieved from https://www.cbc.ca/radio/thecurrent/the-current-for-april-5-

2018-1.4605392/how-bad-is-canada-s-food-waste-problem-among-the-world-s-worst-report-finds-1.4606012.

CEC. 2017. Characterization and Management of Food Loss and Waste in North America. Montreal, Canada: Commission for Environmental Cooperation. 48 pp.

Cerrillo, M., Vi˜nas, M., Bonmatí, A., 2017. Unravelling the active microbial community in a thermophilic anaerobic digester-microbial electrolysis cell coupled system under different conditions. Water Res. 110, 192–201.

Chan, G.Y.S., Chu, L.M., Wong, M.H., 2002. Effects of leachate recirculation on biogas production from landfill co-disposal of municipal solid waste, sewage sludge and marine sediment. Environ. Pollut. 118, 393–399.

Chen, H., Meng, H., Nie, Z., 2013a. Polyhydroxyalkanoate production from fermented volatile fatty acids: Effect of pH and feeding regimes. Bioresource Technology, 128:533-538.

Chen, S., Rotaru, A.E., Liu, F., Philips, J., Woodard, T.L., Nevin, K.P., and Lovley, D.R., 2014a. Carbon cloth stimulates direct interspecies electron transfer in syntrophic co-cultures. Bioresour. Technol. 173, 82–86.

Chen, S., Rotaru, A.E., Shrestha, P.M., Malvankar, N.S., Liu, F., Fan, W., Nevin, K.P., and Lovley, D.R., 2014b. Promoting interspecies electron transfer with biochar. Sci Rep 4,5019.

Chen, S., Yang, D., Dong, B., Li, N., Dai, X., 2020. Sludge age impacted the distribution, occurrence state and structure of organic compounds in activated sludge and affected the anaerobic degradability. Chem. Eng. J. 384, 123261.

Chen, X., Yuan, H., Zou, D., Liu, Y., Zhu, B., Chufo, A., Jaffar, M., Li, X., 2015. Improving biomethane yield by controlling fermentation type of acidogenic phase in two-phase anaerobic co-digestion of food waste and rice straw. Chemical Engineering Journal, 273, 254-260.

Chen, Y., Cheng, J.J., & Creamer, K.S., 2008. Inhibition of anaerobic digestion process: A review. Bioresource Technology, 99(10): 4044-4064.

Chen, Y., Li, X., Zheng, X., 2013b. Enhancement of propionic acid fraction in volatile fatty acids produced from sludge fermentation by the use of food waste and *Propionibacterium acidipropionici*. Water Research, 47(2): 615-622.

Chen, Y., Yu, B., Yin, C., Zhang, C., Dai, X., Yuan, H., Zhu, N., 2016. Biostimulation by direct voltage to enhance anaerobic digestion of waste activated sludge. RXC Adv. 6(2), 1581-1588.

Cheng, H., Li, Y., Guo, G., 2020. Advanced methanogenic performance and fouling mechanism investigation of a high-solid anaerobic membrane bioreactor (AnMBR) for the co-digestion of food waste and sewage sludge. Water Research, 187:116436.

Cheng, K.Y., Kaksonen, A.H., 2017. Integrating microbial electrochemical technologies with anaerobic digestion for waste treatment: possibilities and perspectives. In: Wong JWC, Tyagi RD, pandey A, editors. Current developments in biotechnology and bioengineering, solid waste management. Elsevier; 2017. p. 191e221.

Cheng, Q., Call, D.F., 2016. Hardwiring microbes via direct interspecies electron transfer: Mechanisms and applications. Environ. Sci. Processes Impacts, 18, 968–980.

Cheng, S., Logan, B.E., 2007. Sustainable and efficient biohydrogen production via electrohydrogenesis. PNAS, 104(47): 18871-18873.

Cheng, S.A., Xing, D.F., Call, D.F., Logan, B.E., 2009. Direct biological conversion of electrical current into methane by electromethanogenesis. Environ Sci Technol, 43 (10): 3953-3958.

Choi, K.S., Kondaveeti, S., Min, B., 2017. Bioelectrochemical methane (CH_4) production in anaerobic digestion at different supplemental voltages. Bioresour Technol, 245:826e32.

Choi, J.M., Lee, C.Y., 2019. Bioelectrochemical enhancement of methane production in anaerobic digestion of food waste. Int. J. Hydrogen Energy 44 (4), 2081–2090.

Choi, O., Sang, B.I., 2016. Extracellular electron transfer from cathode to microbes: application for biofuel production. Biotechnol Biofuels, 9(1): 1-14.

Chowdhury, B., Lin, L., Dhar, B.R., Islam, M.N., McCartney, D., Kumar, A., 2019. Enhanced biomethane recovery from fat, oil, and grease through co-digestion with food waste and addition of conductive materials. Chemosphere, 236:124362.

Chugh, S., Chynoweth, D.P., Clarke, W., Pullammanappallil, P., Rudolph, V., 1999. Degradation of unsorted municipal solid waste by a leach-bed process. Bioresour. Technol. 69, 103–115.

Clauwaert, P., Verstraete, W., 2009. Methanogenesis in membraneless microbial electrolysis cells. Appl Microbiol Biotechnol, 82(5): 829-836.

Costa, K.C., Lie, T.J., Jacobs, M.A., Leigh, J.A., 2013. H_2-independent growth of the hydrogenotrophic methanogen Methanococcus maripaludis. mBio, 4 (2): 00062-13.

Coursolle, D.; Baron, D.B.; Bond, D.R.; Gralnick, J.A., 2010. The MTR respiratory pathway is essential for reducing flavins and electrodes in Shewanella oneidensis. J. Bacteriol. 192, 467–474.

Cruz, V.C., Rossetti, S., Fazi, S., Paiano, P., Majone, M., Aulenta. F., 2014. Magnetite particles trigger a faster and more robust syntrophic pathway of methanogenic propionate degradation. Environ Sci Technol, 48(13): 7536-7543.

da Costa, M.S., Rainey, F.A., Moe, W.M., 2015. Brooklawnia. In Bergey's Manual of Systematics of Archaea and Bacteria (eds W. B. Whitman, F. Rainey, P. Kämpfer, M. Trujillo, J. Chun, P. DeVos, B. Hedlund and S. Dedysh). doi:10.1002/9781118960608.gbm00161

D'Alessio, M., Nordeste, R., Doxey, A.C., and Charles, T.C., 2017. Transcriptome Analysis of Polyhydroxybutyrate Cycle Mutants Reveals Discrete Loci Connecting Nitrogen Utilization and Carbon Storage in *Sinorhizobium meliloti*. Molecular Biology and Physiology, 2, 1-22.

Dai, X., Duan, N., Dong, B., 2013. High-solids anaerobic co-digestion of sewage sludge and food waste in comparison with mono digestions: Stability and performance. Waste Management, 33(2):308-316.

Dahiya, S., Sarkar, O., Swamy, Y.V., and Mohan, S.V., 2015. Acidogenic fermentation of food waste for volatile fatty acid production with co-generation of biohydrogen. Bioresource Technology, 182, 103–113.

Dalton, E.F., Surridge, N.A., Jernigan, J.C., Wilbourn, K.O., Facci, J.S., and Murray, R.W., 1990. Charge transport in electroactive polymers consisting of fixed molecular redox sites. Chem. Phys. 141(1), 143–157.

Dang, Y., Holmes, D.E., Zhao, Z., Woodard, T.L., Zhang, Y., Sun, D., Wang, L.Y., Nevin, K.P., Lovley, D.R., 2016. Enhancing anaerobic digestion of complex organic waste with carbon-based conductive materials. Bioresour Technol, 220: 516-522.

Dantas, J.M., Silva, M.A., Pantoja-Uceda, D., Turner, D.L., Bruix, M., Salgueiro, C.A. 2017. Solution structure and dynamics of the outer membrane cytochrome OmcF from Geobacter sulfurreducens. Biochim. Biophys. Acta. Bioenerg., 1858(9), 733-741.

Dearman, B., Bentham, R.H., 2007. Anaerobic digestion of food waste: comparing leachate exchange rates in sequential batch systems digesting food waste and biosolids. Waste Manag. 27, 1792–1799.

de Bok F.A.M., Stams, A.J.M., Dijkema, C., 2001. Pathway of propionate oxidation by a syntrophic culture of *Smithella propionica* and *Methanospirillum hungatei*. Appl Environ Microbiol, 67:1800-4.

de Bok, F., Plugge, C., and Stams, A., 2004. Interspecies electron transfer in methanogenic propionate degrading consortia. Water Res., 38, 1368–1375.

da Costa, M. S., Rainey, F. A. and Moe, W. M., 2015. Brooklawnia. In Bergey's Manual of Systematics of Archaea and Bacteria (eds W. B. Whitman, F. Rainey, P. Kämpfer, M. Trujillo, J. Chun, P. DeVos, B. Hedlund and S. Dedysh).

Dearman, B., Bentham, R.H., 2007. Anaerobic digestion of food waste: Comparing leachate exchange rates in sequential batch systems digesting food waste and biosolids. Waste Management, 27, 1792-1799.

De Groof, V., Coma, M., Arnot, T., 2021. Selecting fermentation products for food waste valorisation with HRT and OLR as the key operational parameters. Waste Management, 127:80-89.

Degueurce, A., Tomas, N., Le Roux, S., Martinez, J., Peu, P., 2016. Biotic and abiotic roles of leachate recirculation in batch mode solid-state anaerobic digestion of cattle manure. Bioresour. Technol. 200, 388–395.

Demirbas, M. F., Balat, M., and Balat, H., 2011. Biowastes-to-biofuels. Energy Conversion and Management, 52(4), 1815–1828.

Desmond-Le Quéméner, E., Bridier, A., Tian, J.H., Madigou, C., Bureau, C., Qi, Y., Bouchez, T., 2019. Biorefinery for heterogeneous organic waste using microbial electrochemical technology. Bioresour. Technol. 292: 121943.

Deutzmann, J.S., Sahin, M., Spormann, A.M., 2015. Extracellular enzymes facilitate electron uptake in biocorrosion and bioelectrosynthesis. mBio, 6(2): e00496-15.

De Vrieze, J.O., Gildemyn, S., Arends, J.B.A., Vanwonterghem, I., Verbeken, K., Boon, N., Verstraete, W., Tyson, G.W., Hennebel, T., Rabaey, K., 2014. Biomass retention on electrodes rather than electrical current enhances stability in anaerobic digestion. Water Res. 54, 211–221.

Dhar, B.R., Ga., Y., Yeo, H., Lee, H.S., 2013. Separation of competitive microorganisms using anaerobic membrane bioreactors as pretreatment to microbial electrochemical cells. Bioresource Technology, 148, 208-214.

Dhar, B.R., and Lee, H.S., 2014. Evaluation of limiting factors for current density in microbial electrochemical cells (MXCs) treating domestic wastewater. Biotechn. Rep. 4, 80-85.

Dhar, B.R., Ryu, H., Ren, H., Santo Domingo, J.W., Chae, J., and Lee, H.S., 2016. High biofilm conductivity maintained despite anode potential changes in a Geobacter-enriched biofilm. ChemSusChem 9 (24), 3485–3491.

Dhar, B.R., Sim, J., Ryu, H., Santo Domingo, J.W., Chae, J., and Lee, H.S., 2017. Microbial activity influences electrical conductivity of biofilm anode. Water Res. 127, 230–238.

Dhar, B.R., Ryu, H., Chae, J., and Lee, H.S., 2018. Recoverability of electrical conductivity of a Geobacter-enriched biofilm. Journal of Power Sources, 40, 198-202.

Dhar, B.R., Park, J.H., Park, H.D., and Lee, H.S., 2019. Hydrogen-based syntrophy in an electrically conductive biofilm anode. Chemical Engineering Journal, 359, 208-216.

Di Maria, F., Barratta, M., Bianconi, F., Placidi, P., Passeri, D., 2017. Solid anaerobic digestion batch with liquid digestate recirculation and wet anaerobic digestion of organic waste: comparison of system performances and identification of microbial guilds. Waste Manag. 59, 172–180.

Dinesh, G.K., Chauhan, R., Chakma, S., 2018. Influence and strategies for enhanced biohydrogen production from food waste. Renewable and Sustainable Energy Reviews, 92:807-822.

Ding, A., Yang, Y.u., Sun, G., Wu, D., 2016. Impact of applied voltage on methane generation and microbial activities in an anaerobic microbial electrolysis cell (MEC). Chem. Eng. J. 283, 260–265.

Ding, Z., Bourven, I., Guibaud, G., van Hullebusch, E.D., Panico, A., Pirozzi, F., Esposito, G., 2015. Role of extracellular polymeric substances (EPS) production in bioaggregation: application to wastewater treatment. Appl. Microbiol. Biotechnol. 99, 9883–9905.

Dinh, H.T., Kuever, J., Mussmann, M., Hassel, A.W., Stratmann, M., Widdel, F., 2004. Iron corrosion by novel anaerobic microorganisms. Nature, 427(6977): 829-832.

Dogan, T., Ince, O., Oz, N.A., 2005. Inhibition of volatile acid production in granular sludge from a UASB reactor. J Environ Sci Health A, 40:633-44.

Doloman, A., Boeren, S., Miller, C.D., Sousa, D.Z., 2022. Stimulating effect of Trichococcus flocculiformis on a coculture of *Syntrophomonas wolfei* and *Methanospirillum hungatei*. Applied and Environmental Microbiology, 88(13): e00391-22.

Dong, L., Zhenhong, Y., Yongming, S., 2010. Semi-dry mesophilic anaerobic digestion of water sorted organic fraction of municipal solid waste (WS-OFMSW). Bioresour. Technol. 101(8):2722-8.

Duan, N.N., Dong, B., Wu, B., Dai, X.H., 2012. High-solid anaerobic digestion of sewage sludge under mesophilic conditions: feasibility study. Bioresour. Technol. 104, 150–156.

Duong, T.H., Grolle, K., Nga, T.T.V., Zeeman, G., Temmink, H., van Eekert, M., 2019. Protein hydrolysis and fermentation under methanogenic and acidifying conditions. Biotechnol Biofuels 12, 254.

El-Naggar, M.Y., Wanger, G., Leung, K.M., Yuzvinsky, T.D., Southam, G., Yang, J., Lau, W.M., Nealson, K.H. and Gorby, Y.A., 2010. Electrical transport along bacterial nanowires

from *Shewanella oneidensis* MR-1. Proceedings of the National Academy of Sciences, 107(42), 18127-18131.

Eisenberg, D., Marcotte, E.M., Xenarios, I., Yeates, T.O., 2000; Protein function in the post-genomic era. Nature, 405:823-826.

Engel, M., Gemünde, A., Holtmann, D., Müller-Renno, C., Ziegler, C., Tippkötter, N., Ulber, R., 2020. Clostridium Acetobutylicum's Connecting World: Cell Appendage Formation in Bioelectrochemical Systems. ChemElectroChem, 7, 414.

Escapa, A., Lobato, A., García, D.M., Morán, A., 2013. Hydrogen production and COD elimination rate in a continuous microbial electrolysis cell: The influence of hydraulic retention time and applied voltage. Environ Prog Sustain, 32(2): 263-268.

European Biogas Association, Statistical Report 2022. https://www.europeanbiogas.eu/__trashed-3/.

European Commission, 2020. Circular economy action plan. https://environment.ec.europa.eu/strategy/circular-economy-action-plan_en

Eurostat, 2022. Food waste and food waste prevention - estimates. Retrieved from https://ec.europa.eu/eurostat/statistics-explained/index.php?title=Food_waste_and_food_waste_prevention_-_estimates

Fagbohungbe, M.O., Dodd, I.C., Herbert, B.M.J., Li, H., Ricketts, L., Semple, K.T., 2015. High solid anaerobic digestion: operational challenges and possibilities. Environ. Technol. Innov. 4, 268-284.

Feng, K., Zhang, Z., Cai, W., Liu, W., Xu, M., Yin, H., Wang, A., He, Z., Deng, Y., 2017. Biodiversity and species competition regulate the resilience of microbial biofilm community. Mol Ecol. 26: 6170– 6182.

Feng, Q., Song, Y.C., Bae, B.U., 2016. Influence of applied voltage on the performance of bioelectrochemical anaerobic digestion of sewage sludge and planktonic microbial communities at ambient temperature. Bioresource Technology, 220, 500-508.

Feng, Q., Song, Y.C., Ahn, Y., 2018. Electroactive microorganisms in bulk solution contribute significantly to methane production in bioelectrochemical anaerobic reactor. Bioresource Technology, 259: 119-127.

Feng, Y., Zhang, Y., Chen, S., Quan, X., 2015. Enhanced production of methane from waste activated sludge by the combination of high-solid anaerobic digestion and microbial electrolysis cell with ironegraphite electrode. Chem Eng J, 259:787e94.

Fernando-Foncillas, C., Varrone, C., 2021. Effect of reactor operating conditions on carboxylate production and chain elongation from co-fermented sludge and food waste. Journal of Cleaner Production, 292:126009.

Fernández-Rodríguez, J., Pérez, M., Romero, L.I., 2014. Dry thermophilic anaerobic digestion of the organic fraction of municipal solid wastes: solid retention time optimization. Chem. Eng. J. 251, 435–440.

Fierro, J., Martínez, J.E., Rosas, J.G., Blanco, D., Gomez, X., 2014. Anaerobic codigestion of poultry manure and sewage sludge under solid-phase configuration. Environ. Prog. Sustain. Energy 33, 866e872.

Fowler, S.J., Torresi E., Dechesne A., Smets B.F., 2023. Biofilm thickness controls the relative importance of stochastic and deterministic processes in microbial community assembly in moving bed biofilm reactors. Interface Focus.13:20220069.

Freguia, S.; Masuda, M.; Tsujimura, S.; Kano, K., 2009. Lactococcus lactis catalyses electricity generation at microbial fuel cell anodes via excretion of a soluble quinone. Bioelectrochemistry, 76, 14–18.

Galushko, A., Kuever, J., 2021. Syntrophobacterium gen. nov. In: Trujillo ME, Dedysh S, DeVos P et al.(eds.) Bergey's Manual of Systematics of Archaea and Bacteria, 1–6.

Gao, Y., Ryu. H., Santo Domingo, J.W., and Lee, H.S., 2014. Syntrophic interactions between H_2-scavangeing and anode-respiring bacteria can improve current density in microbial electrolysis cells. Bioresource Technology, 153, 245-253.

Garcia, J.L., Patel, B.K.C., Ollivier, B., 2000. Taxonomic, phylogenetic, and ecological diversity of methanogenic archaea. Anaerobe, 6(4): 205-226.

Ge, H., Jensen, P.D., Batstone, D.J., 2011. Temperature phased anaerobic digestion increases apparent hydrolysis rate for waste activated sludge. Water Research, 45(4):1597-1606.

Gorby, Y.A.; Yanina, S.; McLean, J.S.; Rosso, K.M.; Moyles, D.; Dohnalkova, A.; Beveridge, T.J.; Chang, I.S.; Kim, B.H.; Kim, K.S., 2006. Electrically conductive bacterial nanowires produced by Shewanella oneidensis strain MR-1 and other microorganisms. Proc. Natl. Acad. Sci. USA, 103, 11358–11363.

Grube, M., Dimanta, I., Gavare, M., Strazdina, I., Liepins, J., Juhna, T., and Kalnenieks, U., 2014. Hydrogen-producing Escherichia coli strains overexpressing lactose permease: FT-IR analysis of the lactose-induced stress. Biotechnology and Applied Biochemistry, 61(2):111-117.

Guendouz, J., Buffiere, P., Cacho, J., Carrere, M., Delgenes, J.P., 2010. Dry anaerobic digestion in batch mode: desing and operation of a laboratory-scale, completely mixed reactor. Water Mana. 30, 1768-1771.

Guo, J., Peng, Y., Ni, B.-J., Han, X., Fan, L., Yuan, Z., 2015a. Dissecting microbial community structure and methane-producing pathways of a full-scale anaerobic reactor digesting activated sludge from wastewater treatment by metagenomic sequencing. Microb. Cell Factories 14, 33.

Guo, N., Ma, X.F., Ren, S.J., Wang, S.G., Wang, Y.K., 2019. Mechanisms of metabolic performance enhancement during electrically assisted anaerobic treatment of chloramphenicol wastewater, Water Res. 156, 199–207.

Guo, X., Liu, J., Xiao, B., 2013. Bioelectrochemical enhancement of hydrogen and methane production from the anaerobic digestion of sewage sludge in single chamber membrane free microbial electrolysis cells. Int J Hydrogen Energy, 38:1342e7.

Ha, P.T., Lindemann, S.R., Shi, L., Dohnalkova, A.C., Fredrickson, J.K., Madigan, M.T., Beyenal, H., 2017. Syntrophic anaerobic photosynthesis via direct interspecies electron transfer. Nat Commun, 8:13924.

Hagos, K., Zong, J., Li, D., 2017. Anaerobic co-digestion process for biogas production: Progress, challenges and perspectives. Renewable and Sustainable Energy Reviews, 76:1485-1496.

Haloua, F., Foulon, E., Allard, A., Hay, B., Filtz, J.R., 2015. Traceable measurement and uncertainty analysis of the gross calorific value of methane determined by isoperibolic calorimetry. Metrologia, 52(6): 741-755.

Hamelers, H.V.M., Ter Heijne, A., Sleutels, T., Jeremiasse, A.W., Strik, D., Buisman, C.J.N., 2010. New applications and performance of bioelectrochemical systems [J]. Appl Microbiol Biotechnol, 85(6): 1673-1685.

Han, S., and Shin, H., 2004. Biohydrogen production by anaerobic fermentation of food waste. International Journal of Hydrogen Energy, 29(6): 569-577.

Hansen, K.H., Angelidaki, I., Ahring, B.K., 1998. Anaerobic digestion of swine manure: inhibition by ammonia. Water Res. 32, 5–12.

Hao, Q., Kulikov, V., and Mirsky, V.M., 2003. Investigation of contact and bulk resistance of conducting polymers by simultaneous two- and four-point technique. Sensors and Actuators B, 94, 352-357.

Hara, M., Onaka, Y., Kobayashi, H., Fu, Q., Kawaguchi, H., Vilcaez, J., Sato, K., 2013. Mechanism of electromethanogenic reduction of CO_2 by a thermophilic methanogen. Energy Procedia, 37: 7021-7028.

Harb, M., Ermer, N., Sawaya, C.B., Smith, A.L., 2020. Increased applied voltage in the presence of GAC enhances microbial activity and methane production during anaerobic digestion of food waste. Environ. Sci: Water Res. Technol., 6, 737.

Hari, A.R., Katuri, K.P., Logan, B.E., Saikaly, P.E., 2016. Set anode potentials affect the electron fluxes and microbial community structure in propionate-fed microbial electrolysis cells. Sci. Rep. 6, 38690.

Hari, A.R., Venkidusamy, K., Katuri, K.P., Bagchi, S., Saikaly, P.E., 2017. Temporal microbial community dynamics in microbial electrolysis cells – influence of acetate and propionate concentration. Front. Microbiol. 8.

Hashimoto, A.G., 1989. Effect of inoculum/substrate ratio on methane yield and production rate from straw. Biol. Wastes 28, 247–255.

Hedderich. R., Whitman, W.B., Physiology and biochemistry of the methane-producing Archaea. In Dworkin M, editor. The Prokaryotes. 3rd ed. New York: Springer-Verlag; 2006. p. 1050–1079. DOI: 10.1007/0-387-30742-7_34

Heller, A., 2006. Electron-conducting redox hydrogels: design, characteristics and synthesis. Current Opinion in Chemical Biology, 10(6):664-672.

Heijne, A.t., Liu, D., Sulonen, M., Sleutels, T., Fabregat-Santiago, F. 2018. Quantification of bio-anode capacitance in bioelectrochemical systems using Electrochemical Impedance Spectroscopy. J. Power Sourc., 400, 533-538.

Hernandez, M.E. and Newman, D.K., 2001. Extracellular electron transfer. Cellular and Molecular Life Sciences CMLS, 58(11), 1562-1571.

Holmes, D.E., Bond, D.R., Lovley, D.R., 2004. Electron transfer by Desulfobulbus propionicus to Fe(III) and graphite electrodes. Appl Environ Microbiol 70 (2), 1234–1237.

Holmes, D.E., Chaudhuri, S.K., Nevin, K.P., Mehta, T., Methe, B.A., Liu, A., Ward, J.E., Woodard, T.L., Webster, J., Lovley, D.R. 2006. Microarray and genetic analysis of electron transfer to electrodes in Geobacter sulfurreducens. Environ. Microbiol., 8(10), 1805-15.

Holmes, D.E., Shrestha, P.M., Walker, D.J.F., Dang, Y., Nevin, K.P., Woodard, T.L., Lovley, D.R., Schloss, P.D., 2017. Metatranscriptomic evidence for direct interspecies electron transfer between *Geobacter* and *Methanothrix* species in methanogenic rice paddy soils. Appl. Environ. Microbiol. 83 (9)

Holm-Nielsen, J.B., Al, Seadi T., Oleskowicz-Popiel, P., 2009. The future of anaerobic digestion and biogas utilization. Bioresource Technol, 100(22), 5478-5484.

Hu, Q., Sun, D., Ma, Y., Zhang, S., Luo, G., 2017. Conductive polyaniline enhanced methane production from anaerobic wastewater treatment. Polymer, 120(30): 236-243.

Huang, Y.J., Hang, D., Lu, L.J., Targeting the human cancer pathway protein interaction network by structural genomics. Mol Cell Proteomics, 7, 2048-60.

Hussain, A., Filiatrault, M., and Guiot, S.R., 2017a. Acidogenic digestion of food waste in a thermophilic leach bed reactor: effect of pH and leachate recirculation rate on hydrolysis and volatile fatty acid production. Bioresource Technology, 245, 1-9.

Hussain, A., Lebrun, F.M., Tartakovsky, B., 2017b. Removal of organic carbon and nitrogen in a membraneless flow-through microbial electrolysis cell. Enzyme Microb. Technol. 102: 41–48.

Hussain, A., Lee, J., Ren, H., Lee, H.-S. 2021. Spatial distribution of biofilm conductivity in a Geobacter enriched anodic biofilm. Chem. Eng. J., 404, 126544.

Imachi, H., Sakai, S., Ohashi, A., 2007. *Pelotomaculum propionicicum* sp. nov., an anaerobic, mesophilic, obligately syntrophic, propionate-oxidizing bacterium. Int J Syst Evol Microbiol. 57:1487–92.

Inaba, R., Nagoya, M., Kouzuma, A., Watanabe, K., 2019. Metatranscriptomic evidence for magnetite nanoparticle-stimulated acetoclastic methanogenesis under continuous agitation. Appl. Environ. Microbiol. 85(23) e01733-19.

Ito, T., Yoshiguchi, K., Ariesyady, H.D., Okabe, S., 2012. Identification and quantification of key microbial trophic groups of methanogenic glucose degradation in an anaerobic digester sludge. Bioresource Technology. 123: 599-607.

Izadi, P., Gey, M.N., Schlüter, N., Schröder, U., 2021. Bidirectional electroactive microbial biofilms and the role of biogenic sulfur in charge storage and release. iScience. 24(8):102822.

Jacobs, P., Suls, J., Sansen, W. 1994. Performance of a planar differential-conductivity sensor for urea. Sens. Actuators, B, 20(2-3), 193-198

Jain, S., Jain, S., Wolf, I.T., Lee, J., Tong, Y.W., 2015. A comprehensive review on operating parameters and different pretreatment methodologies for anaerobic digestion of municipal solid waste. Renew. Sustain. Energy Rev. 52, 142–154.

Jang, H.M., Cho, H.U., Park, S.K., 2014. Influence of thermophilic aerobic digestion as a sludge pre-treatment and solids retention time of mesophilic anaerobic digestion on the methane production, sludge digestion and microbial communities in a sequential digestion process. Water Research, 48:1-14.

Jang, H.M., Kim, M., Ha, J.H., 2015. Reactor performance and methanogenic archaea species in thermophilic anaerobic co-digestion of waste activated sludge mixed with food wastewater. Chemical Engineering Journal, 276:20-28.

Jang, H.M., Ha, J.H., Kim. M., 2016. Effect of increased load of high-strength food wastewater in thermophilic and mesophilic anaerobic co-digestion of waste activated sludge on bacterial community structure. Water Research, 99:140-148.

Jannat, M.A.H., Lee, J., Shin, S.G., Hwang, S., 2021. Long-term enrichment of anaerobic propionate-oxidizing consortia: Syntrophic culture development and growth optimization. Journal of Hazardous Materials, 401, 123230.

Jiang, Z., Yu, Q., Sun, C., Wang, Z., Jin, Z., Zhu, Y., Zhao, Z., Zhang, Y., 2022. Additional electric field alleviates acidity suppression in anaerobic digestion of kitchen wastes via enriching electro-active methanogens in cathodic biofilms, Water Research, Volume 212, 118118.

Jiang, J., Zhang, Y., Li, K., 2013. Volatile fatty acids production from food waste: Effects of pH, temperature, and organic loading rate. Bioresource Technology, 143:525-530.

Jing, Y., Wan, J., Angelidaki, I., Zhang, S., and Luo, G., 2016. iTRAQ quantitative proteomic analysis reveals the pathways for methanation of propionate facilitated by magnetite. Water Research, 108, 212-221.

Kamagata, Y., 2015. Syntrophy in anaerobic digestion. In: Fang HP, Zhang T, editors. Anaerobic Biotechnology: Environmental Protection and Resource Recovery. London: Imperial College Press, World Scientific; p: 13–32.

Karki, R., Chuenchart, W., Surendra, K.C., 2021. Anaerobic co-digestion: Current status and perspectives. Bioresource Technology, 330:125001.

Karthikeyan, O.P., Visvanathan, C., 2013. Bio-energy recovery from high-solid organic substrates by dry anaerobic bio-conversion processes: a review. Rev. Environ. Sci. Biotechnol. 12, 257–284.

Kato, S., Nakamura, R., Kai, F., Watanabe, K., Hashimoto, K., 2010. Respiratory interactions of soil bacteria with (semi)conductive iron-oxide minerals. Environ Microbiol, 12(12): 3114-3123.

Kato, S., Hashimoto, K., and Watanabe, K., 2012. Methanogenesis facilitated by electric syntrophy via (semi)conductive iron-oxide minerals. Environ. Microbiol. 14, 1646–1654.

Kato, S., 2015. Biotechnological aspects of microbial extracellular electron transfer. Microbes Environ. 30, 133–139.

Kaur, G., Johnravindar, D., Wong, J.W.C., 2020. Enhanced volatile fatty acid degradation and methane production efficiency by biochar addition in food waste-sludge co-digestion: A step towards increased organic loading efficiency in co-digestion. Bioresource Technology, 308:123250.

Kayhanian, M., 1994. Performance of a high-solids anaerobic-digestion process under various ammonia concentrations. J. Chem. Technol. Biotechnol. 59 (4), 349–352.

Kendall, M.M., Boone, D.R., 2006. The Order Methanosarcinales. In: Dworkin, M., Falkow, S., Rosenberg, E., Schleifer, KH., Stackebrandt, E. (eds) The Prokaryotes. Springer, New York, NY.

Khalid, A., Arshad, M., Anjum, M., Mahmood, T., and Dawson, L., 2011. The anaerobic digestion of solid organic waste. Waste Management, 31(8), 1737–1744.

Khatami, K., Atasoy, M., Ludtke, M., 2021. Bioconversion of food waste to volatile fatty acids: Impact of microbial community, pH and retention time. Chemosphere, 275:129981.

Kim, D.H., Oh, S.E., 2011. Continuous high-solids anaerobic co-digestion of organic solid wastes under mesophilic conditions. Waste Manage. 31, 1943-1948.

Kim, H.J., Park, H.S., Hyun, M.S., Chang, I.S., Kim, M. and Kim, B.H., 2002. A mediator-less microbial fuel cell using a metal reducing bacterium, *Shewanella putrefaciens*. Enzyme and Microbial Technology, 30(2), 145-152.

Kim, J.; Han, S.J.; Yoo, K., 2022. Dust-Associated Bacterial and Funga Communities in Indoor Multiple-Use and Public Transportation Facilities. Atmosphere, 13, 1373.

Kim, M., Gomec, C.Y., Ahn, Y., Speece, R.E., 2003. Hydrolysis and acidogenesis of particulate organic material in mesophilic and thermophilic anaerobic digestion. Environ. Technol. (United Kingdom). https://doi.org/10.1080/09593330309385659.

Kim, Y.K., Yoo, K., Kim, M.S., Han, I., Lee, M., Kang, B.R., 2019. The capacity of wastewater treatment plants drives bacterial community structure and its assembly. Sci. Rep. 9 (1), 1–9.

Koch, C., Harnisch, F., 2016. Is there a Specific Ecological Niche for Electroactive Microorganisms? ChemElectroChem, 3, 1282.

Korth, B., Rosa, L.F., Harnisch, F. and Picioreanu, C., 2015. A framework for modeling electroactive microbial biofilms performing direct electron transfer. Bioelectrochemistry, 106, 194-206.

Kothari, R., Pandey, A.K., Kumar S., 2014. Different aspects of dry anaerobic digestion for bio-energy: An overview. Renewable and Sustainable Energy Reviews. 39:174-195.

Kouzuma, A.; Kato, S.; Watanabe, K., 2015. Microbial interspecies interactions: Recent findings in syntrophic consortia. Front. Microbiol. 6, 477.

Krcmar, D., Tenodi, S., Grba, N., Kerkez, D., Watson, M., Roncevic, S., and Dalmacija, B, 2018. Preremedial assessment of the municipal landfill pollution impact on soil and shallow groundwater in Subotica, Serbia. Science of the Total Environment, 615(Complete), 1341-1354.

Kumar, M., Dutta, S., You, S., 2021. A critical review on biochar for enhancing biogas production from anaerobic digestion of food waste and sludge. Journal of Cleaner Production, 305:127143.

Kumar, R., Samadder, S.R., 2020. Performance evaluation of anaerobic digestion technology for energy recovery from organic fraction of municipal solid waste：A review. Energy，197：117253.

Kurade, M.B., Saha, S., Salama, E., 2019. Acetoclastic methanogenesis led by Methanosarcina in anaerobic co-digestion of fats, oil and grease for enhanced production of methane. Bioresource Technology, 272:351-359.

Kusch, S., Oechsner, H., Jungbluth, T., 2008. Biogas production with horse dung in solidphase digestion systems. Bioresour. Technol. 99, 1280–1292.

LaBelle, E.V., Marshall, C.W., Gilbert, J.A., May, H.D., 2014. Influence of acidic pH on hydrogen and acetate production by an electrosynthetic microbiome. PLoS ONE, 9, e109935.

Lange, U., Mirsky, V.M., 2008. Separated analysis of bulk and contact resistance of conducting polymers: Comparison of simultaneous two- and four-point measurements with impedance measurements. Journal of Electroanalytical Chemistry, 622, 246-251.

Latif, M.A., Mehta, C.M., Batstone, D.J., 2017. Influence of low pH on continuous anaerobic digestion of waste activated sludge. Water Res. 113, 42–49.

Lee, B., Park, J.G., Shin, W.B., 2017. Microbial communities change in an anaerobic digestion after application of microbial electrolysis cells. Bioresource Technology, 234: 273-280.

Lee, E., Oliveira, D.S.B.L., Oliveira, L.S.B.L., 2020. Comparative environmental and economic life cycle assessment of high solids anaerobic co-digestion for biosolids and organic waste management. Water Research, 171:115443.

Lee, H.S., Torres, C.I., and Rittmann, B.E., 2009. Effects of substrate diffusion and anode potential on kinetic parameters for anode-respiring bacteria. Environmental Science & Technology, 43(19), 7571-7577.

Lee, H.S., Vermaas, W.F. and Rittmann, B.E., 2010. Biological hydrogen production: prospects and challenges. Trends in biotechnology, 28(5), 262-271.

Lee, H.S., Dhar, B.R., An, J., Rittmann, B.E., Ryu, H., Santo Domingo, J.W., Ren, H., and Chae, J., 2016. The Roles of Biofilm Conductivity and Donor Substrate Kinetics in a Mixed-Culture Biofilm Anode. Environmental Scientce & Technology, 50, 12799-12807.

Lee, H.S., 2018. Electrokinetic analyses in biofilm anodes: Ohmic conduction of extracellular electron transfer. Bioresource Technology, 256, 509-514.

Lee, K., Cho, S., Park, S.H., Heeger, A.J., Lee, C.W., Lee, S.H., 2006. Metallic transport in polyaniline. Nature 441:65– 68.

Lee, M., Nagendranatha Reddy, C., Min, B., 2019. In situ integration of microbial electrochemical systems into anaerobic digestion to improve methane fermentation at different substrate concentrations. International Journal of Hydrogen Energy, 44: 2380-2389.

Lei, Y.; Sun, D.; Dang, Y.; Chen, H.; Zhao, Z.; Zhang, Y.; and Holmes, D.E., 2016. Stimulation of methanogenesis in anaerobic digesters treating leachate from a municipal solid waste incineration plant with carbon cloth. Bioresour. Technol. 222, 270–276.

Leng, L., Yang, P., Singh, S., Zhuang, H., Xu, L., Chen, W.-H., Dolfing, J., Li, D., Zhang, Y., Zeng, H., Chu, W., Lee, P.-H., 2018. A review on the bioenergetics of anaerobic microbial metabolism close to the thermodynamic limits and its implications for digestion applications. Bioresour. Technol. 247, 1095–1106.

Li, C., Lesnik, K.L., Fan, Y., and Liu, H., 2016a. Redox Conductivity of Current-Producing Mixed Species Biofilms. PLoS ONE, 11(5): e0155247.

Li, C., Lesnik, K.L., Fan, Y., Liu, H., 2016b. Millimeter scale electron conduction through exoelectrogenic mixed species biofilms. FEMS Microbiol. Lett. 363 (15), 1-6.

Li, C., Lesnik, K.L., and Liu, H., 2017b. Stay connected: Electrical conductivity of microbial aggregates. Biotechnology Advances, 35, 669-680.

Li, C., Lesnik, K.L., and Liu, H., 2018a. Conductive properties of methanogenic biofilms. Bioelectrochemistry, 119, 220-226.

Li, H.J., Chang, J.L., Liu, P.F., Fu, L., Ding, D., Lu, Y., 2015c. Direct interspecies electron transfer accelerates syntrophic oxidation of butyrate in paddy soil enrichments: syntrophic butyrate oxidation facilitated by nanoFe_3O_4. Environ Microbiol, 2015, 17 (5): 1533-1547.

Li, H., Dauphin-Ducharme, P., Arroyo-Currás, N., Tran, C.H., Vieira, P.A., Li, S., Shin, C., Somerson, J., Kippin, T.E., Plaxco, K.W. 2017c. A Biomimetic Phosphatidylcholine-Terminated Monolayer Greatly Improves the In Vivo Performance of Electrochemical Aptamer-Based Sensors. Angew. Chem. Int. Ed., 56(26), 7492-7495.

Li, J., Xiao, L., Zheng, S., Zhang, Y., Luo, M., Tong, C., Xu, H., Tan, Y., Liu, J., Wang, O., Liu, F., 2018c. A new insight into the strategy for methane production affected by conductive carbon cloth in wetland soil: Beneficial to acetoclastic methanogenesis instead of CO2 reduction, Sci. Total Environ. 643: 1024–1030.

Li, L., He, Q., Ma, Y., 2015a. Dynamics of microbial community in a mesophilic anaerobic digester treating food waste: Relationship between community structure and process stability. Bioresource Technology, 189:113-120.

Li, L., Peng, X., Wang, X., Wu, D., 2018b. Anaerobic digestion of food waste: A review focusing on process stability. Bioresource Technology, 248(Pt A): 20-28.

Li, Q., Li H., Wang, G., Wang, X., 2017d. Effects of loading rate and temperature on anaerobic co-digestion of food waste and waste activated sludge in a high frequency feeding system, looking in particular at stability and efficiency. Bioresource Technology, 237: 231-239.

Li., Q., Liu, Y., Yang, X., Zhang, J., Lu, B., Chen, R., 2020. Kinetic and thermodynamic effects of temperature on methanogenic degradation of acetate, propionate, butyrate and valerate. Chemical Engineering Journal, 396(15) 125366.

Li, X., Chen, Y., Zhao, S., 2015b. Efficient production of optically purel-lactic acid from food waste at ambient temperature by regulating key enzyme activity. Water Research, 70:148-157.

Li, X., Sadiq, S., Zhang, W., 2021. Salinity enhances high optically active L-lactate production from co-fermentation of food waste and waste activated sludge: Unveiling the response of microbial community shift and functional profiling. Bioresource Technology, 319: 124124.

Li, X.H., Liang, D.W., Bai, Y.X., Fan, Y.T., and Hou, H.W., 2014. Enhanced H_2 production from corn stalk by integrating dark fermentation and single chamber microbial electrolysis cells with double anode arrangement. Int. J. Hydrogen Energy, 39(17) 8977-8982.

Li, Y., Hua, D., Mu, H., Xu, H., Jin, F., Zhang, X., 2017a. Conversion of vegetable wastes to organic acids in leaching bed reactor: Performance and bacterial community analysis. Journal of Bioscience and Bioengineering, 124(2): 195-203.

Li, Y., Zhang, Y., Liu, Y., Zhao, Z., Zhao, Z., Liu, S., Zhao, H., Quan, X., 2016c. Enhancement of anaerobic methanogenesis at a short hydraulic retention time via

bioelectrochemical enrichment of hydrogenotrophic methanogens. Bioresource Technology, 218, 505-511.

Liang, J., Luo, L., Li, D., 2021. Promoting anaerobic co-digestion of sewage sludge and food waste with different types of conductive materials: Performance, stability, and underlying mechanism. Bioresource Technology, 337:125384.

Liao, X., Zhu, S., Zhong, D., Zhu, J., Liao, L., 2014. Anaerobic co-digestion of food waste and landfill leachate in single-phase batch reactors. Waste Management, 34(11): 2278-2284.

Lim, E.Y., Tian, H.L., Chen, Y.Y., Ni, K.W., Zhang, J.X., Tong, Y.W., 2020. Methanogenic pathway and microbial succession during start-up and stabilization of thermophilic food waste anaerobic digestion with biochar. Bioresour. Technol. 314.

Lim, S.S., Yu, E.H., Daud, W.R.W., Kim, B.H., Scott, K., 2017. Bioanode as a limiting factor to biocathode performance in microbial electrolysis cells. Bioresour. Technol. 238, 313–324.

Lin, C., Wu, P., Liu, Y., Wong, J.W.C., Yong, X., Wu, X., Xie, X., Jia, H., Zhou, J., 2019. Enhanced biogas production and biodegradation of phenanthrene in wastewater sludge treated anaerobic digestion reactors fitted with a bioelectrode system. Chem. Eng. J. 365, 1–9.

Lin, R., Cheng, J., Zhang, J., Zhou, J., Cen, K., Murphy, J.D., 2017. Boosting biomethane yield and production rate with graphene: the potential of direct interspecies electron transfer in anaerobic digestion. Bioresour Technol, 239-345.

Lin, X., Zheng, L., Zhang, M., Qin, Y., Liu, Y., Li, H., Li, C., 2022. Simultaneous boost of anodic electron transfer and exoelectrogens enrichment by decorating electrospinning carbon nanofibers in microbial fuel cell, Chemosphere, Volume 308, Part 2, 2022, 136434,

Lindner, J., Zielonka, S., Oechsner, H., 2015. Effect of different pH-values on process parameters in two-phase anaerobic digestion of high-solid substrates. Environmental Technology, 36(2):198-207.

Lindsay, S., 2006. Molecular wires and devices: Advances and issues. Faraday Discussions 131:403-409.

Liu, C., Sun, D., Zhao, Z., Dang, Y., Holmes, D.E., 2019. *Methanothrix* enhances biogas upgrading in microbial electrolysis cell via direct electron transfer, Bioresour. Technol. 291, 121877.

Liu, F., Rotaru, A.E., Shrestha, P.M., Malvankar, N.S., Nevin, K.P., and Lovley, D.R., 2012a. Promoting direct interspecies electron transfer with activated carbon. Energy Environ. Sci. 5 (10), 8982–8989.

Liu, G., Zhang, R., El-Mashad, H.M., Dong, R., 2009. Effect of feed to inoculum ratios on biogas yields of food and green wastes. Bioresource Technology, 100:5103-5108.

Liu, M., Yuan, Y., Zhang, L., Zhuang, L., Zhou, S., Ni, J., 2010b. Bioelectricity generation by a Gram-positive *Corynebacterium* sp. strain MFC03 under alkaline condition in microbial fuel cells, Bioresource Technology, 101(6):1807-11.

Liu, P., Liang, P., Beyenal, H., Huang, X. 2020. Overestimation of biofilm conductance determined by using the split electrode as the microbial respiration. J. Power Sourc., 453, 227906.

Liu, P.F., Qiu, Q.F., Lu, Y.H., 2011. Syntrophomonadaceae-affiliated species as active butyrate-utilizing syntrophs in paddy field soil. Appl. Environ. Microbiol. 77 (11), 3884–3887.

Liu, Q., Ren, Z.J., Huang, C., 2016b. Multiple syntrophic interactions drive biohythane production from waste sludge in microbial electrolysis cells. Biotechnology for Biofuels, 9: 162.

Liu, J.R., Tanner, R.S., Schumann, P., Weiss, N., McKenzie, C.A., Janssen, P.H., Seviour, E.M., Lawson, P.A., Allen, T.D., Seviour, R.J., 2002. Emended description of the genus *Trichococcus*, description of *Trichococcus collinsii* sp. nov., and reclassification of *Lactosphaera pasteurii* as *Trichococcus pasteurii* comb. nov. and of *Ruminococcus palustris* as *Trichococcus palustri*s comb. nov. in the low-G+C gram-positive bacteria. Int J Syst Evol Microbiol. 52(Pt 4):1113-1126.

Liu, T., Balkwill, D.L., Aldrich, H.C., Drake, G.R., Boone, D.R., 1999. Characterization of the anaerobic propionatedegrading syntrophs Smithella propionica gen. nov., sp. nov. and Syntrophobacter wolinii. International Journal of Systematic Bacteriology, 49, 545-556.

Liu, T., Sung, S., 2002. Ammonia inhibition on thermophilic aceticlasti methanogens. Water Sci. Technol. 45(10), 113-120.

Liu, W., Huang, S., Zhou, A., Zhou, G., Ren, N., Wang, A., and Zhuang, G., 2012b. Hydrogen generation in microbial electrolysis cell feeding with fermentation liquid of waste activated sludge. Int. J. Hydrogen Energy, 37(18), 13859-13864.

Liu, W., Cai, W., Guo, Z., Wang, L., Yang, C., Varrone, C., Wang, A., 2016. Microbial electrolysis contribution to anaerobic digestion of waste activated sludge, leading to accelerated methane production. Renewable Energy 91, 334–339.

Liu, X., Tremblay, P.L., Malvankar, N.S., Nevin, K.P., Lovley, D.R., Vargas, M., 2014. A *Geobacter sulfurreducens* strain expressing *Pseudomonas aeruginosa* type IV pili localizes OmcS on pili but is deficient in Fe(III) oxide reduction and current production. Appl Environ Microbiol 80:1219–1224.

Liu, Y., Kim, H., Franklin, R., and Bond, D.R., 2010a. Gold line array electrodes increase substrate affinity and current density of electricity-producing *G. sulfurreducens* biofilms. Energy & Environmental Science, 3(11), 1782-1788.

Liu, Y., Whitman, W.B., 2008. Metabolic, phylogenetic, and ecological diversity of the methanogenic Archaea. Ann N Y Acad Sci. 1125:171–189.

Logan, B.E., Hamelers, B., Rozendal, R., Schröder, U., Keller, J., Freguia, S., Alterman, P., Verstraete, W., and Rabaey, K., 2006. Microbial fuel cells: methodology and technology. Environmental science & technology, 40(17), 5181-5192.

Logan, B.E., Rabaey, K., 2012. Conversion of wastes into bioelectricity and chemicals by using microbial electrochemical technologies. Science, 337(6095), 686-690.

Logan, B.R., Rossi, R., Ragab, A., Saikaly, P.E., 2019. Electroactive microorganisms in bioelectrochemical systems, Nat. Rev. Microbiol. 17 (2019) 307–319.

Logan, B.E., Wallack, M.J., Kim, K.Y., He, W., Feng, Y. and Saikaly, P.E., 2015. Assessment of microbial fuel cell configurations and power densities. Environmental Science & Technology Letters, 2(8), 206-214.

Lohner, S.T., Deutzmann, J.S., Logan, B.E., Leigh, J., Spormann, A.M., 2014. Hydrogenase-independent uptake and metabolism of electrons by the archaeon *Methanococcus maripaludi*. ISME J, 8(8): 1673-1681.

Lojou, E., Durand, M.C., Dolla, A., Bianco, P., 2002. Hydrogenase activity control at Desulfovibrio vulgaris cell-coated carbon electrodes: Biochemical and chemical factors influencing the mediated bioelectrocatalysis. Electroanalysis, 14, 913–922.

Lovley, D.R., Goodwin, S., 1988. Hydrogen concentrations as an indicator of the predominant terminal electron-accepting reactions in aquatic sediments. Geochim. Cosmochim. Acta, 52, 2993–3003.

Lovley, D.R., 2006. Bug juice: harvesting electricity with microorganisms. Nature Reviews Microbiology, 4(7), 497-508.

Lovley, D.R., 2011. Live wires: direct extracellular electron exchange for bioenergy and the bioremediation of energy-related contamination. Energy & Environmental Science, 4, 4896-4906.

Lovley, D.R., Malvankar, N.S., 2015. Seeing is believing: novel imaging techniques help clarify microbial nanowire structure and function. Environmental microbiology, 17(7), 2209-2215.

Lovley, D.R., 2016. Happy together: microbial communities that hook up to swap electrons. ISME J. 11 (2), 327–336.

Lovley, D.R., 2017. Syntrophy goes electric: direct interspecies electron transfer (DIET). Annual Reviews of Microbiology, 71 (1), 643–664.

Lu, B., Gong, K., Jiang, H.Y., 2021. Performance of AnMBR for the co-digestion of food waste and waste activated sludge. China Environmental Science, 41(5): 2290-2298.

Lu, C.X., Shen, Y.W., Li, C., Zhu, N.W., Yuan, H.P., 2020. Redox-active biochar and conductive graphite stimulate methanogenic metabolism in anaerobic digestion of waste-activated sludge: beyond direct interspecies electron transfer. ACS Sustain. Chem. Eng. 8, 12626–12636.

Lu, F., He, P.J., Hao, L.P., Shao, L.M., 2008. Impact of recycled effluent on the hydrolysis during anaerobic digestion of vegetable and flower waste. Water Sci. Technol. 58 (8), 1637–1643.

Lu, L., Ren, N., Xing, D., and Logan, B.E., 2009. Hydrogen production with effluent from an ethanol-H_2-coproducing fermentation reactor using a single-chamber microbial electrolysis cell. Biosens. Bioelectron. 24, 3055-3060.

Lu, L., and Ren, Z.J., 2016. Microbial electrolysis cells for waste biorefinery: A state of the art review. Bioresource Technology, 215, 254-264.

Ma, J., Carballa, M., Van De Caveye, P., Verstraete, W., 2009. Enhanced propionic acid degradation (EPAD) system: Proof of principle and feasibility. Water Res. 43, 3239–3248.

Magnuson, T.S., Isoyama, N., HODGES-MYERSON, A.L., Davidson, G., Maroney, M.J., Geesey, G.G., Lovley, D.R. 2001. Isolation, characterization and gene sequence analysis of a membrane-associated 89 kDa Fe(III) reducing cytochrome c from Geobacter sulfurreducens. Biochem. J., 359, 147-152.

Malvankar, N.S., Vargas, M., Nevin, K.P., Franks, A.E., Leang, C., Kim, B.C., Inoue, K., Mester, T., Covalla, S.F., Johnson, J.P. and Rotello, V.M., 2011. Tunable metallic-like conductivity in microbial nanowire networks. Nature Nanotechnology, 6(9), pp.573-579.

Malvankar, N.S., Tuominen, M.T., and Lovley, D.R., 2012a. Biofilm conductivity is a decisive variable for high-current-density *Geobacter sulfurreducens* microbial fuel cells. Energy & Environmental Science, 5(2), 5790-5797.

Malvankar, N.S., Lau, J., Nevin, K.P., Franks, A.E., Tuominen, M.T., and Lovley, D.R., 2012b. Electrical conductivity in a mixed-species biofilm. Applied and environmental microbiology, 78(16), 5967-5971.

Malvankar, N.S., Tuominen, M.T., and Lovley, D.R., 2012c. Lack of cytochrome involvement in long-range electron transport through conductive biofilms and nanowires of *Geobacter sulfurreducens*. Energy & Environmental Science, 5(9), 8651-8659.

Malvankar, N.S., Lovley, D.R., 2014. Microbial nanowires for bioenergy applications. Curr. Opin. Biotechnol.27:88–95.

Malvankar, N.S., Yalcin, S.E., Tuominen, M.T., Lovley, D.R., 2014. Visualization of charge propagation along individual pili proteins using ambient electrostatatic force microscopy. Nat Nanotechnol 9:1012–1017.

Malvankar, N.S., Vargas, M., Nevin, K., Tremblay, P.L., Evans-Lutterodt, K., Nykypanchuk, D., Martz, E., Tuominen, M.T., and Lovley, D.R., 2015. Structural basis for metallic-like conductivity in microbial nanowires. mBio 6(2): e00084-15. doi:10.1128/mBio.00084-15.

Malvankar, N.S., Rotello, V.M., Tuominen, M.T., Lovley, D.R., 2016. Reply to 'Measuring conductivity of living Geobacter sulfurreducens biofilms'. Nat. Nanotechnol. 11 (11),913–914.

Marcus, A.K., Torres, C.I. and Rittmann, B.E., 2007. Conduction‐based modeling of the biofilm anode of a microbial fuel cell. Biotechnology and Bioengineering, 98(6), pp.1171-1182.

Marshall, C.W., Ross, D.E., Fichot, E.B., Norman, R.S., May, H.D., 2012. Electrosynthesis of commodity chemicals by an autotrophic microbial community. Appl. Environ. Microbiol. 78, 8412–8420.

Marshall, C.W., Ross, D.E., Fichot, E.B., Norman, R.S., May, H.D., 2013. Long-term operation of microbial electrosynthesis systems improves acetate production by autotrophic microbiomes. Environ. Sci. Technol. 47, 6023–6029.

Marsili, E., Baron, D.B., Shikhare, I.D., Coursolle, D., Gralnick, J.A. and Bond, D.R., 2008. *Shewanella* secretes flavins that mediate extracellular electron transfer. Proceedings of the National Academy of Sciences, 105(10), pp.3968-3973.

Martins G., Salvador A.F., Pereira L., Alves M.M., 2018. Methane production and conductive materials: a critical review. Environmental Science & Technology, 52, 10241-10253.

Massaccesi, L., Sordi, A., Micale, C., Cucina, M., Zadra, C., Di Maria, F., Gigliotti, G., 2013. Chemical characterisation of percolate and digestate during the hybrid solid anaerobic digestion batch process. Process Biochem. 48, 1361–1367.

Mata-Alvarez, J., Mace, S., and Llabres, P., 2000. Anaerobic digestion of organic solid wastes. An overview of research achievements and perspectives. Bioresource Technology, 74, 3-16.

Matsuda, S., Liu, H., Kato, S., Hashimoto, K. and Nakanishi, S., 2011. Negative faradaic resistance in extracellular electron transfer by anode-respiring Geobacter sulfurreducens cells. Environmental Science & Technology, 45(23), 10163-10169.

McCarty, P.L., and Smith, D.P., 1986. Anaerobic wastewater treatment. Environmental Science & Technology, 20(12), 1200-1206.

McGlynn, S.E., Chadwick, G.L., Kempes, C.P., Orphan, V.J., 2015. Single cell activity reveals direct electron transfer in methanotrophic consortia. Nature, 526:531.

McGrath, M.J., Iwuoha, E.I., Diamond, D., Smyth, M.R. 1995. The use of differential measurements with a glucose biosensor for interference compensation during glucose determinations by flow injection analysis. Biosens. Bioelectron., 10(9-10), 937-943.

McInerney, M.J., Struchtemeyer, C.G., Sieber, J., Mouttaki, H., Stams, A.J., Schink, B., Rohlin, L., Gunsalus, R.P., 2008. Physiology, ecology, phylogeny, and genomics of microorganisms capable of syntrophic metabolism. Ann. N. Y. Acad. Sci. 1125 (1), 58–72.

Meena, R.A.A., Rajesh Banu, J., Yukesh Kannah, R., 2020. Biohythane production from food processing wastes – Challenges and perspectives. Bioresource Technology, 298:122449.

Mehariya, S., Patel, A.K., Obulisamy, P.K., 2018. Co-digestion of food waste and sewage sludge for methane production: Current status and perspective. Bioresource Technology, 265:519-531.

Meitl, L.A.; Eggleston, C.M.; Colberg, P.J.S.; Khare, N.; Reardon, C.L.; Shi, L., 2009. Electrochemical interaction of *Shewanella oneidensis* MR-1 and its outer membrane cytochromes OMCA and MTRC with hematite electrodes. Geochim. Cosmochim. Acta, 73, 5292–5307.

Miyazaki, M., Sakai, S., Ritalahti, K.M., Saito, Y., Yamanaka, Y., Saito, Y., Tame, A., Uematsu, K., Löffler, F.E., Takai, K., Imachi, H., 2014. *Sphaerochaeta multiformis* sp. nov., an anaerobic, psychrophilic bacterium isolated from subseafloor sediment, and emended description of the genus Sphaerochaeta. Int J Syst Evol Microbiol. 2014 Dec;64(Pt 12):4147-4154. doi: 10.1099/ijs.0.068148-0. Epub 2014 Sep 23. PMID: 25249566

Morita, M., Malvankar, N.S., Franks, A.E., Summers, Z.M., Giloteaux, L., Rotaru, A.E., Rotaru, C., and Lovley, D.R., 2011. Potential for Direct Interspecies Electron Transfer in Methanogenic Wastewater Digester Aggregates. mBio 2(4): e00159-11.

Morotomi, M., Nagai, F., Watanabe, Y., 2012. Description of *Christensenella minuta* gen. nov., sp. nov., isolated from human faeces, which forms a distinct branch in the order Clostridiales, and proposal of Christensenellaceae fam. nov. International journal of systematic and evolutionary microbiology, PubMed 21357455. Doi: 10.1099/ijs.0.026989-0

Mostafa, A., Im, S., Song, Y.C., Kang, S., Kim, D.H., 2020. Enhanced anaerobic digestion of long chain fatty acid by adding magnetite and carbon nanotubes. Microorganisms 8, 333.

Mu, L., Zhang, L., Zhu, K., 2020. Anaerobic co-digestion of sewage sludge, food waste and yard waste: Synergistic enhancement on process stability and biogas production. Science of The Total Environment,704:135429.

Müller, H., Bosch, J., Griebler, C., Damgaard, L.R., Nielsen, L.P., Lueders, T., Meckenstock, R.U., 2016. Long-distance electron transfer by cable bacteria in aquifer sediments, ISME J. 10, 2010–2019.

Muratçobanoğlu, H., Gökçek, Ö.B., Mert, R.A., 2020. Simultaneous synergistic effects of graphite addition and co-digestion of food waste and cow manure: Biogas production and microbial community. Bioresource Technology, 309:123365.

Nagendranatha Reddy, C., Annie Modestra, J., Naresh Kumar, A., Venkata Mohan, S., 2015. Waste remediation integrating with value addition: biorefinery approach towards sustainable biobased technologies. In: Kalia VC, editor. Microbial factories.Biofuels, waste treatment, vol. 1. Springer India; 2015.p.231-256.

Nakakubo, R., Møller, H.B., Nielsen, A.M., Matsuda, J., 2008. Ammonia inhibition of methanogenesis and identification of process indicators during anaerobic digestion. Environ. Eng. Sci. 25(10): 1487-1496.

Nakamura, R., Kai, F., Okamoto, A., Newton, G.J., Hashimoto, K., 2009. Self-constructed electrically conductive bacterial networks. Anie, 48(3): 508-511.

Nevin, K.P., Kim, B.C., Glaven, R.H., Johnson, J.P., Woodard, T.L., Methe, B.A., Didonato, R.J., Covalla, S.F., Franks, A.E., Liu, A., Lovley, D.R. 2009. Anode biofilm transcriptomics reveals outer surface components essential for high density current production in Geobacter sulfurreducens fuel cells. PLoS One, 4(5), e5628.

Nevin, K.P., Woodard, T.L., Franks, A.E., Summers, Z.M., Lovley, D.R., 2010. Microbial electrosynthesis: Feeding microbes electricity to convert carbon dioxide and water to multicarbon extracellular organic compounds. MBio, 1, e00103-10.

Nevin, K.P., Hensley, S.A., Franks, A.E., Summers, Z.M., Ou, J., Woodard, T.L., Snoeyenbos-West, O.L., Lovley, D.R., 2011. Electrosynthesis of organic compounds from carbon dioxide is catalyzed by a diversity of acetogenic microorganisms. Appl. Environ. Microbiol. 77, 2882–2886.

Nguyen, H.D., Renslow, R., Babauta, J., Ahmed, B. and Beyenal, H., 2012. A voltammetric flavin microelectrode for use in biofilms. Sensors and Actuators B: Chemical, 161(1), 929-937.

Nilsen, R.K., Torsvik, T., Lien, T., 1996. *Desulfotomaculum thermocisternum* sp nov, a sulfate reducer isolated from a hot North Sea oil reservoir. Int J Syst Bacteriol, 46:397–402.

Okamoto, A., Nakamura, R., Nealson, K.H. and Hashimoto, K., 2014a. Bound Flavin Model Suggests Similar Electron‐Transfer Mechanisms in Shewanella and Geobacter. ChemElectroChem, 1(11), pp.1808-1812.

Okamoto, A., Saito, K., Inoue, K., Nealson, K.H., Hashimoto, K. and Nakamura, R., 2014b. Uptake of self-secreted flavins as bound cofactors for extracellular electron transfer in Geobacter species. Energy Environ. Sci.,7(4), 1357-1361.

Oksanen, J., Blanchet, F. G., Friendly, M., Kindt, R., Legendre, P., McGlinn, D., 2019. “Vegan: Community ecology package (version 2.5-6),” in The comprehensive r archive network, http://CRAN.R-project.org/package=vegan.

Pan, Y., Zhi, Z., Zhen, G., 2019. Synergistic effect and biodegradation kinetics of sewage sludge and food waste mesophilic anaerobic co-digestion and the underlying stimulation mechanisms. Fuel, 253:40-49.

Parameswaran, P., Torres, C.I., Lee, H.S., Krajmalnik-Brown, R., and Rittmann, B.E., 2009. Syntrophic interactions among anode respiring bacteria (ARB) and Non-ARB in a biofilm anode: electron balances. Biotechnology and bioengineering, 103(3), 513-523.

Park, J., Lee, B., Tian, D., 2018. Bioelectrochemical enhancement of methane production from highly concentrated food waste in a combined anaerobic digester and microbial electrolysis cell. Bioresource Technology, 247: 226-233.

Parkin, G.F., and Owen, W.F., 1986. Fundamentals of anaerobic digestion of wastewater sludges. Journal of Environmental Engineering, 112(5), 867-920.

Patil, S.A., Arends, J.B.A., Vanwonterghem, I., van Meerbergen, J., Guo, K., Tyson, G.W., Rabaey, K., 2015. Selective enrichment establishes a stable performing community for microbial electrosynthesis of acetate from CO_2. Environ. Sci. Technol. 49, 8833–8843.

Pelletier, E., Kreimeyer, A., Bocs, S., 2008. "*Candidatus* Cloacamonas acidaminovorans": genome sequence reconstruction provides a first glimpse of a new bacterial division. J Bacteriol. 190:2572–9.

Pentassuglia, S., Agostino, V., Tommasi, T., 2018. EAB—Electroactive biofilm: a biotechnological resource. In: Wandelt, K. (Ed.), Encyclopedia of Interfacial Chemistry. Elsevier, Oxford, pp. 110–123.

Pera, A.L., Sellaro, M., Migliori, M., 2021. Dry mesophilic anaerobic digestion of separately collected organic fraction of municipal solid waste: Two-year experience in an industrial-scale plan. Processes, 9(2): 2398-2408.

Pereira, E.L., Cláudio, C.M.M., Motteran, F., 2013. Physicochemical study of pH, alkalinity and total acidity in a system composed of anaerobic baffled reactor (ABR) in series with upflow anaerobic sludge blanket reactor (UASB) in the treatment of pig farming wastewater. Acta. Sci. Technol., 35, 477-483.

Pezzolla, D., Di Maria, F., Zadra, C., Massaccesi, L., Sordi, A., Gigliotti, G., 2017. Optimization of solid-state anaerobic digestion through the percolate recirculation. Biomass Bioenergy 96, 112–118.

Pfeffer, C., Larsen, S., Song, J., Dong, M., Besenbacher, F., Meyer, R.L., Kjeldsen, K.U., Schreiber, L., Gorby, Y.A., El-Naggar, M.Y., Leung, K.M., Schramm, A., Risgaard-Petersen, N., Nielsen, L.P., 2012. Filamentous bacteria transport electrons over centimetre distances, Nature 491 (2012) 218–221.

Pham, T.H.; Boon, N.; Aelterman, P.; Clauwaert, P.; de Schamphelaire, L.; Vanhaecke, L.; De Maeyer, K.; Höfte, M.; Verstraete, W.; Rabaey, K., 2008. Metabolites produced by Pseudomonas sp. enable a Gram-positive bacterium to achieve extracellular electron transfer. Appl. Microbiol. Biotechnol. 77, 1119–1129.

Phan, H., Yates, M.D., Kirchhofer, N.D., Bazan, G.C., Tender, L.M., and Nguyen, T.Q., 2016. Biofilm as a redox conductor: a systematic study of the moisture and temperature dependence of its electrical properties. Phys. Chem. Chem. Phys. 18, 17815–17821.

Pirbadian, S., Barchinger, S.E., Leung, K.M., Byun, H.S., Jangir, Y., Bouhenni, R.A., Reed, S.B., Romine, M.F., Saffarini, D.A., Shi, L., Gorby, Y.A., Golbeck, J.H., El-Naggar, M.Y., 2014. *Shewanella oneidensis* MR-1 nanowires are outer membrane and periplasmic extensions of the extracellular electron transport components. PNAS, 111(35): 12883-12888.

Prabhu, M.S., Mutnuri, S., 2016. Anaerobic co-digestion of sewage sludge and food waste. Waste Management & Research, 34(4):307-315.

Pullammanappallil, P.C., Chynoweth, D.P., Lyberatos, G., Svoronos, S.A., 2001. Stable performance of anaerobic digestion in the presence of a high concentration of propionic acid. Bioresour. Technol. 78, 165e169.

Qian, X., Mester, T., Morgado, L., Arakawa, T., Sharma, M.L., Inoue, K., Joseph, C., Salgueiro, C.A., Maroney, M.J., Lovley, D.R. 2011. Biochemical characterization of purified OmcS, a c-type cytochrome required for insoluble Fe(III) reduction in Geobacter sulfurreducens. Biochim. Biophys. Acta., 1807(4), 404-12.

Quashie, F.K., Feng, K., Fang, A., Agorinya, S., Antwi, P., Kabutey, F.T., Xing, D., 2021a. Efficiency and key functional genera responsible for simultaneous methanation and bioelectricity generation within a continuous stirred microbial electrolysis cell (CSMEC) treating food waste. Sci. Total Environ. 757, 143746.

Quashie, F.K., Fang, A., Wei, L., Kabutey, F.T., Xing, D., 2021b. Prediction of biogas production from food waste in a continuous stirred microbial electrolysis cell (CSMEC) with backpropagation artificial neural network. Biomass Convers. Biorefinery. 1–12.

Rabaey, K., Boon, N., Siciliano, S.D., Verhaege, M. and Verstraete, W., 2004. Biofuel cells select for microbial consortia that self-mediate electron transfer. Applied and environmental microbiology, 70(9), 5373-5382.

Rabaey, K., Boon, N., Höfte, M. and Verstraete, W., 2005. Microbial phenazine production enhances electron transfer in biofuel cells. Environmental science & technology, 39(9), 3401-3408.

Rago, L., Ruiz, Y., Baeza, J.A., Guisasola, A., Cortés, P., 2015. Microbial community analysis in a long-term membrane-less microbial electrolysis cell with hydrogen and methane production. Bioelectrochemistry, 106, 359–368.

Reda, T., Plugge, C.M., Abram, N.J., Hirst, J., 2008. Reversible interconversion of carbon dioxide and formate by an electroactive enzyme. PNAS, 105 (31): 10654-10658.

Reguera, G., McCarthy, K.D., Mehta, T., Nicoll, J.S., Tuominen, M.T., Lovley, D.R., 2005. Extracellular electron transfer via microbial nanowires. Nature, 435(7045): 1098-1101.

Reguera, G., Nevin, K.P., Nicoll, J.S., Covalla, S.F., Woodard, T.L., and Lovley, D.R., 2006. Biofilm and nanowire production leads to increased current in *Geobacter sulfurreducens* fuel cells. Applied and environmental microbiology, 72(11), 7345-7348.

Ren, K., Wu, J., Yan, F., Ju, H. 2014b. Ratiometric electrochemical proximity assay for sensitive one-step protein detection. Sci. Rep., 4(1).

Ren, L., Ahn, Y., Hou, H., Zhang, F. and Logan, B.E., 2014a. Electrochemical study of multi-electrode microbial fuel cells under fed-batch and continuous flow conditions. Journal of Power Sources, 257, 454-460.

Ren, S., Usman, M., Tsang, D.C.W., O-Thong, S., Angelidaki, I., Zhu, X.D., Zhang, S.C., Luo, G., 2020. Hydrochar-facilitated anaerobic digestion: Evidence for direct interspecies electron transfer mediated through surface oxygen-containing functional groups. Environ. Sci. Technol. 54, 5755–5766.

Renslow, R., Babauta, J., Kuprat, A., Schenk, J., Ivory, C., Fredrickson, J., and Beyenal, H., 2013. Modeling biofilms with dual extracellular electron transfer mechanisms. Physical Chemistry Chemical Physics, 15(44), 19262-19283.

Rico, C., Montes, J.A., Muñoz, N., Rico, J.L., 2015. Thermophilic anaerobic digestion of the screened solid fraction of dairy manure in a solid-phase percolating reactor system. J. Clean. Prod. 102, 512–520.

Riggio, S., Torrijos, M., Debord, R., Esposito, G., van Hullebusch, E.D., Steyer, J.P., Escudié, R., 2017. Mesophilic anaerobic digestion of several types of spent livestock bedding in a batch leach-bed reactor: substrate characterization and process performance. Waste Management, 59, 129-139.

Ringeisen, B.R., Henderson, E., Wu, P.K., Pietron, J., Ray, R., Little, B., Biffinger, J.C., Jones-Meehan, J.M., 2006. High power density from a miniature microbial fuel cell using Shewanella oneidensis DSP10, Environ. Sci. Technol. 40, 2629–2634.

Ritalahti, K.M., Justicia-Leon, S.D., Cusick, K.D., Ramos-Hernandez, N., Rubin, M., Dornbush, J., Löffler, F.E., 2012. *Sphaerochaeta globosa* gen. nov., sp. nov. and *Sphaerochaeta pleomorpha* sp. nov., free-living, spherical spirochaetes. Int J Syst Evol Microbiol. 62(Pt 1):210-216.

Rocamora, I., Wagland, S.T., Villa, R., Simpson, E.W., Fernandez, O., Bajon-Fernandez, Y., 2020. Dry anaerobic digestion of organic waste: A review of operational parameters and their impact on process performance. Bioresource Technology, 299 122681.

Rotaru, A.E., Shrestha, P.M., Liu, F., Ueki, T., Nevin, K., Summers, Z.M., and Lovley, D.R., 2012. Interspecies Electron Transfer via Hydrogen and Formate Rather than Direct Electrical Connections in Cocultures of *Pelobacter carbinolicus* and *Geobacter sulfurreducens*. Applied and Environmental Microbiology, 78(21), 7645-7651.

Rotaru, A.E., Shrestha, P.M., Liu, F., Markovaite, B., Chen, S., Nevin, K.P., and Lovley, D.R., 2014a. Direct interspecies electron transfer between *Geobacter metallireducens* and *Methanosarcina barkeri*. Appl. Environ. Microbiol. 80, 4599-4605.

Rotaru, A.E., Shrestha, P.M., Liu, F., Shrestha, M., Shrestha, D., Embree, M., Zengler, K., Wardman, C., Nevin, K.P., and Lovley, D.R., 2014b. A new model for electron flow during anaerobic digestion: Direct interspecies electron transfer to *Methanosaeta* for the reduction of carbon dioxide to methane. Energy Environ. Sci. 7, 408-415.

Rozendal, R.A., Jeremiasse, A.W., Hamelers, H.V., Buisman, C.J., 2008. Hydrogen production with a microbial biocathode. Environ Sci Technol, 42(2): 629-634.

Saha, S., Hussain, A., Lee, J., Lee, E., Lee, H.S., 2023. An integrated leachate bed reactor – anaerobic membrane bioreactor system (LBR-AnMBR) for food waste stabilization and biogas recovery. Chemosphere. 311, 137054.

Saheb-alam, S., Persson, F., 2019. Response to starvation and microbial community composition in microbial fuel cells enriched on different electron donors, (2019). doi:10.1111/1751-7915.13449.

Sakai. S., Takaki. Y., Shimamura. S., Sekine. M., Tajima. T., 2011. Genome sequence of a mesophilic hydrogenotrophic methanogen *Methanocella paludicola*, the first cultivated representative of the order Methanocellales. PLoS One, 6(7): e22898.

Santos, T.C., Silva, M.A., Morgado, L., Dantas, J.M., Salgueiro, C.A. 2015. Diving into the redox properties of Geobacter sulfurreducens cytochromes: a model for extracellular electron transfer. Dalton Trans., 44(20), 9335-9344.

Sarkar, O., Kiran Katari, J., Chatterjee, S., 2020. Salinity induced acidogenic fermentation of food waste regulates biohydrogen production and volatile fatty acids profile. Fuel, 276:117794.

Schmitz, S., Nies, S., Wierckx, N., Blank, L.M. and Rosenbaum, M.A., 2015. Engineering mediator-based electroactivity in the obligate aerobic bacterium Pseudomonas putida KT2440. Frontiers in microbiology, 6.

Schloss, P.D.; Westcott, S.L.; Ryabin, T.; Hall, J.R.; Hartmann, M.; Hollister, E.B.; Lesniewski, R.A.; Oakley, B.B.; Parks, D.H.; Robinson, C.J., 2009. Introducing mothur: Open-source, platform-independent, community-supported software for describing and comparing microbial communities. Appl. Environ. Microbiol. 75, 7537–7541.

Schink, B., 1997. Energetics of syntrophic cooperation in methanogenic degradation. Microbiol. Mol. Biol. Rev., 61, 262–280.

Scholz, V.V., Müller, H., Koren, K., Nielsen, L.P., Meckenstock, R.U., 2019. The rhizosphere of aquatic plants is a habitat for cable bacteria, FEMS Microbiol. Ecol. 95 (2019).

Seib, M.D., Berg, K.J., Zitomer, D.H., 2016. Influent wastewater microbiota and temperature influence anaerobic membrane bioreactor microbial community. Bioresour Technol 216:446-452.

Sharan, R., Ulitsky, I., Shamir, R., 2007. Network-based prediction of protein function. Mo. Syst. Bio., 3, 88.

Shahriari, H., Varith, M., Hamoda, M., Kennedy, K.J., 2012. Effect of leachate recirculation on mesophilic anaerobic digestion of food waste. Waste Manage. 32(3): 400-403.

Shi, Y., Delgado-Baquerizo, M., Li, Y., Yang, Y., Zhu, Y.G., Peñuelas, J., Chu, H., 2020. Abundance of kinless hubs within soil microbial networks are associated with high functional potential in agricultural ecosystems. Environment International, Volume 142, 105869.

Shrestha, P.M., Malvankar, N.S., Werner, J.J., Franks, A.E., Elena-Rotaur, A., Shrestha, M., Liu, F., Nevin, K.P., Angenent, L.T., and Lovley, D.R., 2014. Correlation between microbial community and granule conductivity in anaerobic bioreactors for brewery wastewater treatment. Bioresource Technology, 174, 306-310.

Shofie, M., Qiao, W., Li, Q., Takayanagi, K., Li, Y., 2015. Comprehensive monitoring and management of a long-term thermophilic CSTR treating coffee grounds, coffee liquid, milk waste, and municipal sludge. Bioresource Technology, 192, 202-211.

Shu, C., Xiao, K., Yan, Q., Sun, X., 2016. Comparative Analysis of Type IV Pilin in Desulfuromonadales. Front. Microbiol., 7, 2080.

Sieber, J.R., McInerney, M.J., Gunsalus, R.P., 2012. Genomic insight into syntrophy: the paradigm for anaerobic metabolic cooperation. Annu Rev Microbiol. 66:429–452.

Siriwongrungson, V., Zeng, R.J., Angelidaki, I., 2007. Homoacetogenesis as the alternative pathway for H2 sink during thermophilic anaerobic degradation of butyrate under suppressed methanogenesis. Water Research, 41, 4204-4210.

Snider, R.M., Strycharz-Glaven, S.M., Tsoi, S.D., Erickson, J.S., and Tender, L.M., 2012. Long-range electron transport in *Geobacter sulfurreducens* biofilms is redox gradient-driven. Proceedings of the National Academy of Sciences, 109(38), 15467-15472.

Soleymani, L., Fang, Z., Sargent, E.H., Kelley, S.O. 2009. Programming the detection limits of biosensors through controlled nanostructuring. Nat. Nanotechnol., 4(12), 844-8.

Song, Y.C., Kwon, S.J., Woo, J.H., 2004. Mesophilic and thermophilic temperature cophase anaerobic digestion compared with single-stage mesophilic- and thermophilic digestion of sewage sludge. Water Res. 38 (7), 1653–1662.

Sowers, K.R., Baron, S.F., Ferry, J.G., 1984. *Methanosarcina acetivorans* sp. nov., an Acetotrophic Methane-Producing Bacterium Isolated from Marine Sediments. Appl Environ Microbiol. 47(5):971-8.

Spirito, C.M., Richter, H., Rabaey, K., Stams, A.J.M., Angenent, L.T., 2014. Chain elongation in anaerobic reactor microbiomes to recover resources from waste. Curr. Opin. Biotechnol. 27, 115–122.

Srikanth, S., Mohan, S.V. and Sarma, P.N., 2010. Positive anodic poised potential regulates microbial fuel cell performance with the function of open and closed circuitry. Bioresource technology, 101(14), 5337-5344.

Stams, A.J., De Bok, F.A., Plugge, C.M., Eekert, V., Miriam, H., Dolfing, J., and Schraa, G., 2006. Exocellular electron transfer in anaerobic microbial communities. Environ. Microbiol., 8, 371–382.

Stams AJM, Plugge CM. Electron transfer in syntrophic communities of anaerobic bacteria and Archaea. Nat Rev Microbiol. 2009;7:568–577.

Steendam, C.V., Smets, I., Skerlos, S., and Raskin, L., 2019. Improving anaerobic digestion via direct interspecies electron transfer requires development of suitable characterization methods. Current Opinion in Biotechnology, 57, 183-190.

Steidl, R.J., Lampa-Pastrik, S., and Reguera, G., 2016. Mechanistic stratification in electroactive biofilms of *Geobacter sulfurreducens* mediated by pilus nanowires. Nature communications, 7:12217.

Storck, T., Virdis, B., Batstone, D.J., 2015. Modelling extracellular limitations for mediated versus direct interspecies electron transfer. The ISME Journal, 10(3): 621-631.

Strycharz-Glaven, S. M., Snider, R.M., Guiseppi-Elie, A. and Tender, L.M., 2011. On the electrical conductivity of microbial nanowires and biofilms. Energy & Environmental Science, 4(11), pp.4366-4379.

Strycharz-Glaven, S.M., Tender, L.M. 2012. Reply to the 'Comment on "On electrical conductivity of microbial nanowires and biofilms"' by N. S. Malvankar, M. T. Tuominen and D. R. Lovley, Energy Environ. Sci., 2012, 5, DOI: 10.1039/c2ee02613a. Energy Environ. Sci., 5, 6250-6255.

Summer, Z.M., Fogarty, H.E., Leang, C., Franks, A.E., Malvankar, N.S., and Lovley, D.R., 2010. Direct exchange of electrons within aggregates of an evolved syntrophic coculture of anaerobic bacteria. Science, 330, 1413-1415.

Sun, R., Zhou, A., Jia, J., Liang, Q., Liu, Q., Xing, D., Ren, N., 2015. Characterization of methane production and microbial community shifts during waste activated sludge degradation in microbial electrolysis cells. Bioresour. Technol. 175, 68–74.

Suarez, C., Piculell, M., Modin, O., Langenheder, S., Persson, F., Hermanss, M., 2019. Thickness determines microbial community structure and function in nitrifying biofilms via deterministic assembly. Sci Rep 9, 5110.

Swakshar, S., 2019. Development of a Compact, Energy-positive Food Waste Treatment Process. Master Thesis. University of Waterloo, Waterloo, Canada.

Swakshar, S., Lee, H.S., 2020. High-rate carboxylate production in dry fermentation of food waste at room temperature. Science of the Total Environment, 714, 136695.

Tam, K., Matsumoto, M.R. and Sheppard, J.D., 2005. A Kinetic Model for Suspended and Attached Growth of a Defined Mixed Culture. Biotechnol Progress, 21: 720-727.

Tan, Y., Adhikari, R.Y., Malvankar, N.S., Pi, S., Ward, J.E., Woodard, T.L., Nevin, K.P., Xia, Q., Tuominen, M.T., and Lovley, D.R., 2016. Synthetic Biological Protein Nanowires with High Conductivity. Small, 12(33), 4481-4485.

Tan, Y., Adhikari, R.Y., Malvankar, N.S., Ward, J.E., Woodard, T.L., Nevin, K.P., Lovley, D.R., 2017. Expressing the *Geobacter metallireducens* PilA in *Geobacter sulfurreducens* yields Pili with exceptional conductivity. mBio 8 (1), 16.

Tang, Y.J.J., Meadows, A.L., Keasling, J.D., 2007. A kinetic model describing Shewanella oneidensis MR-1 growth, substrate consumption, and product secretion, Biotechnol. Bioeng. 96, 125–133.

Tang, Y.Q., Shigematsu, T., Morimura, S., Kida, K., 2015. Dynamics of the microbial community during continuous methane fermentation in continuously stirred tank reactors. J Biosci Bioeng, 119 (4): 375-383.

Tartakovsky, B., Manuel, M.F., Wang, H., Guiot, S.R., 2009. High rate membraneless microbial electrolysis cell for continuous hydrogen production. Int J Hydrogen Energy, 34:672e7.

Tatsumi, H., Takagi, K., Fujita, M., Kano, K., Ikeda, T., 1999. Electrochemical study of reversible hydrogenase reaction of *Desulfovibrio vulgaris* cells with methyl viologen as an electron carrier. Anal. Chem. 71, 1753–1759.

Tauch, A., Sandbote, J., 2014. The family Corynebacteriaceae. In: E. Rosenberg., E.F. DeLong., S. Lory., E. Stackebrandt., F. Thompson. The Prokaryotes: Actinobacteria. Pp. 239-277. Springer, Berlin, Heidelberg.

Teodósio, J.S., Simões, M., Melo, L.F., Mergulhão, F.J., 2011. Flow cell hydrodynamics and their effects on E. coli biofilm formation under different nutrient conditions and turbulent flow, Biofouling: The Journal of Bioadhesion and Biofilm Research, 27:1, 1-11.

Thauer, R.K., 1998. Biochemistry of methanogenesis: a tribute to Marjory Stephenson. Microbiology. 144: 2377–2406.

Thauer, R.K., Kaster, A.K.K., Seedorf, H., Buckel, W., Hedderich, R., 2008. Methanogenic archaea: ecologically relevant differences in energy conservaion. Nat. Rev. Microbil. 6: 579-591.

Thiele, J.H., Zeikus, J.G., 1988. Control of interspecies electron flow during anaerobic digestion: Significance of formate transfer versus hydrogen transfer during syntrophic methanogenesis in flocs. Appl. Environ. Microbiol., 54, 20–29.

Tian, T., Qiao, S., Yu, C., Zhou, J., 2018. Bio-electrochemically assisting low-temperature anaerobic digestion of low-organic strength wastewater. Chem. Eng. J. 335, 657–664.

Torres, C.I., Marcus, A.K., and Rittmann, B.E., 2007. Kinetics of consumption of fermentation products by anode-respiring bacteria. Applied microbiology and biotechnology, 77(3), 689-697.

Torres, C.I., Krajmalnik-Brown, R., Parameswaran, P., Marcus, A.K., Wanger, G., Gorby, Y.A., and Rittmann, B.E., 2009. Selecting anode-respiring bacteria based on anode potential: phylogenetic, electrochemical, and microscopic characterization.Environmental science & technology, 43(24), 9519-9524.

Torres, C. I., Marcus, A. K., Lee, H. S., Parameswaran, P., Krajmalnik‐Brown, R., and Rittmann, B. E., 2010. A kinetic perspective on extracellular electron transfer by anode‐respiring bacteria. FEMS microbiology reviews, 34(1), 3-17.

Tran, E., Rampi, M.A., Whitesides, G.M., 2004. Electron transfer in a Hg-SAM//SAM-Hg junction mediated by redox centers. Angewandte Chemie (International ed. Print) 43(29):3835-3839.

Tremblay, P.L., Summers, Z.M., Glaven, R.H., Nevin, K.P., Zengler, K., Barrett, C.L., Qiu, Y., Palsson, B.O., Lovley, D.R., 2011. A c-type cytochrome and a transcriptional regulator responsible for enhanced extracellular electron transfer in Geobacter sulfurreducens revealed by adaptive evolution. Environ Microbiol, 13(1): 13–23.

van Nguyen, P., Plocek, V., Váchová, L., Palková, Z., 2020. Glucose, Cyc8p and Tup1p regulate biofilm formation and dispersal in wild Saccharomyces cerevisiae. NPJ Biofilms Microbiomes, 6(1):7. doi: 10.1038/s41522-020-0118-1. PMID: 32054862; PMCID: PMC7018694.

Vargas, M., Malvankar, N.S., Tremblay, P.L., Leang, C., Smith, J.A., Patel, P., Snoeyenbos-West, O., Nevin, K.P., Lovley, D.R., 2013. Aromatic amino acids required for pili conductivity and long-range extracellular electron transport in Geobacter sulfurreducens. mBio, 4(2): e00105-13.

Veeken, A.H.M., Hamelers, B.V.M., 2000. Effect of substrate-seed mixing and leachate recirculation on solid state digestion of biowaste. Water Sci. Technol. 41, 255-262.

Velasquez-Orta, S.B., Head, I.M., Curtis, T.P., Scott, K., Lloyd, J.R., and Von Canstein, H., 2010. The effect of flavin electron shuttles in microbial fuel cells current production. Applied Microbiology and Biotechnology, 85(5), 1373-1381.

Veluchamy, C., Gilroyed, B.H., Kalamdhad, A.S., 2019. Process performance and biogas production optimizing of mesophilic plug flow anaerobic digestion of corn silage. Fuel, 253, 1097-1103.

Viggi, C.C., Simonetti, S., Palma, E., Pagliaccia, P., Braguglia, C., Fazi, S., Baronti, S., Navarra, M.A., Pettiti, I., Koch, C., Harnisch, F., Aulenta, F., 2017. Enhancing methane production from food waste fermentate using biochar: the added value of electrochemical testing in pre-selecting the most effective type of biochar. Biotechnol. Biofuels 10, 303.

Villano, M., Aulenta, F., Ciucci, C., Ferri, T., Giuliano, A., Majone, M., 2010. Bioelectrochemical reduction of CO_2 to CH_4 via direct and indirect extracellular electron transfer by a hydrogenophilic methanogenic culture. Bioresour Technol, 101(9): 3085-3090.

Voelklein, M.A., Jacob, A., O'Shea, R., Murphy, J.D., 2016. Assessment of increasing loading rate on two-stage digestion of food waste. Bioresource Technology, 202: 172-180.

Vologni, V., Kakarla, R., Angelidaki, I., Min, B., 2013. Increased power generation from primary sludge by a submersible microbial fuel cell and optimum operational conditions. Bioproc Biosyst Eng, 36:635e42.

Wagner, M., Taherzadeh, D., Haisch, C. and Horn, H., 2010, Investigation of the mesoscale structure and volumetric features of biofilms using optical coherence tomography. Biotechnol. Bioeng., 107: 844-853.

Wainaina, S., Parchami, M., Mahboubi, A., Horváth, I.S., and Taherzadeh, M.J., 2019. Food waste-derived volatile fatty acids platform using an immersed membrane bioreactor. Bioresource Technology, 274, 329-334.

Wang, A., Sun, D., Cao, G., Wang, H., Ren, N., Wu, W.M., and Logan, B.E., 2011. Integrated hydrogen production process from cellulose by combining dark fermentation, microbial fuel cells, and a microbial electrolysis cell. Bioresource Technology, 102, 4137-4143.

Wang, B., Liu, W., Zhang, Y., Wang, A., 2020b. Bioenergy recovery from wastewater accelerated by solar power: Intermittent electro-driving regulation and capacitive storage in biomass. Water Res 175, 115696.

Wang, B., Liu, W., Zhang, Y., Wang, A., 2020c. Intermittent electro field regulated mutualistic interspecies electron transfer away from the electrodes for bioenergy recovery from wastewater. Water Res 185, 116238.

Wang, C., Liu, Y., Gao, X., Chen, H., Xu, X., and Zhu, L., 2018a. Role of biochar in the granulation of anaerobic sludge and improvement of electron transfer characteristics. Bioresource Technology, 268, 28-35.

Wang, C., Wang, Y., Wang, Y., 2020a. Genome-centric microbiome analysis reveals solid retention time (SRT)-shaped species interactions and niche differentiation in food waste and sludge co-digesters. Water Research, 181:115858.

Wang, G.J., Li, Q., Li, Y., Xing, Y., Yao, G.F., Liu, Y.Z., Chen, R., Wang, X.C.C., 2020d. Redox-active biochar facilitates potential electron tranfer between syntrophic partners to enhance anaerobic digestion under high organic loading rate. Bioresour. Technol. 298.

Wang, H., and Ren, Z.J., 2013. A comprehensive review of microbial electrochemical systems as a platform technology. Biotechnology Advances, 31, 1796-1807.

Wang, H., Liu, Y., Du, H., Zhu, J., Peng, L., Yang, C., Luo, F., 2021b. Exploring the effect of voltage on biogas production performance and the methanogenic pathway of microbial electrosynthesis. Biochem. Eng. J. 171, 108028.

Wang, H., Vuorela, M., Keranen, A.L., Lehtinen, T.M., Lensu, A., Lehtomaki, A., Rintala, J., 2010. Development of microbial populations in the anaerobic hydrolysis of grass silage for methane production. FEMS Microbiol. Ecol. 72 (3), 496–506.

Wang, L., He, Z.W., Guo, Z.C., Sangeetha, T., Yang, C.X., Gao, L., Wang, A.J., Liu, W.Z., 2019. Microbial community development on different cathode metals in a bioelectrolysis enhanced methane production system. J. Power Sour. 444 (227306),8.

Wang, T., Zhang, D., Dai, L., Dong, B., and Dai, X., 2018b. Magnetite Triggering Enhanced Direct Interspecies Electron Transfer: A Scavenger for the Blockage of Electron Transfer in Anaerobic Digestion of High-Solids Sewage Sludge. Environmental Science & technology, 52, 7160-7169.

Wang, W., Lee, D.J., 2021. Direct interspecies electron transfer mechanism in enhanced methanogenesis: A mini-review. Bioresource Technology, 330, 124980.

Wang, X.T., Zhao, L., Chen, C., Chen, K.Y., Yang, H., Xu, X.J., Zhou, Xu., Liu, W.Z., Xing, D.F., Ren, N.Q., Lee, D.J., 2021a. Microbial electrolysis cells (MEC) accelerated methane production from the enhanced hydrolysis and acidogenesis of raw waste activated sludge. Chemical Engineering Journal, 413 127472.

Wang, X.T., Zhang, Y.F., Wang, B., Wang, S., Xing, X., Xu, X.J., Liu, L., W.Z., Ren, N.Q., Lee, D.J., Chen, C., 2022. Enhancement of methane production from waste activated

sludge using hybrid microbial electrolysis cells-anaerobic digestion (MEC-AD) process-A review, Bioresource Technology, Volume 346, 2022, 126641.

Wang, Y., Wang, C., Wang, Y., 2017. Investigation on the anaerobic co-digestion of food waste with sewage sludge. Applied Microbiology and Biotechnology, 101(20):7755-7766.

Wanger, G., Gorby, Y., El-Naggar, M.Y., Yuzvinsky, T.D., Schaudinn, C., Gorur, A., and Sedghizadeh, P.P., 2013. Electrically conductive bacterial nanowires in bisphosphonate-related osteonecrosis of the jaw biofilms. Oral and Maxillofacial Pathology, 115(1), 71-78.

Ward, A.J., Hobbs, P.J., Holliman, P.J., Jones, D.L., 2008. Optimisation of the anaerobic digestion of agricultural resources. Bioresour. Technol. 99, 7928e7940.

Westerholm, M., Calusinska, M., Dolfin, J., 2022. Syntrophic propionate-oxidizing bacteria in methanogenic systems. FEMS Microbiology reviews, fuab057, 46, 1-26.

Whitman, W.B., Bowen, T.L., Boone, D.R., 2014. The methanogenic bacteria. In: The Prokaryotes; Rosenberg, E.; De Long, E.; Lory, S.; Stackebrandt, E.; Thomson, F., Eds.; Springer Berlin Heidelberg: Berlin, Heidelberg; pp. 123–163.

Wiegel, J., Tanner, R., Rainey, F.A., 2006. In: M. Dworkin., S. Falkow., E. Rosenberg., K-H, Schleifer., E. Stackebrandt. The Prokaryotes Volume 4. Bacteria: Firmicutes, Cyanobacteria. An Introduction to the family Clostridiaceae. Pp 654-678. Springer, U.S.

Wilson, L.P., Sharvelle, S.E., De Long, S.K., 2016. Enhanced anaerobic digestion performance via combined solids- and leachate-based hydrolysis reactor inoculation. Bioresource Technology, 220: 94-103.

Worldometers. 2019. Canada population. Retrieved from https://www.worldometers.info/world-population/canada-population/

Wu, Q., Guo, W., Zheng, H., 2016. Enhancement of volatile fatty acid production by co-fermentation of food waste and excess sludge without pH control: The mechanism and microbial community analyses. Bioresource Technology, 216:653-660.

Xia, X.X., Zhang, J.C., Song, T.Z., Lu, Y.H., 2019. Stimulation of Smithella-dominating propionate oxidation in a sediment enrichment by magnetite and carbon nanotubes. Environ. Microbiol. Rep. 11, 236–248.

Xiao, L.L., Liu, F.H., Lichtfouse, E., Zhang, P., Feng, D.W., Li, F.B., 2020. Methane production by acetate dismutation stimulated by Shewanella oneidensis and carbon materials: an alternative to classical CO_2 reduction. Chem. Eng. J. 389.

Xiao, L.L., Sun, R., Zhang, P., Zheng, S.L., Tan, Y., Li, J.J., Zhang, Y.C., Liu, F.H., 2019. Simultaneous intensification of direct acetate cleavage and CO_2 reduction to generate methane by bioaugmentation and increased electron transfer. Chem. Eng. J. 378.

Xiao, Y., Chen, G., Chen, Z., Bai, R., Zhao, B., Tian, X., Wu, Y., Zhou, X., Zhao, F., 2021. Interspecific competition by non-exoelectrogenic Citrobacter freundii An1 boosts bioelectricity generation of exoelectrogenic Shewanella oneidensis MR-1. Biosensors and Bioelectronics, 194, 113614.

Xie, S.H., Li, X., Wang, C.D., Kulandaivelu, J., Jiang, G.M., 2020. Enhanced anaerobic digestion of primary sludge with additives: Performance and mechanisms. Bioresour. Technol. 316.

Xiong, Z., 2019. Fermentation of Food Waste in a Leach Bed Reactor: Effects of pH and Inoculum to Substrate Ratio. Master Thesis. University of Waterloo, Waterloo, Ontario, Canada.

Xiong, Z., Hussain, A., Lee, J., and Lee, H.S., 2019. Food waste fermentation in a leach bed reactor: Reactor performance, and microbial ecology and dynamics. Bioresource Technology, 274, 153-161.

Xu, S.Y., Karthikeyan, O.P., Selvam, A., and Wong, J.W.C., 2012. Effect of inoculum to substrate ratio on the hydrolysis and acidification of food waste in leach bed reactor. Bioresource Technology, 126, 425–430.

Xu, S.Y., Karthikeyan, O.P., Selvam, A., Wong, J.W.C., 2014. Microbial community distribution and extracellular enzyme activities in leach bed reactor treating food waste: effect of different leachate recirculation practices. Bioresour. Technol. 168, 41–48.

Xu, S.Y., Lam, H.P., Karthikeyan, O.P., Wong, J.W.C., 2011. Optimization of food waste hydrolysis in leach bed coupled with methanogenic reactor: effect of pH and bulking agent. Bioresour. Technol. 102(4):3702-8.

Xu, H., Wang, C., Yan, K., Wu, J., Zuo, J., Wang, K., 2016. Anaerobic granule-based biofilms formation reduces propionate accumulation under high H2 partial pressure using conductive carbon felt particles. Bioresour Technol, 216:677-683.

Xu, J., Zhu, W., Xie, L., 2019. Effect of bioaugmentation on the performance of anaerobic digestion: A review. Chemical Industry and Engineering Progress, 38(9): 4227-4237.

Xu, S.Y., Lam, H.P., Karthikeyan, O.P., Wong, J.W.C., 2011. Optimization of food waste hydrolysis in leach bed coupled with methanogenic reactor: Effect of pH and bulking agent. Bioresource Technology, 102, 3702-3708.

Xu, X.J., Wang, W.Q., Chen, C., Xie, P., Liu, W.-Z., Zhou, X., Wang, X.T., Yuan, Y., Wang, A.J., Lee, D.J., Yuan, Y.X., Ren, N.Q., 2020. Bioelectrochemical system for the enhancement of methane production by anaerobic digestion of alkaline pretreated sludge. Bioresour. Technol. 304, 123000.

Xu, Y., Gong, H., Dai, X., 2021. High-solid anaerobic digestion of sewage sludge: achievements and perspectives. Frontiers of Environmental Science & Engineering, 15(4): 71-88.

Yamada, C., Kato, S., Ueno, Y., Ishii, M., Igarashi, Y., 2014. Conductive iron oxides accelerate thermophilic methanogenesis from acetate and propionate. J Biosci Bioeng, 119(6): 678-682.

Yang, B., Xu, H., Liu, Y., Li, F., Song, X., Wang, Z., Sand, W., 2020. Role of GAC-MnO2 catalyst for triggering the extracellular electron transfer and boosting CH4 production in syntrophic methanogenesis. Chem. Eng. J. 383.

Yates, M.D., Golden, J.P., Roy, J., Strycharz-Glaven, S.M., Tsoi, S., Erickson, J.S., El-Naggar, M.Y., Calabrese Barton, S., and Tender, L.M., 2015. Thermally activated long range electron transport in living biofilms. Phys. Chem. Chem. Phys. 17 (48),32564–32570.

Yates, M.D., Strycharz-Glaven, S.M., Golden, J.P., Roy, J., Tsoi, S., Erickson, J.S., El-Naggar, M.Y., Barton, S.C., and Tender, L.M., 2016a. Measuring conductivity of living *Geobacter sulfurreducens* biofilms. Nature Nanotechnology, 11: 910-913.

Yates, M.D., Eddie, B.J., Kotloski, N.J., Lebedev, N., Malanoski, A.P., Lin, B., Strycharz-Glaven, S.M., and Tender, L.M., 2016b. Toward understanding long-distance extracellular electron transport in an electroautotrophic microbial community. Energy Environ. Sci. 9 (11), 3544–3558.

Ye, C., Cheng, J.J., Creamer, K.S., 2008. Inhibition of anaerobic digestion process: A review. Bioresource Technology, 99(10):4044-4064.

Ye, J., Hu, A.D., Ren, G.P., Zhou, T., Zhang, G.M., Zhou, S.G., 2017. Red mud enhances methanogenesis with the simultaneous improvement of hydrolysis acidification and electrical conductivity. Bioresour Technol, 247:131-137.

Yin, Q., Yang, S., Wang, Z., Xing, L., and Wu, G., 2018. Clarifying electron transfer and metagenomic analysis of microbial community in the methane production process with the addition of ferroferric oxide. Chemical Engineering Journal, 333, 216-225.

Yu, H.G., Fang, H.H., 2002. Acidogenesis of dairy wastewater at various pH levels. Water Sci. Technol. 45(10):201-206.

Yu, Z., Leng, X., Zhao, S., Ji, J., Zhou, T., Khan, A., Kakde, A., Liu, P., and Li, X., 2018. A review on the applications of microbial electrolysis cells in anaerobic digestion. Bioresource Technology, 255, 340-348.

Yu, Z., Liu, W., Shi, Y., Wang, B., Huang, C., Liu, C., Wang, A., 2021. Microbial electrolysis enhanced bioconversion of waste sludge lysate for hydrogen production compared with anaerobic digestion. Sci Total Environ 767, 144344.

Zacharoff, L.A., El-Naggar, M.Y. 2017. Redox conduction in biofilms: From respiration to living electronics. Curr. Opin. Electrochem., 4(1), 182-189.

Zakaria, B.S., and Dhar, B.R., 2019. Progress towards catalyzing electro-methanogenesis in anaerobic digestion process: Fundamentals, process optimization, design and scale-up considerations. Bioresource Technology, 289, 1-12.

Zamanzadeh, M., Hagen, L.H., Svensson, K., Linjordet, R., and Horn, S.J., 2016. Anaerobic digestion of food waste – effect of recirculation and temperature on performance and microbiology. Water Research, 96, 246-254.

Zamora, L., Pérez-Sancho, M., Domínguez, L., Fernández-Garayzábal, J.F., Vela, A.I., 2017. *Jeotgalibaca porci* sp. nov. and *Jeotgalibaca arthritidis* sp. nov., isolated from pigs, and emended description of the genus *Jeotgalibaca*. Int J Syst Evol Microbiol. 2017 May;67(5):1473-1477. doi: 10.1099/ijsem.0.001741. Epub 2017 May 24. PMID: 27983478.

Zeng, D., Yin, Q., Du, Q., Wu, G. 2019. System performance and microbial community in ethanol-fed anaerobic reactors acclimated with different organic carbon to sulfate ratios. Bioresour. Technol., 278, 34-42.

Zhang, B., He, P.J., Lu, F., Shao, L.M., Wang, P., 2007. Extracellular enzyme activities during regulated hydrolysis of high-solid organic wastes. Water Res. 41 (19), 4468–4478.

Zhang, J., Lu, Y., 2016. Conductive Fe_3O_4 nanoparticles accelerate syntrophic methane production from butyrate oxidation in two different lake sediments. Front Microbiol, 7: 1316.

Zhang, J., Zhang, R., Wang, H., 2020. Direct interspecies electron transfer stimulated by granular activated carbon enhances anaerobic methanation efficiency from typical kitchen waste lipid-rapeseed oil. Science of The Total Environment, 704: 135282.

Zhang, W., Zhang, F., Li, Y.X., Jiang, Y., Zeng, R.J., 2019b. No difference in inhibition among free acids of acetate, propionate and butyrate on hydrogenotrophic methanogen of *Methanobacterium formicicum*. Bioresour Technol. 294:122237.

Zhang, X., Jiao, P., Yang, H., Wu, R., Li, Y., Ma, L., 2022. Recent advances in anaerobic co-digestion of excess sludge and food waste. China Environmental Science, 42(5): 2179-2194.

Zhang, Z., Song, Y., Zheng, S., Zhen, G., Lu, X., Kobayashi, T., Xu, K., Bakonyi, P., 2019a. Electro-conversion of carbon dioxide (CO_2) to low-carbon methane by bioelectromethanogenesis process in microbial electrolysis cells: the current status and future perspective, Bioresour. Technol. 279, 339–349.

Zhao, G., Ma, F., Wei, L., Chua, H., Chang, C., Zhang, X., 2012. Electricity generation from cattle dung using microbial fuel cell technology during anaerobic acidogenesis and the development of microbial populations, Waste Manag. 32. 1651–1658.

Zhao, J., Liu, Y., Wang, D., 2017b. Potential impact of salinity on methane production from food waste anaerobic digestion. Waste Management, 67:308-314.

Zhao, J., Zhang, C., Wang, D., Li, X., An, H., Xie, T., Chen, F., Xu, Q., Sun, Y., Zeng, G., Yang, Q., 2016. Revealing the Underlying Mechanisms of How Sodium Chloride Affects Short-Chain Fatty Acid Production from the Cofermentation of Waste Activated Sludge and Food Waste. ACS Sustainable Chemistry & Engineering, 4(9), 4675-4684.

Zhao L., Wang, X.T., Chen, K.Y., Wang, Z.H., Xu, X.J., Zhou, X., Xing, D.F., Ren, N.Q., Lee, D.J., Chen, C., 2021. The underlying mechanism of enhanced methane production using microbial electrolysis cell assisted anaerobic digestion (MEC-AD) of proteins. Water Research, 201 117325.

Zhao, Z., Zhang, Y., Chen, S., Quan, X., Yu, Q., 2014. Bioelectrochemical enhancement of anaerobic methanogenesis for high organic load rate wastewater treatment in an up-flow anaerobic sludge blanket (UASB) reactor. Sci Rep, 4:6658.

Zhao, Z.Q., Zhang, Y.B., Wang, L.Y., Quan, X., 2015. Potential for direct interspecies electron transfer in an electric-anaerobic system to increase methane production from sludge digestion. Sci Rep, 2015, 5: 12.

Zhao, Z., Zhang, Y., Yu, Q., Dang, Y., Li, Y., and Quan, X., 2016a. Communities stimulated with ethanol to perform direct interspecies electron transfer for syntrophic metabolism of propionate and butyrate. Water Research, 102, 475-484.

Zhao, Z., Zhang, Y., Holmes, D.E., Dang, Y., Woodard, T.L., Nevin, K.P., Lovley, D.R., 2016b. Potential enhancement of direct interspecies electron transfer for syntrophic metabolism of propionate and butyrate with biochar in up-flow anaerobic sludge blanket reactors. Bioresour Technol, 209: 148-156.

Zhao, Z., Zhang, Y., Ma, W., Sun, J., Sun, S., Quan, X., 2016c. Enriching functional microbes with electrode to accelerate the decomposition of complex substrates during anaerobic digestion of municipal sludge. Biochem. Eng. J. 111, 1–9.

Zhao, Z., Li, Y., He, J., and Zhang, Y., 2018. Establishing Direct Interspecies Electron Transfer during Laboratory-Scale Anaerobic Digestion of Waste Activated Sludge via Biological Ethanol-Type Fermentation Pretreatment. Sustainable Chem. Eng. 6, 13066−13077.

Zhao, Z., and Zhang, Y., 2019. Application of ethanol-type fermentation in establishment of direct interspecies electron transfer: A practical engineering case study. Renewable energy, 136, 846-855.

Zhao, Z., Wang, J., Li, Y., 2020. Why do DIETers like drinking: Metagenomic analysis for methane and energy metabolism during anaerobic digestion with ethanol. Water Research, 171: 115425.

Zhen, G., Koayashi, T., Lu, X., Kumar, G., Hu, Y., Bakonyi, P., Rozsenberszki, T., Kook, L., Nemestothy, N., Belafi-Bako, K., Xu, K., 2016. Recovery of biohydrogen in a singlechamber microbial electrohydrogenesis cell using liquid fraction of pressed municipal solid waste (LPW) as substrate. Int. J. Hydrogen Energy, 41(40): 17896–17906.

Zhen, G., Lu, X., Kato, H., Zhao, Y., Li, Y.Y., 2017. Overview of pretreatment strategies for enhancing sewage sludge disintegration and subsequent anaerobic digestion: Current advances, full-scale application and future perspectives. Renew. Sustain. Energ. Rev. 69, 559–577.

Zhi, Z., Pan, Y., Lu, X., Zhen, G., Zhao, Y., Zhu, X., Xiong, J., Zhao, T., 2019. Electrically regulating co-fermentation of sewage sludge and food waste towards promoting biomethane production and mass reduction. Bioresour. Technol. 279, 218–227.

Zhou, M., Yan, B., Wong, J. W. C., and Zhang, Y., 2018. Enhanced volatile fatty acids production from anaerobic fermentation of food waste: A mini-review focusing on acidogenic metabolic pathways. Bioresource Technology, 248, 68-78.

Zhu, H., Han, Y.X., Ma, W.C., Han, H.J., Ma, W.W., Xu, C.Y., 2018. New insights into enhanced anaerobic degradation of coal gasification wastewater (CGW) with the assistance of graphene. Bioresour. Technol. 262, 302–309.

Zhuang, H.F., Xie, Q.N., Shan, S.D., Fang, C.R., Ping, L.F., Zhang, C.G., Wang, Z.R., 2020a. Performance, mechanism and stability of nitrogen-doped sewage sludge based activated carbon supported magnetite in anaerobic degradation of coal gasification wastewater. Sci. Total Environ. 737.

Zhuang, L., Tang, J., Wang, Y., Hu, M., Zhou, S., 2015. Conductive iron oxide minerals accelerate syntrophic cooperation in methanogenic benzoate degradation. J hazmat, 293: 37-45.

Zhuang, H.F., Zhu, H., Zhang, J., Shan, S.D., Fang, C.R., Tang, H.J., Xie, Q.N., 2020b. Enhanced 2,4,6-trichlorophenol anaerobic degradation by Fe3O4 supported on water hyacinth biochar for triggering direct interspecies electron transfer and its use in coal gasification wastewater treatment. Bioresour. Technol. 296.

Zotti, G., Zecchin, S., Schiavon, G., Berlin, A., Pagani, G., Canavesi, A., 1995. Conductivity In Redox Modified Conducting Polymers. 2. Enhanced Redox Conductivity in Ferrocene-Substituted Polypyrroles and Polythiophenes. Chemistry of Materials 7(12):2309-2315.